THE DEPARTMENT OF CIVIL ENGINEERING
THE UNIVERSITY OF ASTON IN BIRMINGHAM

THE STRENGTH AND BEHAVIOUR OF BRICKWORK IN FLEXURE

P.M.MASON
C.Eng., F.I.Struct.E., M.I.Mech.E.

A THESIS SUBMITTED FOR THE DEGREE OF DOCTOR OF PHILOSOPHY

FEBUARY 1972

SUMMARY

This thesis is the result of a programme of work concerned with the flexural strength and behaviour of brickwork beams.

The physical properties of the constituent materials are examined in the light of existing knowledge and specific tests of compressive strength, tensile strength, adhesion and modulus of elasticity are carried out for the individual constituent materials (bricks and mortars) and for the composite material (brickwork) that are used in subsequent beam tests.

A theoretical solution is presented for shallow brickwork beams using a theory analogous to that frequently used for beams of laminated cross-sections based upon considerations that the beam is not of a homogenerus material, a number of simply supported beams are tested and analysed by the proposed theory.

Deep beams supported by a vertical shear force at each end are analysed by a theory developed from the Theory of Elasticity using Airey stress functions, stress equations are achieved that result in the ideal conditions of stress free ends at the vertical end faces of the beam. A method for the determination of the stress functions is given from the expansion of a doubly infinite power series.

Tests are carried out to determine the distribution of flexural stress at mid span of some deep beams, these tests validate the proposed theory and give some indication of the arching action that takes place in some deep beams.

Arching action is considered for beams restrained in the longitudinal direction, assuming that a tension failure has taken place. A number of restrained mortar beams are tested to obtain the load/deflection relationships and ultimate strengths for beams of various span/depth ratios.

ACKNOWLEDGEMENTS

The author expresses his sincere gratitude to Professor Malcolm Holmes, B.Sc., Ph.D., C.Eng., F.I.C.E., F.I.Struct.E., F.I.Mun.E., Head of the Department of Civil Engineering, The University of Aston in Birmingham for the opportunity to present this thesis and for his constant help and encouragement throughout the programme of work; to Mr. Walter Parsons, Chief Technician of the Department for his advice on the design and construction of the test rigs and apparatus and to his Assistant Technicians Messrs. John Hollins and Vaughan Williams who prepared the apparatus and test specimens and who both gave valuable assistance in the experimental work.

The author's thanks must also be rendered to Mrs. Marjorie Mills who typed the script and not least of all to his dear wife Patricia for her tolerance and understanding.

PREFACE

Probably the oldest form of building construction known to man is the art of placing small elements of a material one on top of the other to provide a protective shelter against the unfavourable aspects of his environment.

For some thousands of years the simple brick in some form either obtained from natural resources or specifically manufactured has provided man with his most readily adaptable building material. There are numerous examples in the relics of ancient civilisation of sophisticated load bearing bric kwork structures in the shape of bridges, aquaducts, retaining walls, columns, arches and domes that have survived to this day to give evidence of the art and craft that our ancestors must have possessed. It is unlikely that at this time the early masons had the benefit of an ability to carry out a mathematical analysis of the structures that were built and it must be assumed that their work was the result of practical research by trial and error.

Much of the success must have depended upon the intuition and experience of the individual from which it could be expected that the 'academics' of succeeding generations were able to produce rule of thumb methods for simple calculated designs.

It followed over the years that a traditional art of building in brickwork was developed, quite naturally on a very conservative basis and when judged by present day standards cannot be considered to be economical in terms of capital costs for labour and materials.

In recent years the introduction of Building Byelaws permitting the use of calc ulated loadbearing brickwork has generated an interest for research to establish methods of design and construction in order that

a more scientific approach can be made in the assessments of stress distribution in brickwork elements. A better understanding of the material has been achieved whi ch has led to economy in design and utilisation of the available brickwork materials.

Unfortunately, the long standing tradition in the design of load-bearing brickwork has been based on the assumption that brickwork possesses no tensile strength, consequently designers have produced solutions making every attempt to avoid the presence of tensile forces, it is for these reasons that modern research has generally been confined to the behaviour of brickwork in compression. This may well have been satisfactory in the days when weak lime mortars were used, it is a regrettable fact however that more advantage has not been taken of the properties of strength and adhesion of the cement/sand mortars in common use today.
Each day, more use is being made of mortar additives that not only improve the tensile properties of brickwork but with reasonable site supervision can achieve reliable guaranteed strengths for the material in a state of tension.

Recent disasters brought about by gas explosion and other accidental damage have quite clearly shown that brickwork can have a high degree of tensile strength that has previously been ignored. There is still scope therefore that with a better understanding of the flexural strength and behaviour of brickwork there will be an opportunity for further economics to be achieved.

It is for this reason that this thesis has been prepared, within the limitations of the scope of the work presented here it is of course not possible to provide solutions to all of the problems that can arise

when advantage is taken of the tensile strength of brickwork. With these limitations in mind this programme of work has been confined to an investigation, both mathematically and by practical experiment, into the behaviour of brickwork beams.

It has for a long time been the concern of designers that lintols over openings in brick walls become, in a number of practical instances, superfluous once the brickwork has been built and set. The lintol that was in all probability designed to carry the full weight of the brickwork above it, is, in effect, simply a prop that is necessary during the period of construction.

The modern method of multi-storey cross wall construction essentially involves the use of walls that can behave as deep beams supporting vertical loads or providing stability against imposed horizontal forces. Without taking into consideration the tensile strength properties of the brickwork the full economy of the construction cannot be achieved.

Brickwork still remains one of the cheapest, most durable and aesthetically pleasing forms of construction, research in this field must progress in order that the full potential of the material may be exploited.

I N D E X

CHAPTER 1

STATISTICAL PROCEDURES

Statistical procedures used in the presentation of this thesis make it possible to summarise results in a concise and convenient form. Based upon the recommendation of Special Technical Publication 15-C prepared by the American Society for Testing and Materials Committee E-11 on Statistical methods, certain common algebraic functions, the arithmetic mean $\bar{X}$, the coefficient of variation (V) and the number of specimens (n) will be recorded.

The arithmetic mean ($\bar{X}$), popularly called the average, is a measure of central tendency. It corresponds to the centre of gravity of a system and it is expressed in the same units as the observations.

The standard deviation (s) is a measure of variability. It is an indicator of spread or dispersion of a series of measurements about a central point, the mean.

In a mechanical system it corresponds to the radius of gyration measured from the centre of gravity. The larger the standard deviation the larger is the scatter or the wider the spread of the data. It is expressed in the same units as the measurements making up the set of data.

The fundamental formula for the calculation of the standard deviation is:-

$$s = \sqrt{\frac{\sum(x - \bar{x})^2}{n - 1}}$$

where $\bar{X}$ = the arithmetic mean (average)

x = an individual measurement

n = number of specimens or measurements in the sample.

(In small sample statistics n - 1 is used more correctly. If the sample is large n is used as the denominator.)

The standard deviation is best interpreted in terms of the percentage of cases falling within certain limits. In a normal distribution 68.26

per cent of the cases fall within the limits one standard deviation above the mean and one standard deviation below the mean.

The range $\pm$ 2 standard deviation from the mean, includes 95.44 per cent of the cases.
The range $\pm$ 3 standard deviation from the mean includes 99.74 per cent of the cases.

The most simple measure of dispersion is the range (R). It is defined as the difference between the largest and smallest numbers of a set, and numerically defines maximum spread or scatter. Only two numbers are used to calculate the range, whereas all the values in a set of measurements or observations are used to calculate the standard deviation.
Therefore, the standard deviation is a more representative indicator of variability but it is not as easily interpreted.

The coefficient of variation (V) which is also a measure of dispersion or scatter is the ratio of the standard deviation to the arithmetic mean expressed as a percentage. It expresses variability on a relative scale rather than on an absolute scale and is perhaps the most easily interpreted measure of dispersion.

It is calculated from the following:-

$$V = \frac{100\ s}{\bar{X}}$$

where V = coefficient of variation

S = standard deviation

$\bar{X}$ = arithmetic mean

CHAPTER 2

BRICKS

2.1 BRICKS USED FOR EXPERIMENTAL WORK

The bricks used for all tests and sample panels were pressed clay FLETTONS, solid without frogs, supplied by THE LONDON BRICK CO. LTD.

The brick tests were carried out in accordance with BS.3921:1965 "Specification for Bricks and Blocks of Fired Brickearth, Clay or Shale".

2.2 WATER ABSORPTION TESTS

For load bearing bricks other than Engineering Bricks or bricks for damp-proof courses there is no requirement for specific average absorption values imposed on the brick manufacturers by BS.3921. The initial rate of absorption generally decreases as the brick strength increases, there are exceptions of course since the initial rate of absorption is influenced by texture and surface characteristics as well as by the capillary pore structure of the brick.

A brick which is permeated with water may become frozen; even without freezing a wet brick will expand, in both cases severe internal stresses may be set up if the structure is restrained in its movement or damage may occur if free expansion is allowed to take place.

In building structures the general case is that one face of the wall is exposed to weather whilst the inside face remains dry and protected; it must therefore be desirable for a brick to have a low absorption rate.

The requirements of BS.3921 with respect to frost resistance show only the durability of a brick and do not relate to the load bearing capacity under adverse weather and temperature conditions.

The water absorption test is now given less prominence than has often been accorded to it. A low water absorption figure can be used in defining engineering bricks and bricks for damp-proof courses but water absorption, like strength, is not a general index of durability. No limit

can be set, however, that will discriminate generally between durable and non-durable bricks.

Recent work has shown that the saturation coefficient, or ratio of 24 hour cold absorption to total absorption by the boiling or vacuum methods, is less useful as an index of durability than was formerly thought. It is not therefore included in BS.3921.

2.3 Suction Rate of Bricks

Absorption can be defined as the amount of water which will fill those pores in a brick which are open to the air. The rate of absorption is called SUCTION and upon thi s value depends the ease with which bricks may be laid and also their bond strength to the mortar.

Bricks with rough textures on the bed faces and medium values of suction will have high bond because the mortar will key into the irregularities of the brick.

Bricks with low values of suction have bed faces which are often of smooth texture with few irregularities giving low adhesion.

Bricks with high suction can reduce the water content of mortar so rapidly that it stiffens before the upper brick is laid, resulting in a low workability mortar with poor bond. This can result in the mortar adhering much more strongly to the lower than to the upper bricks.

Bricks of high absorption will require wetting to some extent to reduce the suction, particularly in hot dry weather.

PLUMMER (1) states that suction should not exceed 20 g/brick over a face approximately 30 in^2 in area which corresponds with 0.025 $oz/in^2/min$ sometimes quoted.

ALBRECHT and SCHNEIDER (2) quote 15 g/dm^2 (about 35 g/brick) as the critical maximum if a good tensile bond is to be obtained, and recommends the soaking of bric ks to reduce the suction to this value.

(3)

The draft revision to CP.111 (January 1970) states that clay units should not be laid where the suction rate (determined by a specified test) exceeds 2 kg/m^2 per min; where necessary the suction rate on site should be adjusted by wetting. This value corresponds to about 46 g/brick for bricks to BS.3921 (area 35.58 in^2)

The following suction rate test as specified in the draft revision to CP.111 was carried out.

A shallow tray was placed on a level table. Two metal rods of equal size were placed a few inches apart, in the bottom of the dish, and the dish filled with water until the metal rods were covered to a depth of about 3 mm. The brick to be tested, which was dry, was weighed to the nearest gramme and placed, bed face downwards, on the metal rods and left in position for 60 $\pm$ 2 seconds. It was then removed surplus water quickly wiped off with a damp cloth, and re-weighed. The water level was adjusted as necessary between tests.

SPECIMEN NO.	DRY WEIGHT(g)	WET WEIGHT(g)	WEIGHT OF ABSORBED WATER(g)
1	2559	2662	63
2	2573	2639	66
3	2551	2626	75
4	2540	2614	74
5	2544	2620	76
6	2583	2654	71
7	2582	2652	70
8	2557	2646	89
9	2573	2650	77
10	2593	2666	73
11	2530	2604	74
12	2551	2631	80

These results given an arithmetic mean ($\bar{x}$) of 74 g, a standard deviation (S) of 6.65 g and a coefficient of variation (V) of 9%.

Conclusion

The sample bricks tested have a very high suction rate which is in excess of the value specified that would result in an acceptable bond between brick and mortar.

The bricks will therefore be wetted by complete immersion in water for a specified time before sample beams, panels and test pieces are constructed.

2.4 The Compressive Strength of Bricks

Bricks are produced with strengths to satisfy a wide range of architectural and engineering requirements.

Brick crushing strengths range from less than 2000 lb/in^2 to more than 14,500 lb/in^2 with specifications covering all normal building requirements. For load bearing brickwork structures it is usual for the designer to state as his basic specification the required crushing strength of the bric k and the type of mortar to be used.

The main use of the results of compressive strength tests is as a guide to permissable stresses in brickwork. Cp.111 'Recommendation of load-bearing Walls' states limiting design stress values related to the brick crushing strength, the slenderness ratio of the wall, the type of mortar and the condition of eccentric loading.

The crushing strength of a brick is often mistakenly used as a guide to other properties of the brick. Although very approximately the tensile and shear strengths are of the order of 7% and 35% respectively of the particular compressive strength, the crushing strength is not necessarily an index of the durability or absorption rate.

From the manufacturers point of view, the simple crushing strength test is an invaluable aid to the production of a system of quality c ontrol that will enable a guarantee to be given to the user that when random samples are taken from any delivered batch of bricks, there is a specified probability on a statistical basis, that in not more than 1 in 40 samples tested the arithmetic mean of the sample will be below a specified limit of compressive strength.

The method of determination of compressive strength is defined in BS.3921. 1965 'Bricks and Blocks of Fired Brickearth Clay or Shale'.

10 sample bricks were taken from various positions of a stack of 1000 bricks. The overall dimensions of each bed face were measured to the nearest 0.05" and the area of the smaller of the two was taken as the area of the unit for calculating the compressive strength.

For the bed face compression test the bricks were immersed in water for 24 hours before testing between 3 mm plywood at a loading rate of 2000 lb /in^2 MIN all in accordance with Clause 43 d BS.3921.

COMPRESSION TEST ON BRICKS

Carried out in accordance with Clause 43: BS.3921. 1965.

Soaked in water for 24 hours. Tested between 3 mm Plywood at 2000 lb/in^2/MIN.

SPECIMEN NO.	COMPRESSIVE STRENGTH lb/in^2
1	2990
2	4190
3	2950
4	2900
5	3090
6	3050
7	3470
8	2900
9	3160
10	3360

These Results Give:-

ARITHMETIC MEAN $\bar{x}$ = 3206 lb/in^2

STANDARD DEVIATION = 394 lb/in^2

VARIATION = 12.3%

2.5 The Modulus of Elasticity of Bricks

Further compression tests were carried out on the longitudinal axis of 3 selected brick samples for the purpose of investigating the load strain graph for the sample and the calculation of the initial tangent modulus. These tests were carried out on dry bricks.

The opposite 4" faces of each sample were prepared by the application of a thin coat of 'Polyfilla' which was then carefully scraped to provide a smooth face for the strain gauges.

'Tinsley' Type 7A Felt Backed electronic strain gauges of 2" gauge length and a gauge factor of 2.15 were bonded to the prepared face with F88 adhesive cement supplied by the International Dental Co.Ltd. Mexico.

A preliminary load was applied t o each specimen without shock and increased slowly up to a maximum load of 1.5 tons, the load was maintained at this figure for one minute and then reduced gradually to zero. This preliminary loading was carried out in an attempt to prevent the irregularities of the material producing an initial non-linear load-strain relationship.

In order that the initial tangent modulus could be carefully plotted loads were then applied to the specimen in increments of 0.1 ton up to 1.5 tons thereafter in increments of 0.5 tons to failure. Strain gauge readings being taken at each increment of load.

The load strain curves were then plotted for each face of the 3 specimens tested. (Figs. 2.5.1: 2.5.2: and 2.5.3)

For the purpose of the calculation of the tangent modulus the arithmetic mean of the measured strain on the 6 tested faces up to an applied load of 1.5 tons was plotted (Fig.2.5.4)

From the slope of this line it was calculated that:

$$E = 1.25 \times 10^6 \text{ lb/in}^2$$

The arithmetic mean of the crushing strength in the long axis was 2050 lb/in^2 indicating that the crushing strength in this direction is only $\frac{2}{3}$ of the crushing strength in the direction of the normal bed face.

Plate 2.5.1. shows a typical specimen after failure.
All specimens failed by the mode indicated, in each case the diagonal cracks at the top of the brick formed first resulting in a wedge action which produced the vertical split from the intersection of the diagonal cracks to the bottom of the brick.

PLATE 2.5.1

COMPRESSION TEST ON LONG AXIS OF BRICKS

MICRO STRAINS

LOAD (TONS)	SPEC 1		SPEC 2		SPEC 3		$\bar{x}$
	FACE A	FACE B	FACE A	FACE B	FACE A	FACE B	
0.1	5	25	23	20	15	15	17
0.2	15	50	48	30	25	30	33
0.3	20	75	68	45	35	45	48
0.4	30	105	88	60	45	65	65
0.5	40	127	113	70	60	80	82
0.6	55	150	133	85	70	95	98
0.7	66	175	153	100	80	110	114
0.8	85	195	178	110	95	125	131
0.9	100	217	198	130	105	140	148
1.0	115	240	218	145	115	155	165
1.1	133	260	238	160	130	170	182
1.2	155	285	253	180	145	190	201
1.3	167	305	268	195	157	205	216
1.4	190	325	288	210	170	220	234
1.5	205	345	311	225	185	230	267
2.0	325	438	443	305	245	310	344
2.5	415	520	528	400	315	388	428
3.0	565	610	598	520	395	450	523
3.5	670	720	668	660	455	535	618
4.0	785	825	753	780	520	620	714
4.5	910	925	843	910	580	705	
5.0	1050	1035	958	1030	660	785	
5.5	1190	1160	1078	1155	735	880	
6.0	1375	1295	1248	1270	815	975	
6.5	1530	1460	1388	1405	885	1080	
7.0	1745	1665	1588	1550	960	1180	
FAILURE LOAD(TONS)	8.85		9.01		11.9		
CRUSHING STRENGTH lb/in^2	1830		1860		2460		

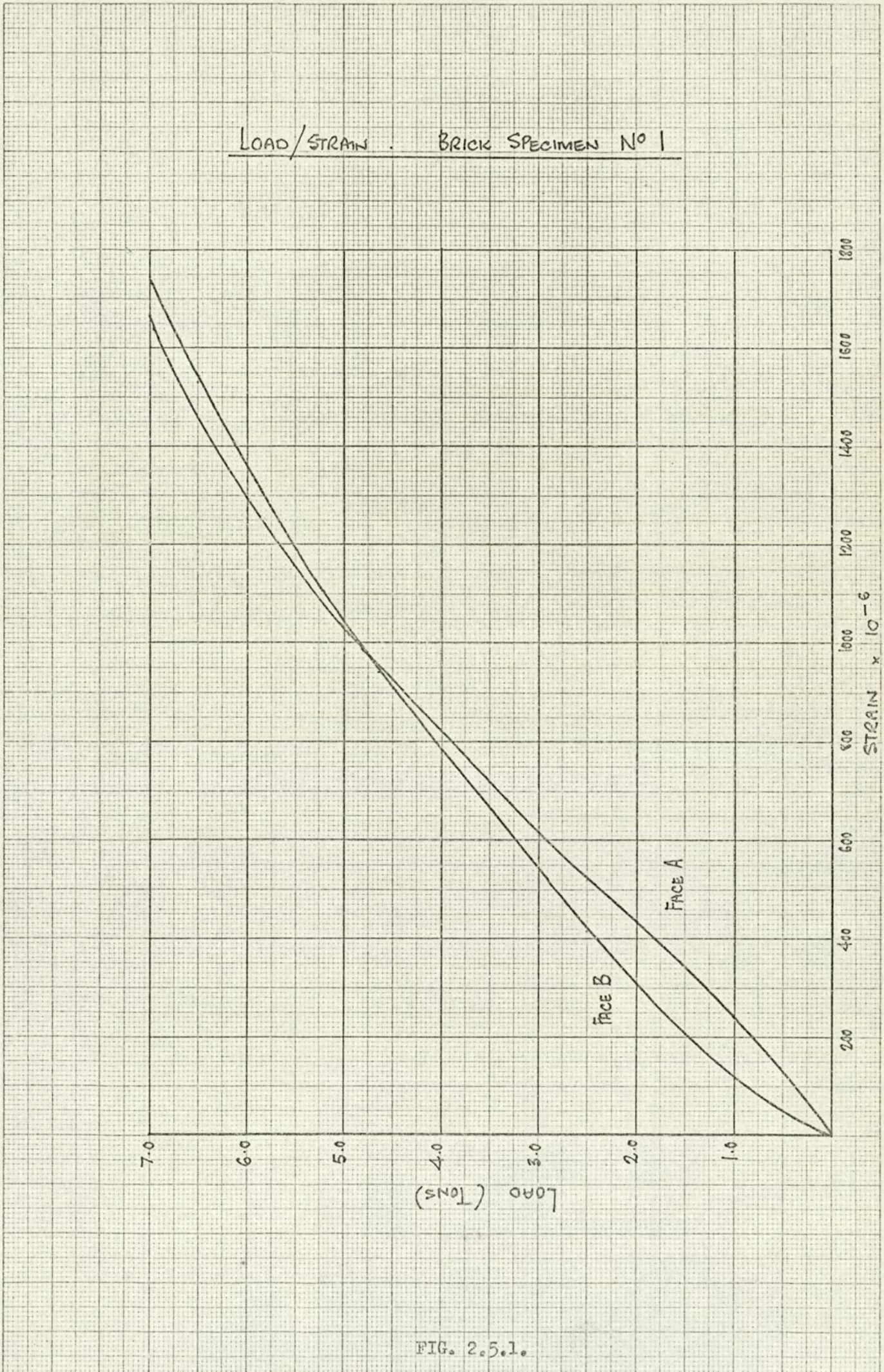
LOAD/STRAIN . BRICK SPECIMEN Nº 1
STRAIN x 10⁻⁶
200
400
600
800
1000
1200
1400
1600
1800
FACE A
FACE B
LOAD (TONS)
7.0
6.0
5.0
4.0
3.0
2.0
1.0

FIG. 2.5.1.

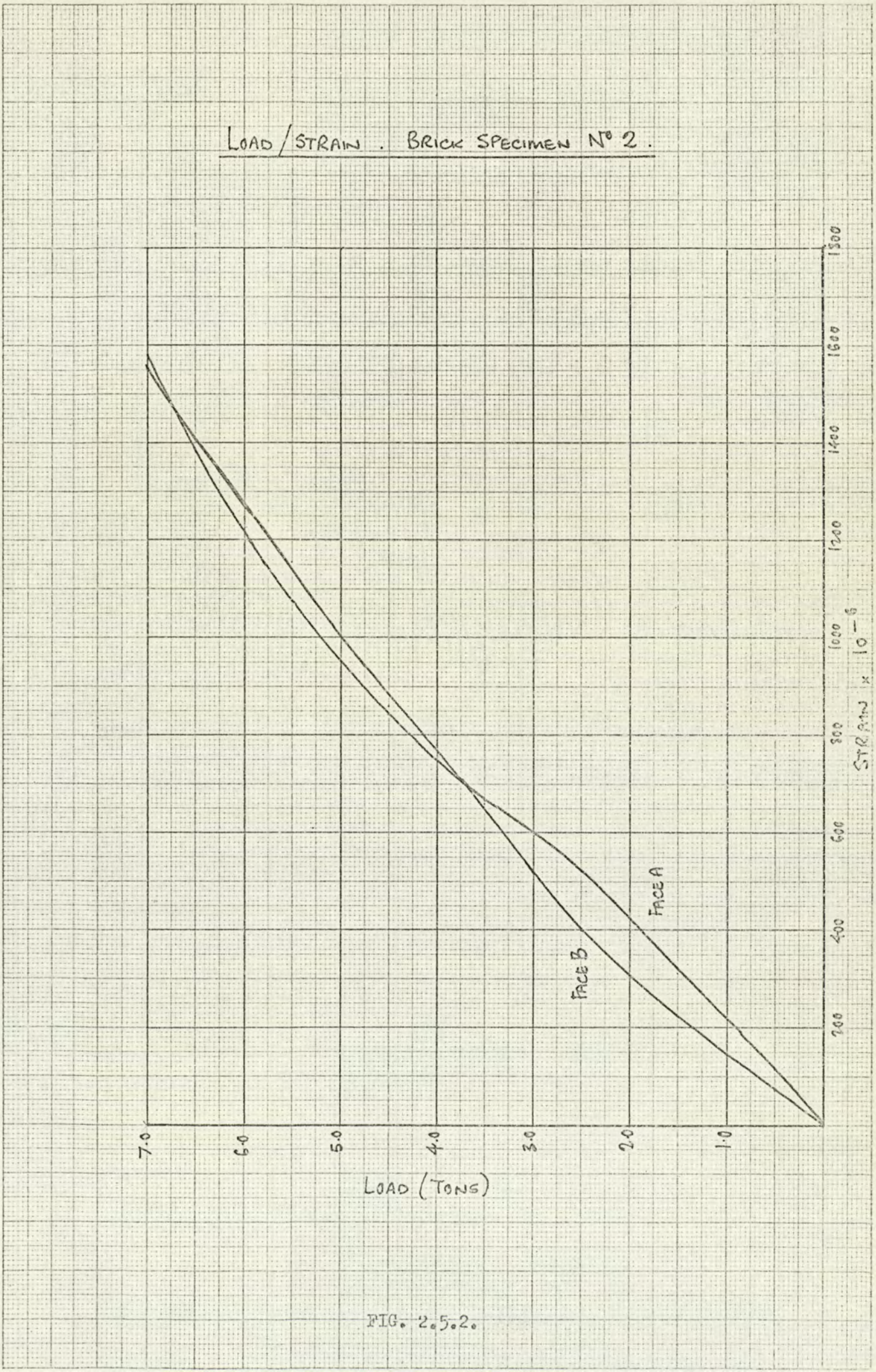
LOAD / STRAIN . BRICK SPECIMEN Nº 2.
FACE A
FACE B
7.0
6.0
5.0
4.0
3.0
2.0
1.0
LOAD (TONS)
200
400
600
800
1000
1200
1400
1600
1800
STRAIN x 10⁻⁶

FIG. 2.5.2.

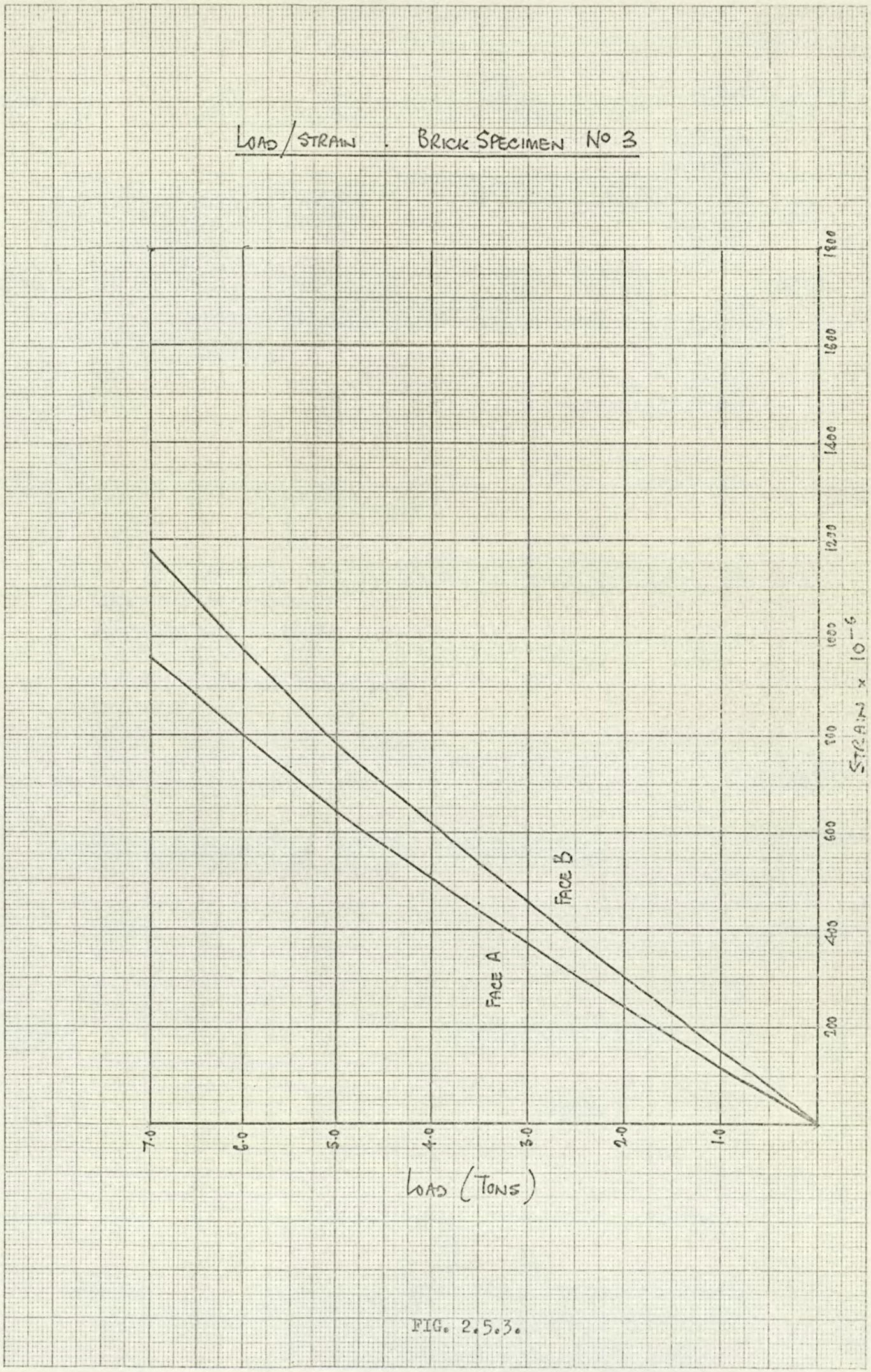
LOAD / STRAIN . BRICK SPECIMEN No 3
FACE B
FACE A
7.0
6.0
5.0
4.0
3.0
2.0
1.0
LOAD (TONS)
1800
1600
1400
1200
1000
800
600
400
200
STRAIN x 10⁻⁶

FIG. 2.5.3.

LOAD / STRAIN

ARITHMETIC MEAN ($\bar{x}$) OF 3 BRICK SPECIMENS

(2.64" × 4.11")

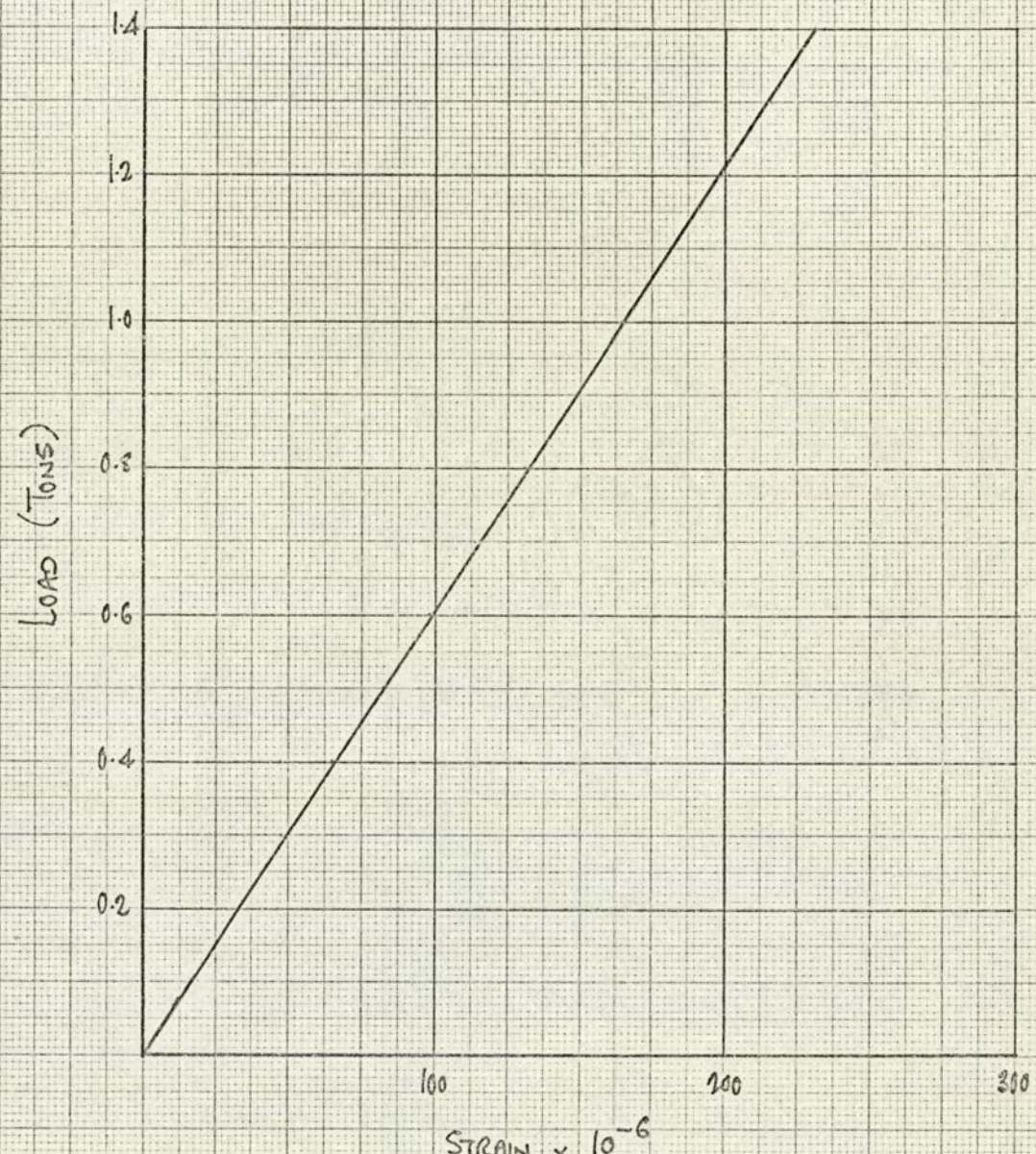

AVERAGE INITIAL TANGENT MODULUS = E = 1.25×10^6 lb/in^2

FIG.2.5.4.

2.6 The Tensile Strength of Bricks

Attempts were first made to obtain the direct tensile strength of the bricks by bonding steel plates to the ends of the brick samples, the steel plates each being fitted with a steel rod suitable for gripping in the jaws of a tensile testing machine.

To obtain the necessary alignment the plates were first fixed into the jaws of the machine and the specimen held in this position until the setting of the bonding agent was complete.

Six samples were prepared and during the test on each sample a fracture occurred within 6 mm from the end of the brick. (see plate No.2.6.1)

It was concluded that this mode of failure was the result of tri-axial tension set up by the restraint to contraction in a direction at right angles to the axis of the applied load at the end of the brick provided by the bond between brick and steel plate.

Further attempts were made to obtain a direct tensile test by bonding hard rubber pads between the steel plates and the specimen brick (see Plate No. 2.6.2).

The test resulted in a tensile failure of the rubber,; After experiencing great difficulty in removing the rubber pad from the steel plate for further use it was decided that this would not in the end produce a satisfactory practical test. Further effort to obtain a suitable grade of rubber was not considered to be worth while.

The direct tensile test was then abandoned in favour of the following 'splitting test'.

Five bricks were taken at random from the stored stack.

Each brick was then cut by the use of a masonry saw into three samples, each being 2.6" x 2.6" in cross section x 4.1" long. Two of the samples being the ends of the bricks, the third being taken from the centre of the brick length.

The standard splitting test was then carried out, the load being applied through 12 mm wide strips of 3 mm plywood.

The load was applied steadily without shock and increased continuously until the specimen failed.

The indirect tensile strength (ft) of each sample was then calculated from $ft = \frac{2P}{\pi . d . l}$

where d = 2.6" the side of the square sample

l = 4.1" the length of the sample

P = the failure load of the sample

Specimen No.		Load (Tons)	ft. (lb/in^2)
Brick No. 1	1 END	2.62	350
	2 CENTRE	2.40	321
	3 END	2.54	340
Brick No. 2	4 END	2.91	390
	5 CENTRE	2.71	362
	6 END	2.85	382
Brick No. 3	7 END	2.72	364
	8 CENTRE	2.52	337
	9 END	2.80	375
Brick No. 4	10 END	2.85	381
	11 CENTRE	2.62	350
	12 END	2.70	361
Brick No. 5	13 END	2.70	361
	14 CENTRE	2.60	348
	15 END	2.79	373

For each brick tested, the sample taken from the centre of the brick length gave the lowest load value of the three specimens, it was therefore concluded that the brick was weaker in tension in the centre than at each end. The values obtained for the centre sample were therefore used to calculate the following statistical results for tensile strength.

Arithmetic mean $\bar{x}$ = 344 lb/in^2

Standard Deviation s = 15.5 lb/in^2

Coefficient of Variation = 4.5%

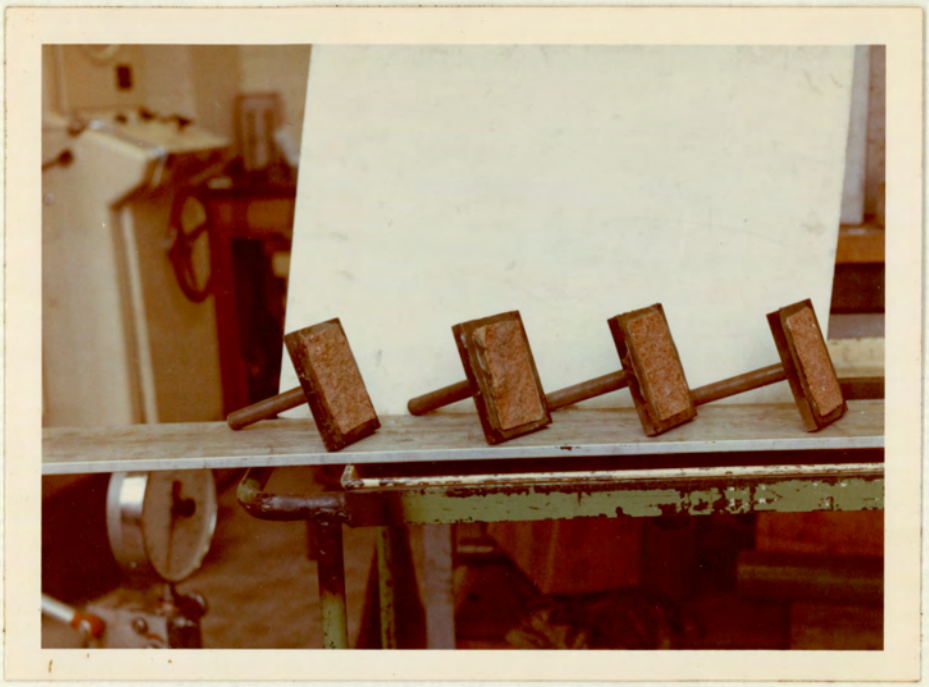

PLATE 2.6.1

PLATE 2.6.2

CHAPTER 3

MORTAR

3.1 The Functions of Mortar

Two of the most important functions of a mortar are to contribute to the structural and weather-resisting abilities of the constructed wall. There are a number of properties of mortar affecting these functions, including drying shrinkage, durability, frost resistance, adhesion, tensile and compressive strength. The freshly mixed mortar must have satisfactory properties for laying the particular type of brick being used.

In the design of mortar all the foregoing factors should be taken into account.

British Standard 4551:1970 'Methods of Testing Mortars' gives details of tests that can be carried out in order that the properties of the mortar can be established but unfortunately gives no guide as to the results that ought to be obtained from these tests. CP.111 'Load Bearing Brickwork' gives in part some details of mortar compressive strengths for various considerations but generally the properties of the mortar are left to the designer to decide and on site to the labourer to achieve.

It is probably these final factors that have been a major influence on the engineers reluctance to view calculated brickwork as an acceptable structural medium .

In consideration of mortars for calculated load-bearing brickwork the major emphasis is placed on achieving certain specified compressive strength requirements. In fact, the racking strength of walls, their ability to withstand lateral loading and their strength as beams bear very little direct relation to the compressive strength of the mortar and are effected in more detail by its transverse strength, tensile strength

or adhesion to the particular bricks in use. There is very little existing information on these important factors at the disposal of the designer. Regardless of the academic approach to brickwork design and the theoretical distribution of stresses in brickwork, as a general case tensile failure of the brickwork is a result of the breakdown in adhesion between brick and mortar.

The mechanism of compressive failure is a vertical splitting of the clay brick due to lateral deformation of the less stiff mortar material in the joint.
The action of the mortar deformation gives rise to lateral compressive stress within its volume. Whilst load between mortar and brick may help to confine the mortar laterally, friction alone would probably provide sufficient resistance.

Lateral confinement of the mortar material and a tri-axial state of compression within its mass are inferred to exist, based on successful results of attempts by several investigators to produce an effective joint by filling it with sand only. A sand joint is necessarily confined by friction, which permits the development, within its mass, of a tri-axial state of compression.

The importance of the influence of mortar tension or bond on the compressive strength only of the assemblage is difficult to conceive within this mechanism of failure and the designer must appreciate the distribution of principal tensile stresses in the loaded brickwork.

To take full advantage of the inherent strength of bricks, the strength properties of the mortar should theoretically be equal to those of the brick.

This implies that to develop the full potential tensile strength of the brickwork, the mortar bond strength should match the tensile strength of the brick.

Such a goal has been partially achieved by the use of an organic polymer added to the construction mortar. The use of high bond mortars makes it possible to consider brickwork as an engineered material. Increasing the bond strength between the masonry units improves the transverse strength of brickwork as well as other structural action on which tension is the mode of failure. Since brickwork in compression fails by tensile splitting and by diagonal tension in shear, the three basic stress conditions in any brickwork structure - compression, tension and shear - are limited by the tensile resistance of the bonded assemblage. Thus any improvement in the bonding action between masonry units indirectly improves shear and compressive strengths. Also, improved bond between the units develops a more monolithic action in the assemblage.

A successful high bond mortar, with respect to both workability and strength has been a 1. $2\frac{1}{4}$ cement - sand ratio with 15% Saran polymer solids (by weight of the cement content). This mortar mix has been used in the United States of America and in addition to having good initial adhesion and proper cohesive mobility it can be stored for up to one hour before being used in the brick laying process.

3.2 Grades of Mortar

A mortar that would suit any requirement for bricklaying would require the following properties:

(a) It must have adequate strength

(b) Bond well to the bricks

(c) Be easily worked

(d) Must stiffen fairly quickly

(e) Have sufficient durability

In any one mortar mix the ideal of all of the above properties cannot be achieved and the designer must decide on the most suitable mix from the design consideration.

The properties of the mortar are decided by the constituent materials and the properties of their mix.

Mortar will work easily if it contains lime, the more lime that it contains, the more workable it will be.
Mortar will stiffen more quickly if it contains cement, the more cement that it contains, the quicker it will stiffen.

Mortar must be capable of the retention of the mixing water, bricks that are very absorbent will take too much water out of the mortar with the result that there will be insufficient retained water to allow the cement to set and harden properly. This will result in a thin layer of mortar adjacent to the bricks that has not properly set and cracks will form between the bricks and the mortar. The addition of lime will help to prevent this.

During the construction of brickwork cracks in the joint may be caused by slight movement of the wall as it settles. If the mortar contains a good proportion of lime it will harden more slowly and be able to take up these movements without serious cracking.

If strength is required in the mortar then it must contain cement (see Fig. 3.3.1). A mortar of non-hydraulic lime or semi-hydraulic lime and sand will of course stiffen slowly but it will never achieve very much strength.

For heavily loaded brickwork it is usual that the highest possible strength is required, in such cases a cement-sand mortar should be used but great care should be taken in such constructions since the mortar will have poor workability and there is the possibility of trouble arising from shrinkage.

The durability of mortar must be such that it can resist frost and the possibility of contact with soluble sulphates.
Weak lime mortar will easily break down under the repeated action of freezing and thawing, the resistance to frost will be dependent upon the strength of the mortar. The question of resistance to sulphate attack is one that unfortunately often receives the least attention. The easiest solution to the problem is to specify bricks that are free from sulphates for any brickwork that is likely to be damp.

Table No. 3.2.1. indicates the strength and nominal mix requirements for the various mortar grades specified in CP.111.

To assist the designer in his choice of Mortars for various classes of work, degree of exposure and time of construction the Ministry of Public Building and Works have produced Advisory Leaflet No.16 based upon the results of investigations carried out at the Building Research Station. These recommendations for mortar mixes are summarised in Table No.3.2.2.

REQUIREMENTS FOR MORTAR
CP.111

GRADE	Compressive Strength at 28 days (MN/m^2)		Type of Mortar Mix*			
	Preliminary (Laboratory Tests)	Works Tests	Cement: Lime: Sand	Cement: Sand(with Plasti-cizor*)	Masonry Cement: Sand	Hydraulic Lime: Sand
I	16.0	11.0	1:0-¼:3	-	-	-
II	8.0	5.5	1:½:4-4½	1:3-4	1:2½-3½	-
III	4.0	2.75	1:1:5-6	1:5-6	1:4-5	-
IV	1.5	1.0	1:2:8-9	1:7-8	1:5½-6½	1:2-3

* The mortar mixes represent dry materials loosely batched in an approved container and may also be used as a guide to what is required where the works compressive strength is specified

TABLE 3. 2. 1

TABLE NO. 3. 2. 2

MORTARS FOR BRICKWORK

(M.P.B.W. Advisory Leaflet No.16)

	TYPE OF CONSTRUCTION	POSITION IN BUILDING	DEGREE OF EXPOSURE TO WIND AND RAIN	TIME OF CONSTRUCTION	RECOMMENDED MIX
EXTERNAL WALLS Clay bricks Clay Blocks Sand-lime bricks Concrete bricks Concrete blocks	Normal construction not designed to withstand heavy loading	Above damp-proof course	Sheltered and moderate conditions	Spring and summer	1:2:8-9,Cement:lime*:sand, or 1:3,Hydraulic lime:sand
			Sheltered and moderate conditions	Autumn and winter	1:1:5-6,Cement:lime*:sand, or 1:2,Hydraulic lime:sand.
			Severe conditions	All seasons	1:1:5-6,Cement:lime*:sand, or 1:2,Hydraulic lime:sand.
		Parapets,free-standing walls or below damp-proof course	All conditions	All seasons	1:1:5-6,Cement:lime*;sand, or 1:3,Cement:sand.
INTERNAL WALLS (including partitions)	Normal	-	-	Spring and summer	1:2:8-9,Cement:lime":sand 1:3:10-12,Cement:lime":sand,or 1:3,Hydraulic lime:sand.
				Autumn and winter	1:2:8-9,Cement:lime*:sand 1:1:5-6,Cement:lime*;sand,or 1:2,Hydraulic lime:sand.
ENGINEERING CONSTRUCTION Clay bricks over 5,000 lb.sq.in. crushing strength		All positions	All conditions	All seasons	1:3,Cement:sand.

SHELTERED CONDITIONS are where the construction is protected by overhanging eaves or by nearby buildings. Typical examples of these conditions occur with ground and first storeys of buildings in the middle of towns.

MODERATE CONDITIONS refer to those in which the construction gets some protection from overhanging eaves or from nearby buildings.

SEVERE CONDITIONS occur when the construction is exposed to the full force of wind and rain.Typical examples are buildings projecting well above the surrounding buildings,and those on elevated and exposed sites and in coastal districts.

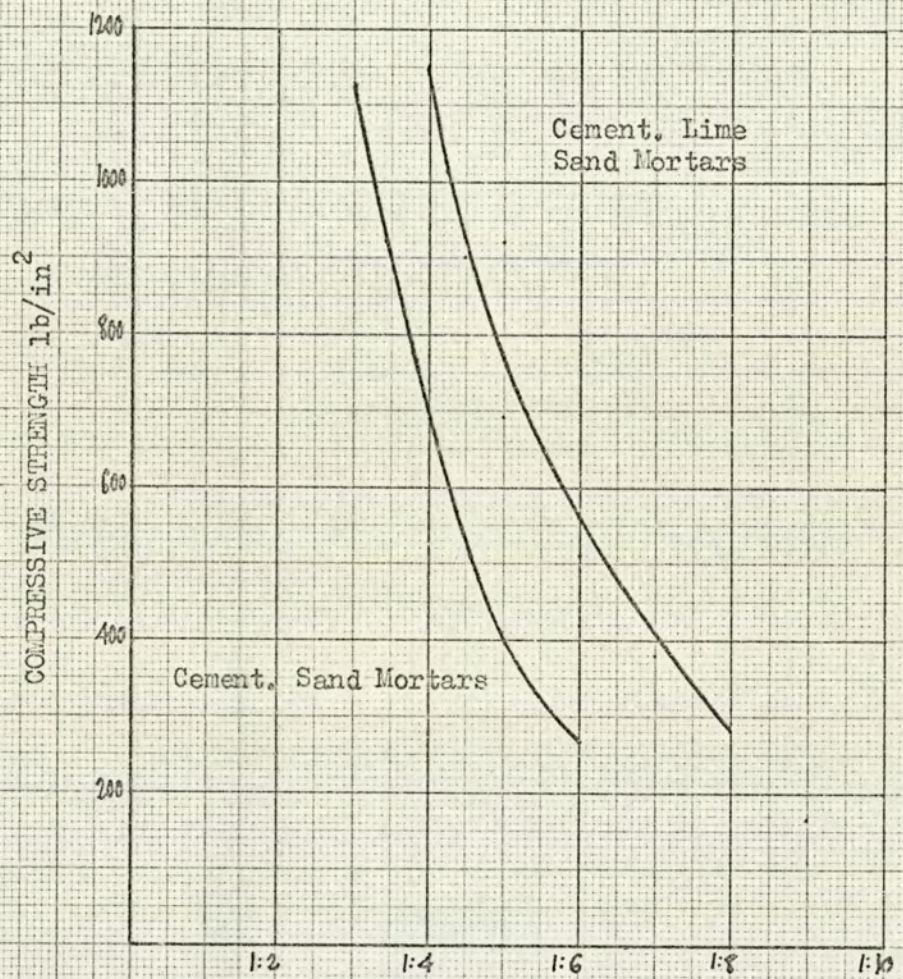

RELATIONSHIP BETWEEN THE 14 DAY COMPRESSIVE STRENGTH OF MORTARS AND THE VOLUME OF CEMENT

FIG. 3.3.1.

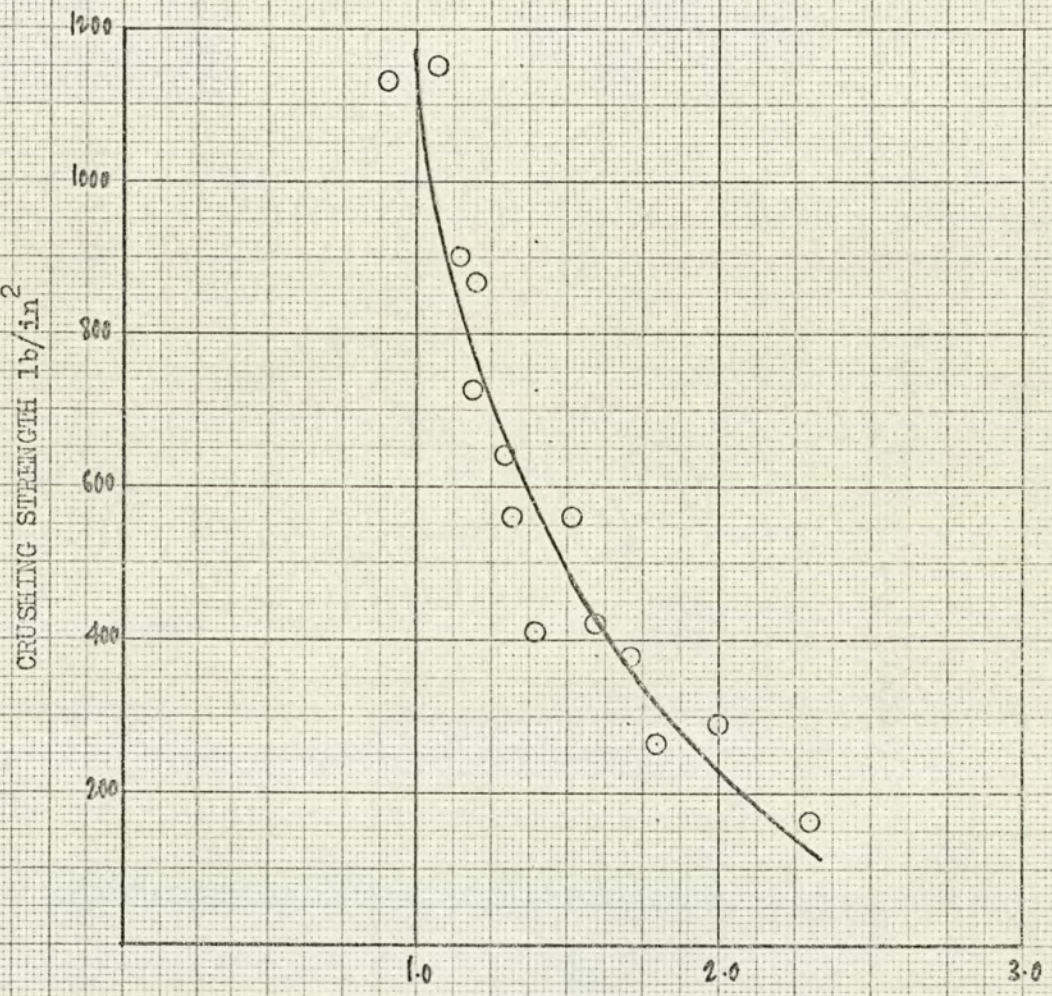

RELATIONSHIP BETWEEN 14 DAY STRENGTH OF 3 INCH CUBES AND WATER/CEMENT RATIO OF VARIOUS MIXES

FIG. 3.3.2.

3.3 The Compressive Strength of Mortar

In the design of load bearing brickwork the permissable stresses are defined in CP.111 relative to the crushing strength of the bricks and the grade of mortar being used.

Table 3.2.1 shows the requirements of CP.111 with respect to minimum 28 day compressive strength for each of the nominal mix mortar grades. These values give a convenient standard of quality control for the particular specified mortars.

The standard method of the determination of the compressive strength of mortar is defined in BS.4551: Part 1. 1970 "Methods of Testing Mortars".

For the purposes of the experimental work related to this thesis it was decided to prepare 4" specimen mortar cubes from locally obtained building sand and ordinary commercial Portland Cement in an attempt to produce specimen representative of those that would be obtained an any well supervised building site.

Cubes of nominal mix 1:0:3 and 1:1:5 cement/lime/sand were made and the bricklayer was allowed to use such amount of mixing water that would produce the correct practical degree of workability. This amount of water was measured and resulted in a water/cement ratio by volume of 1/1.

The specimen cubes were then cured in air and tested at an age of 28 days.

Five cubes of each mortar mix were tested giving the following statistical results:-

1:0:3: Mortar

Crushing Strength Arithmetic Mean	($\bar{X}$)	2890 lb/in^2
Standard Deviation	(S)	243 lb/in^2
Coefficient of Variation	(V)	8.4%

1:1:5: Mortar

Crushing Strength Arithmetic Mean	($\bar{X}$)	925 lb/in^2
Standard Deviation	(S)	15 lb/in^2
Coefficient of Variation	(V)	1.6%

Conclusions:

The crushing strength of mortar is dependent pricipally upon the relative mixtures of the constituent materials and the ratio of water to cement used in the mixing process.

Generally speaking an increase in the volume of cement will result in an increased crushing strength. This relationship is shown in Fig. 3.3.1.

Fig. 3.3.2. shows the relationship between water/cement ratio and mortar crushing strength.

It can be seen that the ratio of 1/1 by volume chosen by the bricklayer for suitable workability produces the best properties for 14 day cube strength.

The specimen mortar cubes gave statistical results of compressive strength much greater than the minimum requirements given for 28 day works test as defined in CP.111.

There was no particular special care taken in the preparation of these specimens since a deliberate attempt was made to reproduce site conditions. It can therefore be concluded that it should be within the capabilities of any well organised site management to produce mortar strengths to the specified requirements of CP.111.

Plates Nos. 3.3.1 and 3.3.2 show 3 of the sample cubes after failure. All cubes failed in this manner which is the classical mode and indicates that the tests were satisfactorily executed.

PLATE 3.3.1

PLATE 3.3.2

3.4 The Tensile Strength of Mortar

CP.111 does not give a specific requirement for the tensile strength of mortar, consequently BS.4551 does not include a standard tensile test. This is not surprising since generally speaking load bearing brickwork structures are designed such that no tensile forces are permitted to exist. However, in such examples as panel walls resisting horizontal wind forces an appreciable tensile stress is often generated in the brickwork, many examples of existing brick retaining walls can only be said to be stable by reason of the ability of the brickwork to sustain a tensile stress due to bending.

Later chapters of this thesis will be dealing with the distribution of stresses in brickwork, for the experimental investigation it will be nec essary to have some knowledge of the tensile strength of brickwork and consequently the tensile strength of mortar.

For these purposes the 'splitting' test was carried out on 4" dia x 8" long mortar cylinders prepared as described in para 3.3 for specimens of 1.0.3 and 1.1.5 cement/lime/sand nominal mixes.

Specimen cylinders were tested in a DENISON compression testing machine, the load being applied through 12 mm wide x 3 mm thick plywood strips.

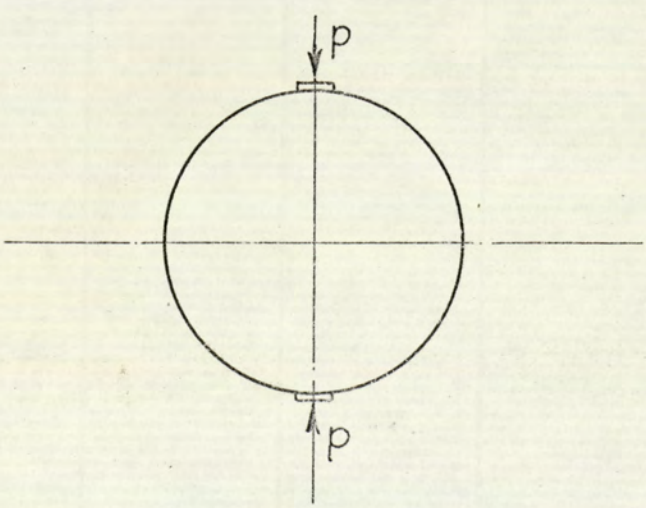

The load was applied steadily without shock and increased continuously until the specimen failed.

All specimens failed on a vertical axis in a line passing through the centre of the specimen.

The indirect tensile strength (ft) of each specimen was then calculated from:-

$$ft = \frac{2P}{\pi . d . l}$$

where d = 4" the diameter of the specimen

l = 8" the length of the specimen

P = the failure load

Specimen No.	1: 0: 3:		1: 1: 5:	
	P(Tons)	ft.(lb/in^2)	P(Tons)	ft(lb/in^2)
1	7.45	332	3.36	150
2	7.73	344	5.10	227
3	6.00	268	4.84	216
4	6.50	290	3.85	172
5	6.40	286	4.66	208
6	7.25	323	3.55	158

Giving the following statistical results:-

1: 0: 3: Mortar

Tensile Strength Arithmetic Mean	($\bar{X}$)	307 lb/in^2
Standard Deviation	(S)	30 lb/in^2
Coefficient of Variation	(V)	9.8%

1: 1: 5: Mortar

Tensile Strength Arithmetic Mean	($\bar{X}$)	180 lb/in^2
Standard Deviation	(S)	34 lb/in^2
Coefficient of Variat ion	(V)	18.9%

3.5 Tests to Obtain the Value of Modulus of Elasticity for Mortar

Specimen cylinders 4" dia x 8" long were prepared from 1. 0. 3 and 1. 1. 5 cement, lime, sand mortar using a water cement ratio of 1:1 By Volume. The specimens were cured in air and tested at an age of 32 days.

Demec points were attached to opposite sides of the specimen and parallel to its axis set to a gauge length of 4" in such a way that the gauge points were symmetrical about the middle of the specimen.

The specimen was placed in the testing machine and its axis carefully aligned with the centre of thrust of the spherically seated platen. No packing other than auxillary steel platens were used between the ends of the specimen and the platens of the testing machine.

The average crushing strength of the mortar mixes had been established by previous crushing tests on 4" cubes. The value (C) given in the following descriptions being one third of the average crushing strength.

Preliminary loading

The load was applied without shock and increased continuously until an average stress of (C + 290) lb/in^2 was reached. The load was maintained at this figure for one minute and then reduced gradually to an average stress of 145 lb/in^2 when Demec gauge readings were taken.

The load was then applied a second time until an average stress of (C + 145) lb/in^2 was reached.

The load was maintained at this figure whilst Demec gauge readings were taken and then gradually reduced to an average stress of 145 lb/in^2 and Demec gauge readings again taken.

Loading:

The load was then applied a third time and Demec gauge readings taken at ten approximately equal increments of stress up to an average of (C + 145) lb/in^2. Gauge readings were taken at each increment of loading. If the average strains observed on the second and third loadings had differed by more than 5% the loading cycle would have been repeated until the difference in strain between consecutive readings at (C + 145) lb/in^2 did not exceed 5%.

The method of testing described above was taken from BS.1881: Part 5: 1970 'Methods of Testing Concrete'.

Calculation:

The strains at the various stages of loading in the last cycle were calculated separately for each gauge and the results plotted against the corresponding load. Straight lines were then drawn through the points plotted for each gauge (Figs. 3.5.1 and 3.5.2). The slope of these two lines was determined and the average value found. The individual values for the slopes were found to differ by less than 15% of the average value, this average value was therefore recorded as the Modulus of Elasticity of the Mortar.

TESTING SEQUENCE:

	1. 0. 3	1. 1. 5
Average Crushing Strength lb/in^2	2890	925
C = $\frac{1}{3}$ Average Crushing Strength	963	309
Preliminary Loading		
(C + 290) lb/in^2	1253	599
i.e TOTAL LOAD (TONS) on 12.59 in^2	7.10	3.40
HOLD FOR 1 MINUTE		
Reduce load to 145 lb/in^2		
i.e TOTAL LOAD (TONS)	0.80	0.80
Take Strain readings.		
Second Cycle loading		
Apply load to (C + 145) lb/in^2		
i.e TOTAL LOAD (TONS)	6.2	2.5
Take Strain readings		
Reduce load to 145 lb/in^2		
i.e TOTAL LOAD (TONS)	0.80	0.80
Third Cycle loading		
Apply load in 10 equal increments up to (C + 145 lb/in^2)		
i.e TOTAL LOAD (TONS)	6.2	2.5

1. O. 3. MORTAR	LOAD TONS	STRAIN x 10^{-5}	
		FACE A	FACE B
PRE-LOAD	0.8	0	0
(Second Cycle)	6.2	63	48
(Third Cycle)	0.8	0	2
	1.4	12	4
	2.0	18	10
	2.6	24	12
	3.2	29	18
	3.8	39	24
	4.4	47	32
	5.0	50	38
	5.6	55	42
	6.2	66	46
	6.8	70	54

1. 1. 5. MORTAR	LOAD TONS	STRAIN x 10^{-5}	
		FACE A	FACE B
PRE-LOAD	0.8	0	0
(Second Cycle)	2.5	49	47
(Third Cycle)	0.8	10	8
	1.0	12	10
	1.2	20	16
	1.4	24	26
	1.6	34	30
	1.8	41	34
	2.0	46	40
	2.2	50	46
	2.4	60	52
	2.6	64	62

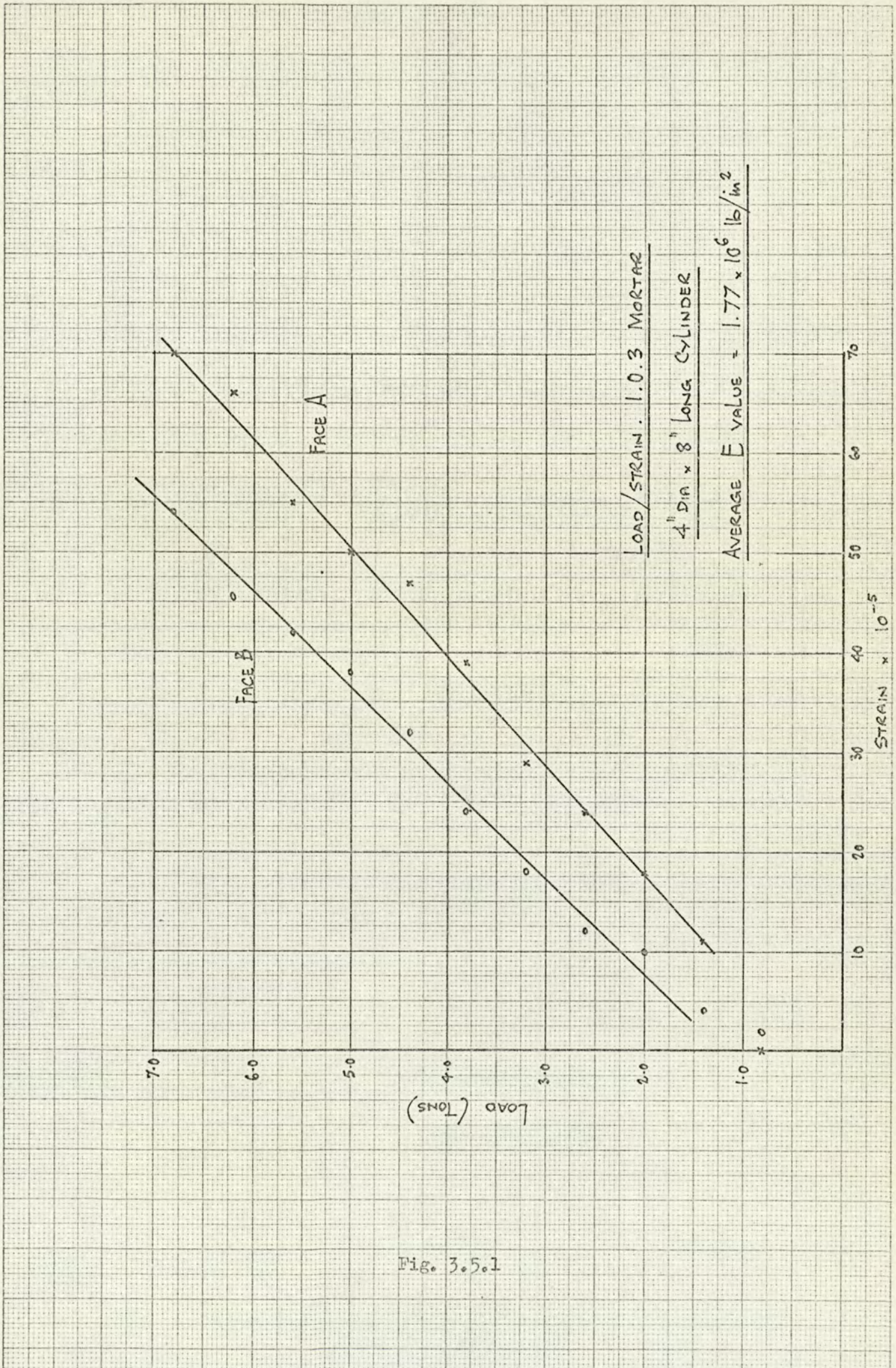
LOAD/STRAIN. 1.0.3 MORTAR
4" DIA x 8" LONG CYLINDER
AVERAGE E VALUE = 1.77 x 10^6 lb/in^2
FACE A
FACE B
LOAD (TONS)
STRAIN x 10^-5
7·0
6·0
5·0
4·0
3·0
2·0
1·0
10
20
30
40
50
60
70

Fig. 3.5.1

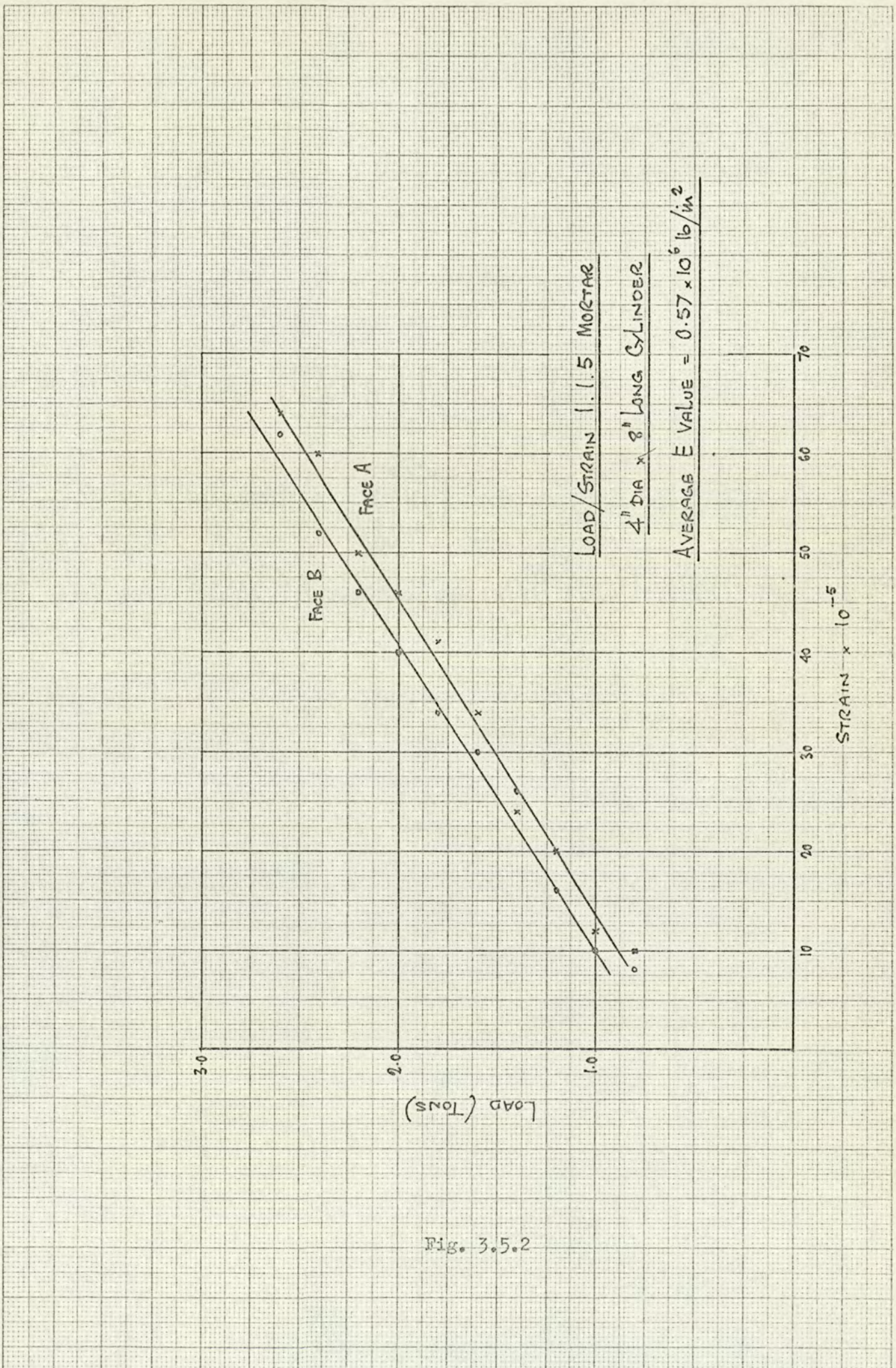
LOAD/STRAIN 1:1.5 MORTAR
4" DIA x 8" LONG CYLINDER
AVERAGE E VALUE = 0.57 x 10⁶ lb/in²
FACE A
FACE B
LOAD (Tons)
STRAIN x 10⁻⁵
1.0
2.0
3.0
10
20
30
40
50
60
70

Fig. 3.5.2

CHAPTER 4

THE BOND OF MORTAR TO BRICK

4.1 Introduction

Factors affecting bond strength include brick absorption, texture of contact surfaces, mortar consistency, workability and water retention.

Bond is obtained by the ability of the mortar to flow into the interstices and irregularities of the brick. To do this, it must be capable of being squeezed out when the upper brick is placed upon it. The ability to be squeezed out is dependent principally on the brick absorption, the water retention and the consistency of the mortar.

By definition, a cement is an adhesive which is used in a plastic form and hardens to bond together various solid surfaces.

Adhesion is the molecular attraction exerted between the surfaces of bodies in contact.

Cohesion is the molecular attraction by which the particles of a body are united throughout the mass, whether like or unlike.

Bond is a term used to describe the extent of contact between a mortar and brick.

For a Portland cement mortar the bond results principally from mechanical key.

The properties of the brick that have the greatest effect on bond are the initial rate of absorption (suction) and the texture of the surfaces in contact with the mortar.

The approximate relationship of bond strength to brick initial absorption is shown in Fig. 4.1.1. taken from ASTM Special Technical Publication No. 320.

4.2 The Theory of Adhesives

The prevailing theories on how adhesives function can be applied to the adhesion of portland cement to itself (cohesion) and to other surfaces (adhesion).

The valence electrons in the outer shell of the atom are the forces that bond the atoms together to form the molecules (electrostatic and covalent bonds). In an electrostatic bond the valence electrons are transferred from one atom to another. The charge on one atom is decreased and the charge on the other is increased by the same amount, resulting in no change in the charge of the molecule. In a covalent bond each atom contributes one electron and the pair are shared equally, again resulting in no change in charge. However, there are a group of compounds which have neither true electrostatic nor covalent bonds. Since the pair of shared electrons are closer to one atom than to the other, this results in a greater negative charge on one and a greater positive charge on the other.

This type of bond is known as a polar covalent bond. Such substances (called polar compounds) are used as adhesives. Portland cement is a similar compound. It is reasonable to assume therefore, that these forces account for the adhesive and cohesive strength of the mortar.

The strength of these forces vary inversely with the cube of the distance. Any material which increases these distances reduces these forces and consequently the strength of the mortar. Sand, water, air and lime have such an effect.

The forces of adhesion are similar to those of cohesion except for the additional factor of mechanical key. The surfaces of bricks have numerous voids, cracks and fissures into which the mortar can flow. The cohesive forces between the mortar in the surface voids and the mortar outside these voids produce an increase in bond strength.

For an organic type mortar (such as an epoxy resin mortar) the bond strength results principally from the intermolecular forces.

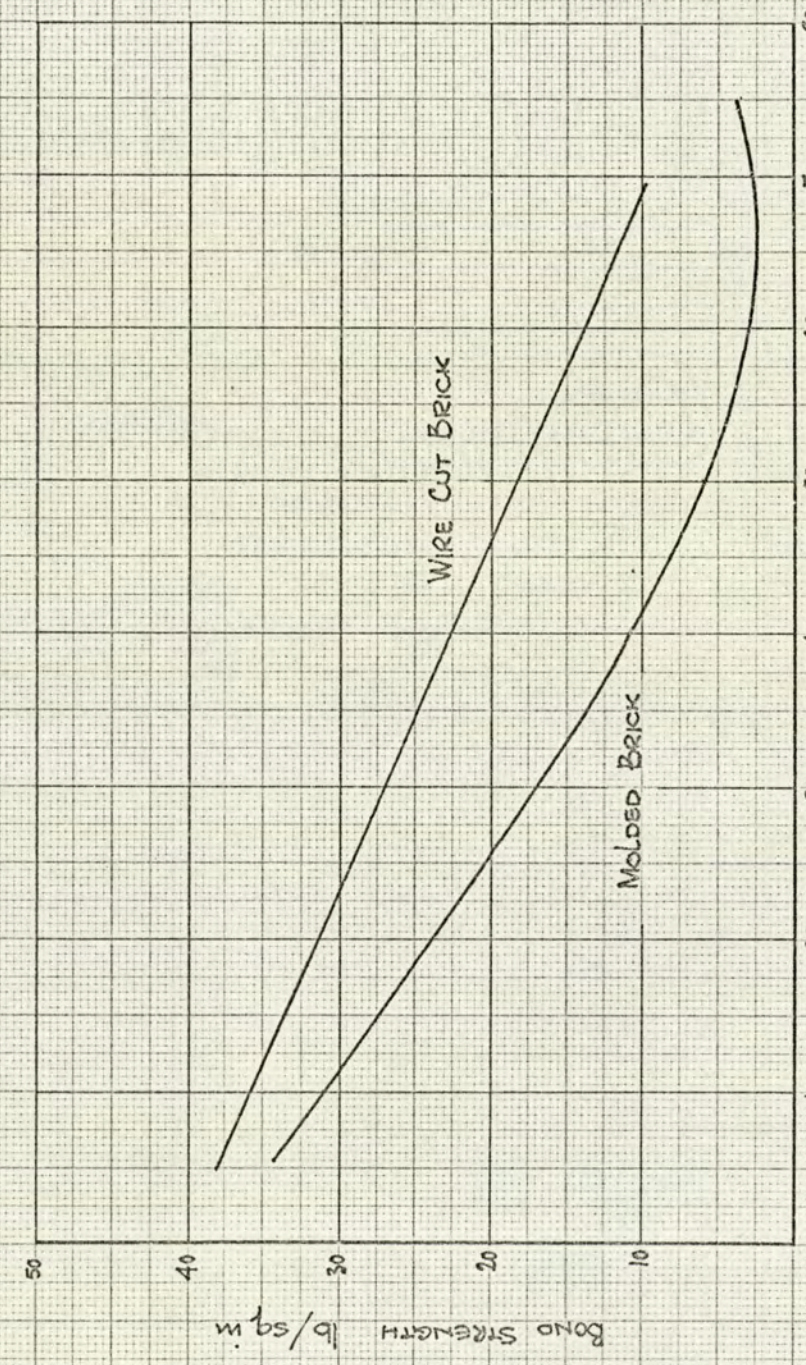
Bond Strength lb/sq in
50
40
30
20
10
Wire Cut Brick
Molded Brick
10
20
30
40
50
60
70
80
Initial Rate of Absorption (Suction) G = Grams of Water per 30 sq ins.
When Immersed in 1/8" of Water for 60 Secs.

Fig.4.1.1

4.3 The Tensile Bond Strength of Mortar to Brick

Experimental work carried out to investigate the flexural strength of brickwork resulted without exception in failure due to a breakdown in the bond between bricks and mortar.

The factors affecting bond strength have previously been stated. By reason of the number of parameters, a general value for bond strength cannot be given to cover the wide range of materials available to the designer.

CP.111 states that in special cases tensile stress in bending may be taken into account at the discretion of the designer. In such cases the wall should be built with units prepared before laying according to CP.121.101. For mortar not weaker than Grade III other than plasticised mortar or masonry cement mortar, the permissable tensile stress in bending should not exceed 0.07 MN/m^2 (10 lb/in^2) when the direction of this stress is at right angles to the bed joints and should not exceed 0.14 MN/m^2 (20 lb/in^2) when the direction of tensile stress is as right angles to the perpend joint. The higher value should not be used where the crushing strength of the unit is less than 10.5 MN/m^2 (1500 lb/in^2).

The above values are presumably based upon the results of experimental work and the higher value of tensile stress should be applied only to brickwork in blockwork walls consisting of squared units built to horizontal courses, with broken vertical joints.

If ultimate loads are to be predicted and they are dependent upon the bond strength then the bond strength of the mortar and brick being used in any particular application must be known.

The values for working stress given in CP.111 to be applied generally to all bricks without limitation other than a minimum crushing strength may well in fact be dangerous on the one hand or even very conservative on the other hand.

A simple test was therefore designed in order that the tensile bond strength could be easily measured without the necessity of complicated clamping arrangements to apply a direct tensile force to the brick or mortar.

Sample brick couplets were prepared each with a $\frac{3}{8}$" mortar joint, the longitudinal axes of the bricks being arranged at 90° to give an effective bed face of $4\frac{1}{8}$" x $4\frac{1}{8}$".

The use of the steel jig shown in Plate No. 4.3.1 applied a tensile force to the mortar joint when the assembled jig was subjected to a compressive load.

PLATE 4.3.1

In consideration of the magnitude of the ultimate loads it can be assumed that the mortar joint is in direct tension only and by reason of the very small deflections in the brick the stresses due to bending can be neglected and the brick considered to be in a state of shear only.

The London Common Brick previously described was used for all tests and mortar type 1: 0: 3: and 1: 1: 5: cement/lime/sand were investigated. All specimens were tested at an age of 28 days.

	1: 1: 5: Mortar		1: 0: 3: Mortar	
Specimen No.	Failure Load tons	Ultimate Stress lb/in^2	Failure Load tons	Ultimate Stress lb/in^2
1	0.373	49	0.397	52
2	0.385	51	0.342	45
3	0.290	38	0.377	50
4	0.279	37	0.400	53
5	0.234	31	0.435	57
6	0.321	42	0.277	36
7	0.379	50	0.386	51
8	0.346	46	0.464	61
9	0.276	36	0.294	39
10	0.398	52	0.426	56
11	0.213	28	0.527	69
12	0.497	65	0.380	50

GIVING THE FOLLOWING STATISTICAL RESULTS:

1: 1: 5: Mortar

Arithmetic mean ($\bar{x}$)	44 lb/in^2
Standard Deviation (S)	10.4 lb/in^2
Coefficient of Variation (V)	23.8%

1: 0: 3: Mortar

Arithmetic Mean ($\bar{x}$)	52 lb/in^2
Standard Deviation (S)	9 lb/in^2
Coefficient of Variation (V)	17.3%

Conclusions:

The statistical results indicate a load factor of 4.4 for 1.1.5 mortar and 5.2 for 1.0.3. mortar when compared with the lower value of tensile stress specified in CP.111.

The coefficient of Variation is high and from the consideration that the specimens were carefully prepared to give full mortar joints in each case (whereas on practical building sites this condition is rarely achieved) it must be concluded that special supervision must be given to brickwork that is designed to resist tensile bending stresses.

The values of tensile bond strength obtained from the tests represent a bond strength of 12.8% of the brick tensile strength and a bond strength of 24.5% and 16.9% of the tensile strength of 1.1.5 mortar and 1.0.3. respectively.

It can therefore be expected that in any brickwork flexural strength or tensile strength test using London Common Pressed Clay bricks, failure of the specimen will be by a breakdown in the bond of mortar to brick.

CHAPTER 5

THE MODULUS OF ELASTICITY OF BRICKWORK

5.1 Introduction

In the design of load-bearing brickwork structures the engineer must be aware not only of the compressive, tensile and shear strength of the bricks and mortar being used, he must also have an accurate knowledge of the Modulus of Elasticity of the assembled brickwork.

Particular problems occur when different strength bricks are used in the same structure; for example if the E value of the two leaves of a cavity wall supporting a concrete slab are different then the load will not be shared equally between the two leaves.
A wall with a high E value will deflect less than a wall with a low E value.
A wall supported on a beam will impose a greater load on the beam if it has a low E value rather than a high E value.
Further problems arise when framed steel or concrete buildings are erected with brickwork in-fill panels, the distribution of load into the in-fill panel will be dependent upon the E value of the brickwork.

It must further be noted that the value of the Modulus of Elasticity of the brickwork will vary with the direction of principal stress being considered.

Modulus of Elasticity by definition is the relationship of normal stress to corresponding strain.
For perfectly elastic materials this value is constant throughout the stress range, i.e. the stress/strain relationship is linear.

Brickwork is not a perfectly elastic material and in common with other imperfect materials will creep under load. The higher the load the greater the creep. Therefore, the stress strain relationship will not be linear and the ratio of stress to strain will vary according to the value of the stress i.e. according to the point at which the slope is measured so does the value of E differ.

However, the value of E at any point on the stress/strain curve will be directly dependent upon the individual values of E for the bricks and mortar in the assemblage.

5.2 The Presentation of the Modulus of Elasticity

There are four methods (Fig. 5.2.1) in general use for presenting the Modulus of Elasticity value when considering a non-linear stress/strain relationship:

(a) The Initial Tangent Modulus:

The slope of the curve is taken at zero stress and consequently zero creep.

(b) The Chord Modulus:

A chord is drawn between 2 selected stress values and the slope of the chord is calculated.

(c) The Tangent Modulus:

The slope of the tangent to the stress/strain curve is measured at the selected stress.

(d) The Secant Modulus:

The slope of a straight line joining the points of zero stress to design stress.

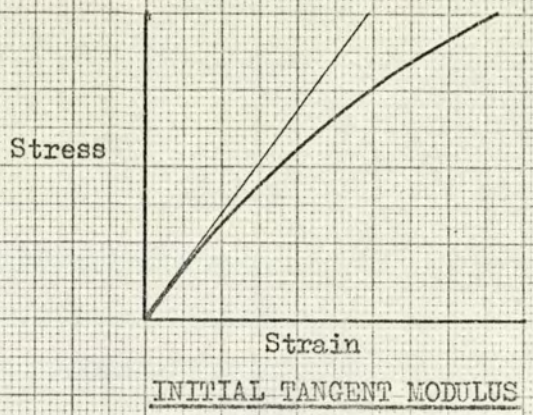

INITIAL TANGENT MODULUS

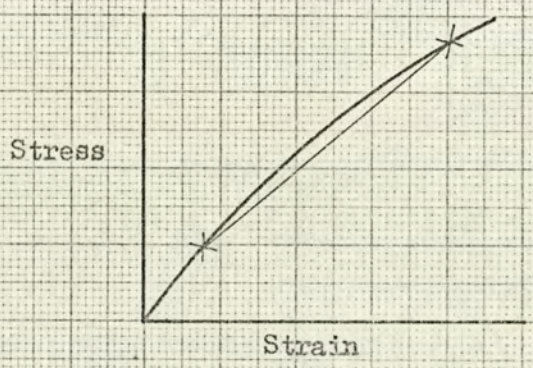

CHORD MODULUS

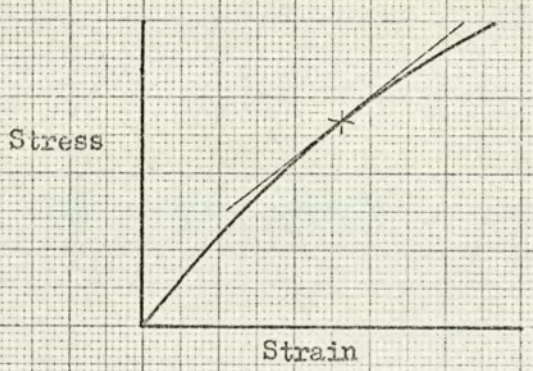

TANGENT MODULUS

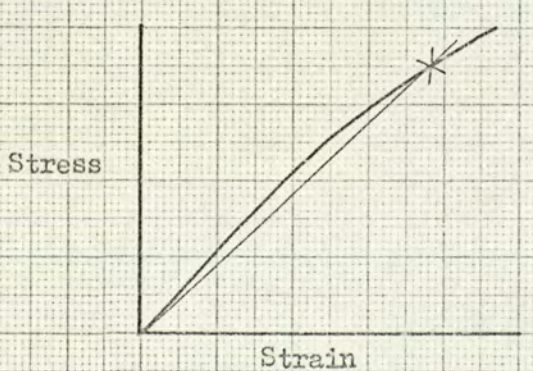

SECANT MODULUS

FIG. 5.2.1.

5.3 The Value of Young's Modulus for Brickwork

The value of Young's Modulus of brickwork is dependent upon the physical properties of the constituent materials in the assemblage. Fig. 5.3.1 shows that there is almost a linear relationship between the brickwork strength and the value of Young's Modulus.

From the existing Codes of Practice the designer is unable to obtain any direct information with respect to the value of Young's Modulus to be used in the design of calculated loadbearing brickwork. In fact, Young's Modulus is not referred to in CP.111 for conditions other than reinforced brickwork where the modular ratio, i.e. the ratio of elastic modulus of steel to that of the brickwork, is given in tabular form relative to the average compressive strength of the brick for Mortar grades I, II and III. It seems likely that in the absence of other design data Engineers will use the above information to obtain a value of E for use in the preparation of their calculations.

Fig. 5.3.2 shows the relationship of Young's Modulus for brickwork to brick strength calculated from the modular ratio values given in CP.111 on the basis that E steel = 200 MN/m^2 (29 x 10^6 lb/in^2).

A comparison of these results with those obtained by experiment indicates that the authors of CP.111 have taken no account of creep.
To predict the deflection in brickwork, it is not sufficient simply to consider the instantaneous deflection since some allowance must be made for deflections due to creep with the ageing of the brickwork.

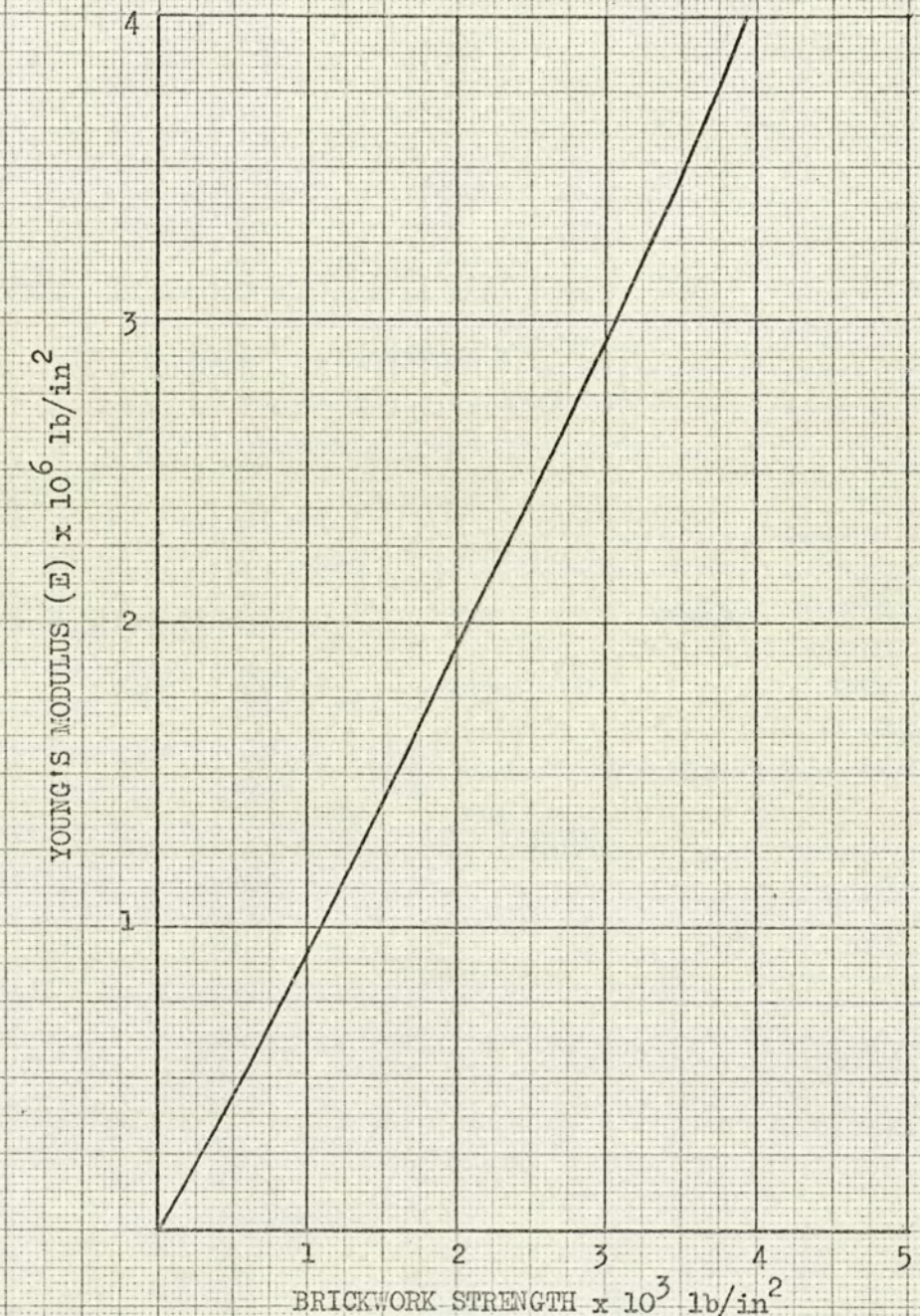

YOUNG'S MODULUS OF BRICKWORK versus BRICKWORK STRENGTH

FIG 5.3.1.

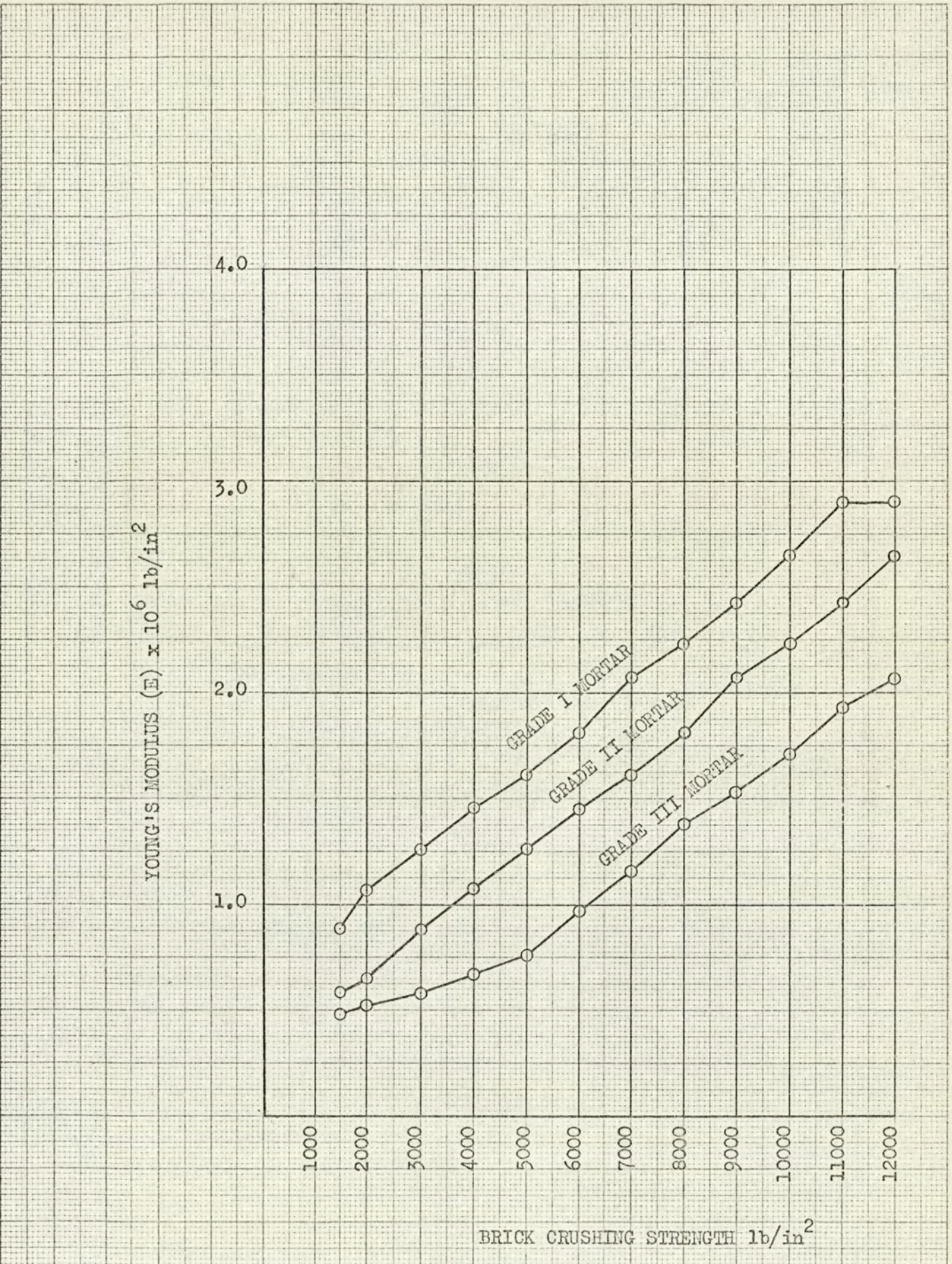

The Relationship of Young's Modulus for Brickwork to Brick Crushing Strength calculated from CP.111

Fig. 5.3.2

5.4 Creep in Brickwork

Brickwork being an imperfect material will creep when subjected to a load, consequently there will be an increase in strain without a change in stress.

The value of this increase in strain will be dependent upon the difference in time between loading the specimen and measuring the strain. It can therefore be reasonably concluded that the value of E will decrease as time increases. Since brickwork structures are designed to last a number of years it is the effective Modulus of Elasticity after x years that the engineer should consider when calculating the deflection of walls under load.

The factors that will influence the magnitude of creep in brickwork are:-

(a) The stress history

(b) The properties of the sand

(c) The air humidity

(d) The properties of the brick

(e) The proportions of the mortar mix

(f) The ability of the mortar to retain moisture after absorption of moisture from the mortar by the brick

From previous work[4] on concrete and mortar it is suggested that the creep of brickwork will be approximately $\frac{1}{4}$ to 1/5 that of concrete under similar circumstances.

Assuming that the brickwork will be stressed according to CP.111, the strain can be calculated using the known E value of the brickwork.

The value for creep will vary according to the actual strength of the brickwork, it will also vary according to the stress therein. Having regard to the degree of accuracy involved in obtaining the value of Young's Modulus and other information in the calculation, it is suggested[4] that a value of 100×10^{-6} for creep strain after 10 years would apply to all

all strengths of brickwork when stressed to the limiting value as specified in Table 3.1 of CP.111.

By adding the two strains, the effective value for E after 10 years can be calculated.

Figures 5.4.1, 5.4.2 and 5.4.3 show the relationship of Young's Modulus to Brick Strength for Mortar Grades I, II and III when the above allowance for creep strain has been included.

For comparison, the values calculated previously and shown in Fig.5.3.2 have again been included.

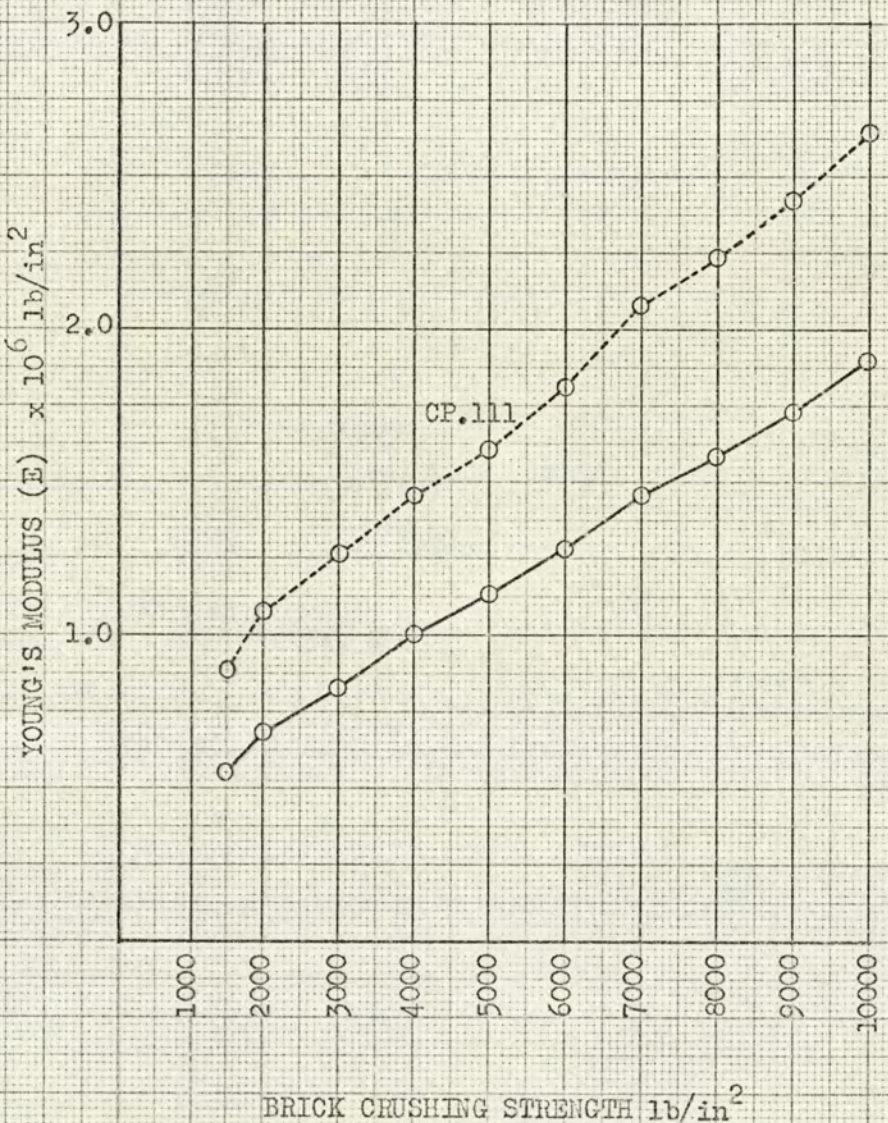

THE RELATIONSHIP OF YOUNG'S MODULUS FOR BRICKWORK TO BRICK CRUSHING STRENGTH INCLUDING ALLOWANCE FOR CREEP

GRADE I MORTAR

Fig.5.4.1

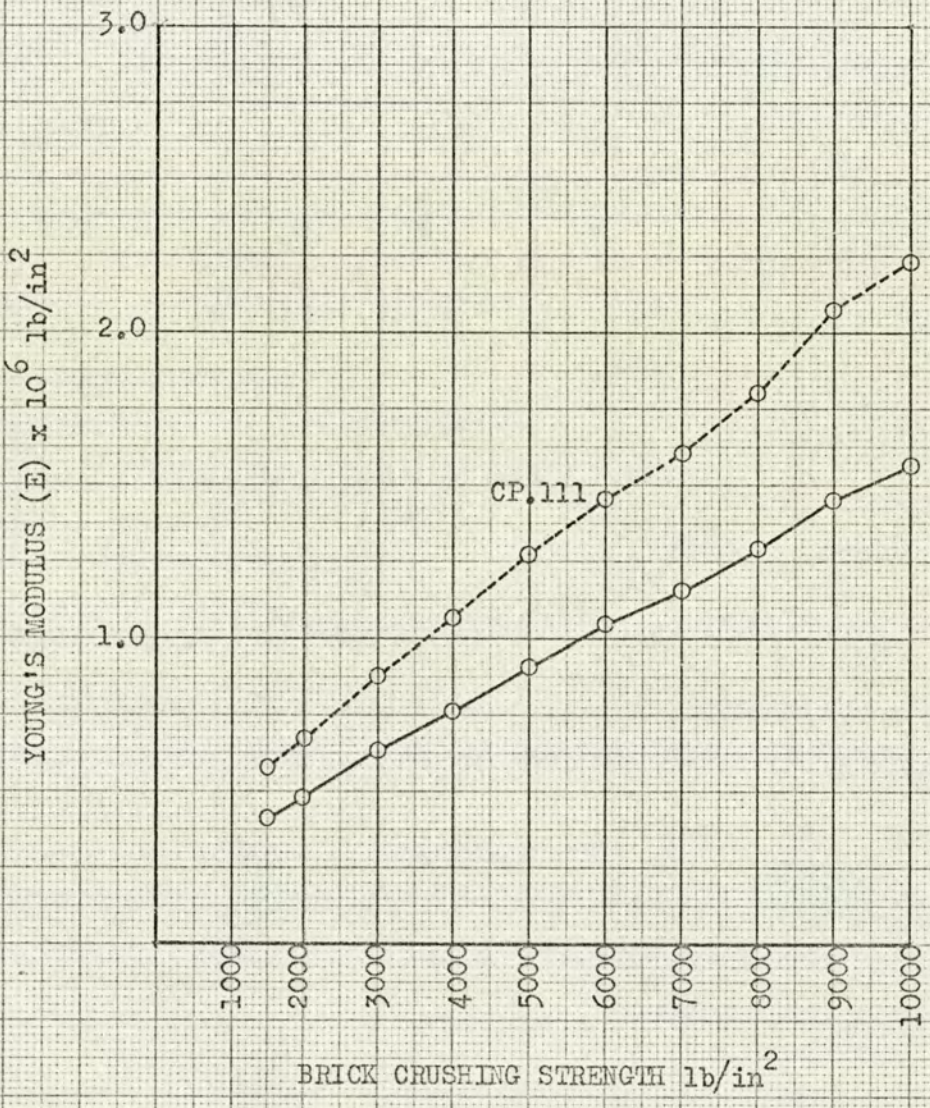

THE RELATIONSHIP OF YOUNG'S MODULUS FOR BRICKWORK TO BRICK CRUSHING STRENGTH INCLUDING ALLOWANCE FOR CREEP

GRADE II MORTAR

Fig.5.4.2

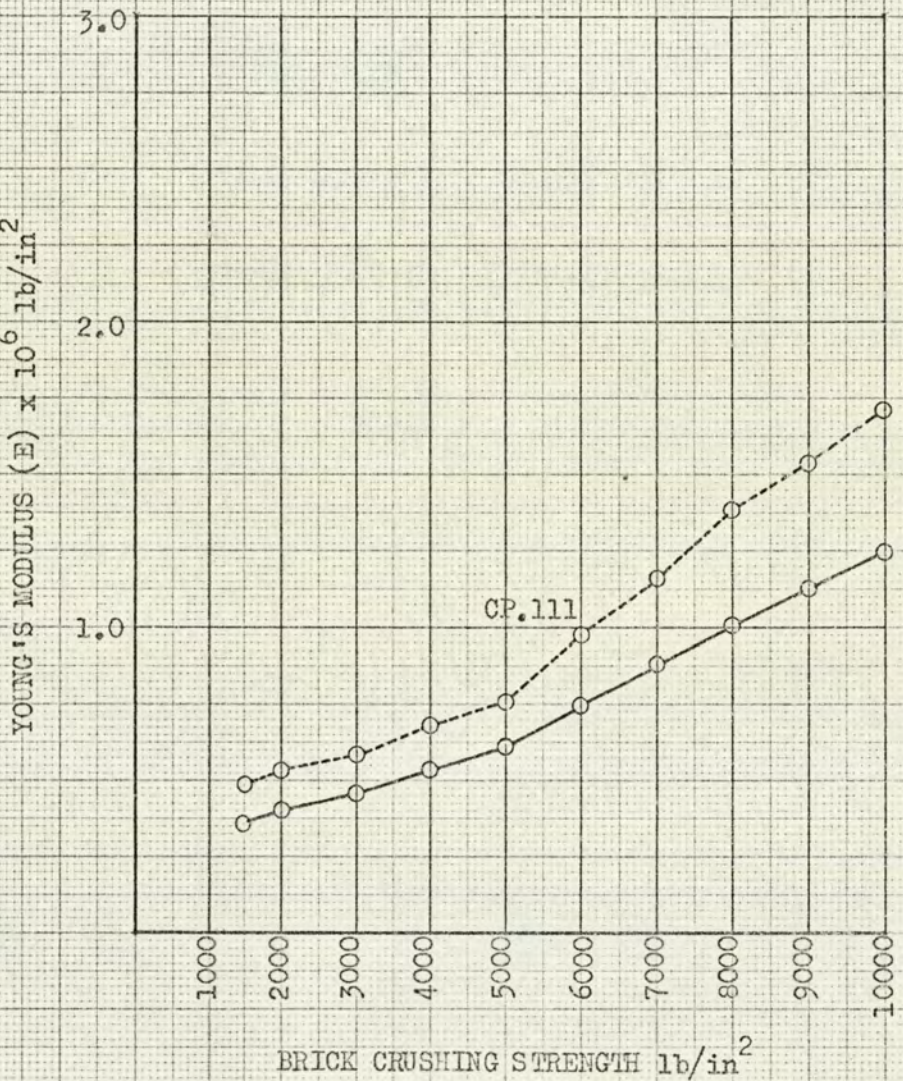

THE RELATIONSHIP OF YOUNG'S MODULUS FOR BRICKWORK

TO BRICK CRUSHING STRENGTH INCLUDING ALLOWANCE FOR CREEP

GRADE III MORTAR

Fig.5.4.3

5.5 The Relationships between the Modulus of Elasticity of Brickwork, Bricks and Mortar

It has been previously shown that the value of Young's Modulus for brickwork is related to the crushing strength of the brickwork which in turn is dependent upon the strength of the bricks and mortar that constitute the assemblage.

These relationships can be conveniently shown in a simple mathematical form where:-

Em = Modulus of Elasticity of Mortar

Eb = Modulus of Elasticity of Brickwork

tm = thickness of mortar joint

tb = thickness of brick

l = length of brick

em = strain in mortar in direction of load

eb = strain in brick in direction of load

ebwk = strain in brickwork in direction of load

σ = compressive stress in brick and mortar bed joint

Consider a specimen assemblage made up from one brick and one mortar joint

5.5.1 In a Direction at Right Angles to the Bed Joints

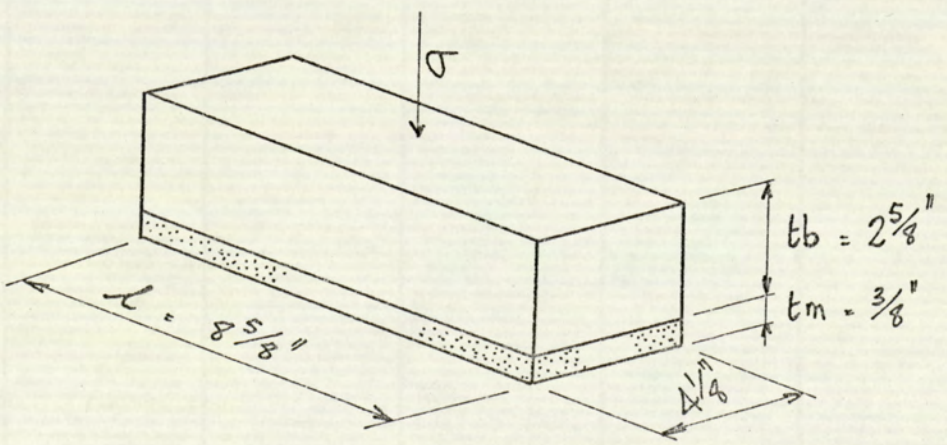

$tm + tb = \frac{3}{8}" + 2\frac{5}{8}" = 3"$

$em = \frac{\text{Vertical deflection in mortar bed joint}}{\frac{3}{8}"}$

$eb = \frac{\text{Vertical deflection in brick}}{2\frac{5}{8}"}$

$ebwk = \frac{\text{Vertical deflection in one brick + joint}}{3"}$

The vertical deflection in one brick and joint $= 3\ ebwk$

$= 2\frac{5}{8}\ eb + \frac{3}{8}\ em$

$\therefore ebwk = \frac{2\frac{5}{8}\ eb + \frac{3}{8}\ em}{3}$

$= \frac{7}{8}\ eb + \frac{em}{8}$

$Ebwk = \frac{\sigma}{ebwk} = \frac{8\sigma}{7eb + em}$

$= \frac{8\sigma}{\frac{7\sigma}{Eb} + \frac{\sigma}{Em}}$

$\therefore Ebwk = \frac{8.Eb.Em}{7\ Em + Eb}$

5.5.2. In a Direction at Right Angles to the Perpend Joints

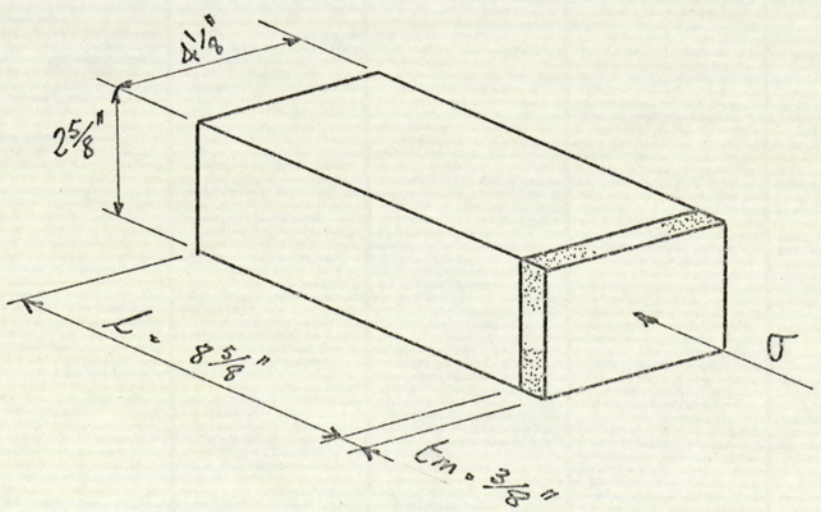

$tm + l = \frac{3}{8} + 8\frac{5}{8} = 9"$

The vertical deflection in one brick and joint = 9 ebwk

$= 8\frac{5}{8}\ eb + \frac{3}{8}\ em$

$$\therefore \text{ebwk} = \frac{8\frac{5}{8}\ eb + \frac{3}{8}\ em}{9}$$

$$= \frac{23}{24}\ eb + \frac{em}{24}$$

$$Ebwk = \frac{\sigma}{ebwk} = \frac{24\ \sigma}{23\ eb + em}$$

$$= \frac{24\ \sigma}{\frac{23\sigma}{Eb} + \frac{\sigma}{Em}}$$

$$\therefore Ebwk = \frac{24\ Eb.Em}{23\ Em + Eb}$$

The above calculations show that the Modulus of Elasticity of Brickwork when considering load in a direction at right angles to the bed joint will have a value different to that when considering load in a direction at right angles to the perpend joint.

It can be seen that for the case when Eb = Em producing a 'homogeneous ' spec imen the equations reduce to give a value of Modulus of Elasticity equal in both directions.

5.5.3. Theoretical curves (Figs. 5.5.1 and 5.5.2) can now be drawn showing the relationship of $\frac{Em}{Eb}$ to $\frac{Ebwk}{Eb}$

(a) Considering the condition at right angles to the perpend joints

$$k = \frac{Em}{Eb} \quad \therefore Em = k\ Eb$$

$$Ebwk = \frac{24\ Eb\ Em}{23\ Em + Eb}$$

$$\frac{Ebwk}{Eb} = \frac{24\ E\ m}{23\ Em + Eb}$$

$$= \frac{24\ k\ Eb}{23\ k\ Eb + Eb} = \frac{24\ k}{23k + 1}$$

(b) Considering condition at right angles to the bed joint similarly to 5.5.3(a)

$$\frac{Ebwk}{Eb} = \frac{8\,k}{7k + 1}$$

5.5.4 Conclusions

Figs. 5.5.1 and 5.5.2 show the calculated relationships between the values of Young's Modulus for brickwork, bricks and mortar. These figures clearly show brickwork to be anisotropic.

However, the maximum difference for the value of Young's Modulus for brickwork when measured at right angles to the bed joints and when measured at right angles to the perpend joints is 0.25 Eb when the value of Em/Eb is 0.10, when the value of Em/Eb is greater than 8 the difference in E values remains very nearly constant.

Further consideration must also be given to the possible coefficient of variation that can occur between a number of measured specimens each made up from identical materials and the unknown variables than can exist.

Within the range of materials normally used for loadbearing brickwork it can be concluded that calculations involving the value of Young's Modulus for brickwork can be carried out with sufficient accuracy for all practical design purposes on the assumption that brickwork is isotropic.

From the equations obtained for Ebwk the following values were calculated for brickwork constructed with pressed clay frogless Flettons supplied by The London Brick Co. Ltd.

1. In a direction at right angles to the bed joints

1.0.3. Mortar mix Ebwk = 1.30×10^6 lb/in^2

1.1.5. Mortar Mix Ebwk = 1.09×10^6 lb/in^2

2. In a direction at right angles to the perpend joints

1.0.3. Mortar Mix	$E_{bwk} = 1.27 \times 10^6$ lb/in^2
1.1.5. Mortar Mix	$E_{bwk} = 1.19 \times 10^6$ lb/in^2

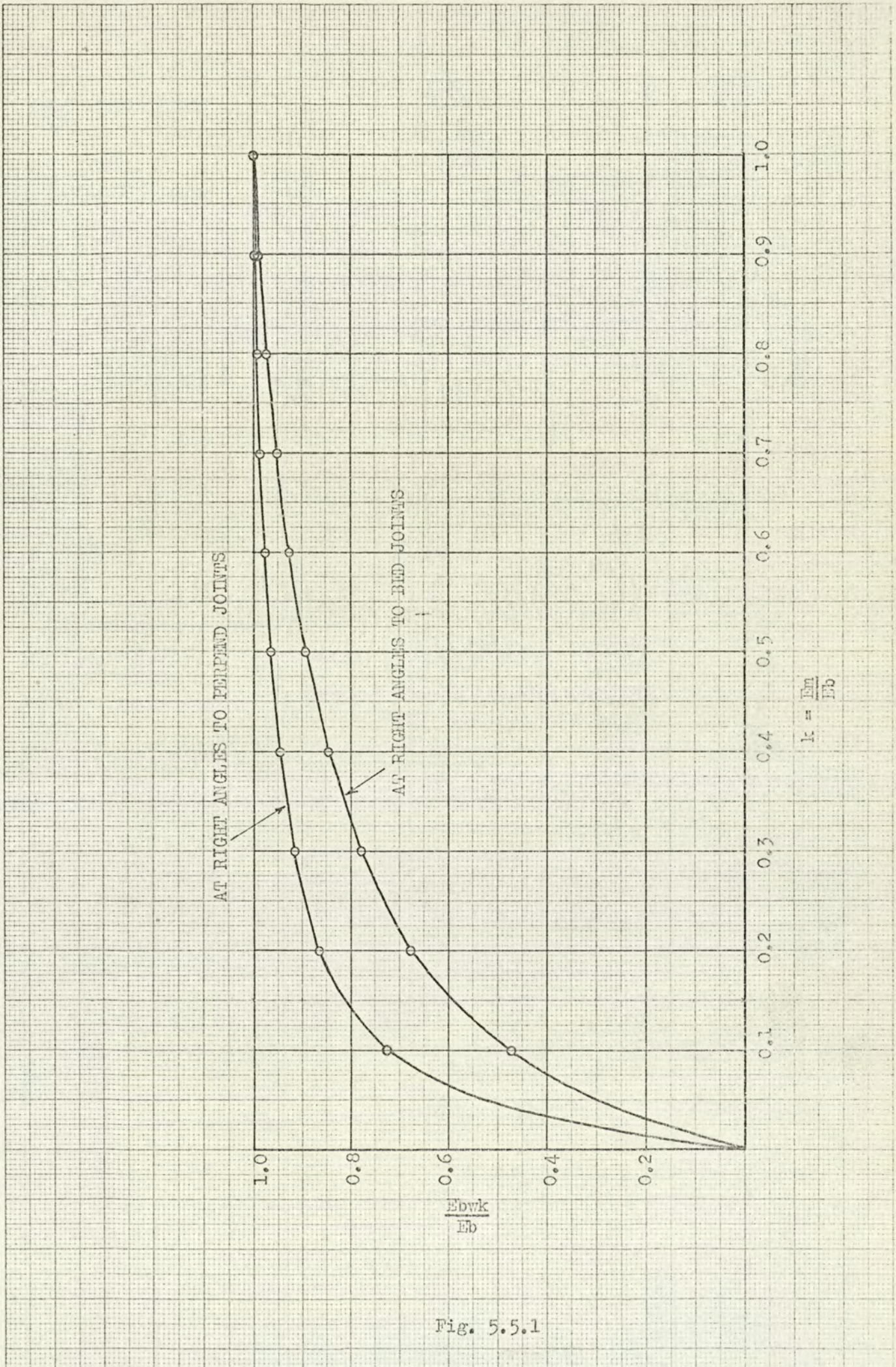
AT RIGHT ANGLES TO PERPEND JOINTS
AT RIGHT ANGLES TO BED JOINTS
1.0
0.8
0.6
0.4
0.2
Ebwk / Eb
0.1
0.2
0.3
0.4
0.5
0.6
0.7
0.8
0.9
1.0
k = Em / Eb

Fig. 5.5.1

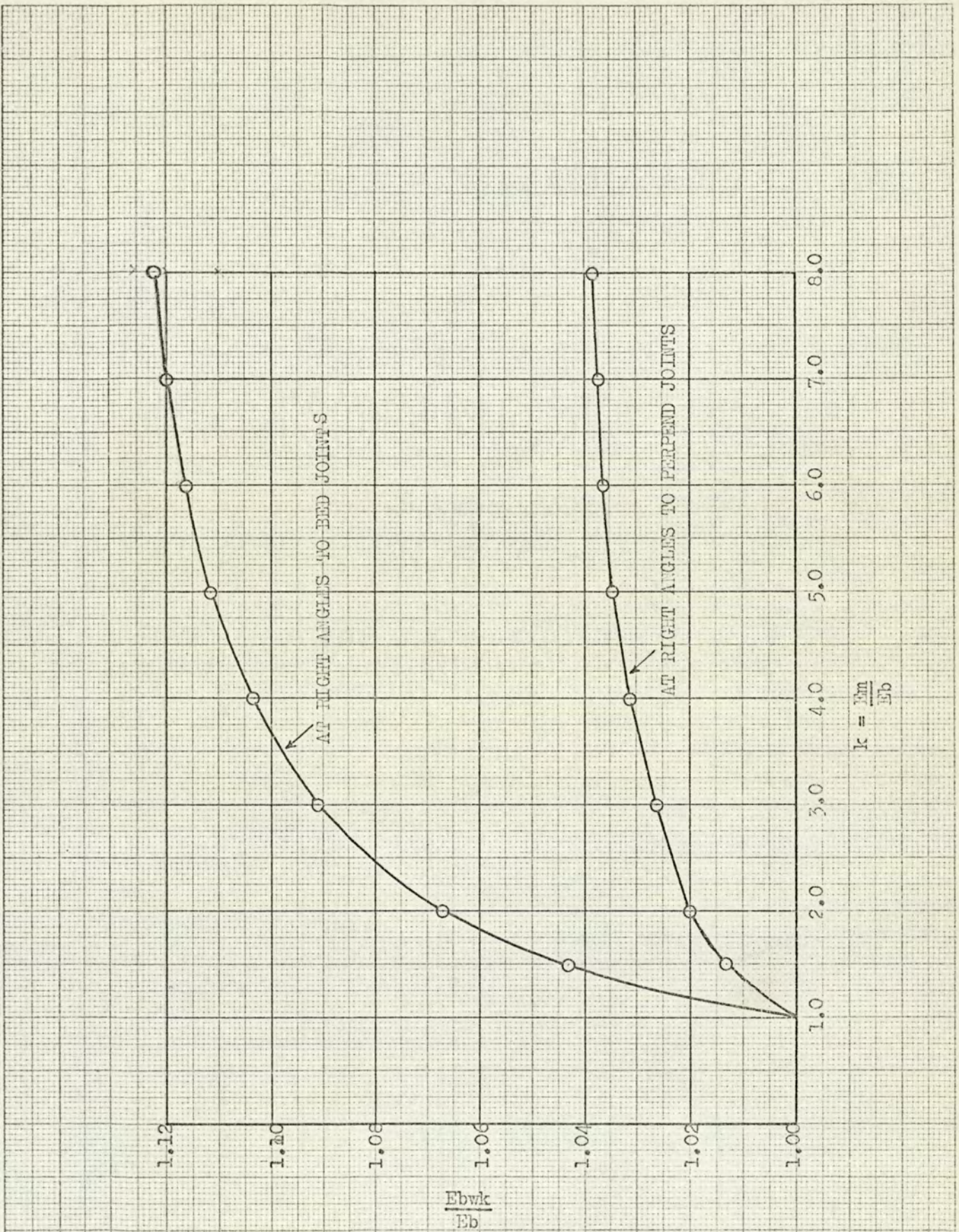
AT RIGHT ANGLES TO BED JOINTS
AT RIGHT ANGLES TO PERPEND JOINTS
1.12
1.10
1.08
1.06
1.04
1.02
1.00
Ebwk / Eb
1.0
2.0
3.0
4.0
5.0
6.0
7.0
8.0
k = Em / Eb

Fig. 5.5.2

5.6 Tests to obtain the values of Modulus of Elasticity of Brickwork for Sample Brickwork Panels

5.6.1 Introduction

Previous work by the author has indicated that brickwork samples prepared using 'dry' bricks will have different mechanical properties to brickwork samples prepared using bricks that have been 'wetted' before laying. The effect of this process was investigated as part of this programme by comparing the results obtained for 'dry' samples with those obtained for samples in which the bricks had been immersed in water for 1 minute before laying.

3 No. sample panels of brickwork of nominal size 18" x 18" x 4" were prepared for each mortar mix of 1. 0. 3 and 1. 1. 5 cement/lime/Sand each using the pressed clay frogless fletton brick supplied by The London Brick Co. Ltd. 1 No. panel was prepared using 'dry' bricks, the other 2 No. panels were prepared using 'wetted' bricks. The 'dry' sample and 1 No. 'wetted' sample were used for tests with a direction of compressive stress at right angles to the bed joints (Fig. 5.6.1), the remaining 'wetted' sample of each mix was used for tests with a direction of compressive stress at right angles to the perpend joints (Fig.5.6.2.)
All tests were carried out on a Denison Compression Testing Machine using Demec Strain gauges, the Demec spots being fixed with F88 dental cement to each face of the panel under test plated at 8" centres both vertically and horizontally in a symmetrical position about the centre line of the panel.

By reason of the fact that there does not exist a specific Code of Practice for the experimental procedure to be used in the determination of Young's Modulus for brickwork a system of pre-loading was arranged in an attempt to overcome the initial non-linear stress/strain relationship set up by

any small cracks and voids that may be present due to the manufacturing process for the bric ks and workmanship in the construction of the sample panels.

5.6.2 Method of Testing

The prepared sample panels (Table 5.6.2. 1) were carefully aligned in the testing machine and the uniformly distributed load gradually increased from zero up to 4.00 tons, this load being maintained for 1 minute.

The load was then gradually reduced to 0.20 tons and strain gauge readings taken.

The load was again gradually increased up to 4.00 tons, strain gauge readings taken and then reduced to 0.20 tons, the strain readings checked for comparison with the previous loading phase.

For the final phase, load increments of 0.4 tons were applied, the values of vertical strain being measured at each increment. For the purposes of plotting the stress/strain relationship (Fig. 5.6.3) the average vertical strain of the 2 readings measured per face was calculated and recorded (Table 5.6.2. 2)

5.6.3 Analysis of Test Results

From the slopes of the relevant load/strain curves shown in Fig.5.6.3 the values (Table 5.6.3. 1) for the Modulus of Elasticity of the brick-work samples (Ebwk) were calculated:

	VALUES OBTAINED BY TEST	THEORETICAL VALUES FROM FIGS.5.5.1 & 5.5.2	VALUES ALLOWED BY CP111(Fig 5.3.2)
Panel No.	Ebwk (lb/in^2)	Ebwk (lb/in^2)	Ebwk (lb/in^2)
1	0.58×10^6	1.09×10^6	0.58×10^6
2	0.60×10^6	1.30×10^6	1.25×10^6
3	1.17×10^6	1.30×10^6	1.25×10^6
4	1.32×10^6	1.27×10^6	1.25×10^6
5	1.13×10^6	1.09×10^6	0.58×10^6
6	1.41×10^6	1.19×10^6	0.58×10^6

TABLE 5.6.3. 1

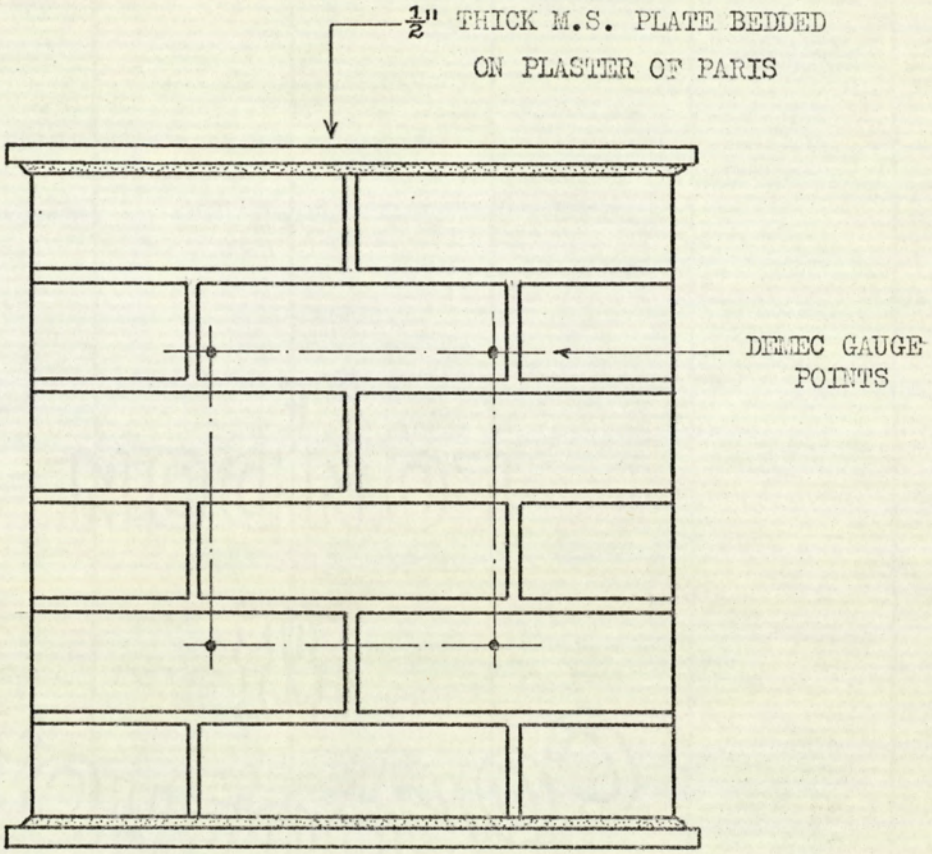

Fig.5.6.1

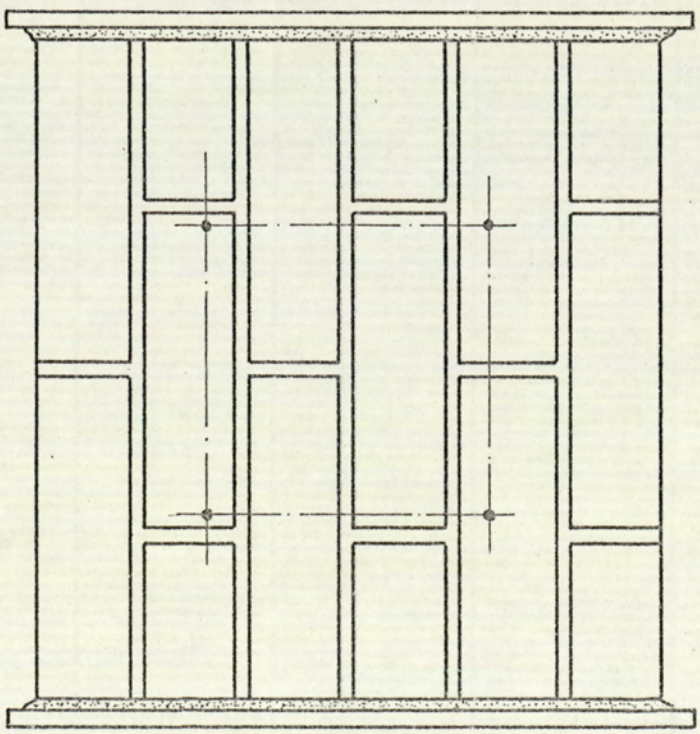

Fig.5.6.2

DETAILS OF PANEL TESTS

PANEL NO.	MIX	DATE BUILT	DATE TESTED	DIRECTION OF APPLIED LOAD	STATE OF BRICKS
1	1.1.5	9. 9.70	27.10.70	AT RIGHT ANGLES TO BED JOINTS	DRY
2	1.0.3	9. 9.70	3.11.70	AT RIGHT ANGLES TO BED JOINTS	DRY
3	1.0.3	5.11.70	16. 2.71	AT RIGHT ANGLES TO BED JOINTS	WETTED
4	1.0.3	5.11.70	16.2.71	AT RIGHT ANGLES TO PERPEND JOINTS	WETTED
5	1.1.5	5.11.70	9. 2.71	AT RIGHT ANGLES TO BED JOINTS	WETTED
6	1.1.5	5.11.70	9. 2.71	AT RIGHT ANGLES TO PERPEND JOINTS	WETTED

TABLE 5.6.2 1.

	AVERAGE MICROSTRAINS IN DIRECTION OF APPLIED LOAD					
LOAD(TONS)	PANEL NO.1	PANEL NO.2	PANEL NO.3	PANEL NO.4	PANEL NO.5	PANEL NO.6
0.2	42.5	30.0	0	0	11.6	0
0.6	66.0	41.0	12.5	11.8	24.9	17.5
1.0	86.0	62.5	20.0	18.0	29.9	23.75
1.4	111.0	82.5	34.0	24.2	36.5	31.25
1.8	130.0	111.0	41.25	32.8	54.8	43.75
2.2	152.0	122.0	56.75	48.8	68.0	52.5
2.6	174.0	151.0	63.75	55.0	69.7	53.75
3.0	196.0	159.0	77.0	65.0	83.6	65.0
3.4	212.0	191.0	85.0	72.0	97.9	77.5
3.8	239.0	204.5	95.0	89.0	111.2	85.0
5.0	300.0	271.0	113.75	101.0	140.8	112.5

LOAD/STRAIN TEST RESULTS

TABLE 5.6.2 2.

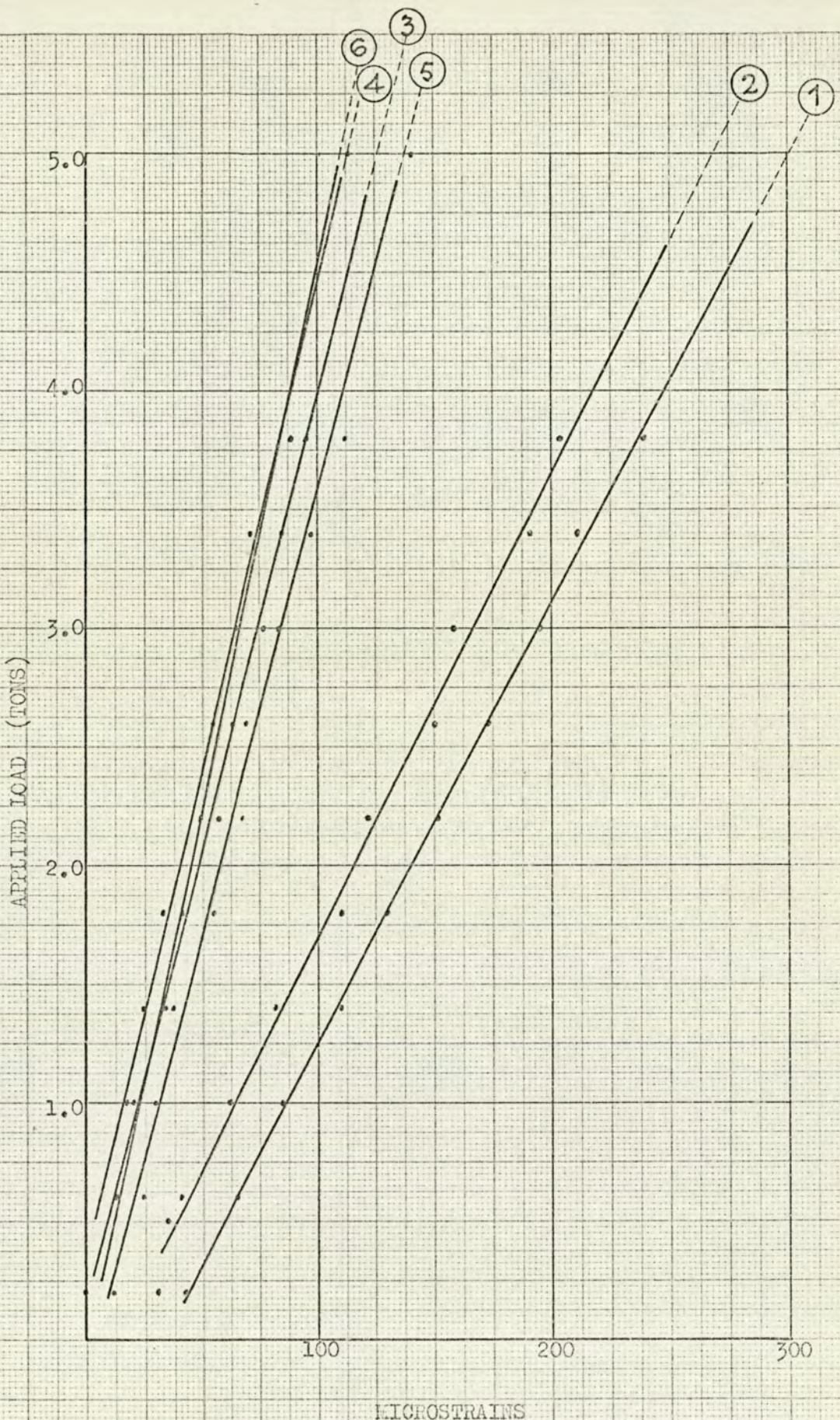

SAMPLE BRICKWORK PANELS

LOAD/STRAIN RELATIONSHIP

Fig. 5.6.3

5.6.4. Conclusions

The values obtained from the tests for the Modulus of Elasticity of brickwork built with 'dry' bricks were approximately 50% of the corresponding values for brickwork built with 'wetted' bricks. This gives further support to the requirement for brickwork to be constructed with bricks that have an acceptable suction rate. Not only would the resulting deflection of 'dry' brickwork be 50% greater than for 'wetted' brickwork, but additionally, the 'dry' brickwork would be more susceptible to vertical splitting under a compressive load due to the magnified difference in lateral strain between the two adjacent materials brick and mortar.

The resulting reduced stiffness of the brickwork can be attributed entirely to the resulting weak mortar from the action of the dry brick sucking moisture from the wet mortar. This action gives a layer of poorly hydrated cement matrix adjacent to the contact faces of each brick.

A comparison between the values obtained by test, the theoretical calculated values and values for Ebwk allowed by CP.111 is shown in Table 5.6.3. 1.

The Code of Practice does not give information with respect to the basis of the Ebwk values specified, it must therefore be concluded that in order that the designer may use these values he must be satisfied that the materials of construction conform to the Code of Practice for suction rate and strength properties.

For the 1.0.3. cement/lime/sand mix the Ebwk values show a comparable relationship, the CP.111 specified Ebwk values for the 1.1.5 mix could possibly be increased by up to 100% for properly constructed brickwork.

From Fig. 5.6.1. the 8" gauge length adopted for the tests can be seen to span 3 mortar joints, this gives a brick/mortar ratio over the gauge length equal to 6.10.

In general building construction with brickwork built at 4 courses to 1' 0" the brick/mortar ratio is 7.01 i.e. $2\frac{5}{8}$" brick with $\frac{3}{8}$" mortar joint. The resulting difference in Ebwk values can by calculation on the basis of para: 5.5. be shown to be negligable.

CHAPTER 6

THE SHEAR STRENGTH OF BRICKWORK

6.1 Shear Strength Parallel to the Bed Face

In consideration of structural design problems such as brick retaining walls, infill panels subject to racking loads, the restraint of brick walls subject to horizontal wind forces etc. it is necessary to know the resistance of the brickwork to horizontal shearing forces.

CP.111 states that in the case of walls resisting horizontal forces in the plane of the wall, the permissable shear stress should be calculated on the area of the mortar in the horizontal bed joint.
For walls built with mortar not weaker than Grade III, the permissable shear stress should range from 0.10 MN/m^2 (14.5 lb/in^2), when the compressive stress due to dead load at the level under consideration is zero, to an upper limit of 0.50 MN/m^2 (72.5 lb/in^2) when the compressive stress due to dead load is 2.5 MN/m^2 (362.5 lb/in^2). Linear interpolation between these values is permitted.

The resistance of brickwork to horizontal shearing stresses has for many years been accepted as the combination of mortar to brick bond shear strength and the friction between the mortar and the brick set up by the compressive forces.

This can be expressed by the simple mathematical equation:-

$$\sigma_s = \sigma_{bs} + \mu\sigma_c$$

where σ_s = ultimate shear stress of the brickwork

σ_{bs} = bond shear strength of mortar to brick

μ = coefficient of friction between mortar and brick

σ_c = compressive stress at right angles to the bed joint

The value for μ is directly dependent upon the surface roughness of the brick, but it has been found by experiment to be independent of the strength of the mortar. It is more likely to be dependent upon the grading of the mortar sand since this will influence the surface texture of the finished mortar.

Experiments to establish the value of μ indicates that for similar brickwork specimens the value of μ appears to decrease substantially with increasing normal compressive stress, it is therefore necessary to adopt an average value for μ.

For average solid brickwork $\mu = 0.6$ can be used as a basic guide.

An investigation into the shear strength of brickwork carried out by Stafford-Smith and Carter (5) suggests that the shear strength of brickwork is dependent upon the tensile strength of the mortar layers. It is assumed that failure occurs when the principal tensile stress in the mortar exceeds its strength; finite element stress analysés were carried out to determine the maximum principal tensile stresses in brickwork triplets resulting from applied shear and normal compressive forces.

Experimental results of shear tests on brickwork triplets with varying normal compressive stress when compared with the finite element analysis give some support to the proposition.

In order that the possibility of a shear failure in brickwork may be predicted by the method of finite element analysis the designer must be able to establish the maximum local values of stress for the specified loading condition on the structure under consideration. Such an analysis for a full scale brick structure is at present quite impractical. If the 'tensile failure' hypothesis is to be of use to the designer a simple method of analysing the stresses in brickwork structures will have to be developed.

A further important design parameter that must be considered is the fact that in brick structures subject to horizontal forces the normal compressive stress may be very small, generally speaking it is usually due only to the self weight of the brickwork. For this reason, the resistance to horizontal forces is developed principally by the bond shear strength of brick to mortar. The additional resistance due to friction being small since the normal compressive stress is small.
If the horizontal shear strength of brickwork is to be dependent upon the tensile strength of the mortar, then the adhesion of mortar to brick must be of such magnitude by the addition of bond shear strength and friction that the joint will not fail before the mortar fails.

An investigation by the author of practical cases of shear failure in brickwork shows that in all cases failure was brought about by a bond failure between bric k and mortar resulting in the brick course being displaced by sliding over the mortar layer.
Plates Nos. 6.1.1, 6.1.2 and 6.1.3 shows some typical failures of this type.

Tests on model and full scale structures were carried out by Prof. A.W. Hendry (6) to establish the relationship between precompression and shear strength.
The results of these tests, are summarised in Fig. 6.1.1. and compared with the value allowed by CP.111.
Tests indicate that failure of multi-storey cross-wall brickwork structures under lateral load will occur as a result of shear in the lowermost storey and that calculation of the shear resistance of the structure may be based on the cross-sectional area of the brickwork that is resisting the lateral shear multiplied by the permissable shear stress appropriate to the value of the precompression.

PLATE 6.1.1

PLATE 6.1.2

PLATE 6.1.3

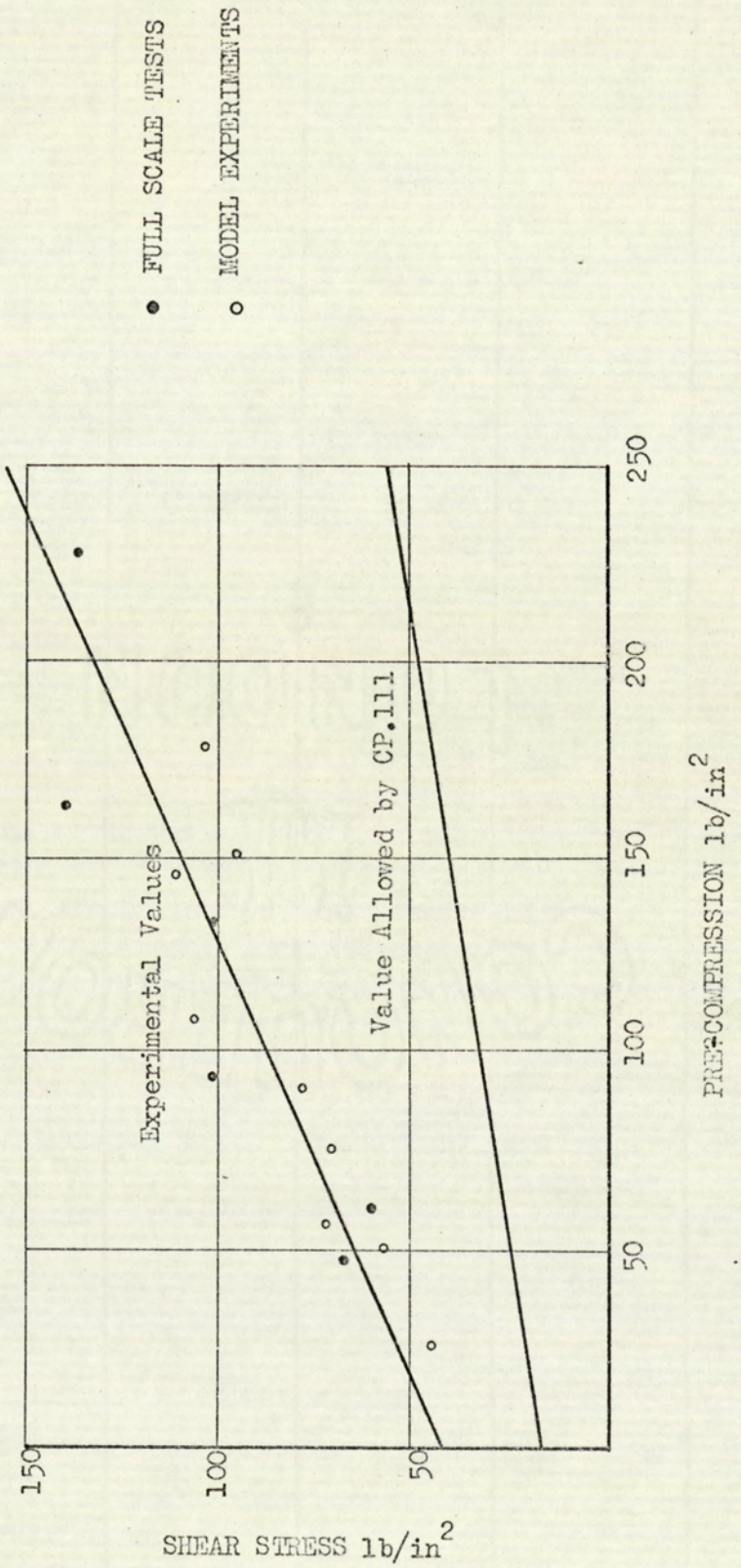

VARIATION OF SHEAR STRENGTH WITH PRE-COMPRESSION

(DUE TO PROFESSOR A. W. HENDRY)

Fig. 6.1.1

6.2 The 'Vertical' Shear Strength

Experimental work carried out by the author on unreinforced brick beams in no case resulted in a shear failure, this was not surprising, since brickwork is well known to be weak in tension and it can reasonably be expected that in the case of unreinforced brickwork flexural tension will always be the mode of failure.

In structures of reinforced brickwork such as the case of walls acting as beams the designer must consider the shear stresses and if necessary provide reinforcement to accommodate all such stresses.

CP.111 states that the permissable shear stresses (given in 6.1) may be used in the case of reinforced brick walls acting as beams.
However, when the permissable shear stress is to exceed 0.1 MN/m^2 ($14.5 lb/in^2$) particular care should be taken to ensure that the assumed compressive stresses are developed at right angles to the shear plane.

When calculated shear stresses exceed 0.1 MN/m^2 ($14.5\ lb/in^2$) or in the appropriate case 0.5 MN/m^2 ($72.5\ lb/in^2$) shear reinforcement should be provided to accommodate ALL of the shear stress.
Stresses taken by the steel in this manner should not exceed twice those calculated as permissable in the brickwork alone.

In a state of simple shear in beams the vertical shear stress is accompanied by a horizontal shear stress and diagonal tension and compressive stresses of equal intensity. Since brickwork is very much weaker in tension than in any other state of simple stress, the typical shear failure in brick beams will be a diagonal tension failure. This mode of failure must therefore be investigated.

6.3 The Diagonal Tensile Strength of Brickwork

At the suggestion of Professor Neils Thompson and Frank Johnson of the University of Texas, a method of testing brickwork to establish its diagonal tensile strength has been pioneered by the Structural Clay Products Research Foundation of the U.S.A. (S.C.R.)

The 15 inch diameter x 4 inch nominal thickness circular test specimens shown in Fig. 6.3.1. are placed between the loading surfaces of a compression testing machine such that the bed joint is orientated at 45° to the horizontal. As the specimen is loaded in the direction of its vertical diameter, the middle portion of this diameter is subjected to tensile forces perpendicular to it until the specimen fails suddenly by splitting along a vertical plane. The load is applied to a $\frac{1}{8}$" thick plywood strip that is $1\frac{1}{4}$" wide (i.e. 1/12 of the specimen diameter).

The usual mode of failure is by splitting along the loaded diameter being the result of the induced transverse tensile stresses.

Fig. 6.3.2. indicates that the vertical diameter of the circular specimen is a plane of principal tensile stress for approximately 80% of its length, the stress being approximately constant for about 60% of its length.

The maximum tensile stresses which act across the loaded diameter and therefore considered to have a constant magnitude of

$$f_t = \frac{2P}{D.t.\pi}$$

where P = load at failure (lb)

D = Specimen diameter (in)

t = Specimen thic kness (in)

It can be seen immediately that this is now the well known 'Brazilian' test for obt aining the indirect tensile strength of concrete cylinders. This method of testing is based upon the theory that the material is ideally elastic, it has been suggested that since the method has been successfully applied to concrete cylinders which are neither truly elastic nor homogeneous then the test would be equally suitable for bric kwork specimens.

The stress distribution shown in Fig. 6.3.2 would apply to a truly elastic material, in brickwork specimens shears in the mortar joints may be expected to produce stress concentrations, further compressive stresses in brickwork produce shears in the mortar joints due to a difference in Modulus of Elasticity between brick and mortar. However, the results obtained from a diagonal tensile strength 'splitting ' test calculated on the basis that $ft = 2P/D.t.\pi$ would, by reason of the presence of additional shears or stress concentrations, indicate that the calculated results of the splitting test would be below the true tensile strength of the assemblage.

It is therefore reasonable to use this method of test to establish the design value of the ultimate diagonal tensile strength (ft) of a brickwork specimen.

It would NOT be acceptable however to use this method of test and the calculated results in order that (ft) could be stated as the maximum tensile stress in the assemblage.

Published work on this subject by Stafford-Smith, Carter and Choudhury[7] is in error. The work employs the methods of Finite Element Analysis to investigate the distribution of stress in a circular specimen similar to that shown in Fig. 6.3.1. Firstly, these authors do not consider the effects of the value of adhesion between brick and mortar and erroneously continue with a mathematical analysis assuming that a breakdown in 'bond' will not be the mode of failure.

Secondly, having progressed to the determination of a modification factor to the simple equation $ft = \frac{2P}{\pi Dt}$ and using the equation $ft = \frac{NP}{\pi Dt}$ where (N) for all values of Eb/Em stated to be greater than 2, the authors produce a curve of Diagonal Tensile Strength related to Mortar Tensile Strength suggesting that $\frac{NP}{\pi Dt}$ gives a lower value than $\frac{2P}{\pi Dt}$.

This obviously is a mathematical error and unfortunately leads to the erroneous conclusion that the diagonal tensile strength of brickwork is approximately equal to the tensile strength of the mortar or bricks, whichever is the weaker.

TEST RESULTS

The value of diagonal tensile strength calculated from the S.C.R. Testing Programme[8] vary with brick and mortar strengths from 131 lb/in^2 to 354 lb/in^2. The arithmetic mean of the tests being 246 lb/in^2 with a coefficient of variation of 10.3%.

The ratio of diagonal tensile strengths to the compressive strength of the brickwork assemblage decreased from 6.3% for 2700 lb/in^2 brickwork to 2.5% for 6,500 lb/in^2 brickwork.

Since the diagonal tensile strength does not vary linearly with the compressive strength, previous investigators have related tensile resistance to the square root of the compressive strength.

$$ft = K\sqrt{fc}$$

The ratio K of splitting tensile strength to the square root of the compressive strength is a measure of the capacity of brickwork specimens to sustain diagonal tension failure.

From 27 specimens tested only one case revealed a splitting ratio (K) below the value of 2.

In 90% of the specimens the ratio (K) was between the values 2.5 and 4.5. Thus, it could be conservatively predicted that the lower limit of diagonal tensile strength would be $(ft) = 2.5\sqrt{fc}$

where fc = the crushing strength of the brickwork assemblage.

Diagonal splitting tests carried out by the author in this programme on sample 'wetted' brickwork panels using pressed clay frogless 'Flettons' supplied by the London Brick Co. Ltd. results in an arithmetic mean of diagonal tensile strength of 155 lb/in^2 for 1.0.3. mortar and 119 lb/in^2 for 1.1.5 cement/lime/sand mortar.

Plate No. 6.3.1 shows a typical sample brickwork panel after failure, the influence of 'bond' failure can clearly be seen and was apparent in all spec imens that were tested.

The mode of failure cannot be accurately predicted by reason of the factors such as bond strength, workmanship etc. that influence the mode of failure.

Some specimens failed by reason of the high shears set up by the compressive stress at the load points causing a segment of the specimen to split along a bed joint and not in the central portion of the specimen due to the tensile stress.

This mode of failure is undesirable since it is intended that the tensile stress should initiate fracture.

Since all tests were included irrespective of the mode of failure, the reported strengths are the APPARENT diagonal tensile strengths of the specimens.

PLATE 6.3.1

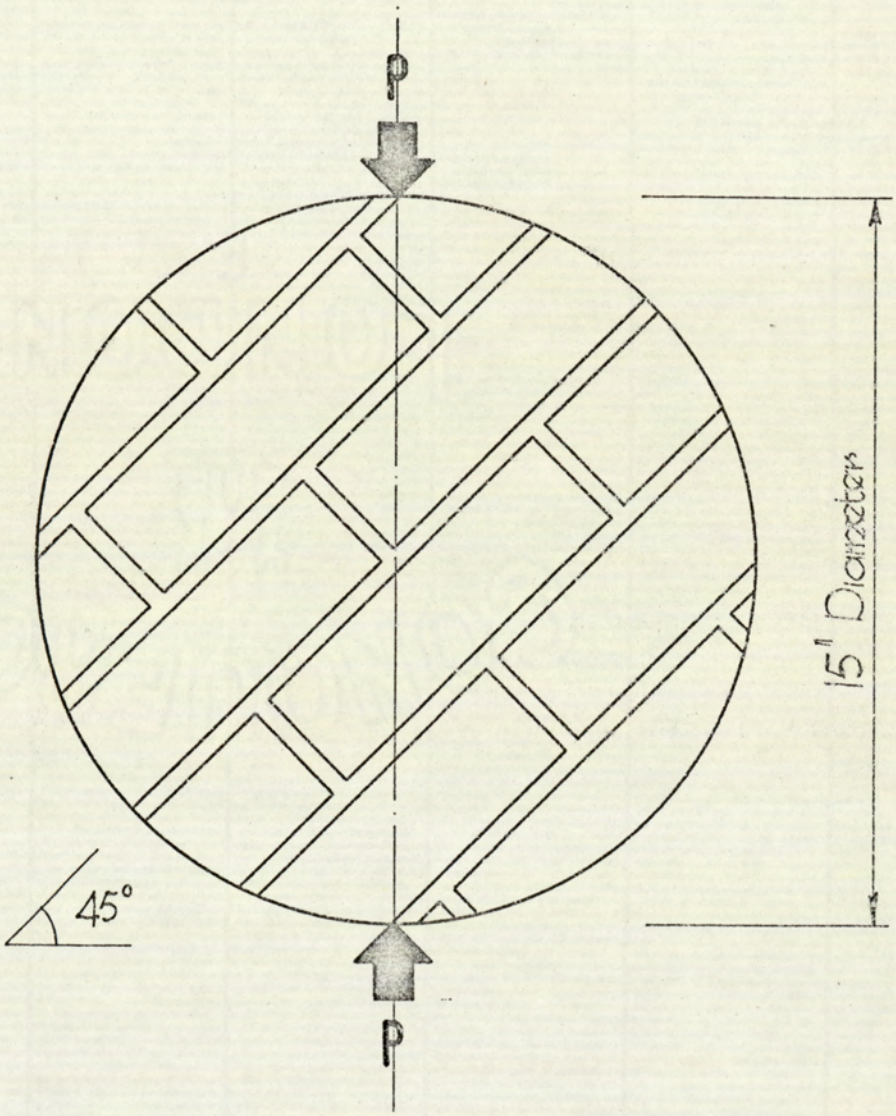

TEST SPECIMEN USED BY S.C.R.

Fig.6.3.1

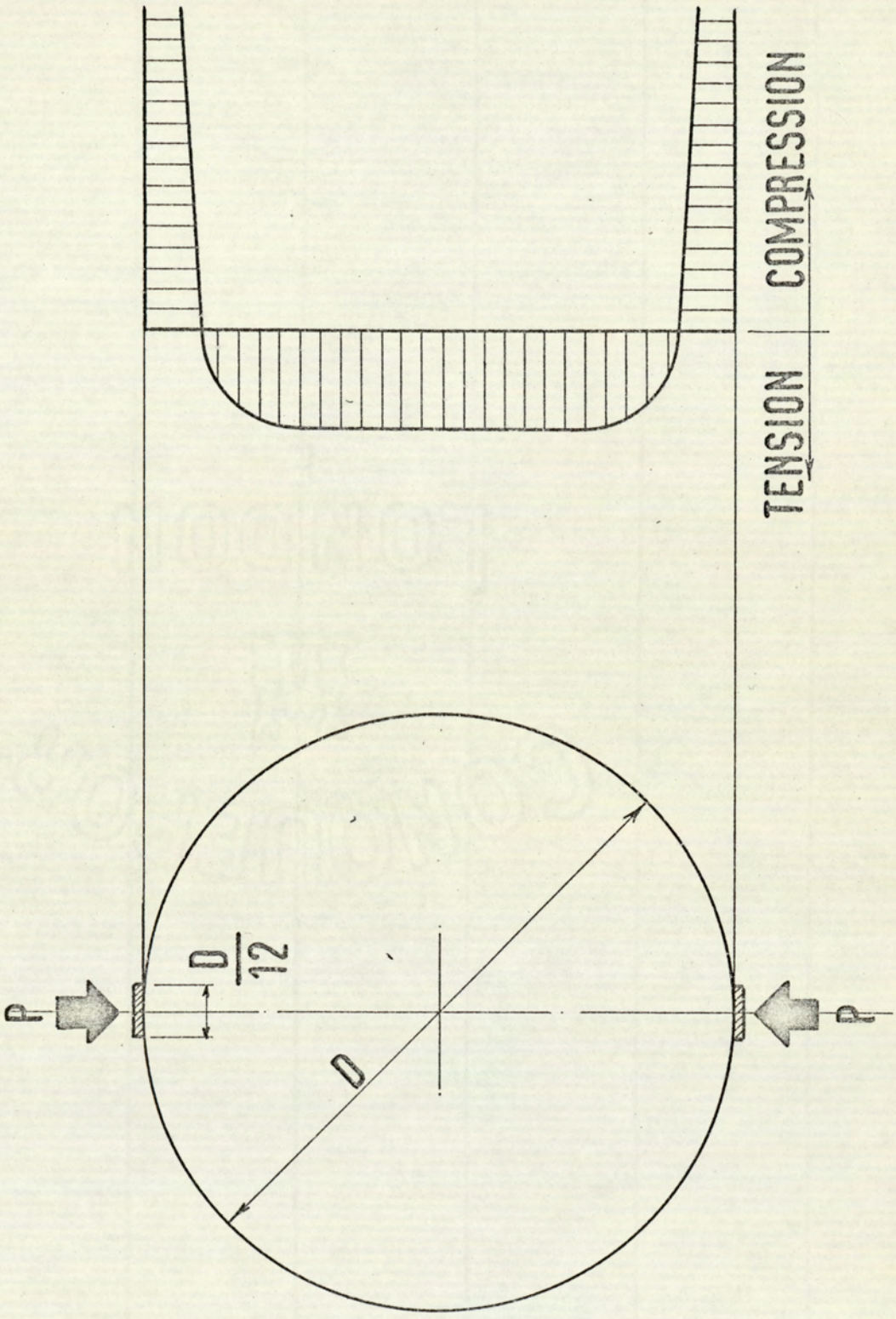

STRESS DISTRIBUTION IN TENSILE SPLITTING TEST

Fig. 6.3.2

Factors Affecting the Diagonal Tensile Strength

The influence of the mortar mix on the diagonal tensile strength is shown in Fig. 6.3.3.

These are the results of diagonal splitting tests carried out on 15" dia. x 4" thick specimens each made with a controlled brick having an average compressive strength of 11.771 lb/in^2 and initial rate of absorption of 10.6 grams per min per 30 sq. ins. Each point shown on the curve is the arithmetic mean of 5 specimens built with the indicated mortar mix all with a $\frac{3}{8}$" joint thickness.

It is clearly shown that diagonal tensile strength increases with mortar tensile strength, this is due not only to the increase in bond strength but by some extent due to the ability of stronger mortars to sustain the additional shears and stress concentration that are set up in a loaded non-homogeneous specimen.

The bond strength of mortar to brick is of primary importance in the development of diagonal tensile strength. The brick with the poorest bond characteristics as shown by the flexural strength values (which were all bond failures) also yields the lowest diagonal tensile strengths.

Fig. 6.3.4. shows the diagonal tensile strength plotted against the flexural strength of similar brickwork specimens. The wide scatter of these results clearly shows that it would be unwise to predict diagonal tensile strength from a knowledge of the flexural strength or vice-versa; however, the tendency for assemblages with the poorest bond strength to produce the lowest diagonal tensile strengths can be seen.

Fig. 6.3.5 shows the diagonal tensile strength plotted against the suction rate of the brick used in the assemblage. Again, there is a wide scatter of results showing a general tendency for bricks with a high suction

rate to yield low diagonal tensile strength. This of course can be expected since the suction rate of the brick is one of the factors that inf luence the bond strength. The wide scatter of these results is the direct result of the various other brick and mortar properties which decide the bond strength of mortar to brick.

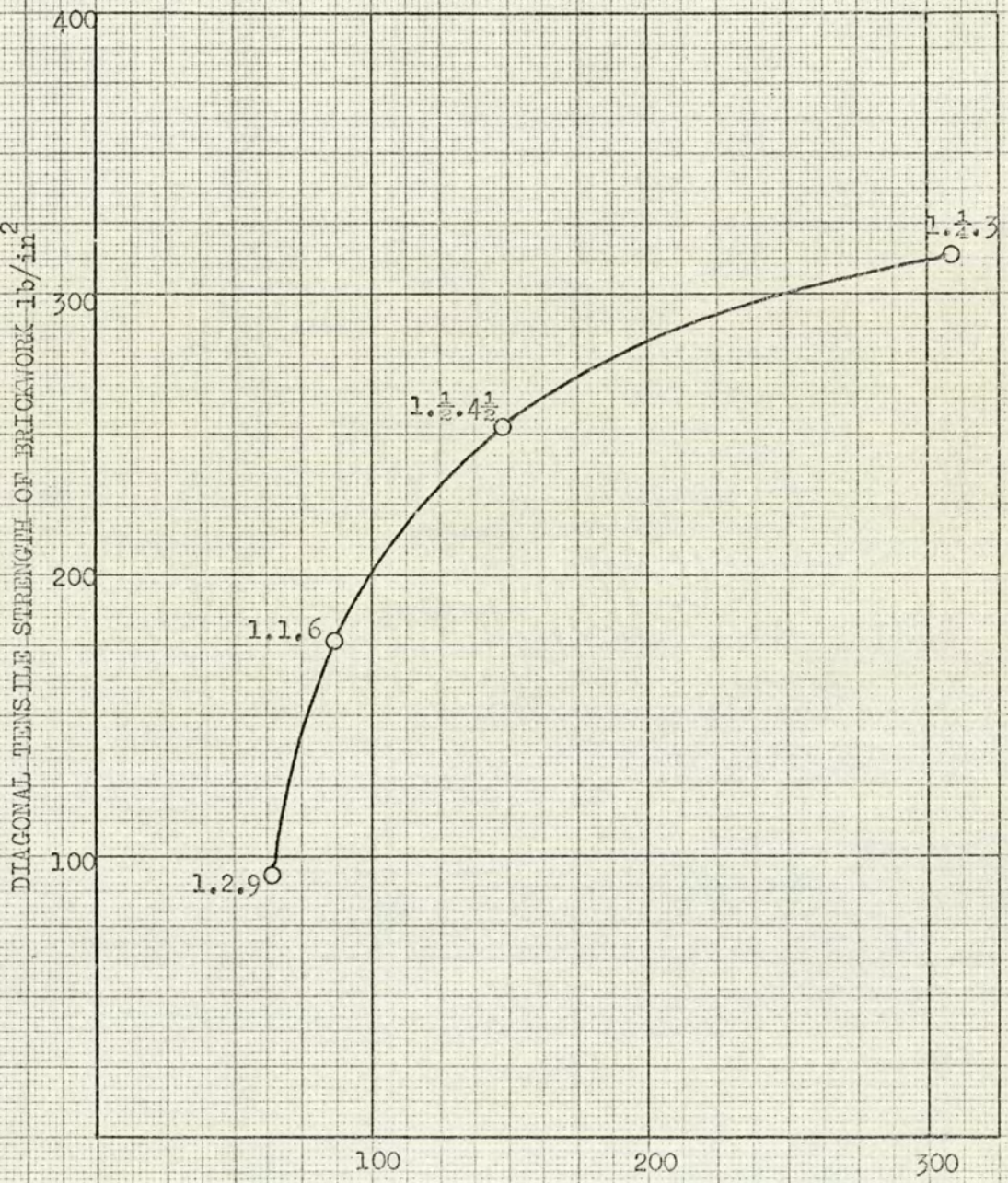

THE RELATIONSHIP OF DIAGONAL TENSILE STRENGTH OF BRICKWORK TO MORTAR TENSILE STRENGTH

Fig. 6.3.3

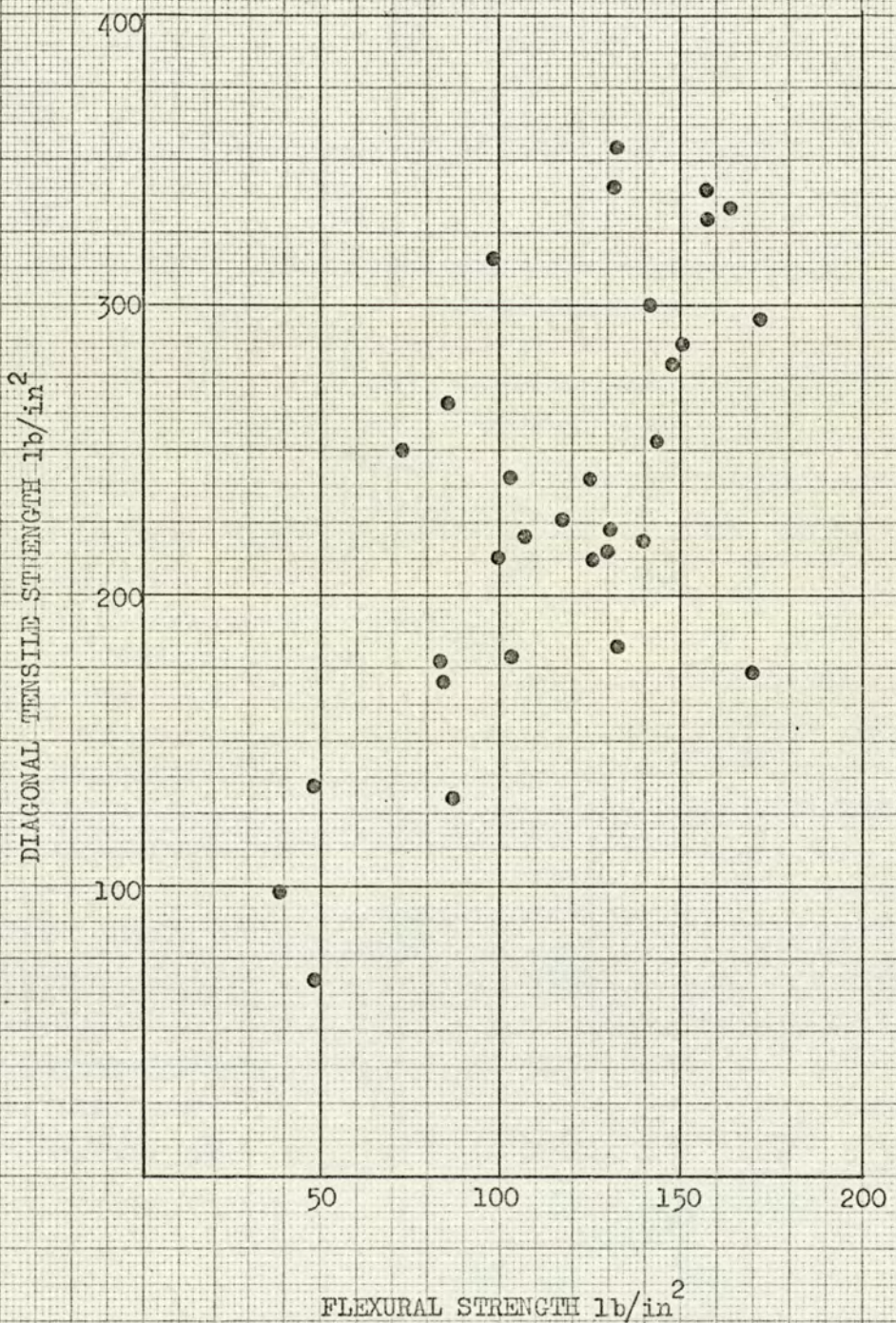

DIAGONAL TENSILE STRENGTH PLOTTED AGAINST FLEXURAL STRENGTH OF SIMILAR BRICKWORK SPECIMENS

Fig. 6.3.4

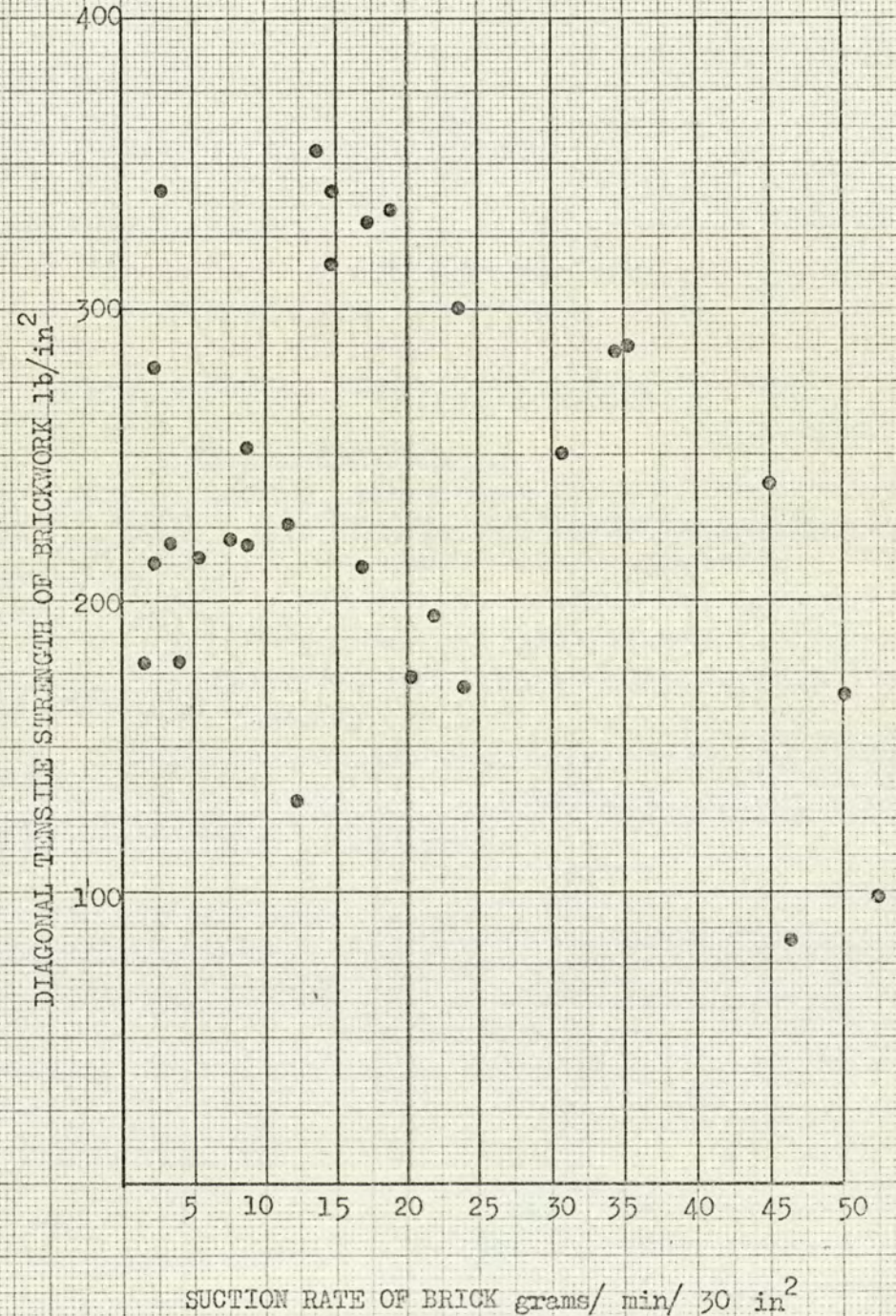

DIAGONAL TENSILE STRENGTH OF BRICKWORK PLOTTED AGAINST SUCTION RATE OF BRICKS

Fig. 6.3.5

CHAPTER 7

THE FLEXURAL STRENGTH OF BRICKWORK WITH THE DIRECTION OF BENDING STRESS AT RIGHT ANGLES TO THE BED JOINTS

7.1 Small Scale assemblages

As part of the National Testing Programme (8) carried out in 1964 by the Structural Clay Products Research Foundation, Geneva, Illinois, a series of 135 brick assemblies using 5 specimens from each of 27 different types of brick, each specimen 16" x 16" x 4" thick using a mortar mix of 1.$\frac{1}{2}$.4$\frac{1}{2}$ Cement.Lime.Sand with bricks of varying compressive strength were tested to obtain the Modulus of Rupture as a measure of the flexural strength. These results however are only valid for conditions when the direction of the principal tensile stress is at right angles to the mortar in the bed joint.

It was concluded that there was no relationship between the compressive strength of the brick and the flexural strength of the assemblages, the flexural strength being dependent upon the bond of mortar to brick, the tensile strength of the mortar and the thickness of the bed joint.

ALL specimens failed in bond between brick and mortar. No tensile failures in the mortar itself were observed.

The matter of the effects of joint thickness and mortar tensile strength were left in a somewhat inexplicable situation.
It is suspected that the improved performance of specimens with thinner joints can be attributed to the greater pressures required on the part of the bricklayer in laying the units.
This is a human variability to which a simple mathematical analysis cannot be appli ed.

The lowest flexural strength values corresponded to extremes in the initial rate of absorption (suction) of the brick. There was considerable scatter and overlapping in the test results considered in part to be due to the difficult to control practice of wetting higher suction rate bricks in order to reduce suction at the time of laying. It was also appreciated that another variable is the roughness of the bedding surface and the extent to which mechanical interlocking of the mortar with brick is achieved.

This latter variable was not investigated as part of the programme.

The method of test (Fig. 7.1.1.) was developed to impose a uniform bending stress upon all five bed joints by applying an eccentric load to the specimen mounted in a vertical position. The plane of loading in parallel to and has 10 inches eccentricity to the neutral axis of the specimen. Rotation of top and bottom of the test specimen results in almost pure bending.

The mode of failure is the opening of the weakest bed joint, since all five bed joints are subjected to a uniform bending stress.

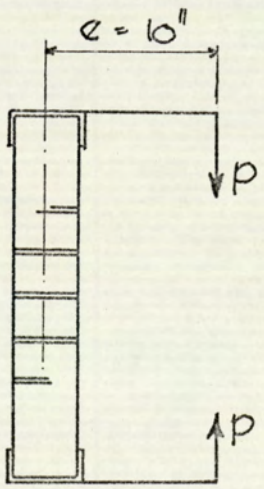

DIAGRAMATIC ARRANGEMENT OF TEST ASSEMBLY

Fig. 7.1.1.

The Modulus of Rupture of the specimen was calculated from:-

$$MR = \frac{P}{bd}\left(\frac{6e}{d} - 1\right)$$

where	MR	= Modulus of Rupture	lb/in^2
	P	= Ultimate load	lb
	b	= Width of specimen	inches
	e	= Load eccentricity	inches

From the test results the calculated Modulus of Rupture values range from 49 lb/in^2 to 172 lb/in^2 the group average being 123 lb/in^2 for 135 specimens tested. Statistically it can be shown from cumulative frequency distribution that 90% of the specimens have Modulus of Rupture values in excess of 85 lb/in^2.

Fig. 7.1.1. shows the relationship of the type of mortar and the resulting Modulus of Rupture related for convenience as mortar tensile strength to Modulus of Rupture. The results plotted are the arithmetic means of a group of 5 samples for each mortar type.

The influence of mortar joint thickness is shown in Fig. 7.1.2. Sets of 5 specimens each were built with $\frac{1}{4}$", $\frac{3}{8}$", $\frac{1}{2}$", $\frac{5}{8}$" and $\frac{3}{4}$" thick bed joints using the central brick and $1.\frac{1}{2}.4\frac{1}{2}$ Cement/Lime/Sand mortar.

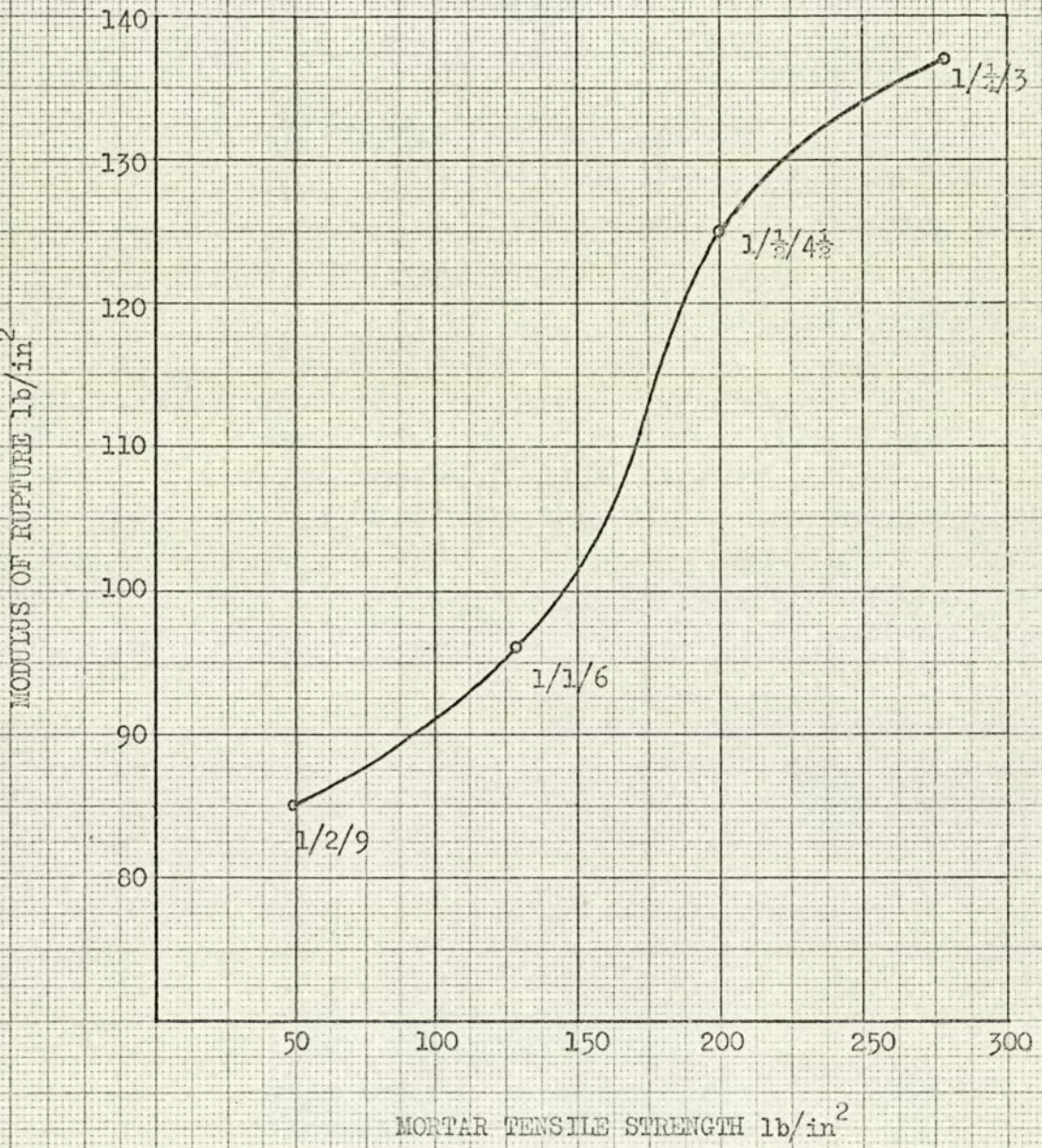

FLEXURAL STRENGTH AS A FUNCTION OF MORTAR TENSILE STRENGTH

Fig. 7.1.1.

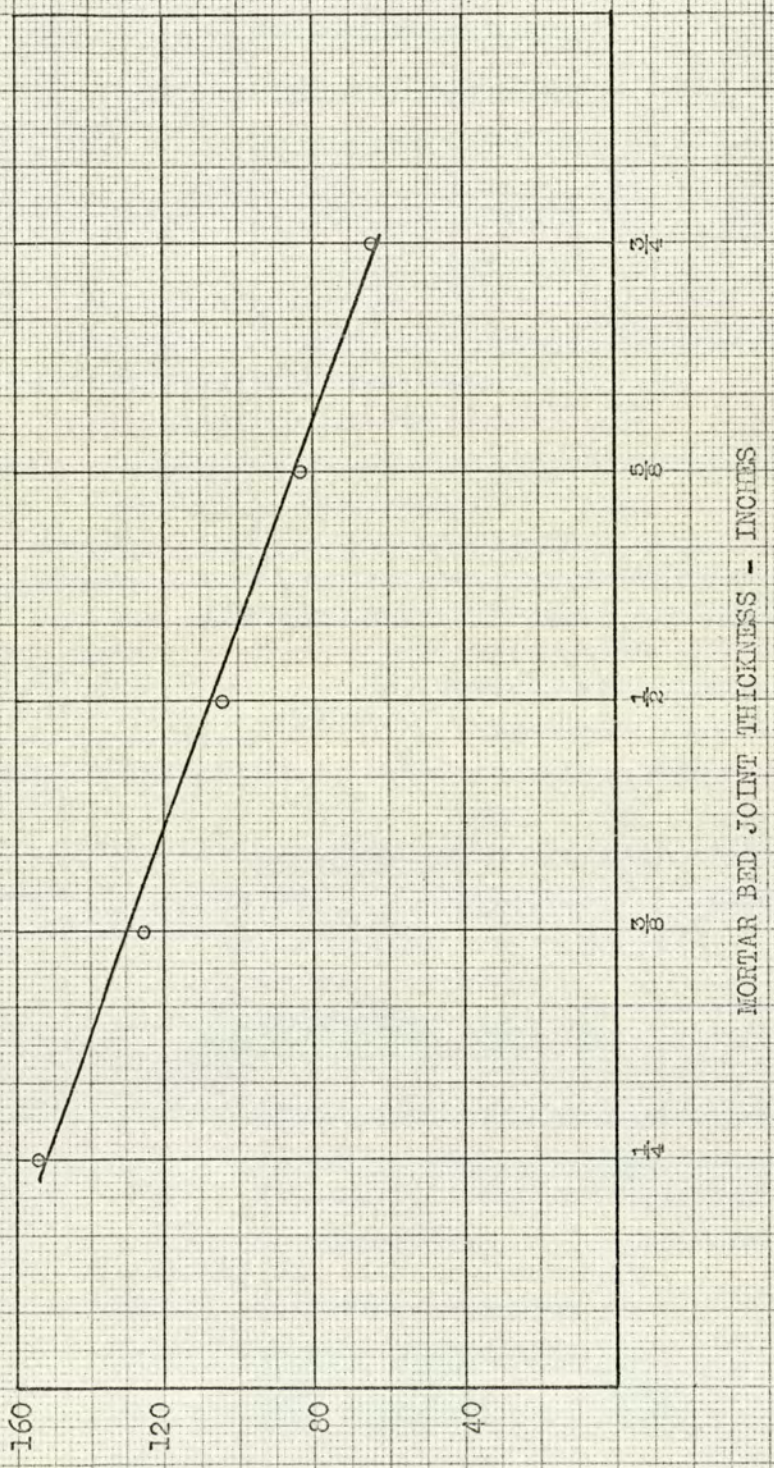

FLEXURAL STRENGTH AS A FUNCTION OF MORTAR JOINT THICKNESS

Fig. 7.1.2

7.2 Full Scale Panels

Subsequent research work investigating the flexural strength of brickwork panels 4' wide x 8' long tested by the application of a uniformly distributed load over a specimen span of 7' 6" was carried out by S.C.R.

It is not proposed to reproduce the results of this work here, since full reports are given in the Structural Clay Products Research Foundation Research Reports Nos. 8, 9 and 10.

However, it is interesting to note that again all specimens failed when a bed joint opened on the tension face as a result of bond failure at the extreme tension fibres of the brick-mortar interface.

Tests on walls of various thickness clearly show the influence of the width of the mortar bed on the flexural strength of the specimen. The flexural strength is directly related to the mortar bed width, the narrower the bed, the lower the strength. This has been attributed to the greater likelihood of more rapid drying of the narrow bed, resulting in a more unfavourable curing condition and a consequent lower strength.

The flexural strength of the small scale (16" x 16" x 4") assemblages were on average somewhat lower than those of the full size wall specimens.

CHAPTER 8

AN INVESTIGATION INTO THE DISTRIBUTION OF BENDING STRESSES IN NON-REINFORCED SHALLOW BRICK BEAMS

8.1 Introduction

The limitations imposed upon the designer by present day Codes of Practice relating to structural brickwork, prevent full advantage being taken of the tensile strength that brickwork must possess. The result of these limitations is that very little information on the true strength of brickwork in flexure is available and that in the majority of cases the designer is forced to neglect the self strength of brickwork completely and to provide additional steel or reinforced concrete beams to carry brickwork over an opening. The supporting beams being designed in themselves to carry the entire weight of the brickwork.
This cannot be the true requirement, since the supporting beam will not take load until the brickwork has deflected under load either by its own weight or by some external applied load.

For shallow brick beams the physical size of the brick and mortar element are generally not small in relation to the height, breadth and length of the beam. It may be therefore that such beams should not be considered as a 'plate' of homogeneous material when analysing the internal stresses due to bending.

Probably the most serious method of analysis would be one using the method of 'finite elements'. However such a rigorous method of analysis would be of little use to the practical designer by reason of the wide range of parameters that would need to be considered in order that appropriate design charts could be produced.

This investigation has the intention of producing a simple mathematical solution to the theoretical behavior of simple shallow beams by considering them to be 'laminated' and obeying the simple theories of elastic bending.

Tests are carried out on a number of simply supported beams to establish the stress/strain relationship at various cross-sections and the deflection characteristics of the beam.

8.2 Theoretical behaviour

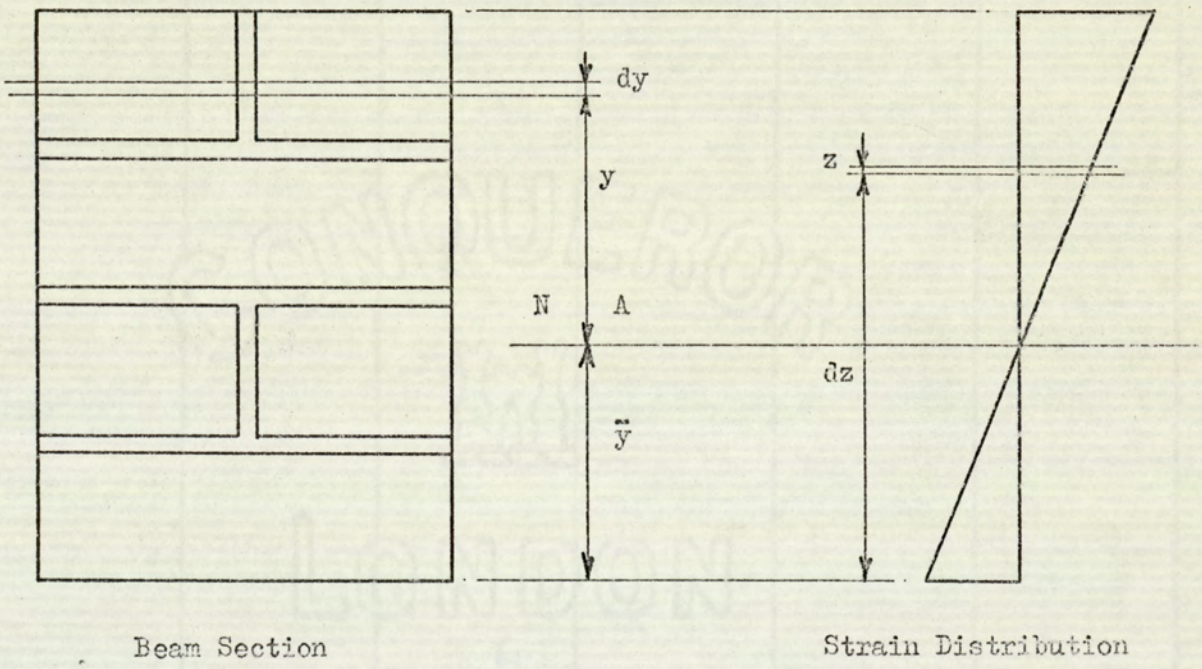

Fig 8.2.1

Consider a strip of height dy at a height y above the neutral axis. The width of the strip is (B) part of it being brick (Bb) and the remainder mortar (Bm).

The strain at a height y is given by the usual bending theory as $e = y/R$, R being the radius of curvature of the neutral axis. In this strip the brick will be subjected to a stress of $\sigma_b = Ebe$ and the mortar subjected to a stress of $\sigma_m = Eme$. Hence the total force on the strip (P) is given by

$$P = \sigma_b . Bb . dy + \sigma_m . Bm . dy .$$

$$= (Eb\ Bb + Em\ Bm) \frac{y}{R} dy$$

The total force on the section (P) is found by summing the forces on the strips so that

$$P = \int (Eb\ Bb + Em\ Bm) \frac{Y}{R} dy \qquad [1]$$

In the case of a beam without any direct force $P = 0$

$$\therefore \int (Eb\ Bb + Em\ Bm)\ y . dy . = 0 \qquad [2]$$

If the height of the strip is measured from the bottom of the section so that $z = y + \bar{y}$ equation [2] becomes:

$$\int (Eb\ Bb + Em\ Bm)(z - \bar{y})\ dz = 0$$

$$\therefore \bar{y} = \frac{\int (Eb\ Bb + Em\ Bm)\ z\ dz}{\int (Eb\ Bb + Em\ Bm) dz} \qquad [3]$$

If $Eb = Em$ then this equation reduces to the usual equation $\bar{y} = \frac{\int z dz}{\int dz}$ for finding the centre of gravity of the section.

The moment of resistance of the beam to bending is found in the manner of the usual elastic theory by taking moments about the neutral axis. The resultant of the external forces which produce bending is a couple, this external couple must be balanced by the internal forces in the beam, and the resultant of these internal forces must therefore be a couple because

only a couple will balance a couple. The two forces which form the internal couple will be the resultants of the tensile and compressive stresses, therefore these resultants being the total tension and the total compression must be equal and parallel.

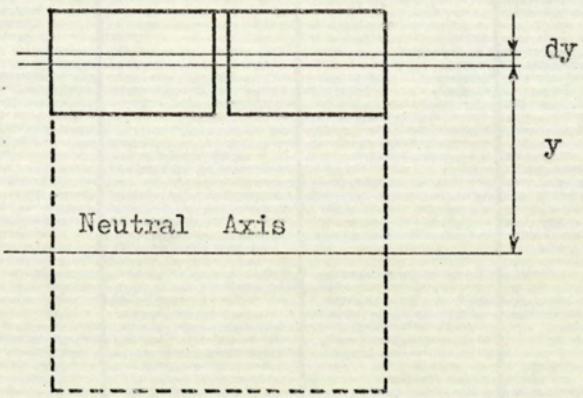

Total Force on Strip = P = $(Eb.Bb + Em.Bm.) \frac{y}{R} dy$

Moment of Resistance of Strip = $(Eb\ Bb + Em\ Bm) \frac{y^2}{R} dy$

M = Total Moment of Resistance of Section = $\sum (Eb\ Bb + Em\ Bm) \frac{y^2}{R} dy$

THE SUMMATION BEING MADE ABOVE AND BELOW THE NEUTRAL AXIS

$\therefore$ Since $I = \sum By^2\ dy$

$$M = \frac{(Eb\ Ib + Em\ Im)}{R} \qquad [4]$$

Where Ib and Im are the second moments of area about the neutral axis for the total section of brick and mortar.

Since $R = \frac{y}{e}$ and $e = \frac{\sigma}{E}$

$\frac{1}{R}$ can be written as $\frac{\sigma}{E.y}$

The section shown in Fig. 8.2.1. can be considered as a laminated beam made from a material containing brick and mortar so that a horizontal section of the beam vertical section can be either brick, mortar, or part brick and part mortar.

It is assumed that the simple theory of elastic bending may be used and that plane sections remain plane. With sections composed of one material we are used to stating that the neutral plane passes through the centre of gravity, but this does not apply to a section built up from several materials with different moduli of elasticity. Since the elastic modulus of brick (Eb) is different from the elastic modulus of mortar (Em) the first step will be to find the position of the neutral axis.

If we now consider the side elevation of the brick beam (Fig. 8.2.2) it can be seen that the cross section is not constant throughout the beam due to the method of brick bonding. This will result in a shift of the neutral axis throughout the length of the beam. i.e. the neutral axis for sections 1.1, 2.2, 3.3 will not be in the same positions.

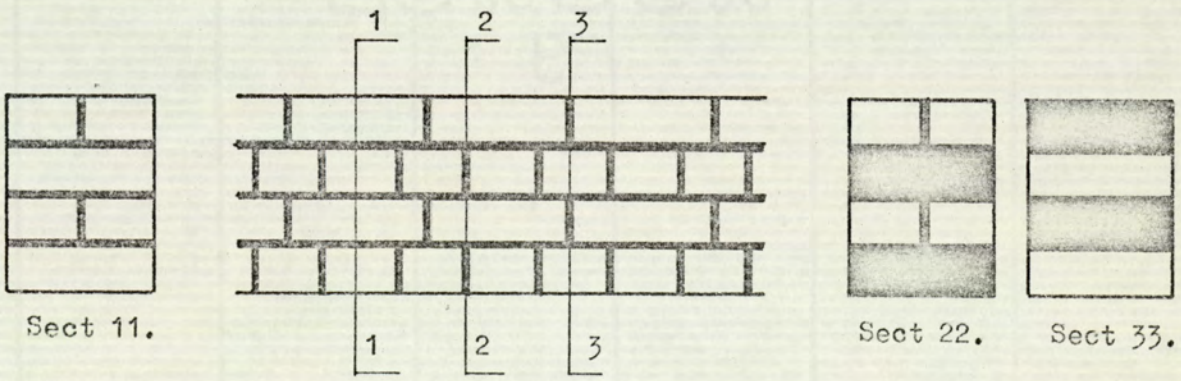

Fig. 8.2.2.

If failure of the section occurs in the mortar at a height ym under a stress of σ_m then

$$M = (Eb.IB + Em\ Im)\ \frac{\sigma_m}{Em\ ym} \qquad [5]$$

Similarly if failure occurs in the brick at a height yb under a stress of σ_b then

$$M = (Eb.IB + EmIm)\ \frac{\sigma_b}{Eb.yb} \qquad [6]$$

If EB = Em and I is said to be the total second moment of area of the section then the above equations reduce to $M = \frac{\sigma I}{y}$ which is the general expression of finding the moment of resistance of a homogeneous section.

The two materials, brick and mortar, which comprise the beam will have different ultimate values of stress. In materials of usual construction the limiting condition will be either the value of the adhesion of mortar to brick or the ultimate tensile strength of the mortar and by reason of the methods of 'bond' a failure of the mortar at the extreme fibres will not be the ultimate bending moment capacity of the beam.
An added complication is the 'shift' of the neutral axis along the beam elevation. The elevational stress failure pattern must now be examined.

Consider a small length of the beam elevation:—

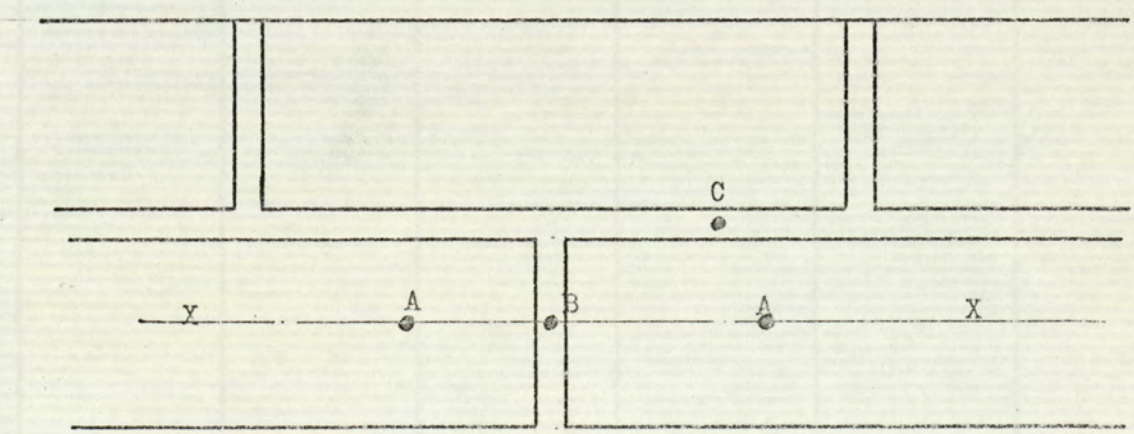

On the line XX, since Em does not equal Eb and further since the position of the neutral axis is not common to both vertical sections at A and B

the strain at A will not be equal to the strain at B.

The numerical value of the strain across the perpend mortar joint must by reasons of equilibrium vary from the value of the brick strain at the bonded face to the max value of the mortar strain in the centre of the perpend joint.

The strain across the vertical section of the bed joint say at point C can possibly have more complicated effects. A complete tensile failure of the mortar alone is not likely to occur if Em is less than EB since under conditions of equal stress the strain in the mortar will be greater than the strain in the brick, the result being that there will either be a failure of the bond between brick and mortar or that the movement of the mortar will cause a tensile failure in the brick.

This vertical splitting is the general mode of failure when brickwork is subjected to axial compression and is of course the result of horizontal tension. The reason for this type of failure is not at first apparent until the different strain characteristics of brick and mortar are considered.
The lateral strain of the mortar being greater than that of the brick forces the bricks apart and hence the tensile failure by vertical splitting. The tensile strength of the brick is therefore an important factor.

It is anticipated that the strength of brick beams will increase as the strength of both brick and mortar increases, usually resulting in an increase in the value of the 'bond' strength being the value of the adhesion on Mortar to brick.

The modulus of rupture of the beam may not be dependent upon the ultimate strength of the brick and mortar at the extreme fibres of the section, higher value of tensile stress may be present in the bed joint immediately below the extreme fibres where we have the addition of the calculated stress due to the applied bending moment and the local stress set up as described when the brick restricts the horizontal strain in the mortar. It is not likely however that this condition would exist in very shallow beams unless some method is employed to achieve a 'bond' stress that is greater than both the ultimate tensile strengths of the mortar and brick.

Theoretical Solution of Test Beams

The following values of Modulus of Elasticity have been established by previous experiments:

$Eb = 1.25 \times 10^6$ lb/in^2

$Em(1.0.3) = 1.77 \times 10^6$ lb/in^2

$Em(1.1.5) = 0.57 \times 10^6$ lb/in^2

$Ebwk(1.0.3) = 1.3 \times 10^6$ lb/in^2

$Ebwk(1.1.5) = 1.1 \times 10^6$ lb/in^2

It is predicted that failure of the beams will occur at a section M.B.M. for 3 course beams and at a section B.M. for 2 course beams due to a failure of adhesion between brick and mortar. This will be equivalent to a failure in the mortar and the Modulus of Rupture which is by definition the apparent stress at the extreme fibres at collapse, can be calculated from Equation [5] which can be expressed as:-

$$\text{Modulus of Rupture} = \bar{\sigma}_{mc} = \frac{Mc.\ Em.\ ym}{EbIb + EmIm} \qquad [7]$$

where Mc is the total bending moment at collapse due to the applied load, the weight of the apparatus and the self weight of the beam.

THE THEORETICAL POSITION OF THE NEUTRAL AXIS

3 COURSE BEAMS (Fig. 8.3.2)

By reasons of the symmetry of brick and mortar the neutral axis for cross-sections B.B.B: B.M.B: and M.B.M. will be in the centre of the beam.

2 COURSE BEAMS (Fig. 8.3.3)

SECTION B.B.

Again, by reasons of symmetry the neutral axis will be in the centre of the beam.

SECTION B.M.

Since the test beams are $\frac{1}{2}$ brick (4" wide), Equation [3] can be reduced to:-

$$\bar{y} = \frac{\int (Eb + Em)\ z.\ dz}{\int (Eb + Em)\ dz} \qquad [8]$$

1.0.3 Mortar Mix

$$\bar{y} = \frac{\int_0^{3.00} 1.77.\ z.\ dz + \int_{3.00}^{5.625} 1.25\ z.\ dz}{\int_0^{3.00} 1.77\ dz + \int_{3.00}^{5.625} 1.25\ dz}$$

$$\therefore\ \bar{y} = \frac{\left(\frac{1.77 \times 3^2}{2}\right) + \frac{1.25}{2}\ (5.625^2 - 3^2)}{(1.77 \times 3) + 1.25(5.625 - 3.00)}$$

$$= 2.57"\ \text{(from bottom of beam)}$$

1.1.5 Mortar Mix

$$\bar{y} = \frac{\int_0^{3.00} 0.57\, z.\, dz + \int_{3.00}^{5.625} 1.25\, z\, dz}{\int_0^{3.00} 0.57\, dz + \int_{3.00}^{5.625} 1.25\, dz}$$

$$= \frac{\left(\frac{0.57 \times 3^2}{2}\right) + \frac{1.25}{2}\left(5.625^2 - 3^2\right)}{(0.57 \times 3) + 1.25(5.625 - 3.00)}$$

$$= 3.34'' \text{ (from bottom of beam)}$$

SECTION M.B

By a reverse of the above calculations

1.0.3. Mortar Mix

$\bar{y}$ = (5.63 - 2.57) = 3.06" (from bottom of beam)

1.1.5 Mortar Mix

$\bar{y}$ = (5.63 - 3.34) = 2.29" (from bottom of beam)

The experimental values of the beam deflection will be compared to the theoretical values calculated, (using the appropriate Ebwk value) on the assumption that the beam is constructed from a homogeneous material.

THE MODULUS OF RUPTURE

(i) 3 Course Beams

For 1.0.3. Mortar Mix

Considering section M.B.M. for failure in the mortar at the outer fibres

From Equation [7]

$$\sigma_{mc} = \frac{Mc(\text{lb ins}) \times 1.77 \times 4.33}{(1.25 \times 4.125 \times \frac{2.625^3}{12}) + 3.54 \left[(\frac{4.125 \times 3^3}{12}) + (4.125 \times 3 \times 2.813^2)\right]}$$

$\therefore$ Modulus of Rupture $= \sigma_{mc} = 0.0195\ Mc\ \text{lb/in}^2$ [9]

For 1.1.5 Mortar Mix

Considering section M.B.M. for failure in the mortar at the outer fibres

From Equation [7]

$$\sigma_{mc} = \frac{Mc(\text{lb ins}) \times 0.57 \times 4.313}{(1.25 \times 4.125 \times \frac{2.625^3}{12}) + 1.14 \left[(\frac{4.125 \times 3^3}{12}) + (4.125 \times 3 \times 2.1813^2)\right]}$$

$\therefore$ Modulus of Rupture $= \sigma_{mc} = 0.0189\ Mc\ \text{lb/in}^2$ [10]

(ii) 2 Course Beams

For 1.0.3. Mortar Mix

Considering section B.M. for a tension failure in the mortar at the outer fibres (Fig.8.2.3)

From Equation [7]

$$\sigma_{mc} = \frac{Mc\ (\text{lb ins}) \times Em \times ym}{Eb\ Ib + Em\ Im}$$

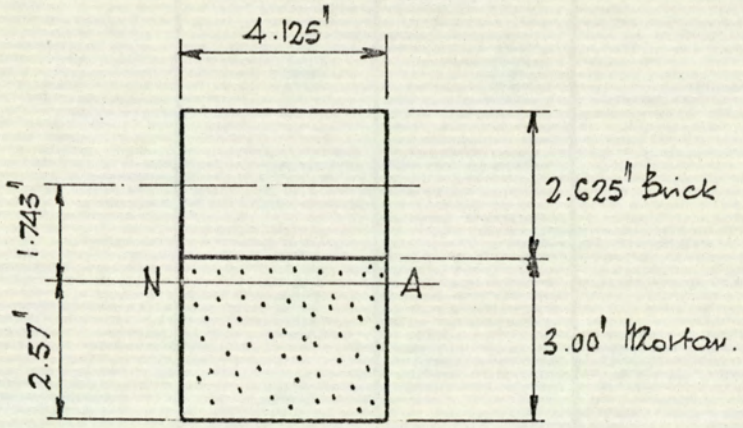

Fig. 8.2.3.

$$Im = \frac{(4.125 \times 2.57^3)}{3} + \frac{(4.125 \times 0.43^3)}{3}$$

$$= 23.44 \text{ in}^4$$

$$Ib = \frac{(4.125 \times 2.625^3)}{12} + (4.125 \times 2.625 \times 1.743^2)$$

$$= 39.12 \text{ in}^4$$

$$\therefore \quad \sigma_{mc} = \frac{Mc(\text{lb ins}) \times 1.77 \times 2.57}{(1.25 \times 39.12) + (1.77 \times 23.44)}$$

$$\sigma_{mc} = 0.051 \text{ Mc lb/in}^2 \qquad [11]$$

For 1.1.5 Mortar

Considering section B.M. for a tension failure in the mortar at the outer fibres (Fig.8.2.4)

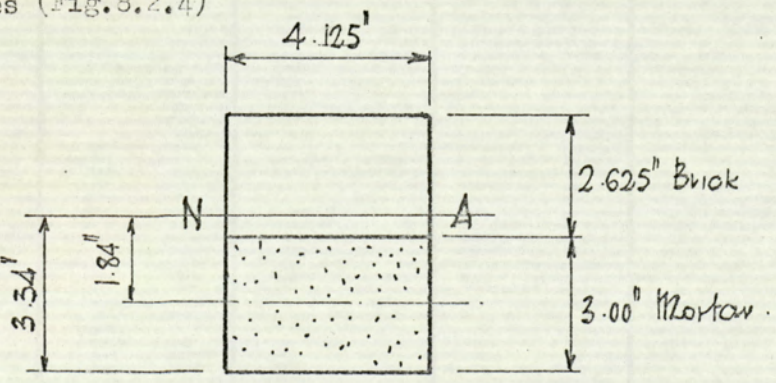

Fig.8.2.4.

$$Ib = \frac{(4.125 \times 2.285^3)}{3} + \frac{(4.125 \times 0.34^3)}{3}$$

$$= 16.46 \text{ in}^4$$

$$Im = \frac{(4.125 \times 3^3)}{12} + (4.125 \times 3 \times 1.84^2)$$

$$= 51.2 \text{ in}^4$$

$$mc = \frac{Mc \text{ (lb ins)} \times 0.57 \times 3.34}{(1.25 \times 16.46) + (0.57 \times 51.2)}$$

$$\therefore \sigma_{mc} = 0.0382 \text{ Mc lb/in}^2 \qquad [12]$$

LOADING SYSTEM FOR EXPERIMENTAL WORK

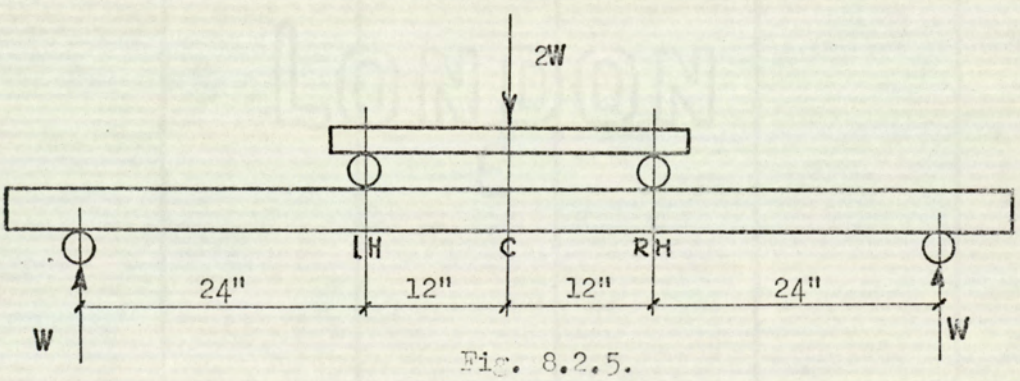

Fig. 8.2.5.

Bending Moment over 24" centre section of beam due to an applied load (2 W) = 24 W lb ins

Deflection (inches) at centre of beam (C) = $\frac{13248 \times W \text{ (lb)}}{E(\text{lb/in}^2) \times I \text{ (in}^4)}$ [13]

BEAM DEFLECTIONS

The Theoretical beam deflection calculated on the average Ebwk value for the relevant mortar mix and the gross Moment of Inertia assuming a homogeneous section will be compared to the experimental value of the beam deflection at mid-span.

Considering the theoretical deflection at mid-span of the beam due to an applied load (2W) distributed as shown in Fig. 8.2.5. Therefore from Equation [8]

3 COURSE BEAM ($I = 220.6\ in^4$)

1.0.3. Mortar

$$\text{Deflection at C} = \frac{13248.\ W}{1.3 \times 10^6 \times 220.6} = 0.046 \times 10^{-3}\ W \text{ inches}$$

1.1.5 Mortar

$$\text{Deflection at C} = \frac{13248.\ W}{1.1 \times 10^6 \times 220.6} = 0.055 \times 10^{-3}\ W \text{ inches}$$

2 COURSE BEAM ($I = 61.16\ in^4$)

1.0.3. Mortar

$$\text{Deflection at C} = \frac{13248.\ W}{1.3 \times 10^6 \times 61.16} = 0.167 \times 10^{-3}\ W \text{ inches}$$

1.1.5 Mortar

$$\text{Deflection at C} = \frac{13248\ W}{1.1 \times 10^6 \times 61.16} = 0.197 \times 10^{-3}\ W \text{ inches}$$

8.3 Beam Tests

This investigation was restricted to non-reinforced brick beams:-

(a) 2 courses deep
(b) 3 courses deep

} Built with pressed clay frogless 'Flettons' 'wetted' before laying

All beams were 7' 0" long x $\frac{1}{2}$ brick (4") wide and for ease of handling into the test rig were constructed on a steel channel base plate (Fig. 8.3.1)

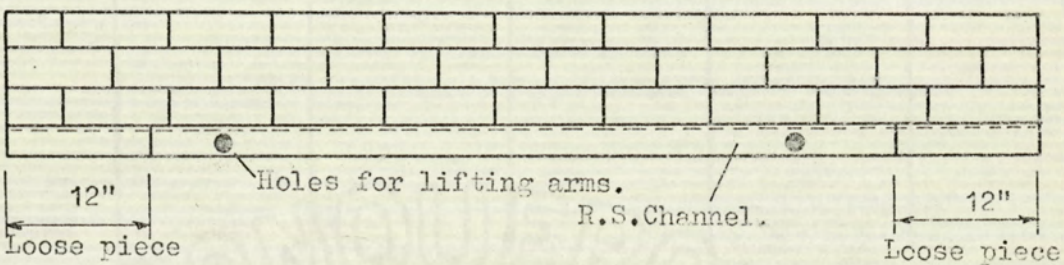

Fig 8.3.1.

It was the original intention to use 'Demec' strain gauges and for this purpose gauge spots were fixed to the sides of the beam at $\frac{1}{2}$" vertical centres. During the preliminary tests it was found that 'Demec' gauges could not be used with sufficient accuracy since the small value of the applied loads resulted in corresponding small values of horizontal strain. Therefore for subsequent tests, 1" electrical resistance strain gauges were used fixed at $\frac{1}{4}$" vertical centres to the side of the beam in the centre 2' 0" section in position shown in Figs. 8.3.2 and 8.3.3.

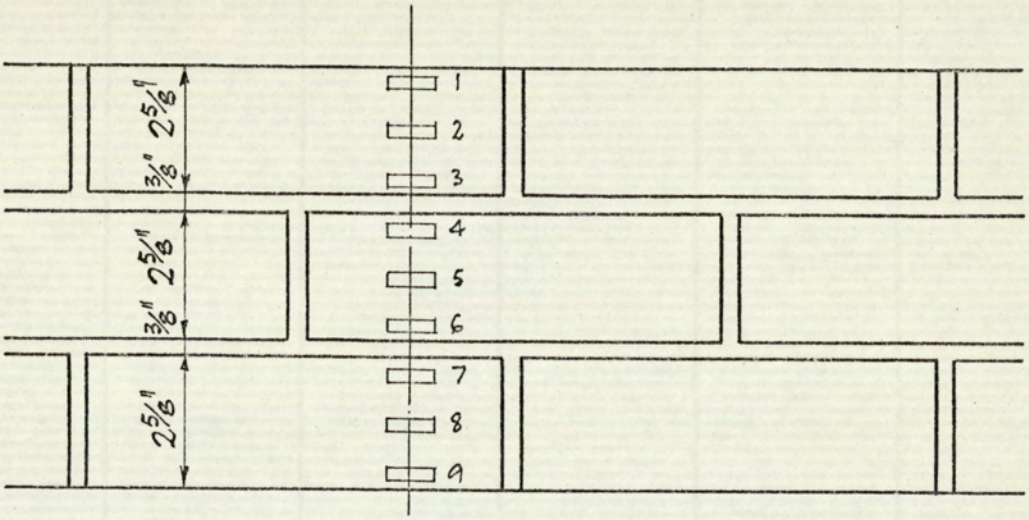

SECTION B.B.B.

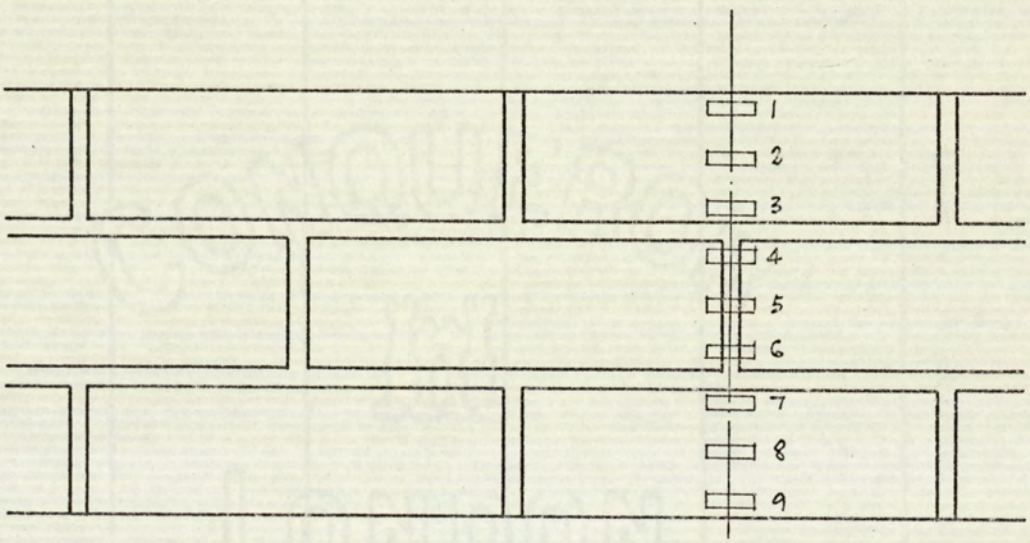

SECTION B.M.B.

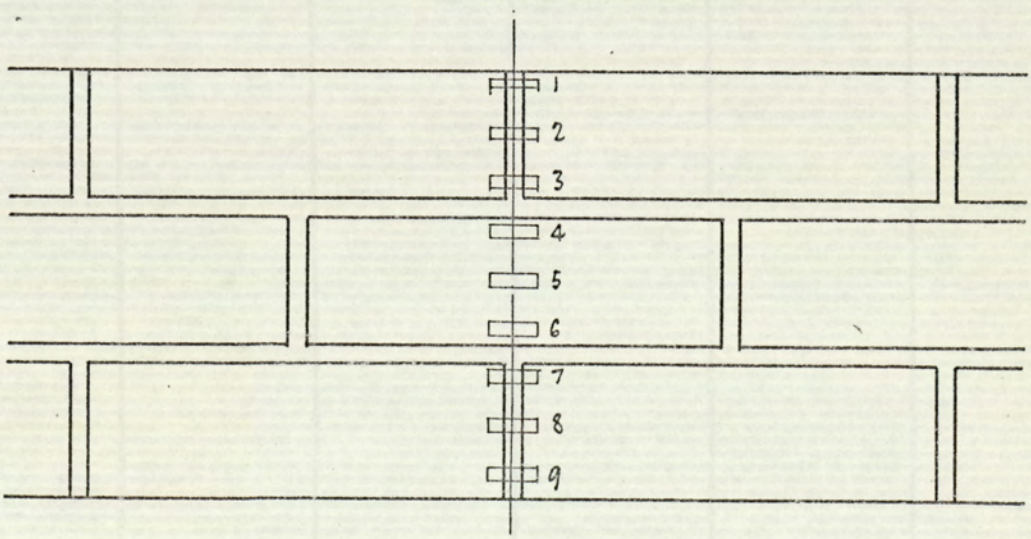

SECTION M.B.M.

STRAIN GAUGE POSITIONS FOR 3 COURSE BEAMS
Fig.8.3.2

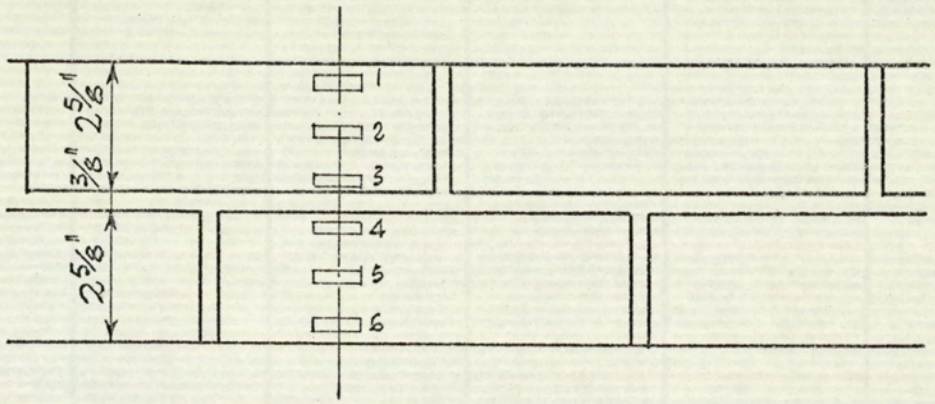

SECTION B.B

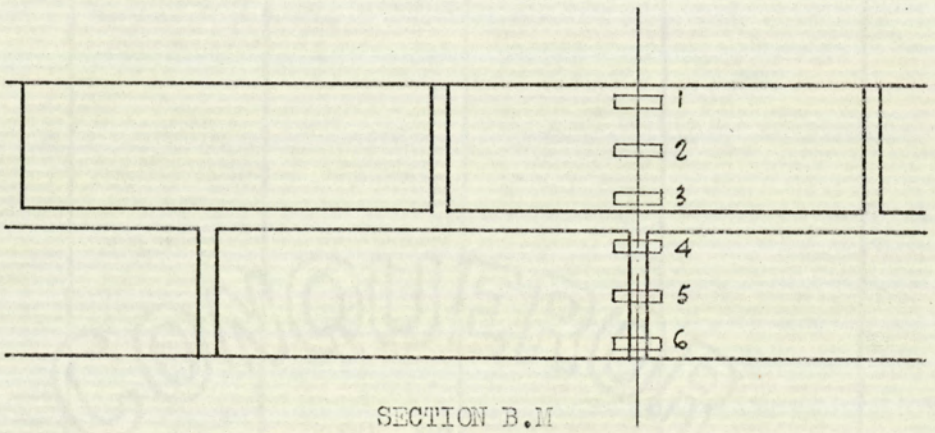

SECTION B.M

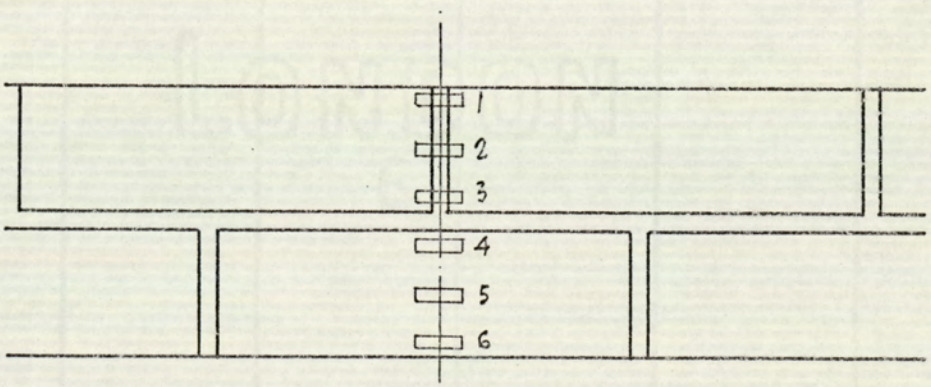

SECTION M.B.

STRAIN GAUGE POSITIONS FOR 2 COURSE BEAMS

Fig. 8.3.3.

The beams were lifted into the testing rig (Plates 8.1 and 8.2) together with the channel base plate upon which they were constructed such that it was possible to place the beams into the test rig whilst they remained fully supported and free from the stresses that would be set up due to their self weight.

At this stage, strain gauge readings were taken and used as the zero from which future strains were measured.

The beams were then lowered onto the supporting rollers which were fixed at 6' 0" centres. (Steel plates bedded in plaster of Paris separated the brick beams from the supporting rollers) and the supporting channels lowered clear of the beam. The channels were allowed to remain in a position just clear of the beam in order that they were able to support the test specimen after fracture, thus preventing complete collapse of the beam and loading apparatus (Plate 8.3)

Strain gauge readings were then taken giving the horizontal strain in the beams due to the self weight only.

The test loads were then applied to the beam by a hand operated hydraulic jack transmitting the applied load through a proving ring to a steel I beam supported by steel rollers on the top face of the beam. There loading rollers were positioned at 12" on either side of the beam centre line to produce a loading system that resulted in a constant bending moment and zero shear in the centre 2' 0" section of the beam.

Dial gauges fixed to the test rig at the bottom face of the beam measured the vertical beam deflection at the loading points and at the centre of the beam span.

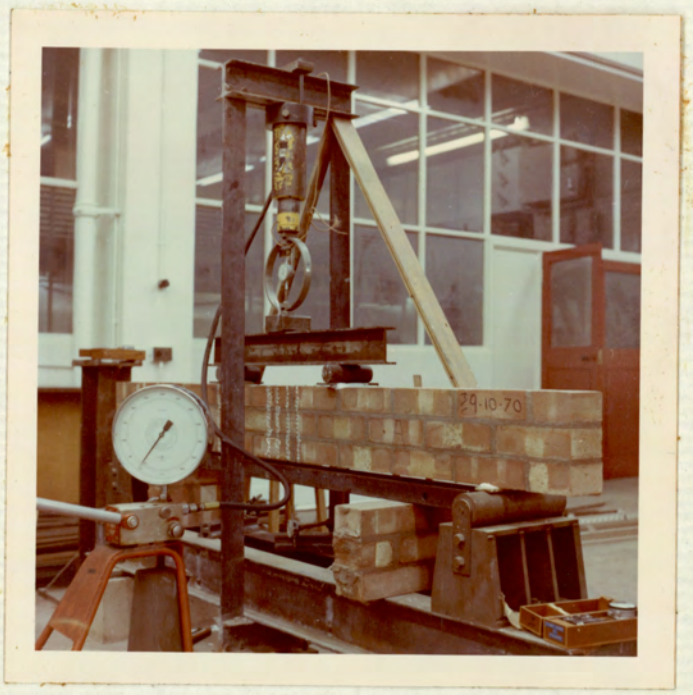

PLATE 8.1

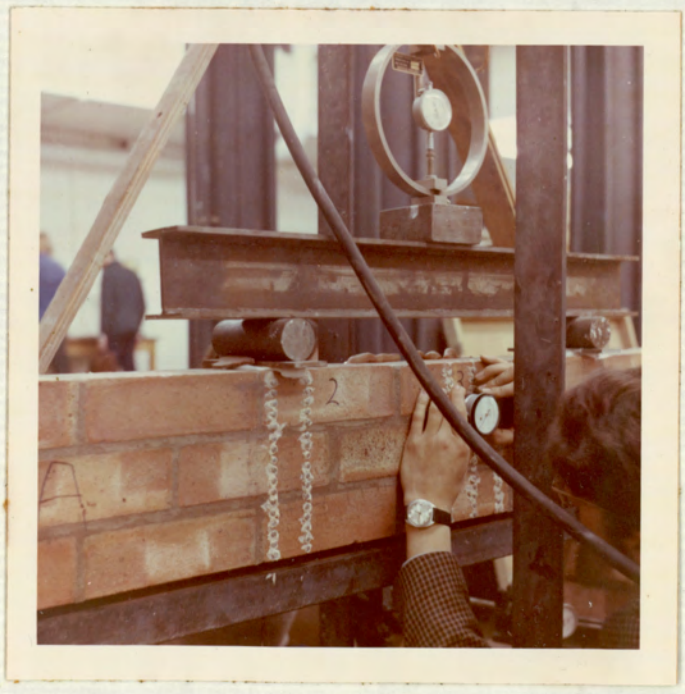

PLATE 8.2

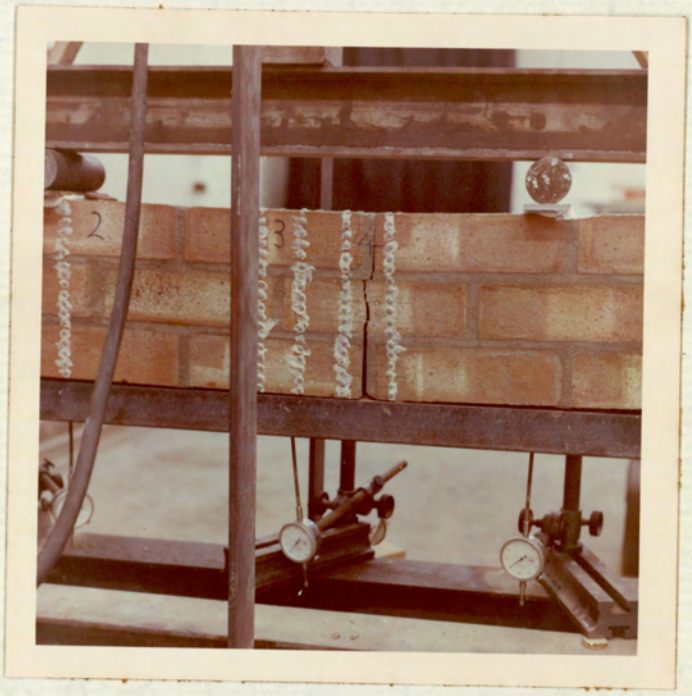

PLATE 8.3

8.4 TEST RESULTS

BEAM NO.	COURSES DEPTH	MORTAR MIX	DATE BUILT	DATE TESTED
* 1	3	1.0.3	13.10.70	17.11.70
2	3	1.0.3	16.12.70	26. 1.71
3	3	1.0.3	16.10.70	2. 2.71
+4	3	1.1.5	16.10.70	12. 1.71
5	3	1.1.5	16.10.70	19. 1.71
6	2	1.0.3	13.10.70	24.11.70
7	2	1.0.3	16.12.70	2. 2.71
8	2	1.1.5	16.10.70	26.1. 71

* TESTED USING DEMEC GAUGES UNSATISFACTORY STRAIN READING RESULTS NOT INCLUDED

\+ FAULT IN STRAIN GAUGES RESULTS NOT INCLUDED

SUMMARY OF TEST BEAMS

8.4.1. BEAM DEFLECTIONS

BRICK BEAM NO.2

Mortar Mix 1.3
Depth 3 course

Constructed 16.12.70
Tested 26.1.71

	Deflection (Inches x 10^{-3})		
LOAD lbf	Left Hand	Right Hand	Central
50	0.9	1.0	2
100	1.5	2.4	2.5
150	3.2	3.5	3.5
200	4.6	5.3	5.0
250	6.4	7.0	6.75
300	6.75	11.4	9
350	15.7	16.5	15.4

BRICK BEAM NO.3

Mortar Mix 1.3
Depth 3 Course

Constructed 16.10.70
Tested 2.2.71

	Deflection (Inches x 10^{-3})		
LOAD lbf	Left Hand	Right Hand	Central
50	1.1	1.8	1.2
100	2.3	2.9	2.4
150	3.4	4.0	3.7
200	4.8	5.3	5.2
250	6.1	6.5	6.5
300	7.8	8.1	8.3
350	9.4	9.4	10.2
400	10.8	10.7	11.7
450	12.2	12.1	13.3
500	14.1	15.0	13.7

BRICK BEAM NO.4

Mortar Mix 1.1.5
Depth 3 course

Constructed 16.10.70
Tested 12.1.71

	Deflection (Inches x 10^{-3})		
LOAD lbf	Left Hand	Right Hand	Central
50	1.0	1.6	1.5
100	1.7	2.4	2.7
150	2.9	3.4	4.0
200	4.1	4.6	5.5
250	5.6	6.0	7.0
300	6.9	7.1	8.5
350	8.1	8.5	10.0
400	11.0	13.1	13.8
450	13.5	16.0	16.7

BRICK BEAM NO.5

Mortar Mix 1.1.5
Depth 3 course

Constructed 16.10.70
Tested 19.1.71

	Deflection ($I_n$ches x 10^{-3})		
LOAD lbf	Left Hand	Right Hand	Central
50	0.7	1.1	1.3
100	1.8	2.3	2.6
150	2.8	3.4	3.9
200	4.0	4.8	5.3
250	5.2	5.9	7.0
300	6.9	7.5	8.8
350	9.7	10.9	12.5
400	13.1	15.0	17.2

BRICK BEAM NO.6

Mortar Mix 1.3
Depth 2 course

Constructed 13.10.70
Tested 24.11.70

	Deflection (Inches x 10^{-3})		
LOAD lbf	Left Hand	Right Hand	Central
10	0.8	0.5	0.7
20	1.8	1.5	1.7
30	2.6	2.1	2.5
40	3.3	3.0	3.3
50	4.3	4.0	4.5
60	4.9	4.9	5.2
70	5.8	5.8	6.2
80	6.6	6.5	7.2
90	7.4	7.2	8.1
100	8.3	8.1	9.0
110	8.8	9.2	9.9
120	9.9	10.1	10.9

BRICK BEAM NO.7

Mortar Mix 1.3
Depth 2 course

Constructed 16.12.70
Tested 2.2.71

	Deflection (Inches x 10^{-3})		
LOAD lbf	Left Hand	Right Hand	Central
10	0.3	1.2	0.3
20	1.2	2.1	1.2
40	2.8	3.9	3.2
60	4.5	5.3	5.3
80	6.2	7.4	7.4
100	8.0	9.2	9.8
120	9.9	11.1	12.0

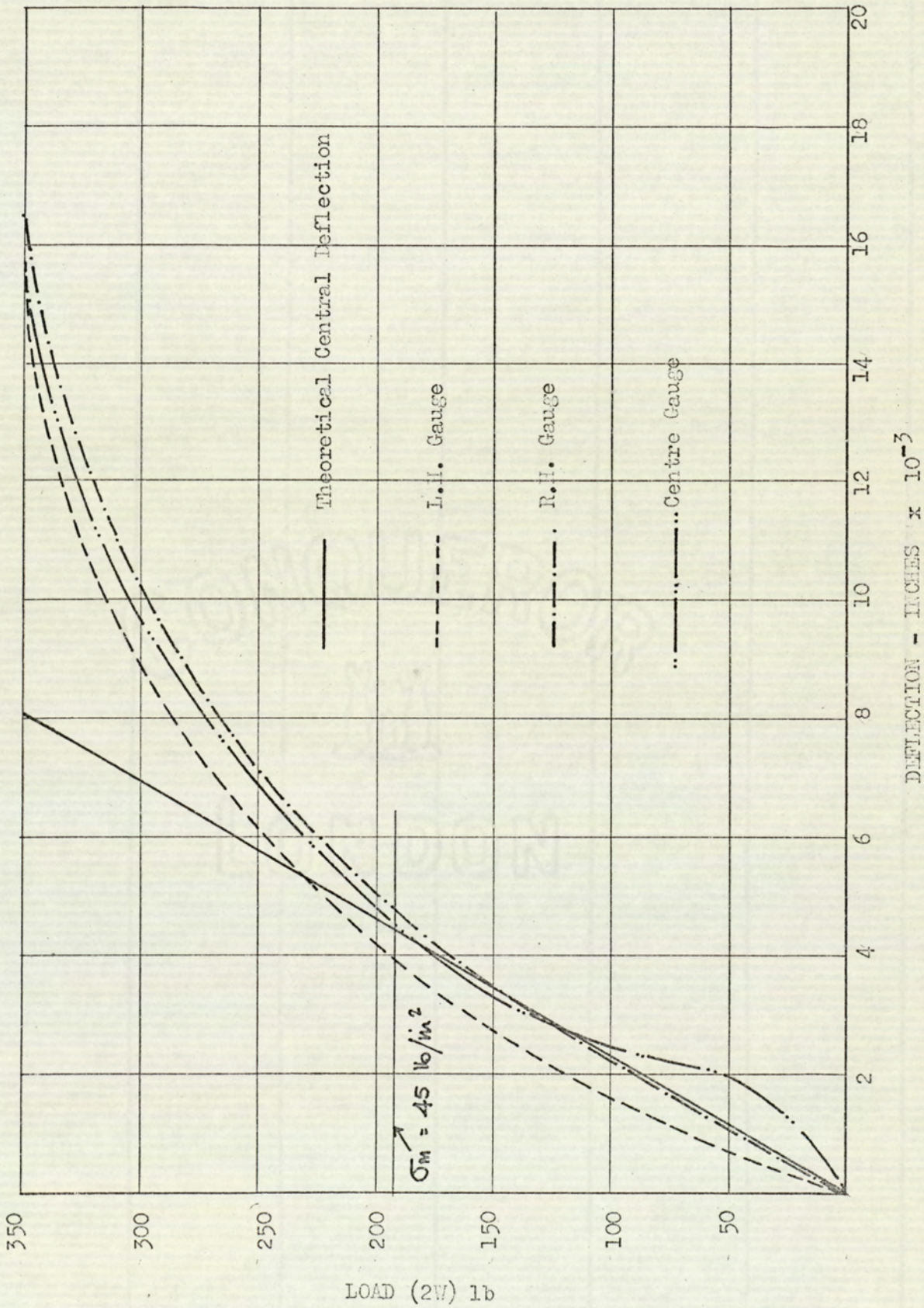

LOAD/DEFLECTION RELATIONSHIP BEAM NO.2

Fig. 8.4.1. 1

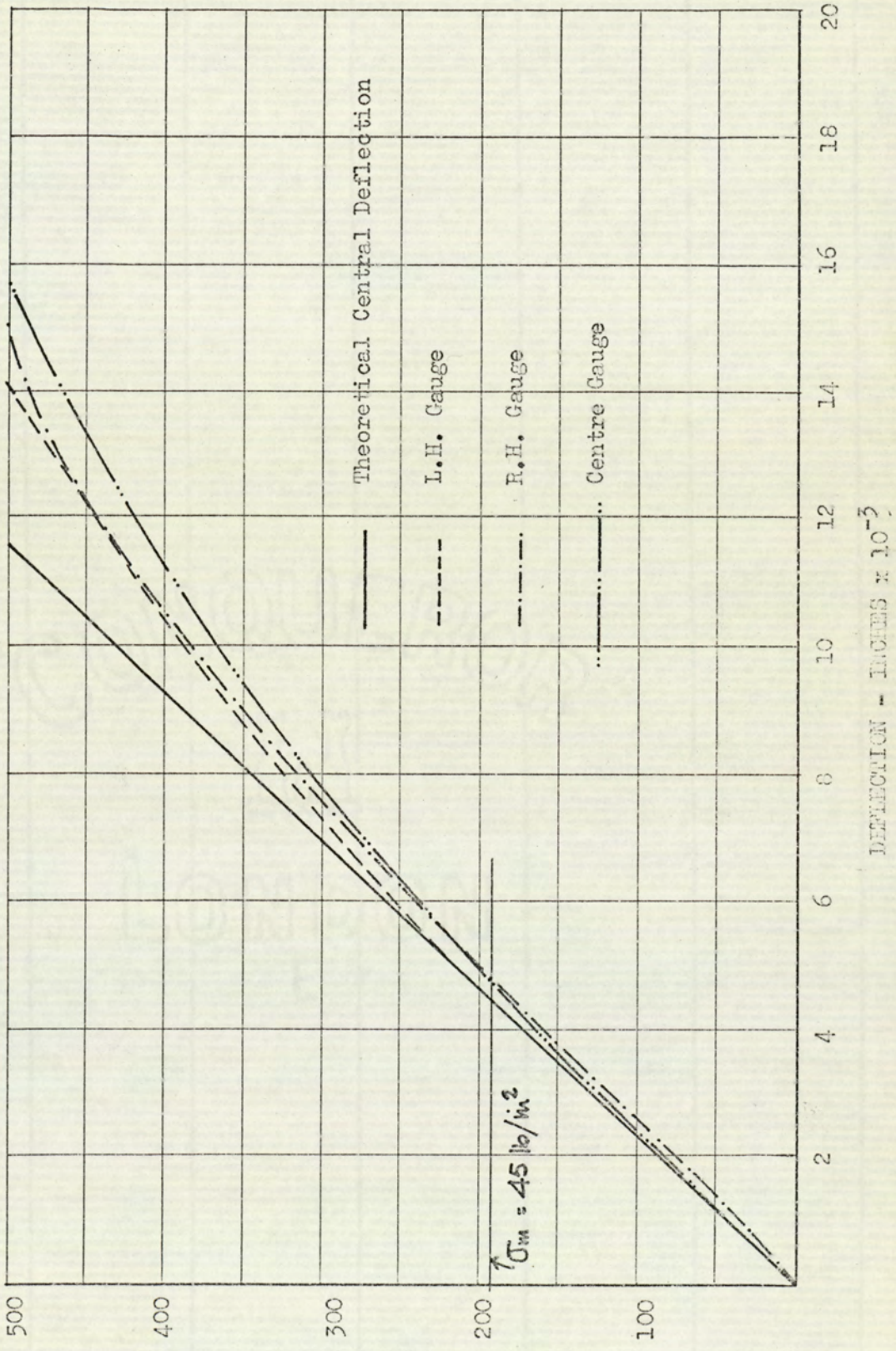

LOAD/DEFLECTION RELATIONSHIP BEAM NO.3

Fig. 8.4.1. 2

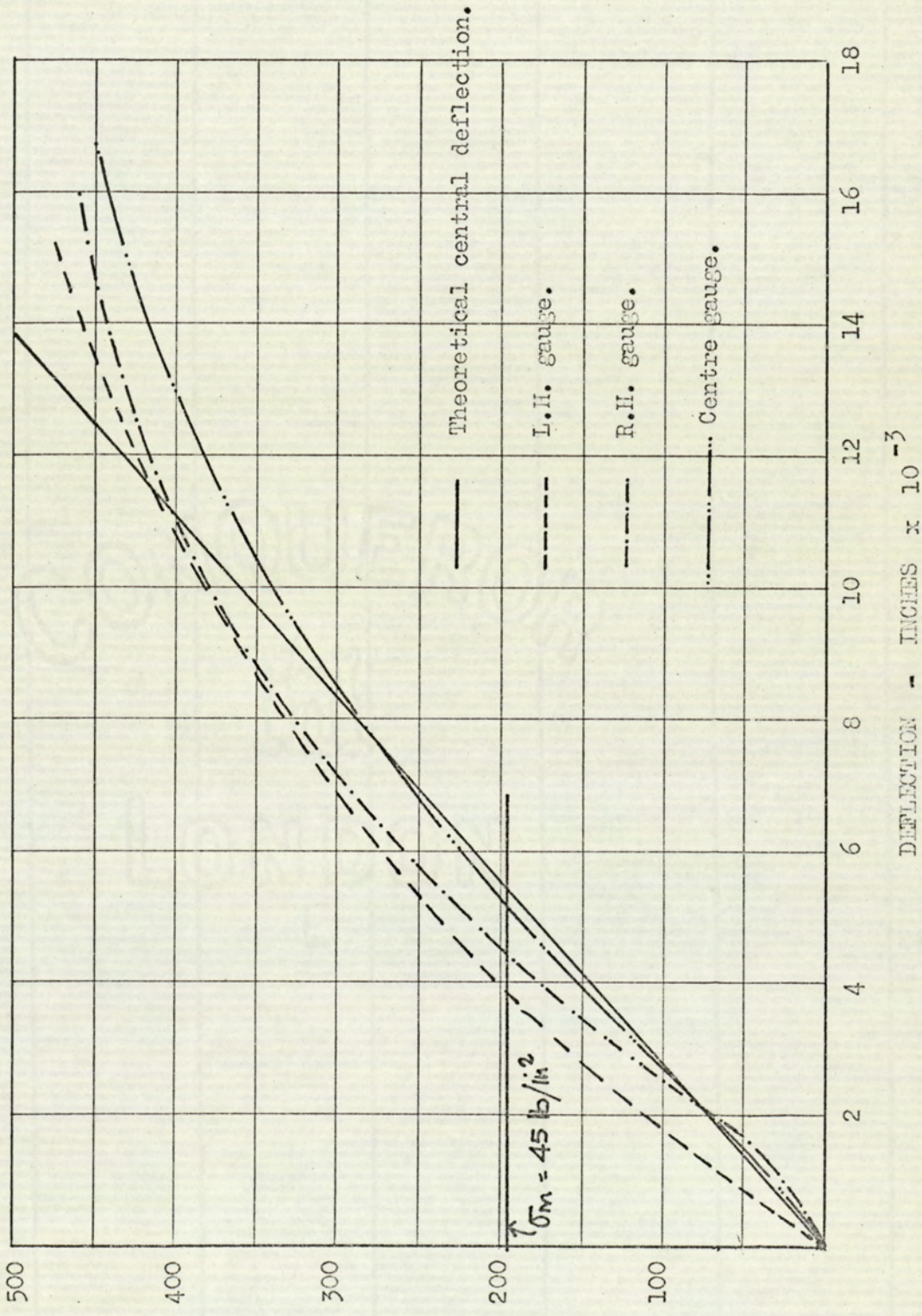

LOAD/DEFLECTION RELATIONSHIP BEAM NO.4

Fig.8.4.1. 3

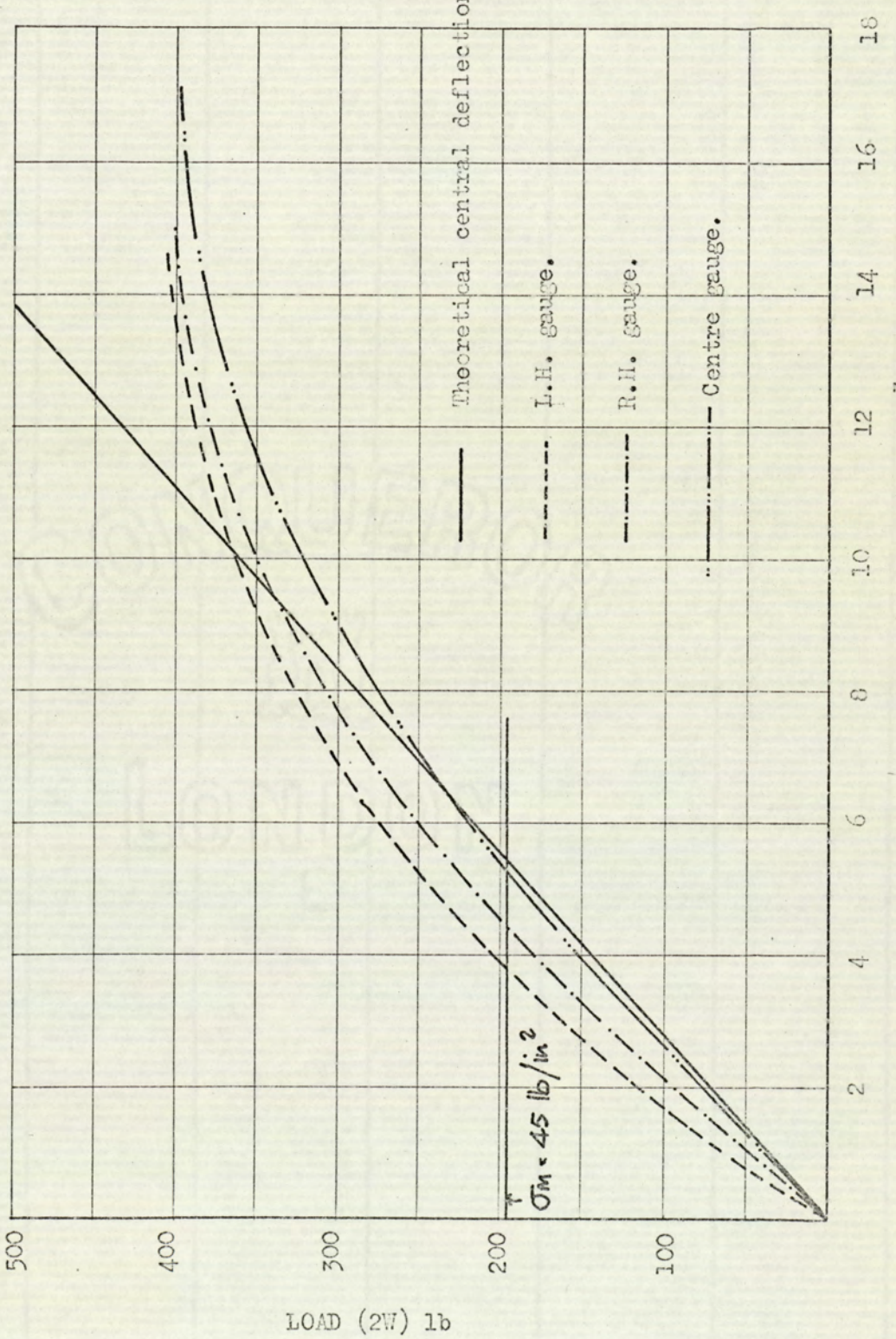

LOAD/DEFLECTION RELATIONSHIP BEAM NO.5

Fig.8.4.1 4

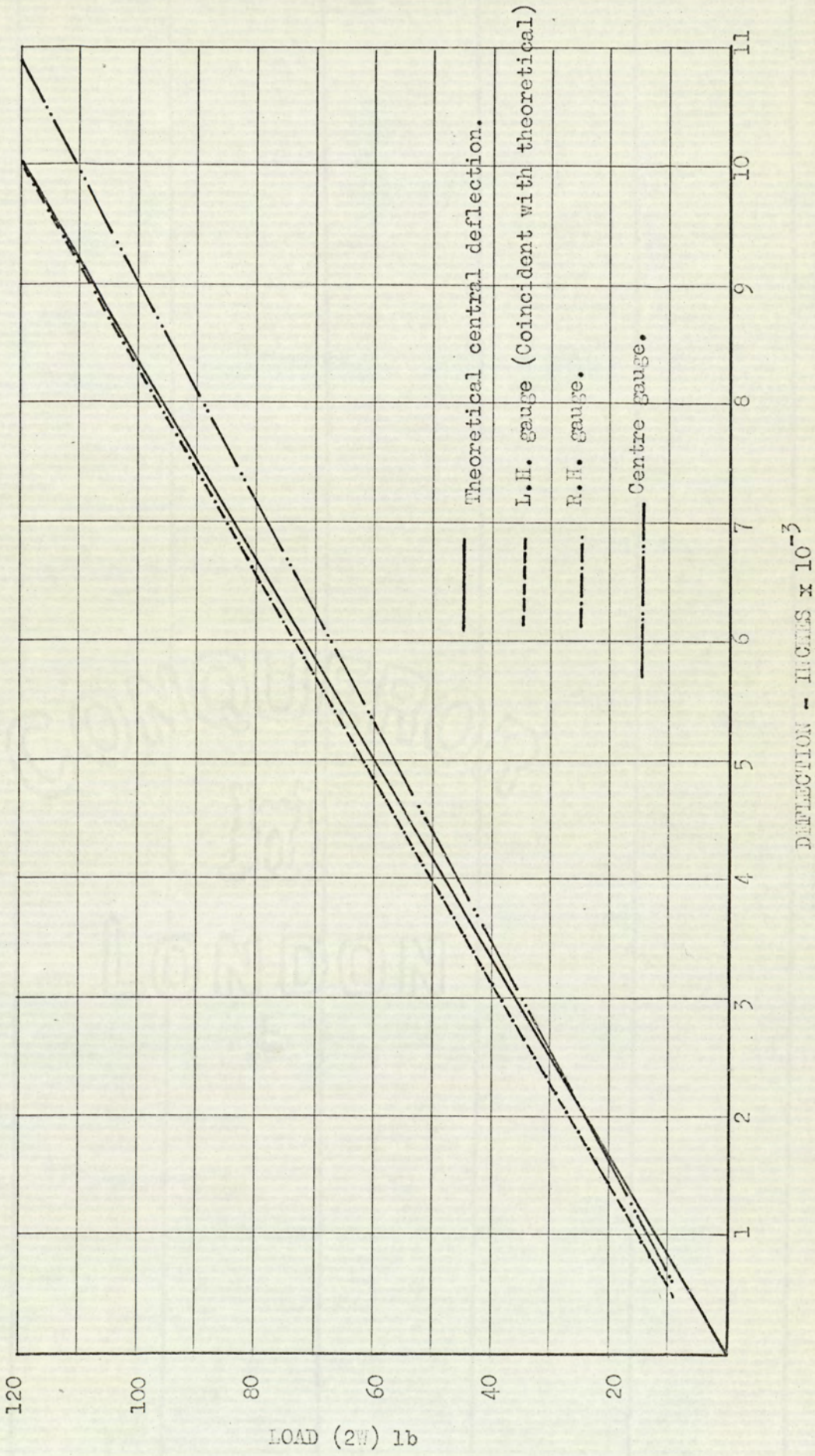

LOAD/DEFLECTION RELATIONSHIP BEAM NO.6

Fig. 8.4.1. 5

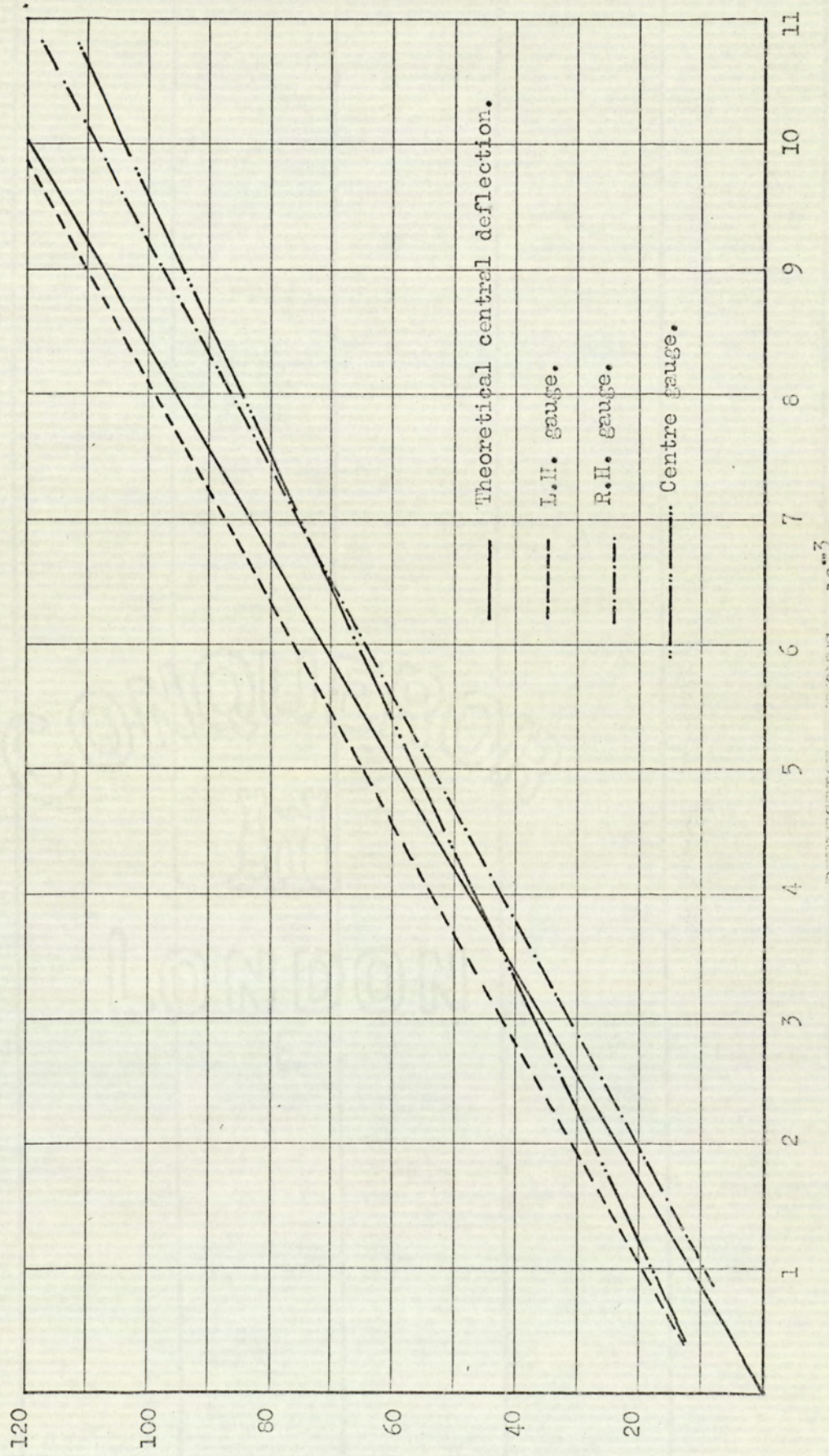

LOAD/DEFLECTION RELATIONSHIP BEAM NO. 7

Fig.8.4.1 6

8.4.2 LONGITUDINAL STRAINS

BRICK BEAM NO.2

Mortar Mix 1.3
Depth 3 course
Section No. B-M-B

Constructed 16.12.70
Tested 26.1.71

Load lbf	MICROSTRAINS								
	1	2	3	4	5	6	7	8	9
Self Wt	-27	-24	-10	-2	-1	+11	+26	+26	+29
50	-48	-46	-29	-23	-21	-5.5	+7	+15	+16
100	-57	-55	-35	-27	-20	-1	+7	+20	+21
150	-64.5	-61.5	-43	-32	-20.5	-2	+12	+24	+23
200	-73	-68	-50	-31	-20	0	+17	+37	+27
250	-86	-77	-52	-27	-10	+8	+26	+24	+38
300	-102	-86	-50	-28	-7	+10	+26	+35	+37
350	-147	-104	-50	-5	+17	+22	+32	+32	+32.5
$\bar{x}$	-82	-71	-44	-25	-12	+5	+18	+27	+28

BRICK BEAM NO.2

Mortar Mix 1.3
Depth 3 course
Section No. M-B-M

Constructed 16.12.70
Tested 26.1.71

Load lbf	MICROSTRAINS								
	1	2	3	4	5	6.	7	8	9
Self Wt	-17	-12	-8	-4	+3	+9	+54	+70	+87
50	-46	-34	-25	-16	-6	.0	+64	+89	+121
100	-54.5	-37	-30	-21	-11	+4	+110	+160	+240
150	-67	-50	-45	-27	-11	+7	+139	+260	+407
200	-78	-58	-51	-30.3	-9	+19	+311	+302	+653
250	-84.5	-60	-49	-26	-5	+38	+503.5	+604	+1005
300	-115	-80	-61	-17	+11	+98	+1054	+1069	+1948
350	-246	-114	-55	-9	+64	+144			
$\bar{x}$	-99	-62	-45	-21	+5	+44	+363	+412	+729

The magnitude of strain readings for gauges 7, 8 & 9, suggest that these were either faulty readings or that some type of premature failure that had not been detected had taken place.

BRICK BEAM NO.2

Mortar Mix 1.3
Depth 3 course
Section No. B-B-B

Constructed 16.12.70
Tested 26.1.71

Load lbf	MICROSTRAINS								
	1	2	3	4	5	6	7	8	9
Self Wt	-13	-12	-11	-5	-2	+3	+6	+15	+22
50	-30	-28	-27	-22	-16	-10	-6	+4	+13
100	-36	-29	-30	-21	-17	-8	+1	+8	+20
150	-45	-42	-37	-27	-19	-9.5	-1	+12	+25
200	-51	-45	-42	-30	-19	-9	+2	+18	+29
250	-57	-50	-48	-35	-21	-9	+4.5	+20.5	+29
300	-61	-44	-43	-28	-14.5	-1	+13	+29	+38
350	-62.5	-55	-51	-33	-16	-4	+11	+26	+36.5
$\bar{x}$	-49	-42	-40	-28	-18	-7	+3	+17	+27

BRICK BEAM NO.3

Mortar Mix 1.3
Depth 3 course
Section No. M-B-M

Constructed 16.10.70
Tested 2.2.71

Load lbf	MICROSTRAINS								
	1	2	3	4	5	6	7	8	9
Self Wt	-55	-44	-42	-38	-25	-18	+9	+40	+70
50	-44	-32	-28	-22	-10	0	+32	+65	+98
100	-44	-29	-23	-18	-7	+11	+48	+90	+131
150	-46	-32	-22	-17	-2	+15	+64	+118	+176
200	-50	-35	-26	-18	-4	+19	+77	+148	+215
250	-52	-38	-27	-20	-5	+26	+107	+191	+285
300	-64	-53	-41	-30	-11	+17	+117	+217	+320
350	-62	-47	-32	-22	+1	+27	+146	+259	+371
400	-67	-50	-32	-21	-1	+41	+174	+300	+424
450	-71	-55	-35	-24	+3	+49	+205	+347	+486
500	-74	-57	-35	-23	+5	+59	+239	+397	+550
$\bar{x}$	-57	-49	-30	-22	-16	+26	+120	+213	+306

BRICK BEAM NO.3

Mortar Mix 1.3
Depth 3 course
Section No. B-B-B

Constructed 16.10.70
Tested 2.2.71

Load lbf	MICROSTRAINS								
	1	2	3	4	5	6	7	8	9
Self Wt	-58	-65	-61	-59	-42	-41	-25	-16	-7
50	-39	-46	-42	-33	-18	-17	-1	+3	+19
100	-37	-39	-38	-27	-8	-8	+10	+17	+33
150	-40	-40	-34	-25	-7	0	+16	+25	+39
200	-44	-42	-36	-24	-5	-1	+19	+29	+47
250	-47	-44	-38	-23	-4	+4	+24	+36	+53
300	-71	-68	-62	-48	-26	-20	+1	+12	+34
350	-62	-60	-49	-32	-7	0	+25	+37	+60
400	-65	-63	-53	-32	-6	+6	+28	+42	+66
450	-71	-69	-54	-36	-8	+4	+32	+47	+72
500	-73	-68	-55	-33	-2	+9	+39	+53	+80
$\bar{x}$	-55	-54	-46	-31	-9	-2	+19	+31	+50

BRICK BEAM NO.3

Mortar Mix 1.3
Depth 3 course
Section No. B-M-B

Constructed 16.10.70
Tested 2.2.71

Load lbf	MICROSTRAINS								
	1	2	3	4	5	6	7	8	9
Self Wt	-57	-60	-54	-35	-34	-13	-1	+2	+23
50	-43	-39	-31	-19	-12	-4	+12	+22	+44
100	-42	-33	-26	-14	-7	+3	+19	+30	+54
150	-48	-36	-28	-13	-5	+6	+23	+35	+62
200	-57	-44	-31	-18	-6	+5	+25	+39	+68
250	-62	-48	-33	-15	-4	+9	+28	+45	+75
300	-90	-83	-57	-31	-18	-1	+21	+35	+70
350	-77	-61	-43	-22	-6	+10	+37	+50	+89
400	-86	-65	-44	-23	-8	+9	+31	+52	+94
450	-91	-70	-46	-22	-5	+12	+35	+60	+103
500	-100	-73	-48	-24	-3	+15	+40	+63	+107
$\bar{x}$	-69	-55	-39	-20	-7	+6	+27	+43	+77

BRICK BEAM NO.5

Mortar Mix 1.1.5
Depth 3 course
Section No. B-M-B

Constructed 16.10.70
Tested 19.1.71

Load lbf	MICROSTRAINS								
	1	2	3	4	5	6	7	8	9
Self Wt	-28	-20	-16	-13.5	-1	+5	+15	+18	+32
50	-33	-26	-16	-16	-0.5	+6	+14	+21	+35
100	-36	-27	-17	-19	0	+8	+17	+29	+46
150	-41	-33	-19	-19	-1	+11	+22	+36	+54
200	-47	-33	-19	-20	+4	+16	+29	+42	+63
250	-53	-40	-26	-23	+5	+17	+30	+46	+72
300	-60	-43	-24	-24	+10	+27	+37	+55	+84
350	-81	-58	-21	(-1)	+48	+58	+52	+59	+82
400	-90	-59	-10	(+27)	+84	+91	+68	+66	+85
$\bar{x}$	-55	-40	-19	-20	+18	+29	+34	+44	+65

BRICK BEAM NO.5

Mortar Mix 1.1.5
Depth 3 course
Section No. M-B-M

Constructed 16.10.70
Tested 19.1.71

Load lbf	MICROSTRAINS								
	1	2	3	4	5	6	7	8	9
Self Wt	-28	-59.5	-74	-16	-5	+4	+3.5	+14	+21
50	-29	-67	-88	-19	-5	+4.5	+10	+17	+27
100	-37	-83	-106	-23	-7	+10	+11.5	+20	+34
150	-42	-90	-115	-22	-6	+10	+14	+24	+38
200	-47	-101	-127	-23	-5	+14	+20	+33	+48
250	-54	-114	-141	-25	-2	+19	+24	+34	+52
300	-62	-130	-162	-35	-2	+20	+28	+38	+59
350	-69	-141	-172	-32	-3	+21	+34	+41.5	+64
400	-67	-149	-181	-25	+5	+33	+51	+58	+84
$\bar{x}$	-51	-109	-136	-25	-4	+16	+24	+33	+51

BRICK BEAM NO.5

Mortar Mix 1.1.5
Depth 3 course
Section No. B-B-B

Constructed 16.10.70
Tested 19.1.71

Load lbf	MICROSTRAINS								
	1	2	3	4	5	6	7	8	9
Self Wt	-33	-24	-12	-10	-7	-5	+19	+13	+13
50	-37	-33	-18	-12	-9	-4	+24	+17	+15
100	-36	-33	-21	-16	-13	-4	+28	+23	+19
150	-38	-36	-23	-21	-11	-3	+34	+28	+19
200	-39	-36	-19	-13	-4	+4	+42	+39	+24
250	-43	-40	-22	-16	-7	+3	+48	+42	+24
300	-48	-52	-25	-15	-8	+7	+60	+51	+27
350	-47	-41	-12	-02	+5	+24	+64	+67	+46
400	-51	-41	-5	+11	+17	+35	+73	+76	+52
$\bar{x}$	-42	-39	-18	-10	-4	+8	+47	+43	+28

BRICK BEAM NO.6

Mortar Mix 1.3
Depth 2 course

Constructed 13.10.70
Tested 24.11.70

Section No. B-M

Load lbf	MICROSTRAINS					
	1	2	3	4	5	6
10	-1	-4.5	-4.5	-7.5	-4.5	-1.5
20	-5.5	-14	-8	-7.5	-4.5	-0.5
30	-11.5	-17.5	-11.5	-14.5	-6.5	+10.5
40	-13	-21.5	-15.5	-14.5	-4.5	+5
50	-18	-31	-22	-21.5	-8.5	+1
60	-21.5	-36	-26	-23.5	-6.5	+1
70	-23	-38.5	-27.5	-25.5	-5.	+5.5
80	-28	-48.5	-32	-30.5	-5.5	+4
90	-33	-59.5	-39	-30.5	-6.5	+6
100	-33	-61.5	-39	-30.5	-7.5	+6
110	-36	-65.5	-40	-24.5	-3.5	+16
120	-33	-64.5	-34	-24.5	+6.5	+27
$\bar{x}$	-21	-39	-25	-21	-4.7	+7

BRICK BEAM NO.6

Mortar Mix 1.3
Depth 2 course
Section No. M-B

Constructed 13.10.70
Tested 24.11.70

Load lbf	MICROSTRAINS					
	1	2	3	4	5	6
10	-12.5	-10	-10.5	-3	+2	+5.5
20	-18	-16	-14	-3.5	+1	+6.5
30	-26	-25	-20.5	-7.5	+1	+6.5
40	-35	-32	-25	-7	+3	+10.5
50	-42	-43	-32	-11	0	+5.5
60	-51.5	-51.5	-38	-15	-2	+8
70	-55	-54	-39.5	-13	0	+10
80	-62	-62	-44	-13	+3	+12.5
90	-73	-71	-50	-16	+2	+13.5
100	-79	-76	-52	-16	+4	+14.5
110	-88	-82	-55	-18	+4	+12.5
120	-89	-80	-50	-10	+13	+21.5
$\bar{x}$	-53	-50	-36	-11	+2.5	+10.6

BRICK BEAM NO.7

Mortar Mix 1.3
Depth 2 course
Section No. B-M

Constructed 16.12.70
Tested 2.2.71

	MICROSTRAINS					
LOAD lbf	1	2	3	4	5	6
SELF WT	-19	-7	+3	+22	+34	+38
10	-22	-8	+3	+26	+40	+43
20	-23	-9	+4	+28	+44	+50
40	-37	-11	+3	+30	+50	+56
60	-45	-11	+5	+33	+58	+63
80	-52	-20	+3	+37	+64	+71
100	-61	-22	+1	+39	+71	+78
120	-68	-25	+2	+44	+78	+89
140	-71	-27	+3	+50	+90	+98
160	-74	-33	0	+54	+100	+106
180	-84	-39	-3	+58	+112	+115
$\bar{x}$	-54	-20	+2	+40	+71	+77

BRICK BEAM NO.7

Mortar Mix 1.3
Depth 2 course
Section No. B-B

Constructed 16.12.70
Tested 2.2.71

	MICROSTRAINS					
LOAD LBF	1	2	3	4	5	6
SELF WT	+3	+10	+15	+24	+37	+14
10	-1	+13	+19	+31	+38	+28
20	-3	+13	+19	+33	+44	+41
40	-5	+14	+20	+37	+46	+63
60	-10	+11	+21	+40	+53	+82
80	-14	+9	+22	+44	+57	+107
100	-16	+7	+23	+45	+62	+131
120	-23	+7	+25	+52	+67	+156
140	-29	+3	+26	+58	+73	+176
160	-35	+3	+27	+61	+76	+194
180	-38	+1	+28	+62	+75	+189
200	-40	0	+25	+64	+79	+186
$\bar{x}$	-19.5	+7	+33	+48	+61	+123

BRICK BEAM NO.7

Mortar Mix 1.3
Depth 2 course
Section No. M-B

Constructed 16.12.70
Tested 2.2.71

	MICROSTRAINS					
LOAD LBF	1	2	3	4	5	6
SELF WT	-24	-3	+10	+34	+46	+50
10	-24	-5	+9	+35	+47	+55
20	-24	-5	+10	+38	+53	+60
40	-28	-8	+10	+39	+53	+67
60	-36	-12	+8	+39	+58	+72
80	-38	-14	+10	+43	+64	+80
100	-43	-16	+9	+49	+70	+86
120	-52	-20	+9	+52	+77	+95
140	-55	-24	+10	+54	+84	+101
160	-62	-27	+8	+55	+83	+106
180	-75	-32	+3	+57	+86	+115
$\bar{x}$	-44	-16	+9	+46	+67	+ 84

BRICK BEAM NO.8

Mortar Mix 1.1.5
Depth 2 course
Section No. B-B

Constructed 16.10.70
Tested 26.1.71

	MICROSTRAINS					
	*	2	3	4	5	6
SELF WT	-26	-10	-7	+1	+9	+22
10	-24	-7	-7	+1	+10	+24
20	-28	-4	-7	+1	+11	+27
30	-35	-7	-13	-2	+11	+25
$\bar{x}$	-29	-6	- 9	0	+11	+26

BRICK BEAM NO.8

Mortar Mix 1.1.5
Depth 2 course
Section No. M-B

Constructed 16.10.70
Tested 26.1.71

	MICROSTRAINS					
	1	2	3	4	5	6
SELF WT	-62	-33	-24	+1	+12	+23
10	-61	-36	-23	+3	+13	+27
20	-66	-38	-25	+3	+14	+29
30	-67	-37	-25	+3	+17	+29
$\bar{x}$	-65	-37	-25	+3	+15	+28

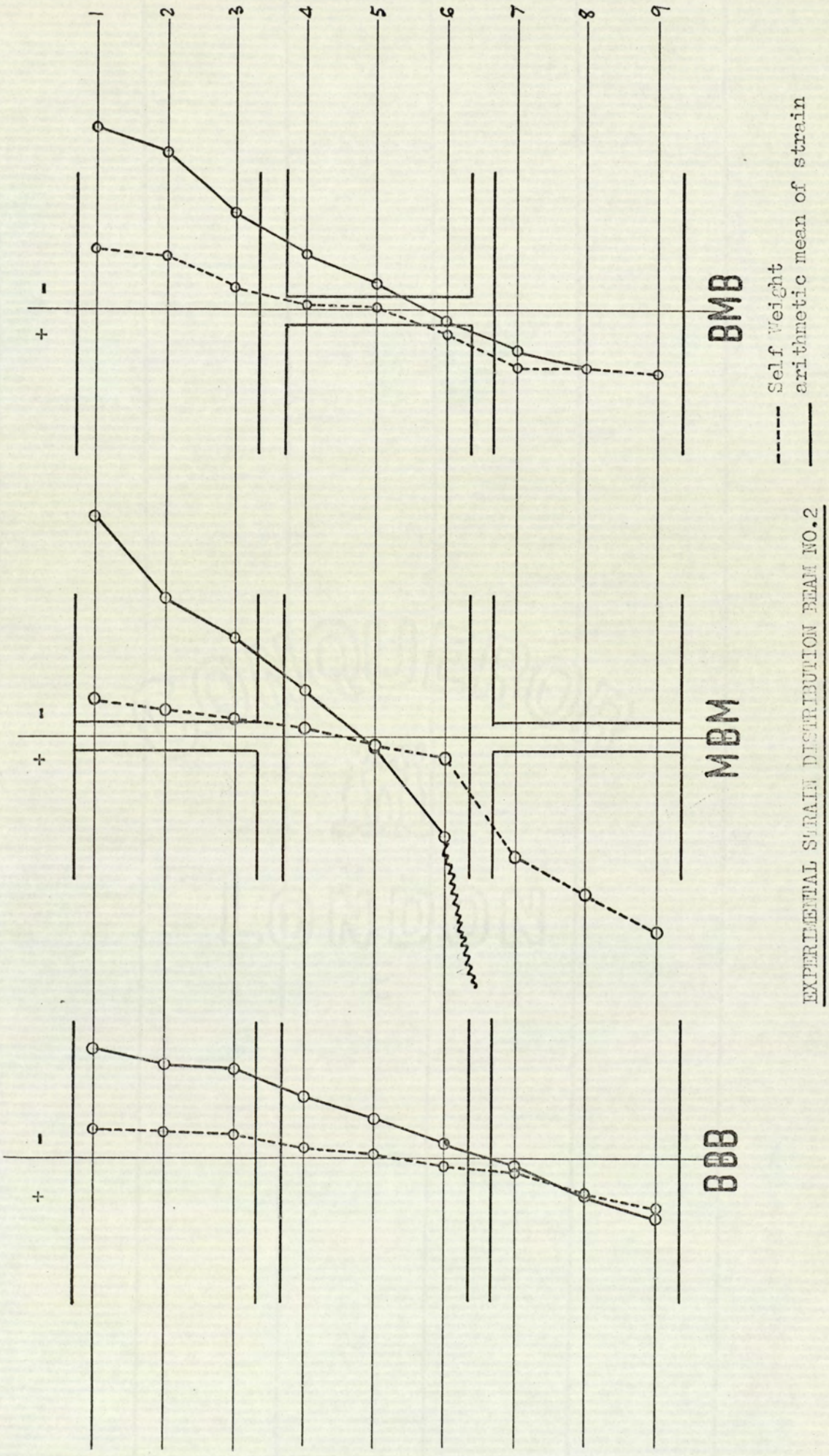

EXPERIMENTAL STRAIN DISTRIBUTION BEAM NO.2

Fig. 8.4.2. 1

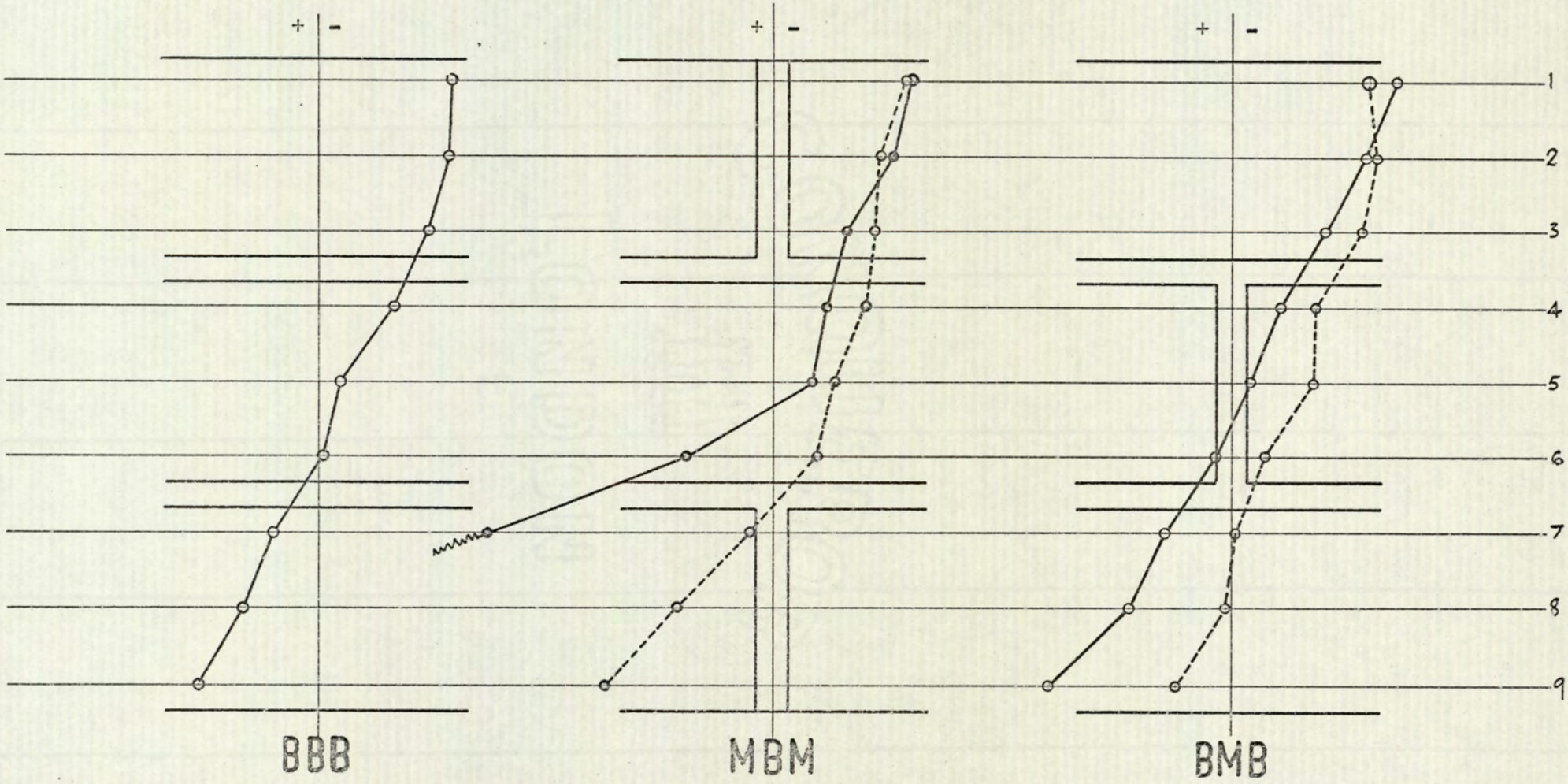

(Strain readings for self weight unsatisfactory)

----- Self Weight

_____ arithmetic mean of strain

EXPERIMENTAL STRAIN DISTRIBUTION BEAM NO.3

Fig.8.4.2. 2

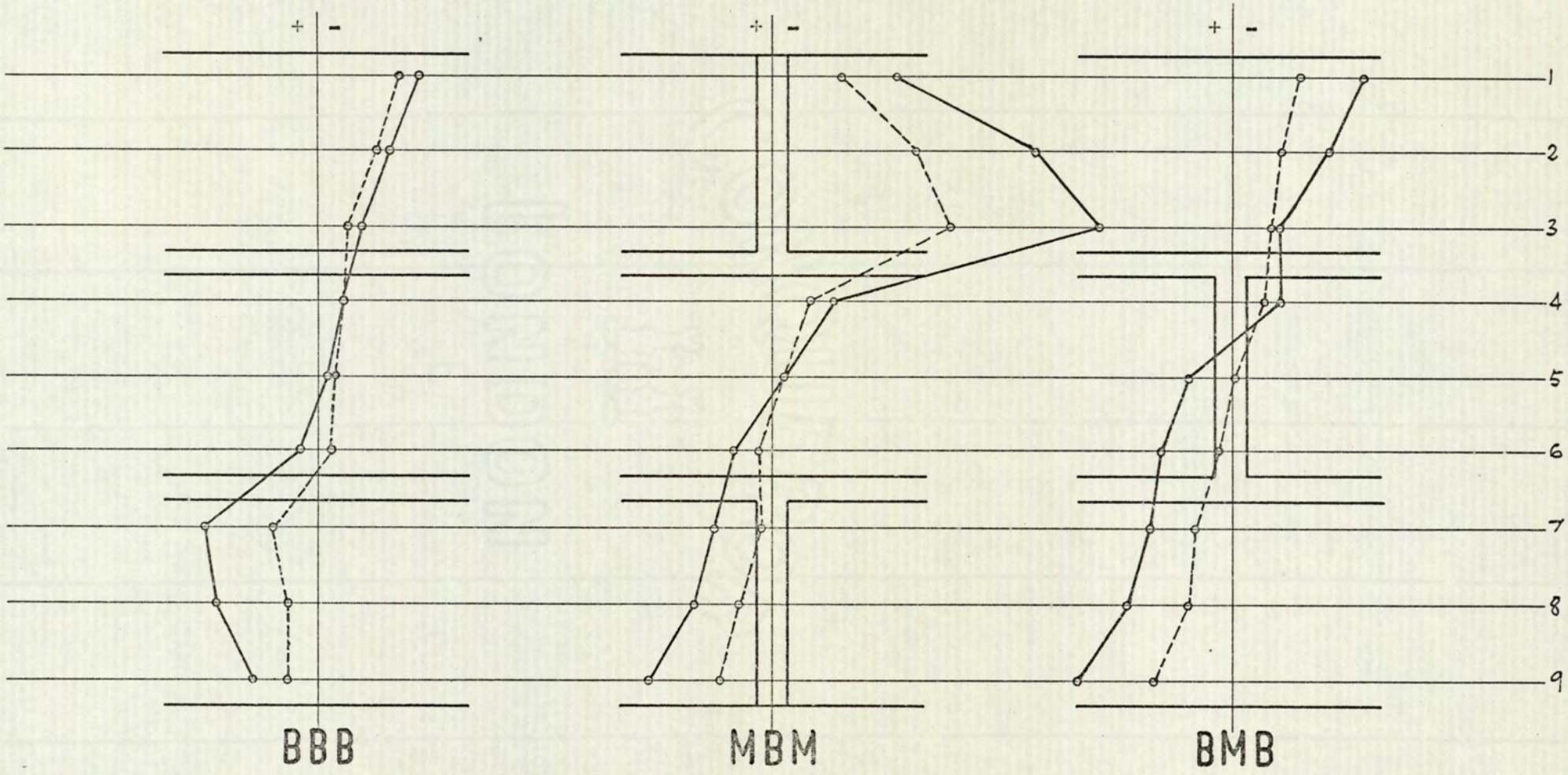

EXPERIMENTAL STRAIN DISTRIBUTION BEAM NO.5

Fig. 8.4.2. 3

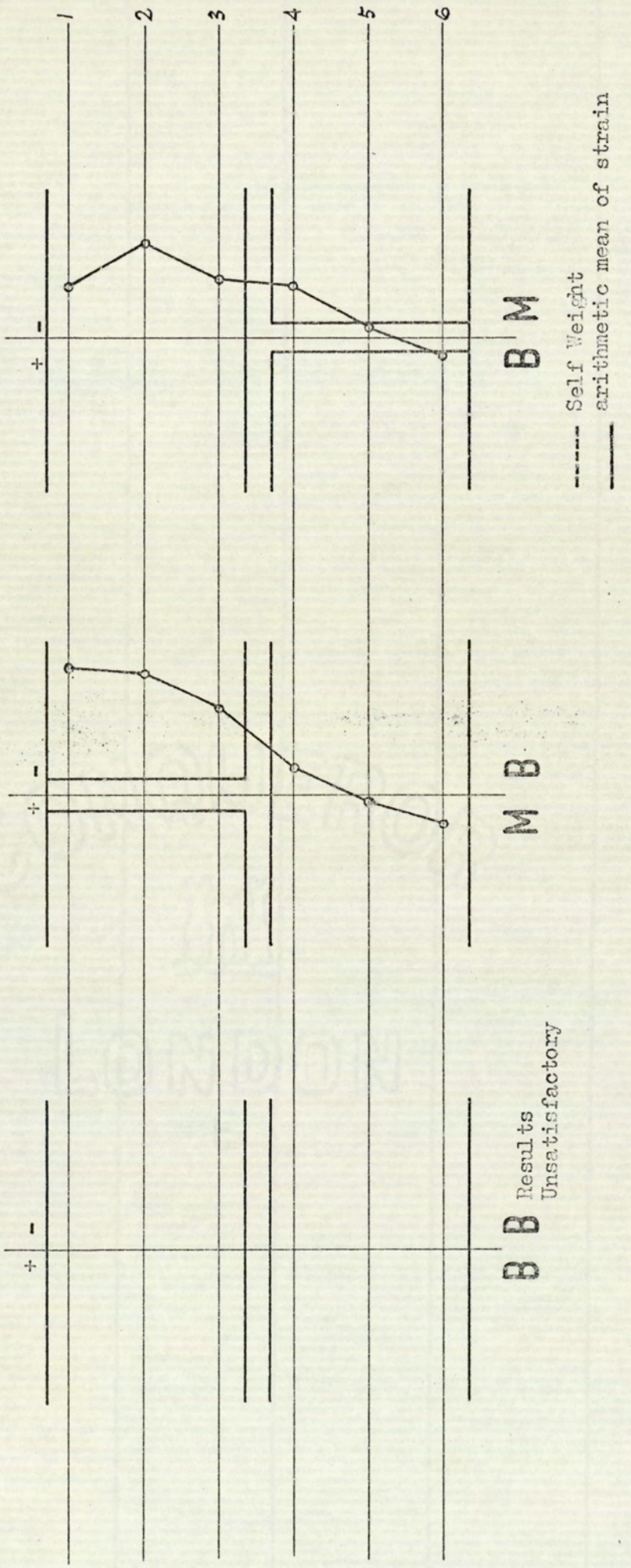

EXPERIMENTAL STRAIN DISTRIBUTION BEAM NO.6

Fig.8.4.2. 4

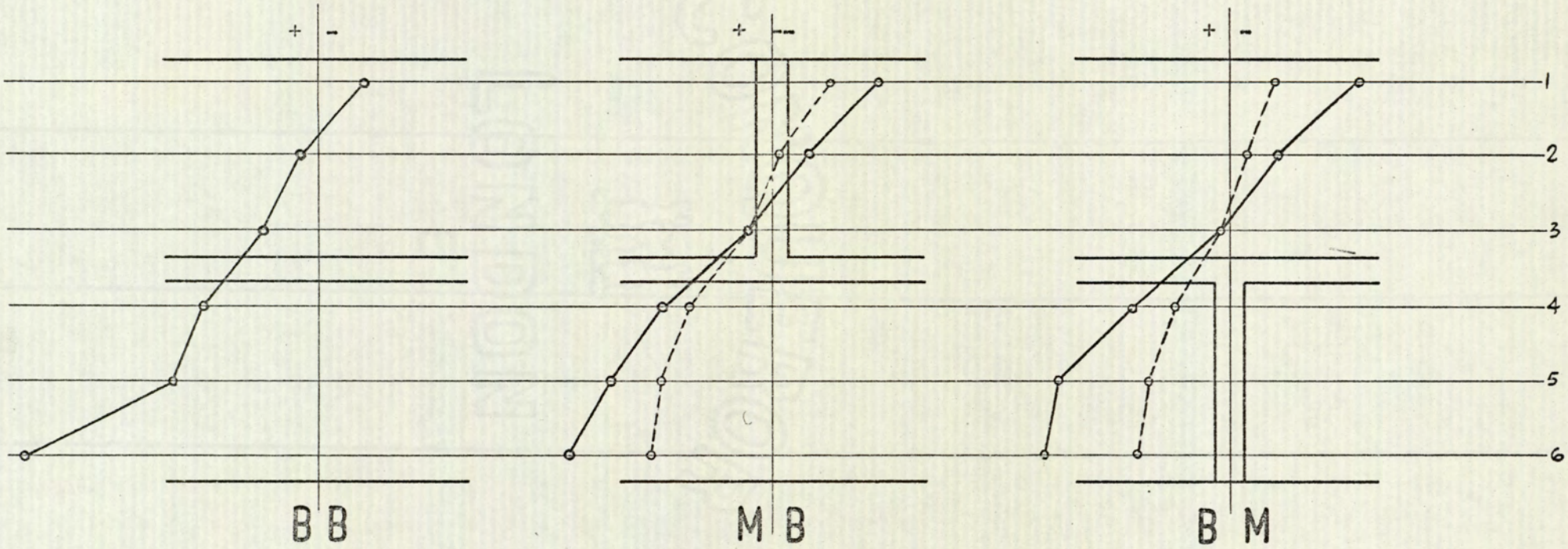

(Strain readings for self weight unsatisfactory)

----- Self Weight

_____ arithmetic mean of strain

EXPERIMENTAL STRAIN DISTRIBUTION BEAM NO.7

Fig.8.4.2. 5

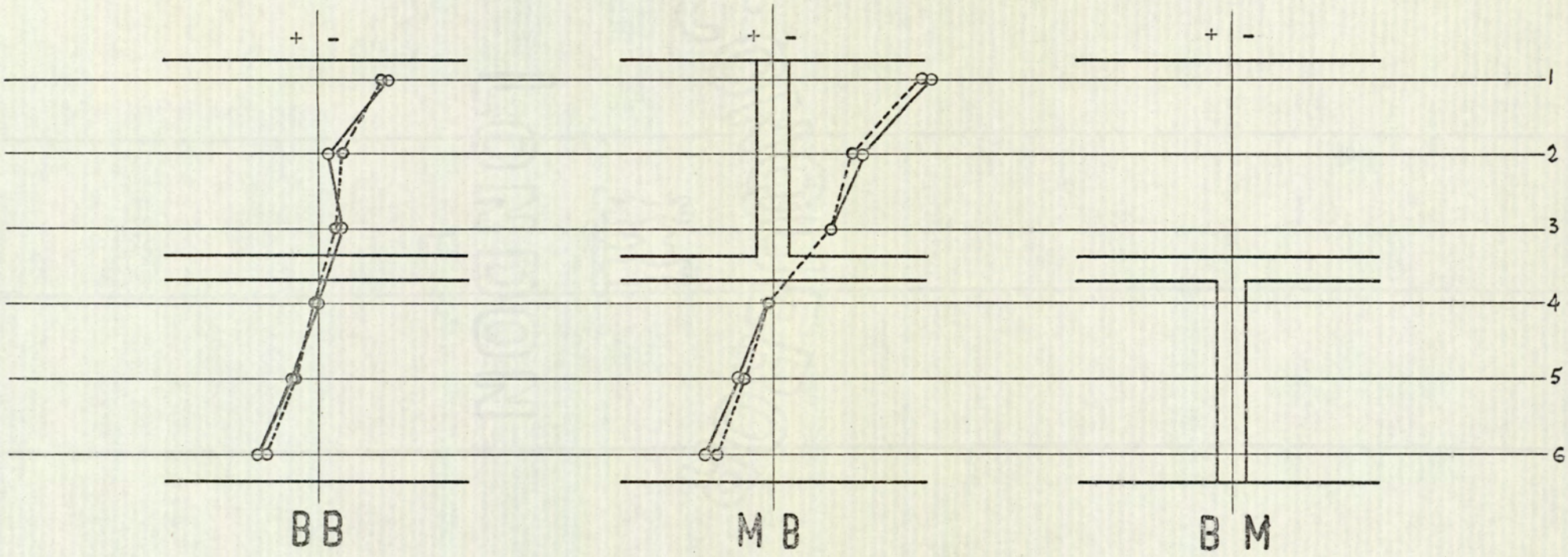

(Unsatisfactory Strain Readings)

----- Self Weight

_____ arithmetic mean of strain

EXPERIMENTAL STRAIN DISTRIBUTION BEAM NO.8

Fig. 8.4.2 6

8.5 Conclusions

Figures 8.4.1. 1 to 8.4.1. 6 inclusive show the experimental load/deflection relationships at the points of application of load to the beams and at the mid-span points.
Superimposed upon these figures are the straight lines of calculated theoretical deflection from Eqn [13] for the mid-span point of the beam based upon the Ebwk and gross Moment of Inertia Values.

Beams Nos. 3. 6 and 7 show a comparable relationship between theoretical and actual deflections.
Beams Nos. 2, 4 and 5 clearly show the effect of creep strain in the relative higher regions of applied load resulting in a non-linear load/deflection relationship. However, in the cases of these beams exhibiting the effects of creep the relationship can be said to be linear up to a mortar stress approximately 45 lb/in^2 at the extreme outer fibres of the beam material due to the applied load.

In practical design cases the flexural stress would be limited to 20lb/in^2 (as allowed by CP.111). It can therefore be concluded that in such designs the load/deflection relationship can be considered to be linear and that calculations based upon the Ebwk and gross Moment of Inertia values would predict deflection with an acceptable degree of accuracy.

Figs. 8.4.2 1 to 8.4.2. 6 inclusive have been prepared to show for the sections of beams tested the distribution of strain due to self weight and the arithmetic mean ($\bar{x}$) of the strains measured at each increment of load.

This method of presentation has been chosen in order that the general tendency rather than the particular distribution of strain for a given load can be shown graphically.

In consideration of the inconsistency of the constituent materials, the variability of workmanship and the possible limits of experimental error, it can be concluded that shallow brick beams exhibit a linear strain distribution with the neutral axis in a position predicted by the theory.

It is suggested by the author that more conclusive evidence would be obtained if specimen beams were constructed using an additive to the mortar that would considerably improve the strength of adhesion between bricks and mortar.

During the testing programme considerable difficulty was experienced in some cases due to a premature breakdown of the adhesion, resulting in strain gauge readings that suggested rapid changes in the position of the beam neutral axis.

The test rig and loading apparatus used prevented an accurate measurement of the load causing failure of the beam.

It was not possible to observe initial cracking at the extreme outer fibres, failure was sudden and without warning, thus making it necessary to c arefully observe the proving ring dial gauge between increments of load being applied through the hand operated hydraulic jack. By this method the approximate failure loads were noted and are recorded in Table 8.5.1.

The mode of failure for all beams tested was a breakdown in adhesion between brick and mortar in the perpend joint nearest to the mid-span point of the beam. * i.e. nearest to the point of maximum bending moment.

The failure loads of Table 8.5.1. are used to calculate the failure bending moments(Mc) given in Table 8.5.2. and are recorded as total moments being the addition of the moments due to the applied load at failure, the weight of the apparatus (50 lbs) and the self weight of the beam.
(3 course beams = 199 lb : 2 course beams = 130 lb)

From these failure moments, the mode of failure is considered as a mortar failure and the Modulus of Rupture (σ_{mc}) is calculated using Eqns [9], [10], [11] or [12] whichever is applicable to the beam size and mortar mix. A comparison is given (σ_x) of the Modulus of Rupture calculated from the simple beam formula $M = fZ$ where $Z = \frac{bd^2}{6}$ for the section.

As would be expected, Beams Nos. 2 and 3 which are constructed 3 courses deep with 1.0.3. mortar such that $\frac{Eb}{Em} = 0.706$ and are symmetrical at the M.B.M. failure section show almost identical results from σ_{mc} and σ_x.

Beams Nos. 4 and 5 again are 3 courses deep and symmetrical at the M.B.M. failure section, but in these instances the Eb/Em ratio which is equal to 2.193 has a more appreciable influence on the stress that would be predicted at failure.

For 3 course beams analysed by the theory presented here the Modulus of Rupture is of a value less than that which would be given by a simple analysis based upon the properties of an equivalent homogeneous section.

Similarly, for a given limiting design stress, the analysis of a 3 course beam by the theory presented here would result in a greater allowable bending moment than would be given by the simple beam analysis.

Clearly, these conditions are reversed for 2 course beams Nos. 6 and 7. At the B.M. failure section the cross section of the beam is not symmetrical, consequently a shift of the neutral axis towards the extreme outer tension fibres for the case when Em>Eb results in a Modulus of Rupture greater than would be predicted by using the section modulus of the homogeneous section.

Beam No. 8 of course is constructed with Eb/Em = 2.193 resulting in a mathematical shift of the neutral axis towards the extreme outer compression fibres. σ_{mc} will therefore be less than σ_x.

The limited number of tests carried out are insufficient to give a specific conclusion regarding the ultimate strength of the beams. It can certainly be concluded that the limiting allowable design stress of 20 lb/in^2 given in CP.111 is very conservative, discounting Beam No. 8 which is apparently an inconsistent result the arithmetic mean of the Modulus of Rupture values is 153.86 lb/in^2, suggesting that there would be a load factor against failure of 7.69. However, even allowing for the inconsistent results that must be catered for in the process of safe structural design, Beam No. 8 would have a load factor of 4.18.

The conservative values of flexural stress allowed by CP.111 are said to be for reasons including the inconsistency of workmanship. Present day standards of quality control and site supervision are such that the performance reliability of brickw ork could be at least equal to that obtained for reinforced concrete. On the brief evidence of the experimental work presented in this chapter it is clear that it would be possible to take more advantage of the flexural strength of brickwork than is at present allowed.

Beam No.	Mortar Mix	Courses Deep	Applied Load (2W) lb at Failure	Failure Section
2	1.0.3	3	375	M.B.M.
3	1.0.3	3	525	M.B.M
4	1.1.5	3	450	M.B.M
5	1.1.5	3	425	M.B.M
6	1.0.3	2	120	B.M
7	1.0.3	2	125	B.M
8	1.1.5	2	35	B.M

TABLE NO. 8.5.1

Beam No.	Failure Moment (Mc) lb.ins	Modulus of Rupture σ_{mc} lb/in^2	Modulus of Rupture σ_x lb/in^2
2	6891	134.37	134.07
3	8691	169.47	169.08
4	7791	147.24	151.57
5	7491	141.58	145.70
6	3210	163.70	147.59
7	3270	166.77	150.34
8	2190	83.66	100.68

TABLE NO.8.5.2

CHAPTER 9

THE APPLICATION OF THE THEORY OF ELASTICITY TO THE SOLUTION OF STRESSES IN BEAMS

9.1 Introduction

The theory of simple bending based upon the 'straight line' theory of stress distribution is in error since the mathematical theory of elasticity shows the presence of additional stresses in the x direction.

These additional stresses however are dependent entirely upon the depth of the beam. It is proposed here to establish a simple mathematical process by which the stresses in a beam can be calculated using the 'Theory of Elasticity' and to investigate the significant importance of the theory upon the stresses in brick beams.

There are several available methods for the solution of plane stress problems based upon the mathematical theories of elasticity and the solution is usually said to be found when the correct stress function or a sufficient approximation to it has been found.

(9)

G. B. Airy (1801 - 1892) obtained the differential equations of equilibrium

$$\frac{\partial \sigma_x}{\partial x} + \frac{\partial \tau_{xy}}{\partial y} = 0 \qquad \text{(i)}$$

$$\frac{\partial \sigma_y}{\partial y} + \frac{\partial \tau_{xy}}{\partial x} = 0 \qquad \text{(ii)}$$

and proved that these equations would be satisfied if expressions for the stress components are derived from a function ϕ such that

$$\sigma_x = \frac{\partial^2 \phi}{\partial y^2} \qquad \sigma_y = \frac{\partial^2 \phi}{\partial x^2} \qquad \tau_{xy} = \frac{\partial^2 \phi}{\partial x \, \partial y} \qquad \text{(iii)}$$

It is proposed here to find a solution to the problem of a simple beam subject to its own weight and to an external load applied to the top face of the beam by establishing a ϕ function in the form of a polynomial that will satisfy the 'Airy' equations of equilibrium, the specified boundary conditions and the equation of compatibility (iv).

$$\left[\frac{\partial^2}{\partial x^2} + \frac{\partial^2}{\partial y^2}\right](\sigma_x + \sigma_y) = 0 \qquad \text{(iv)}$$

In brick beams of usual construction the size of the elements (brick and mortar) is usually small compared to the overall size of the beam and the material can be assumed to be homogeneous for the purposes of overall stress analysis, the thickness of the beam is again usually small compared to the length and height.

The problem can therefore be said to reduce to one of plane stress in which the variation of the stress componenets σ_x, σ_y and σ_z across the thickness may be neglected and $\sigma_{xx} = \sigma_{yz} = \sigma_{xz} = 0$.

The problem therefore reduces to one of a two dimensional system.

Considering the stress function ϕ to be a permissable 'Airy' function, the compatibility equation (iv) can be written in terms of the stress function:-

$$\nabla^4\phi = \frac{\partial_4\phi}{\partial x^4} + \frac{2\,\partial_4\phi}{\partial x^2\partial y^2} + \frac{\partial_4\phi}{\partial y^4} = 0 \qquad \text{(v)}$$

Considering the general case of body forces and assuming that these forces have a potential. Then the component of the body force in the y direction can be defined as Y and is given by the equation:-

$$Y = -\frac{\partial V}{\partial y} \qquad \text{(vi)}$$

When the body force is simply the self weight of the body, the potential V is - Dy where D is the unit density of the body material.

In problems of plane stress, all compatibility equations cannot be satisfied, however it can be shown that for thin plates the errors caused by neglecting some of the compatibility equations are small and can be neglected.

It is necessary only to consider the compatibility equation

$$\nabla^4\phi = \frac{\partial_4\phi}{\partial x^4} + \frac{2\partial^4\phi}{\partial x^2\partial y^2} + \frac{\partial^4\phi}{\partial y^4} = -(1-\nu)\nabla^2 V \qquad \text{(vii)}$$

therefore since $\nabla^2 V = \frac{\partial_2 V}{\partial y^2} + \frac{\partial^2 V}{\partial x^2}$

and $V = -Dy$

then $\nabla^2 V = 0$

$\therefore \nabla^4\phi = 0$ when body forces are included.

The stresses due to body forces in an element of the body can be obtained from the ϕ stress function as follows:-

$$\sigma_x = \frac{\partial_2\phi}{\partial y^2} + V \qquad \text{(viii)}$$

$$\sigma_y = \frac{\partial_2\phi}{\partial x^2} + V \qquad \text{(ix)}$$

$$\tau_{xy} = -\frac{\partial^2\phi}{\partial x\partial y} \qquad \text{(x)}$$

9.2 THE DETERMINATION OF THE AIRY STRESS FUNCTION

The stress function ϕ can be expressed in the form of a doubly infinite power series

$$\phi = \sum_{m=0}^{\infty} \sum_{n=0}^{\infty} C_{m n} . x^m . y^n \qquad [1]$$

where m and n are positive integers and Cmn are undetermined coefficients which can be arranged in the matrix:-

~~C00~~	~~C01~~	C02	(C03)	C04	(C05)	C06	"
~~C10~~	(C11)	C12	(C13)	C14	C15	C16	"
(C20)	(C21)	C22	(C23)	C24	C25	C26	"
C30	C31	C32	C33	C34	C35	C36	"
C40	C41	C42	C43	C44	C45	C46	"
C50	C51	C52	C53	C54	C55	C56	"
C60	C61	C62	C63	C64	C65	C66	"
"	"	"	"	"	"	"	"

By substitution into Equation [1] the components of stress in an element are given by:-

$$\sigma_x = \frac{\partial^2 \phi}{\partial y^2} = \sum_{m=0}^{\infty} \sum_{n=2}^{\infty} n(n-1)\, C_{mn} . x^m . y^{n-2} \qquad [2]$$

$$\sigma_y = \frac{\partial^2 \phi}{\partial x^2} = \sum_{m=2}^{\infty} \sum_{n=0}^{\infty} m(m-1)\, C_{mn} . x^{m-2} . y^n \qquad [3]$$

$$\tau_{xy} = \frac{-\partial^2 \phi}{\partial x\, \partial y} = -\sum_{m=1}^{\infty} \sum_{n=1}^{\infty} m . n . C_{mn} . x^{m-1} . y^{n-1} \qquad [4]$$

The coefficients C00, C01, and C10 do not appear in the equations for stress [2], [3] and [4] and can therefore be immediately deleted from the matrix.

The biharmonic equation of compatibility

$$\nabla^2 \nabla^2 \phi = 0 \qquad [5]$$

where $\nabla^2 = \frac{\partial^2}{\partial x^2} + \frac{\partial^2}{\partial y^2}$

by substitution into equation [1] can be expressed in the following form:

$$\sum_{m=2}^{\infty} \sum_{n=2}^{\infty} x^{m-2}.y^{n-2} \Big[(m+2)(m+1)m(m-1)C_{m+2,n-2} + 2m(m-1)n(n-1)C_{mn} + (n+2)(n+1)n(n-1)C_{m-2,n+2} \Big] = 0$$

The condition of compatibility is not dependent upon x and y such that $x^{m-2}.y^{n-2} = 0$

$$\therefore (m+2)(m+1)m(m-1)C_{m+2,n-2} + 2m(m-1)n(n-1)C_{mn} + (n+2)(n+1)n(n-1)C_{m-2,n+2} = 0 \qquad [6]$$

Equation [6] by the recurrence relationship establishes the inter-relationships between any three alternate Cmn coefficients in the diagonals of the matrix running in a line from the lower left to the upper right starting with the group [C40, C22, C04]

e.g. The group [C60, C42, C24] is related by:-

(6.5.4.3) C60 + 2(4.3)(2.1)C42 + (4.3.2.1.)C24 = 0

The problem of the determination of the ϕ equation is therefore reduced to finding values of Cmn in Equation [1] that satisfy the boundary conditions of the problem and the inter-relationship among the Cmn coefficients in Equation [6]

9.3 A shallow beam with no body forces (i.e. self weight neglected)

Consider the beam shown in Fig. 9.3.1 to be the left hand half of a beam supported by a shear force (W) at the left hand edge.

The beam is rectangular in cross section, of unit width and carries a uniformly distributed load of w per unit area on the top face such that

W = wL

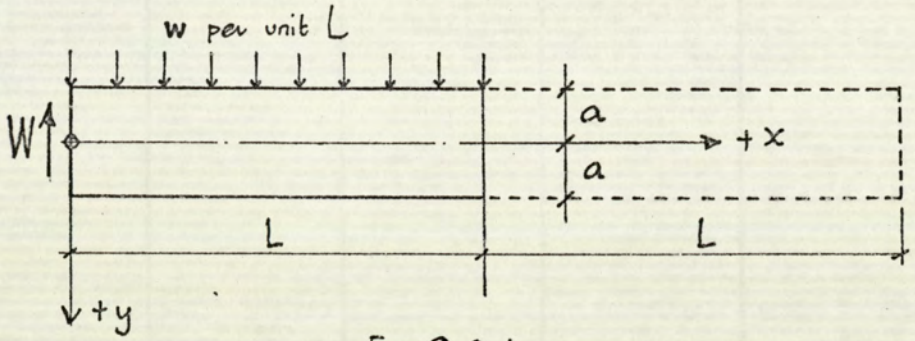

Fig 9.3.1

The matrix of undetermined coefficients can again be written:-

-	-	C02	(C03)	C04	(C05)	C06	⋰
-	(C11)	C12	(C13)	C14	C15	C16	⋰
(C20)	(C21)	C22	(C23)	C24	C25	C26	⋰
C30	C31	C32	C33	C34	C35	C36	⋰
C40	C41	C42	C43	C44	C45	C46	⋰
C50	C51	C52	C53	C54	C55	C56	⋰
C60	C61	C62	C63	C64	C65	C66	⋰
⋰	⋰	⋰	⋰	⋰	⋰	⋰	⋰

The boundary condition that $\tau_{xy} = 0$ at $y = \pm a$ for values of x greater than 0 and less than L, is therefore independent of x and demands therefore that all powers of x in equation [4] are zero.

$$\sum_{n=1}^{\infty} n.C_{mn}.a^{n-1} = 0 \quad \text{for} \quad m \geqslant 1 \qquad [7]$$

$$\sum_{n=1}^{\infty} n.C_{mn}(-a)^{n-1} = 0 \quad \text{for} \quad m \geqslant 1 \qquad [8]$$

addition and subtraction of Equations [7] and [8] multiplied by (a) give:

$$\sum_{n=2.4.6}^{\infty} n.C_{mn}.a^{n} = 0 \quad \text{for} \quad m \geqslant 1 \qquad [9]$$

$$\sum_{n=1.3.5}^{\infty} n.\ Cmn\ a^{n} = 0 \quad \text{for } m \geqslant 1 \qquad [10]$$

Similarly, the boundary condition that $\sigma_y = 0$ at $y = +a$ for values of x greater than 0 and less than L demands that:-

$$\sum_{n=0}^{\infty} C\,m\,n.a^{n} = 0 \quad \text{for } m \geqslant 2 \qquad [11]$$

Further, the boundary condition that $\sigma_y = -w$ at $y = -a$ for values of x greater than 0 and less than L demands that:-

$$-w = \sum_{m=2}^{\infty} \left[\sum_{n=0}^{\infty} Cmn(-a)^{n} \right] m(m-1)x^{m-2} \qquad [12]$$

these equations being obtained from Equation [3]

hence

$$\sum_{n=0}^{\infty} Cmn(-a)^{n} = 0 \quad \text{for } m \geqslant 3 \qquad [13]$$

$$2\sum_{n=0}^{\infty} C2n(-a)^{n} = -w \qquad [14]$$

addition and subtraction of Equation [11] for values of $m \geqslant 3$ and [13] give:-

$$\sum_{n=0.2.4}^{\infty} Cmn\ a^{n} = 0 \quad \text{for } m \geqslant 3 \qquad [15]$$

$$\sum_{n=1.3.5}^{\infty} Cmn\ a^{n} = 0 \quad \text{for } m \geqslant 3 \qquad [16]$$

Equations [9] for $m \geqslant 3$ and [15] can both be satisfied by

$Cmn = 0$ for $m \geqslant 3$, $n = 0.2.4$

and similarly Equations [10] for $m \geqslant 3$ and [16] give

$Cmn = 0$ for $m \geqslant 3$ $n = 1.3.5$

These values of Cmn can now be deleted from the matrix.

The compatibility relationship Equation [6] gives C14 = 0 since

C50 = C32 = 0.

By the same considerations all of the coefficients Cmn below the diagonal running from C60 to C06 will be zero and can be deleted from the matrix.

The matrix has now been reduced and it is possible to write Equations [9] [10] [11] and [14] for m = 2.

$$2\ C22\ a^2 = 0$$

$$C21\ a + 3\ C23\ a^3 = 0$$

$$C20 + C21a + C22a^2 + C23a^3 = 0$$

$$C20 - C21a + C22a^2 - C23\ a^3 = -\frac{w}{2}$$

from which is obtained

$$C22 = 0, \qquad C20 = -\frac{w}{4}$$

$$C21 = \frac{3w}{8a} \qquad C23 = -\frac{w}{8a^3}$$

the compatibility relationships of Equation [6] give:-

$$C04 = 0 \qquad C05 = -\frac{C23}{5} = \frac{w}{40a^3}$$

Equations [9] and [10] for m = 1 give:-

$$C12 = 0 \qquad C11 = -3\ C13\ a^2$$

The remaining unknown coefficients of Cmn are C02, C03, C13 and the stress function can be written in terms of these coefficients:-

$$\phi = C02.y^2 + C03.y^3 + \frac{w}{40a^3}\ y^5 - 3.C13.a^2.x.y.$$

$$+C13.x.y^3 - \frac{w.x^2}{4} + 3\ \frac{w.x^2.y}{8a} - \frac{w.x^2.y^3}{8a^3} \qquad [17]$$

C02, C03 and C13 can be solved for a shallow beam by considering the boundary conditions at the free end (x = 0) at which point there must be a zero resultant horizontal force producing a zero couple for the resulting system of forces to be statically equivalent to zero. At the same point the resulting shear force must be equal to W.

$\therefore$ when x = 0

$$\int_{-a}^{a} \frac{\partial^2 \phi}{\partial y^2} \, dy = 0 \qquad [18]$$

$$\int_{-a}^{a} \frac{\partial^2 \phi}{\partial y^2} \, y \, dy = 0 \qquad [19]$$

$$\int_{-a}^{a} -\frac{\partial^2 \phi}{\partial x \, \partial y} \, dy = W = wL \qquad [20]$$

Substitution of Equation [17] into Equations [18,] [19] and [20] gives:-

$$C02 = 0$$

$$C03 = \frac{-w}{20\,a}$$

$$C13 = \frac{wL}{4\,a^3}$$

The resulting ϕ stress function can now be written:-

$$\phi = -\frac{w}{20a} y^3 + \frac{w}{40a^3} y^5 - \frac{3wL}{4a} x\,y + \frac{wL}{4a^3} xy^3$$

$$\frac{-wx^2}{4} + 3\,\frac{wx^2 y}{8a} - \frac{w\,x^2 y^3}{8a^3} \qquad [21]$$

Substituting for $w = 160\ A\ a^3$

The fifith power algebraic ϕ function can be expressed as:-

$$\phi = A(4y^5 - 20\ x^2y^3 + 60\ x^2y\ a^2 - 40\ x^2a^3 + 40\ xy^3L - 120\ xyLa^2 - 8\ y^3a^2) \qquad [22]$$

and can be verified as a permissable 'Airy Function' by substitution into the biharmonic equation

$$\nabla^4\phi = \frac{\partial^4\phi}{\partial x^4} + \frac{2\partial^4\phi}{\partial x^2\partial y^2} + \frac{\partial^4\phi}{\partial y^4} = 0$$

$$\frac{\partial^4\phi}{\partial x^4} = A(0 - 0 + 0 - 0 + 0 - 0 - 0)$$

$$\frac{2\partial^4\phi}{\partial x^2\partial y^2} = 2A(0 - 240y + 0 - 0 + 0 - 0 - 0)$$

$$\frac{\partial^4\phi}{\partial y^4} = A(480y - 0 + 0 - 0 + 0 - 0 - 0)$$

$$\therefore\ \nabla^4\phi = 480\ Ay - 480\ Ay = 0$$

Substitution of Equation [22] into the equations for stress give:

$$\sigma_x = \frac{\partial^2\phi}{\partial y^2} = A\left[80y^3 - 120y(x^2 - 2xL) - 48\ ya^2\right] \qquad [23]$$

$$\sigma_y = \frac{\partial 2\phi}{\partial x^2} = A(-40y^3 + 120ya^2 - 80a^3) \qquad [24]$$

$$\tau_{xy} = -\frac{\partial 2\phi}{\partial x\partial y} = -120A(-xy^2 + xa^2 + y^2L - La^2) \qquad [25]$$

The resulting stress equations [23] [24] and [25] can now be checked against the specified boundary conditions.

At the ends of the beam when x = 0 the total shear force must be equal to the reaction. i.e. $\int \tau_{xy} = 160\ A\ a^3 L$ for a beam of unit thickness.

i.e. at x = 0

$$\int_{-a}^{+a} \tau_{xy}.\ dy = \pm wL = 160\ A\ a^3 L$$

$$-120A \int_{-a}^{+a} (-xy^2 + x a^2 + y^2 L - La^2)\ dy$$

$$= 120\ A \left[\frac{-xy^3}{3} + xa^2 y + \frac{y^3 L}{3} - La^2 y \right]_{-a}^{+a}$$

then at x = 0

$$\int_{-a}^{+a} \tau_{xy}.\ dy = -120\ A \left[\frac{y^3 L}{3} - La^2 y \right]_{-a}^{+a}$$

$$= -120A \left(\frac{a^3 L}{3} - a^3 L\right) + 120A\left(a^3 L - \frac{a^3 L}{3}\right)$$

$$= 160\ A\ a^3\ L$$

At the ends of the beam when x = 0 the total resultant of σ_x must be zero.

i.e. at x = 0

$$\int_{-a}^{+a} \sigma_x.\ dy = 0$$

$$\therefore\ A \int_{-a}^{+a} (80y^3 - 120\ y\ x^2 + 240\ y\ x\ L - 48\ y\ a^2)\ dy = \int_{-a}^{+a} \sigma_x\ dy$$

$$A \left[\frac{80y^4}{4} - \frac{120\ y^2 x^2}{2} + \frac{240\ y^2 xL}{2} - \frac{48\ y^2\ a^2}{2} \right]_{-a}^{+a} = \int_{-a}^{+a} \sigma_x\ dy$$

$$\therefore\ A(20a^4 - 60a^2 x^2 + 120a^2 xL - 24a^4) - A(20a^4 - 60a^2 x^2 + 120a^2 xL - 24a^4) = 0$$

At the ends of the beam when x = 0 the total moment of σ_x must be zero.

i.e. at x = 0

$$\int_{-a}^{+a} \sigma_x . y . dy = 0$$

$$\therefore A \int_{-a}^{+a} (80y^4 - 120\, y^2x^2 + 240\, y^2xL - 48\, y^2a^2)\, dy = \int_{-a}^{+a} \sigma_x . y . dy$$

$$A \left[\frac{80y^5}{5} - \frac{120y^3x^2}{3} + \frac{240y^3xL}{3} - \frac{48y^3a^2}{3} \right]_{-a}^{+a} = \int_{-a}^{+a} \sigma_x . y . dy$$

$$\therefore A(16a^5 - 40a^3x^2 + 80\, a^3xL - 16\, a^5) - A(-16a^5 + 40a^3x^2 - 80a^3xL + 16a^5) = 0$$

At the top face of the beam when y = -a, σ_y is equal to $-160Aa^3$ which is the applied load.

$\therefore$ when y = -a

$$\sigma_y = A(-40y^3 + 120\, y\, a^2 - 80\, a^3)$$
$$= A(40\, a^3 - 120\, a^3 - 80\, a^3)$$
$$= -160\, A\, a^3$$

At the bottom face of the beam when y = +a σ_y must be zero.

i.e. when y = +a

$$\sigma_y = A(-40y^3 + 120y\, a^2 - 80\, a^3)$$
$$= A(-40a^3 + 120\, a^3 - 80a^3)$$
$$= 0$$

It is therefore proved that the resulting stress equations [23] [24] and [25] satisfy the specified boundary conditions.

Consider now the centre of the beam span i.e. $x = L$

the maximum value of σ_x will occur at $y = \pm a$

$\therefore$ At $y = \pm a$, $\sigma_x = \pm A\left[80\,y^3 - 120y(x^2 - 2xL) - 48ya^2\right]$

$= \pm A\left[32\,a^3 + 120\,a\,L^2\right]$

The term $120\,A.\,a.\,L^2$ is the stress resulting from the 'straight line' theory of simple bending.

The term $32\,A\,a^3$ is therefore the influence of the 'Theory of Elasticity' on the value of the maximum flexural stress in the beam and is constant for all span/depth ratios.

An analysis of equation [23] shows the presence of a σ_x value at $x = 0$. This should not be the case.

However, it has been shown that when $x = 0$, σ_x has a zero resultant and also a zero moment $\int \sigma_x . y . dy$ so that the end section conditions at $x = 0$ for σ_x are statically equivalent to zero.

9.4 Saint Venant's Principle

Saint Venant's Principle, known as the 'elastic equivalence of a statically equipollent system of load' states that the application to a small part of its surface of a system of forces statically equivalent to zero force and zero couple are of negligable magnitude at distances which are large compared with the linear dimensions of the part.

It can therefore be said that for practical design considerations in beams with a length greater than the depth, the effect of the presence of a σ_x stress at the end of the beam will have died down at a short distance from the end of the beam, and can be neglected when considering the stresses in the beam at mid-span, by the application of the 'Theory of Elasticity'.

9.5 The Stresses due to the Self Weight of the Beam

When the load carried by the beam is simply its self weight (where D = the unit density of the beam material) the previous solution for top face loading Equations [23], [24] and [25] must be modified by putting $160\ A\ a^3 = 2.\ D.\ a$ i.e. $A = \frac{D}{80a^2}$ into the equations for stress [viii], [ix] and [x] and adding to the solution the following stresses:-

$\sigma_x = 0$

$\sigma_y = D\,(a - y)$

$\tau_{xy} = 0$

Thus when the stresses obtained from this solution are added to the stresses obtained from the previous solution with $160\ A\ a^3$ replaced by 2.D.a for top face loading, the resulting stresses on both the top and bottom faces is zero and the only load carried by the beam will be that due to its own weight.

The above additional stresses can be obtained from the algebraic function

$$\phi = \frac{D}{2}\left(ax^2 + \frac{y^3}{3}\right) \qquad [26]$$

which can be proved to be a permissable 'Airy' function by substitution into the biharmonic equation:-

$$\nabla^4\phi = \frac{\partial_4\phi}{\partial x^4} + \frac{\partial_4\phi}{\partial y^4} + 2\,\frac{\partial_4\phi}{\partial x^2\partial y^2} = 0$$

then, by substitution into the equations for stress [viii] [ix] and [x]

$$\sigma_x = \frac{\partial_2\phi}{\partial y^2} - Dy = Dy - Dy = 0$$

$$\sigma_y = \frac{\partial_2\phi}{\partial x^2} - Dy = Da - Dy = D(a-y)$$

$$\tau_{xy} = \frac{2\,\partial_2\phi}{\partial x^2\partial y^2} = 0$$

The stress equations for body forces which are entirely due to the self weight of the beam can now be written:

$$\sigma_x = \frac{D}{80a^2}\left[80y^3 - 120y(x^2 - 2xL) - 48\,ya^2\right] \qquad [27]$$

$$\sigma_y = \frac{D}{80a^2}(-40y^3 + 120\,ya^2 - 80a^3) + D(a-y) \qquad [28]$$

$$\tau_{xy} = \frac{3D}{2a^2}(-xy^2 + xa^2 + y^2L - La^2) \qquad [29]$$

These equations can now be checked against the specified boundary conditions.

when $y = +a$, $\sigma_y = 0$

$$\sigma_y = \frac{D}{80a^2}(-40a^3 + 120a^3 - 80a^3) = 0$$

when $y = -a$, $\sigma_y = 0$

$$\sigma_y = \frac{D}{80a^2}(+40a^3 - 120\,a^3 - 80a^3) + D(a + a) = 0$$

At the end of the beam when $x = 0$ the total vertical shear must be equal to the reaction

i.e. for a beam of unit thickness.

$$\therefore \text{ at } x = 0 \quad \int_{-a}^{+a} \tau_{xy}\,dy = D\,a\,L$$

$$\frac{3D}{2a^2}\int_{-a}^{+a}(y^2L - L\,a^2)\,dy = \frac{3D}{2a^2}\left[\frac{y^3L}{3} - La^2y\right]_{-a}^{+a}$$

$$= \frac{3D}{2a^2}\left[\frac{a^3L}{3} - a^3L\right] - \frac{3D}{2a^2}\left[-\frac{a^3L}{3} - a^2L\right]$$

$$= D\,a\,L$$

At the end of the beam when x = 0 the total resultant of σx must be zero

i.e. at x = 0 $\quad \int_{-a}^{+a} \sigma x \, . \, dy = 0$

$$\frac{D}{80a^2} \int_{-a}^{+a} (80y^3 - 120\, y\, x^2 + 240\, y\, x\, L - 48\, y\, a^2)\ dy$$

$$= \frac{D}{80a^2} \left[20y^4 - 24\, y^2 a^2 \right]_{-a}^{+a} \qquad \text{at } x = 0$$

$$= \frac{D}{80a^2} \left[20a^4 - 24a^4 \right] - \frac{D}{80a^2} \left[20a^4 - 24a^4 \right]$$

$$= 0$$

At the end of the beam when x = 0 the total moment of σx must be zero

i.e. at x = 0 $\quad \int_{-a}^{+a} \sigma x . \ y \, . \, dy = 0$

$$\frac{D}{80a^2} \int_{-a}^{+a} (80y^4 - 120\, y^2 x^2 + 240\, y^2 x L - 48\, y^2 a^2)\ dy$$

$$= \frac{D}{80a^2} \left[16\, y^5 - 16\, y^3 a^2 \right]_{-a}^{+a} \qquad \text{at } x = 0$$

$$= \frac{D}{80a^2} \left[16a^5 - 16a^5 \right] - \frac{D}{80a^2} \left[-16a^5 + 16a^5 \right]$$

$$= 0$$

It is therefore proved that the resulting stress equations [27] [28] and [29] satisfy the specified boundary conditions.

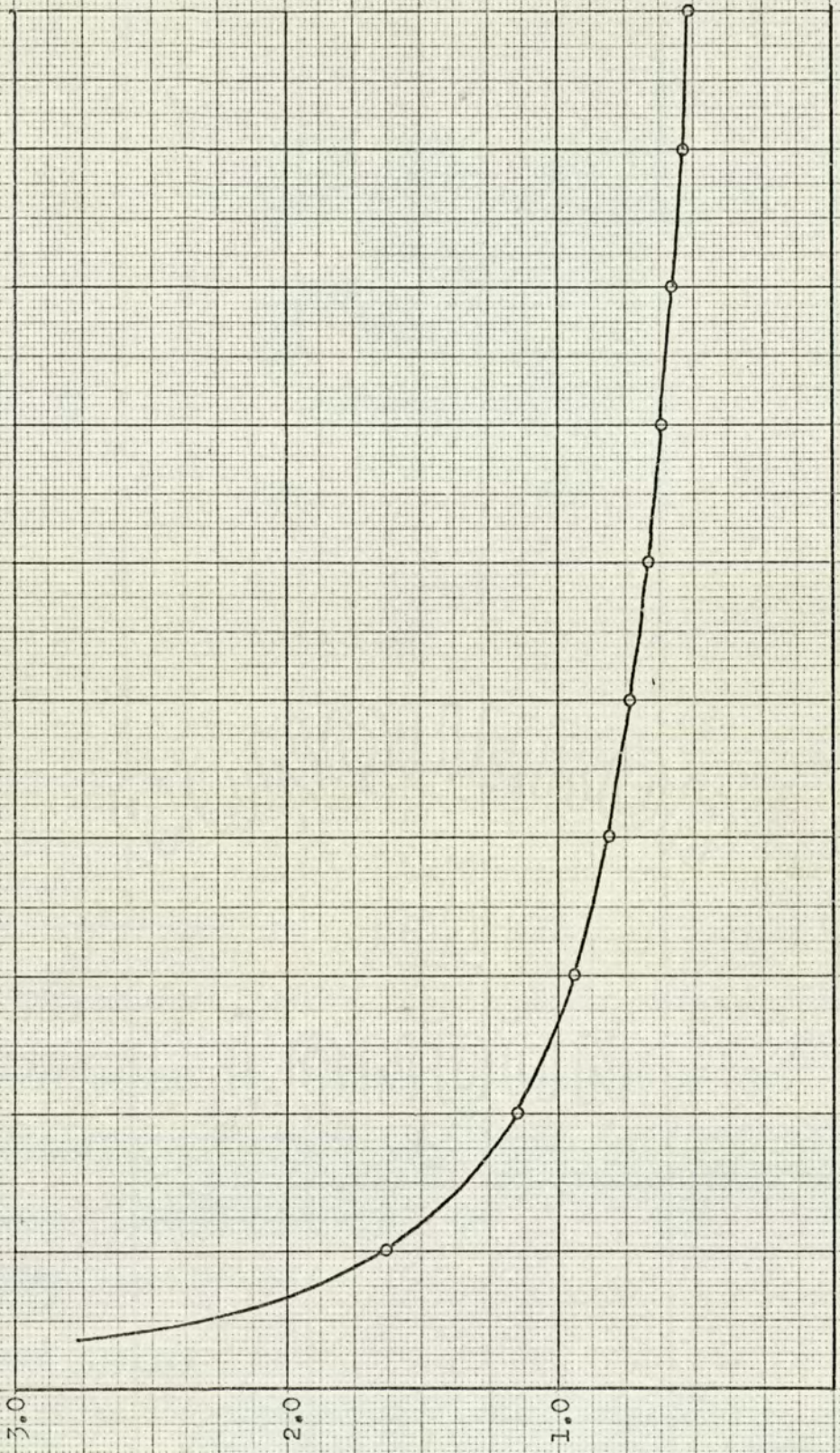

THE EFFECT ON THE MAXIMUM VALUE OF σ_x AT MID-SPAN OF BEAM DUE TO THE THEORY OF ELASTICITY

Fig. 9.2.

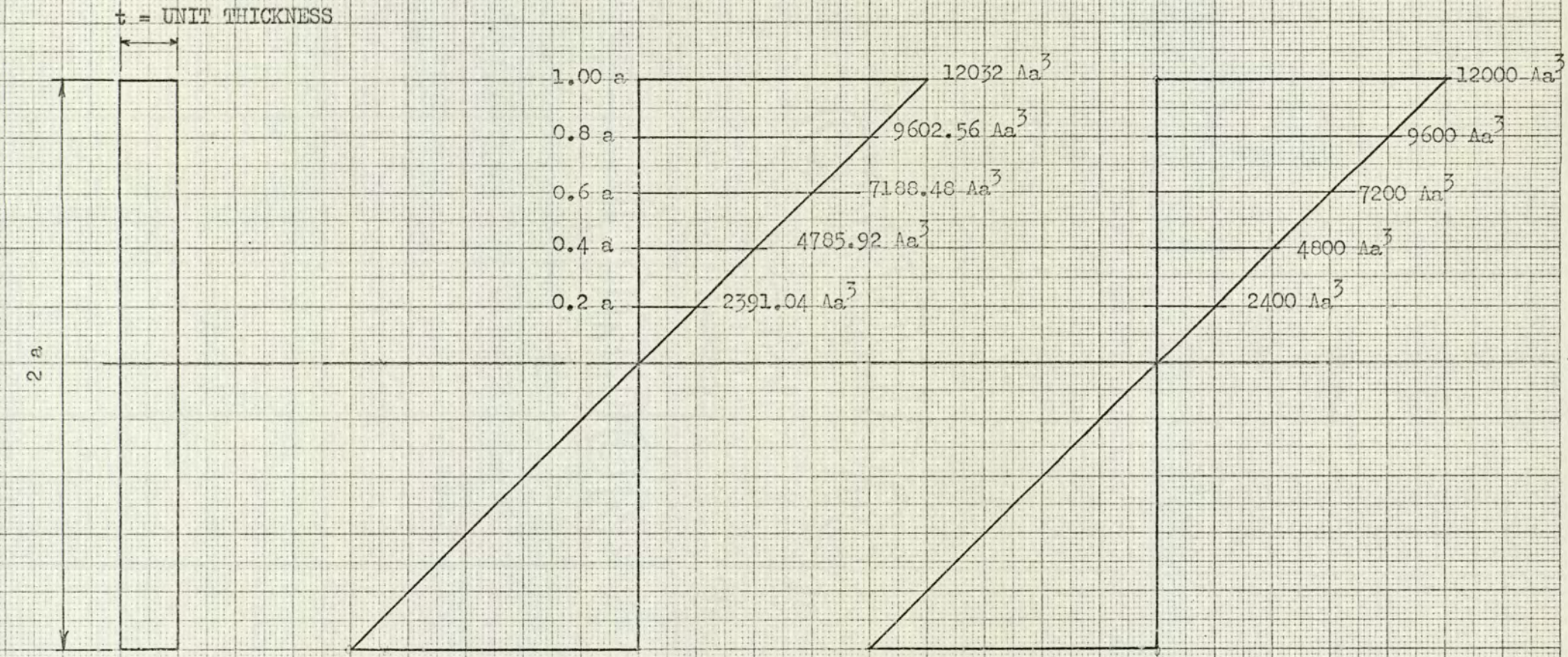

DISTRIBUTION OF σ_x STRESSES AT MID-SPAN DUE TO TOP FACE LOADING = 160 A a^3 per UNIT LENGTH

SPAN/DEPTH RATIO = 10

Fig.9.1

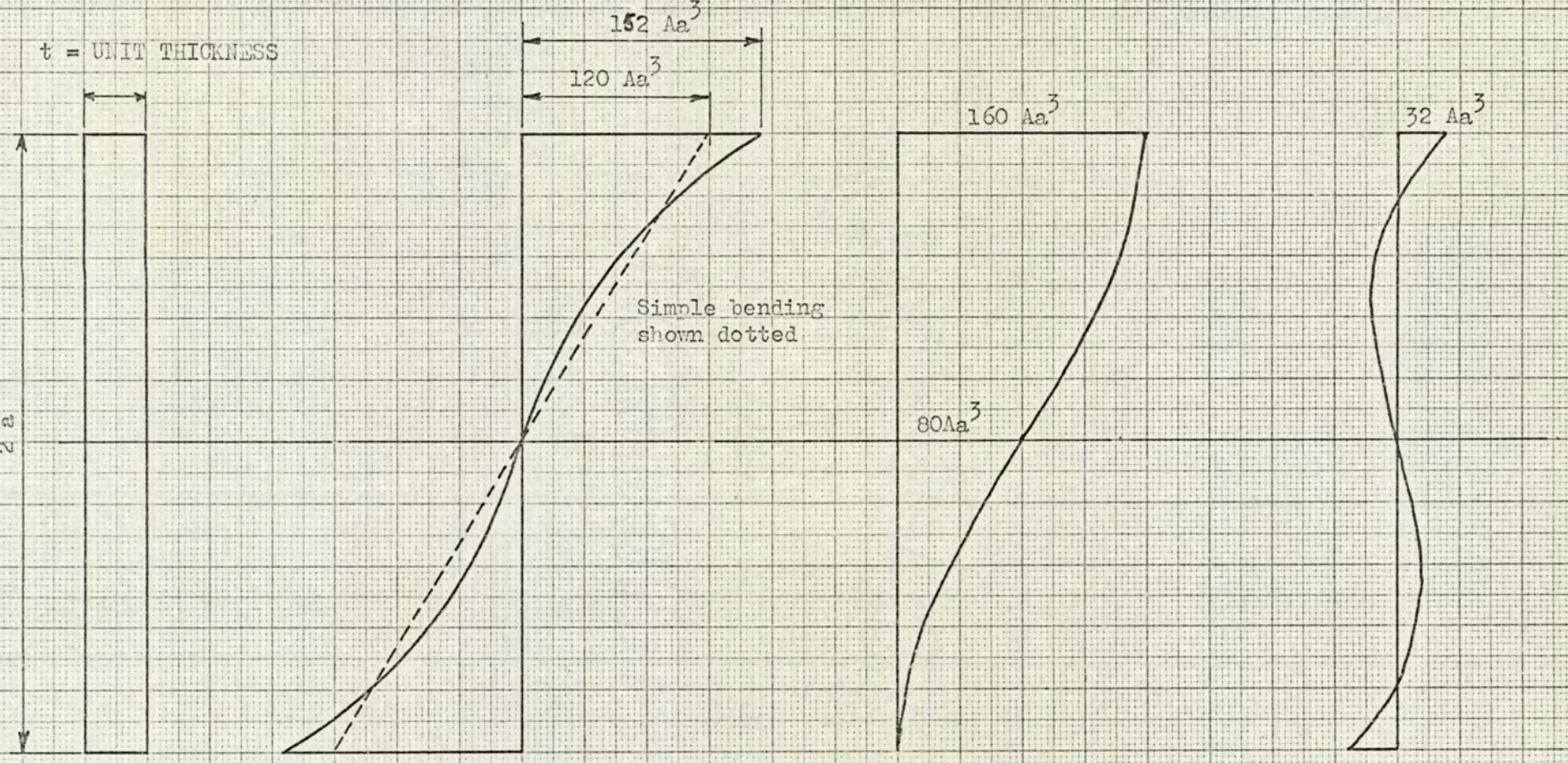

DISTRIBUTION OF σ_x STRESSES AT MID-SPAN DUE TO TOP FACE LOADING = 160 Aa^3 PER UNIT LENGTH

SPAN/DEPTH RATIO = 1.00

Fig.9.3

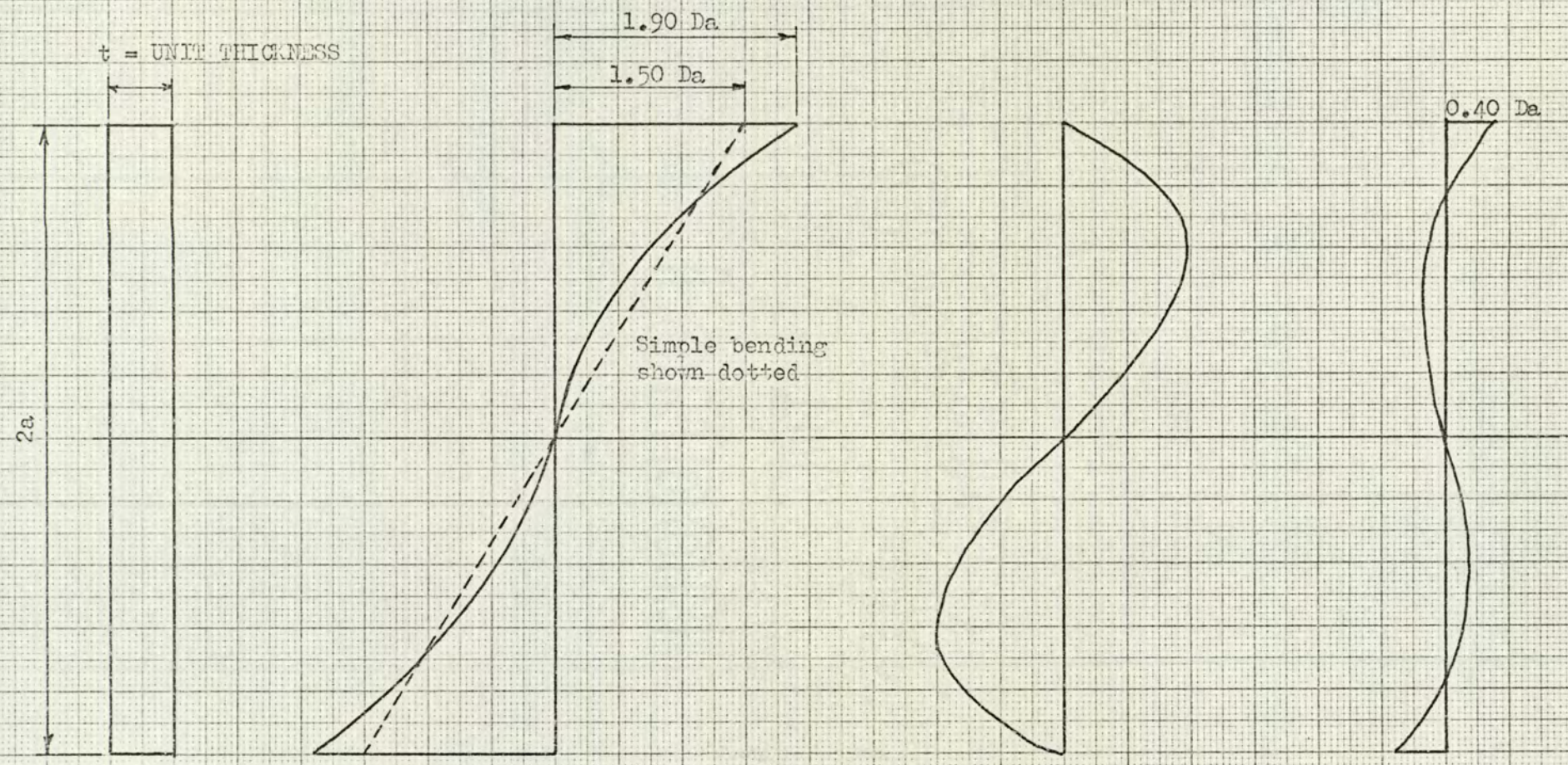

DISTRIBUTION OF STRESSES AT MID-SPAN DUE TO SELF WEIGHT OF BEAM

SPAN/DEPTH RATIO = 1.00

Fig.9.4

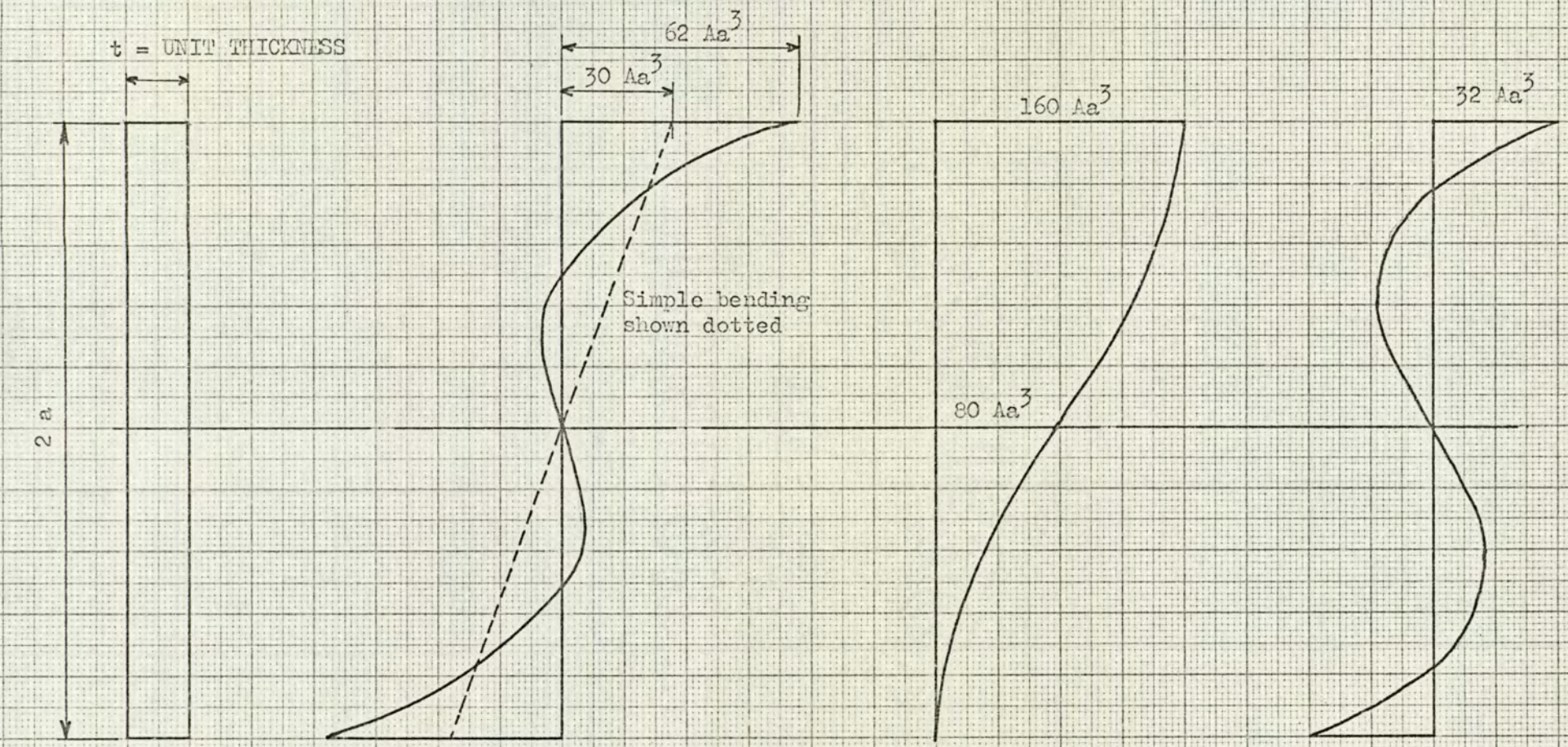

DISTRIBUTION OF STRESSES AT MID-SPAN DUE TO TOP FACE LOADING = 160 Aa^3 PER UNIT LENGTH

SPAN/DEPTH RATIO = 0.50

Fig.9.5

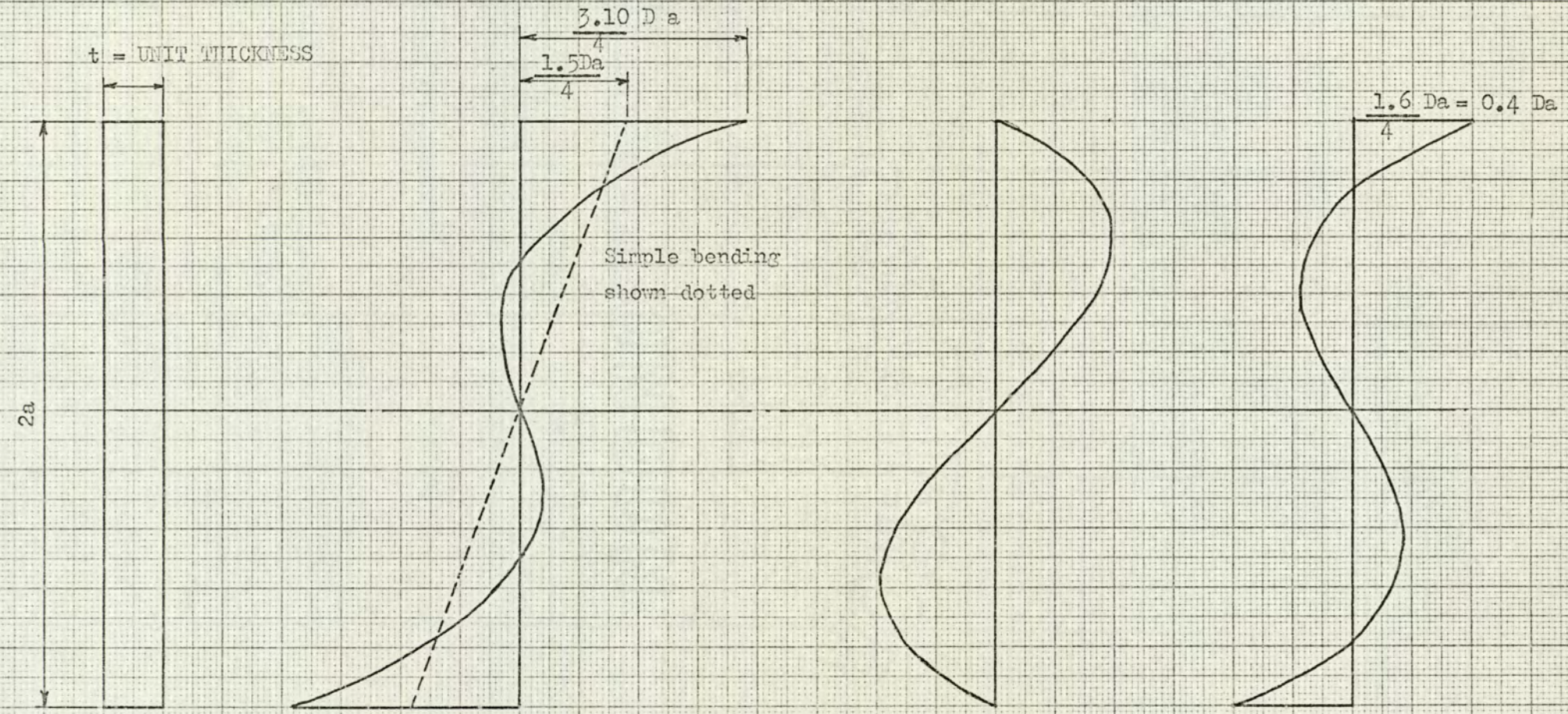

DISTRIBUTION OF STRESSES AT MID-SPAN DUE TO SELF WEIGHT OF BEAM

SPAN/DEPTH RATIO = 0.50

9.7 Conclusions

The derived ϕ equation [22] although being in itself a permissable 'Airy' stress function that does not satisfy all boundary conditions and conditions of compatibility, results in stress equations for σx, σy and τxy stresses [23] [24] [25] [27] [28] and [29] that are acceptable for the theoretical analysis of shallow beams.

Fig. 9.1. shows the comparison of σx distribution at mid-span of a beam due to T O P face loading calculated from the derived stress equation based upon the 'Theory of Elasticity' and from the 'Straight Line' theory of simple bending for a rectangular beam of Span/Depth ratio = 10. This comparison clearly shows that the additional longitudinal stresses obtained from the Theory of Elasticity can be neglected for shallow beams. It is therefore sufficient only to consider the simple theory of bending in the design of shallow beams.

The effect of the Theory of Elasticity is to increase the maximum value of σx obtained by the 'Theory of Simple Bending' by a constant value of $32\ Aa^3$ for all values of Span/Depth ratio due to the applied load $160\ A\ a^3$ per unit area. At some stage in the Span/Depth ratio range the effect of the 'Theory of Elasticity' will become of significant importance.

Fig. 9.2. shows the effect of the 'Theory of Elasticity' on σx as a percentage of σx calculated from the 'Theory of Simple Bending.' In effect, this figure shows the point in the Span/Depth ratio range when a 'shallow beam' becomes a 'deep beam' for the purposes of stress analysis.

It is suggested by the author that a 10% error in the stress analysis of brick beams would be the acceptable limit. This limit is reached at a Span/Depth Ratio of 1.63; at Span/Depth Ratios less than this value the beam should be analysed as a 'deep beam'. The effect of the 'Theory of Elasticity' can be clearly seen to be of rapidly increasing significance as the Span/Depth ratio decreases from 1.5 to 0.5, there being an increase in σx of 100% at the latter value.

A true conclusion with respect to the rate of increase of σx with a decrease in Span/Depth ratio cannot however be given at this stage. It is likely that further investigations with 'deep beams' will result in modified stress equations that do not have such a significant effect on the maximum value of σx. It must be emphasised that Fig. 9.2. is dependant upon stress equations that may not be acceptable for 'deep beam' analysis such that the part of the curve in Fig. 9.2. for Span/Depth ratios less than 1.00 will probably be invalid.

Figs. 9.3, 9.4, 9.5 and 9.6 have been prepared to show the effect of the 'Theory of Elasticity' on deep beams using the derived Equation [22]. Figs. 9.3 and 9.4 drawn for a Span/Depth Ratio = 1.00 indicate that the stress distribution is just beginning to seriously deviate from the straight line distribution and that the difference in the maximum value of σx is such that the effects of the additional longitudinal stresses could not be ignored in the design of brick beams.
Figs. 9.5 and 9.6 drawn for a Span/Depth Ratio = 0.50 show the magnified effect of the resulting deviation from the straight line theory of stress distribution. The magnitude of the deviation is such that there is a reversal of stress in zones that the 'Straight Line' Theory would indicate to be entirely tension or compression. Again, this cannot be the final conclusion since the stress equations that will be derived for 'deep beams'

may well show a modified stress distribution for beams of Span/Depth Ratio less than 1.00.

It will therefore be necessary for further investigations to be made with respect to the effect of the 'Theory of Elasticity' on deep beams. The principle of Saint Venant as described in para. 9.4. may not be acceptable in the case of deep beams since the effect of a σx stress at the ends of the beam may have a significant effect on the σx value at mid-span.

The derived ϕ equation [22] for a shallow beam may therefore be required to be modified in order that the resulting stress equations can become acceptable for the stress analysis of deep beams.

CHAPTER 10

THE APPLICATION OF THE THEORY OF ELASTICITY TO THE SOLUTION OF STRESSES IN DEEP BEAMS

10.1 Introduction

It was shown in Chapter 9 that the determination of two dimensional stress distribution in an elastic body can be achieved by finding an Airy Stress function ϕ which satisfies the boundary conditions of a given problem and the biharmonic equation of compatibility.

The stress function developed showed the presence of a σx stress at the vertical ends of the beams which gave end conditions that were statically equivalent to zero. It was concluded that by the application of St. Venant's principle this state of stress would be acceptable for the consideration of shallow beams.

The effect of end stresses on a deep beam would have some influence on the state of flexural stress at sections throughout the length of the beam, with the result that when considering deep beams it is necessary to satisfy the boundary conditions for zero σx stress at the ends of the beam if an accurate analysis of the beam stresses is to be achieved.

Previous authors investigating the problem of deep beams and the end problem of rectangular strips have employed the method of Finite Difference or principles of Strain Energy to obtain further stress functions by the use of complex eigenfunctions or Fourier series resulting in the form of an infinite integral. These functions are an approximate solution to the finite half plate problem of elasticity and when superimposed upon the solution obtained for the beam loading condition gives a solution that is sufficiently approximate to the ideal condition of a stress free end.

It is proposed here to consider further the general case of a finite beam carrying a uniformly distributed load and to investigate the effect of the Theory of Elasticity on the maximum value and distribution of bending stresses at the mid-span section of the beam for deep beams of various span/depth ratios.

The additional stress function required to eliminate the end stresses resulting from the solution in Chapter 9 will be determined according to the method developed by Timoshenko[10][11], which gives a stress function in the form of a series with adjustable parameters by applying the principle of least work to the strain energy integral.

The stress function so obtained for the elimination of the resultant end stresses will be used to examine the validity of St. Venant's principle where the applied distribution of end stress is a self equilibrative system as is the case of this problem.

10.2 The determination of the stress function for end stresses

The strain energy for a plate of unit thickness is given by

$$U = \frac{1}{2E}\iint\left[\sigma_x^2 + \sigma_y^2 - 2\nu\sigma_x\sigma_y + 2(1+\nu)\tau_{xy}^2\right] dx\, dy \qquad [1]$$

The rectangular plate under consideration is the case of a simply connected boundary and as such the stress distribution does not depend upon the elastic constants of the material.

Equation [1] can therefore be simplified by taking Poissons' ratio ($\nu = 0$)

$$\therefore U = \frac{1}{2E}\iint\left[\sigma_x^2 + \sigma_y^2 + 2\tau_{xy}^2\right] dx\, dy \qquad [2]$$

which from Eqns 9.2 [2] [3] and [4] can be written

$$U = \frac{1}{2E}\iint\left[\left(\frac{\partial^2\phi}{\partial y^2}\right)^2 + \left(\frac{\partial^2\phi}{\partial x^2}\right)^2 + 2\left(-\frac{\partial^2\phi}{\partial x\partial y}\right)^2\right] dx\, dy \qquad [3]$$

in which ϕ is the stress function which makes Eqn [3] a minimum and which also satisfies the prescribed boundary conditions.

The application of variational calculus to determine the minimum value of Eqn [3] results in

$$\frac{\partial^4\phi}{\partial x^4} + 2\,\frac{\partial^4\phi}{\partial x^2\partial y^2} + \frac{\partial^4}{\partial y^4} = 0 \qquad [4]$$

which is the equation of compatibility shown in Chapter 9.

The method developed by Timoshenko arrives at an approximate solution for the problem by taking the stress function in the form of a series

$$\phi = \phi_0 + \alpha_1\phi_1 + \alpha_2\phi_2 + \alpha_3\phi_3 + \ldots\ldots \qquad [5]$$

such that the boundary conditions are satisfied.

$\alpha_1, \alpha_2, \alpha_3$ etc. are constants to be determined.

Substituting Eqn [5] into Eqn [3] V is given as a function of the second degree in $\alpha_1, \alpha_2, \alpha_3$ etc.

The magnitude of these undetermined coefficients is then calculated from the conditions

$$\frac{\delta V}{\delta \alpha_1} = 0 \qquad \frac{\delta V}{\delta \alpha_2} = 0 \qquad \frac{\delta V}{\delta \alpha_3} = 0 \text{ etc.} \qquad [6]$$

which are linear equations in $\alpha_1, \alpha_2, \alpha_3$ .....

A suitable choice of the functions ϕ_1, ϕ_2, ϕ_3 etc. will usually give a satisfactory approximate solution by using only a few terms in the series of Eqn [5].

The function ϕ_0 is determined to satisfy the boundary conditions of the problem.

The remaining functions ϕ_1, ϕ_2, ϕ_3 etc. are chosen so that the stresses corresponding to them vanish at the boundary.

To ensure this, the expression $(x^2 - L^2)^2 \ (y^2 - a^2)^2$ is taken as a factor in all these functions.

The x y origin being taken at the centre point of the beam.

The second derivative of this expression with respect to x vanishes at the edges $y = \pm a$ and the second derivative with respect to y vanishes at the sides $x = \pm L$. The second derivative $\frac{\partial^2}{\partial x \partial y}$ vanishes on all four boundaries of the beam.

The stress equations can be written from Eqn [5]

$$\sigma_x = \frac{\partial^2 \phi}{\partial y^2} = \frac{\partial^2 \phi_0}{\partial y^2} + \alpha_1 \frac{\partial^2 \phi_1}{\partial y^2} + \alpha_2 \frac{\partial^2 \phi_2}{\partial y^2} + \alpha_3 \frac{\partial^2 \phi_3}{\partial y^2} \ldots \text{etc.} \quad [7]$$

$$\sigma_y = \frac{\partial^2 \phi}{\partial x^2} = \frac{\partial^2 \phi_0}{\partial x^2} + \alpha_1 \frac{\partial^2 \phi_1}{\partial x^2} + \alpha_2 \frac{\partial^2 \phi_2}{\partial x^2} + \alpha_3 \frac{\partial^2 \phi_3}{\partial y^2} \ldots \text{etc} \quad [8]$$

$$\tau_{xy} = -\frac{\partial^2 \phi}{\partial x \partial y} = -\frac{\partial^2 \phi_0}{\partial x \partial y} - \alpha_1 \frac{\partial^2 \phi_1}{\partial x \partial y} - \alpha_2 \frac{\partial^2 \phi_2}{\partial x \partial y} - \alpha_3 \frac{\partial^2 \phi_3}{\partial x \partial y} \ldots \text{etc} \quad [9]$$

The linear equations for the determination of the α values take the typical form

$$\iint \left[\left(\frac{\partial^2 \phi_0}{\partial x^2} + \sum \alpha_M \frac{\partial^2 \phi_M}{\partial x^2} \right) \frac{\partial^2 \phi_n}{\partial x^2} + \left(\frac{\partial^2 \phi_0}{\partial y^2} + \sum \alpha_M \frac{\partial^2 \phi_M}{y^2} \right) \frac{\partial^2 \phi_n}{\partial y^2} + 2 \left(\frac{\partial^2 \phi_0}{\partial x \partial y} + \sum \alpha_M \frac{\partial^2 \phi_M}{\partial x \partial y} \right) \frac{\partial^2 \phi_n}{\partial x \partial y} \right] dx\, dy = 0 \quad [10]$$

The first equation is obtained by taking n = 1 the second by taking n = 2 and so on, the summations in each case comprising all of the terms $\alpha_M \phi_M$ from $\alpha_1 \phi_1$ to the end of the series.

Putting all terms in ϕ_0 on the right hand side of the equation, Eqn [10] can be written:-

$$\iint \left[\sum_M \alpha_M \frac{\partial_2 \phi_m}{\partial x^2} \cdot \frac{\partial_2 \phi_n}{\partial x^2} + \sum_M \alpha_M \frac{\partial_2 \phi_m}{\partial y^2} \cdot \frac{\partial_2 \phi_n}{\partial y^2} + 2 \sum_M \alpha_M \frac{\partial_2 \phi_m}{\partial x \partial y} \cdot \frac{\partial_2 \phi_n}{\partial x \partial y} \right] dx\, dy$$

$$= - \iint \left[\frac{\partial_2 \phi_0}{\partial x^2} \cdot \frac{\partial_2 \phi_n}{\partial x^2} + \frac{\partial_2 \phi_0}{\partial y^2} \cdot \frac{\partial_2 \phi_n}{\partial y^2} + 2 \cdot \frac{\partial_2 \phi_0}{\partial x \partial y} \cdot \frac{\partial_2 \phi_n}{\partial x \partial y} \right] dx\, dy \qquad [11]$$

Consider the rectangle bounded by $x = \pm L$ and $y = \pm a$

If the distribution of end stress at $x = \pm L$ is symmetrical about both x and y axes the ϕ stress function will contain only even powers of x & y and can be written:-

$$\phi = \phi_0 + (x^2 - L^2)^2 (y^2 - a^2)^2 \left[\alpha_1 + \alpha_2 x^2 + \alpha_3 y^2 + \alpha_4 x^2 y^2 \right] \text{..etc.} [12]$$

A typical loading condition for which this would be a suitable stress function is shown in Fig. 10.2.1.

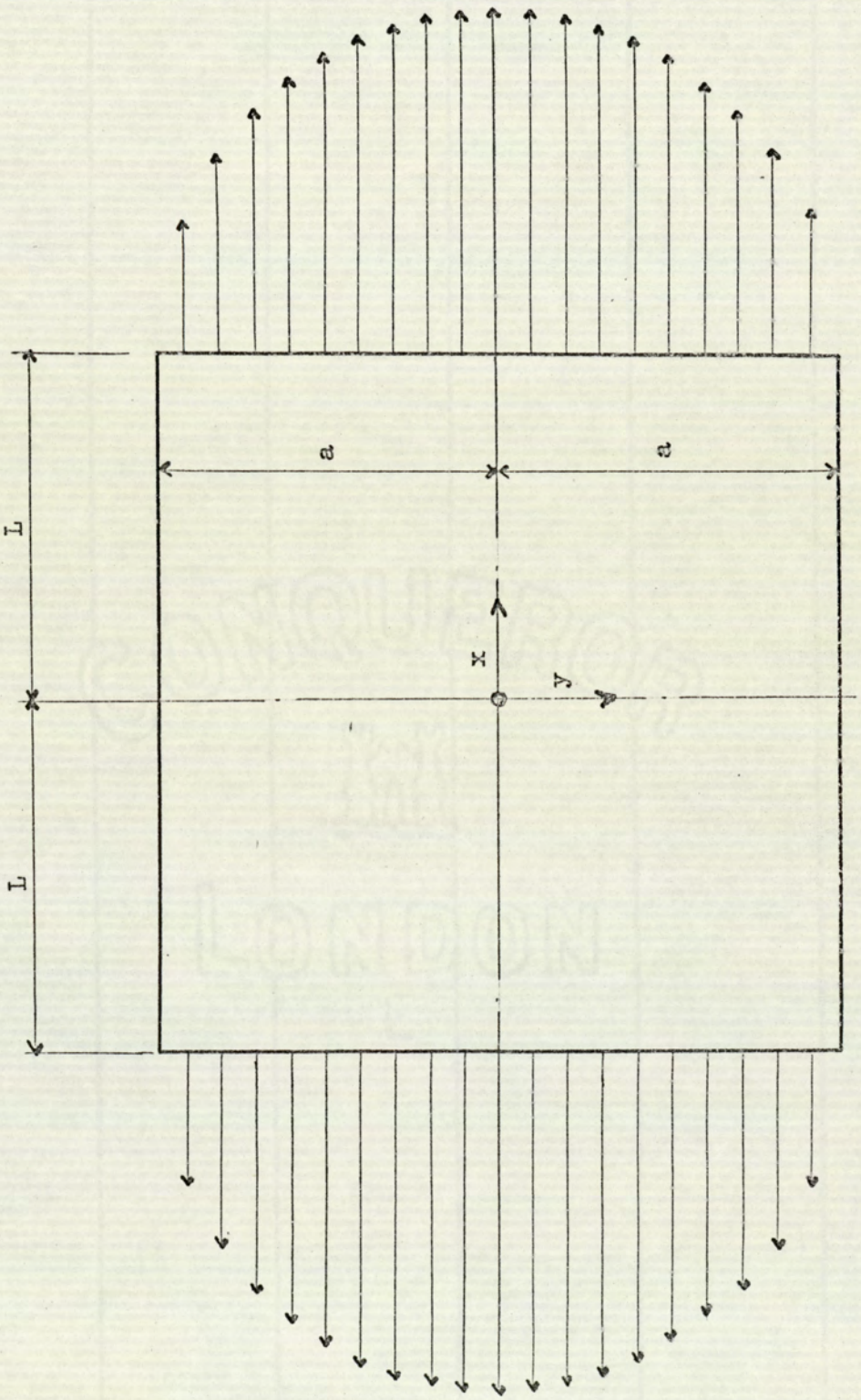

Fig. 10.2.1

If only four parameters ($\alpha 1, \alpha 2, \alpha 3$ and $\alpha 4$) are used in Eqn [12] for the solution of a given problem then the solution of Eqn [11] will give four equations from which the unknown (α) parameters can be determined.

Writing $\frac{a^2}{L^2} = K$ these four equations are:-

$$\left[\frac{64}{7} + \frac{256}{49} K + \frac{64}{7} K^2\right] \alpha 1 + \left[\frac{64}{77} + \frac{64}{49} K^2\right] \alpha 2 \, L^2$$

$$+ \left[\frac{64}{49} + \frac{64}{77} K^2\right] \alpha 3 \, a^2 + \left[\frac{64}{539} + \frac{64}{539} K^2\right] \alpha 4 \, a^2 L^2$$

$$= -\frac{9.5.5}{128 L^9 a^5} \int_0^L \int_0^a \left[\frac{\partial^2 \phi_0}{\partial x^2} \cdot \frac{\partial^2 \phi_1}{\partial x^2} + \frac{\partial^2 \phi_0}{\partial y^2} \cdot \frac{\partial^2 \phi_1}{\partial y^2} \right.$$

$$\left. + 2 \cdot \frac{\partial^2 \phi_0}{\partial x \partial y} \cdot \frac{\partial^2 \phi_1}{\partial x \partial y} \right] dx \, dy \qquad [13]$$

$$\left[\frac{64}{11} + \frac{64}{7} K^2\right] \alpha 1 + \left[\frac{192}{143} + \frac{256}{77} K + \frac{192}{7} K^2\right] \alpha 2 \cdot L^2$$

$$+ \left[\frac{64}{77} + \frac{64}{77} K^2\right] \alpha 3 \cdot a^2 + \left[\frac{192}{1001} + \frac{192}{77} K^2\right] \alpha 4 \, a^2 L^2$$

$$= -\frac{9.7.5.5}{128 L^{11} a^5} \int_0^L \int_0^a \left[\frac{\partial^2 \phi_0}{\partial x^2} \cdot \frac{\partial^2 \phi_2}{\partial x^2} + \frac{\partial^2 \phi_0}{\partial y^2} \cdot \frac{\partial^2 \phi_2}{\partial y^2} \right.$$

$$\left. + 2 \cdot \frac{\partial^2 \phi_0}{\partial x \partial y} \cdot \frac{\partial^2 \phi_2}{\partial x \partial y} \right] dx \, dy \qquad [14]$$

$$\left[\frac{64}{7}+\frac{64}{11}K^2\right]\alpha_1+\left[\frac{64}{77}+\frac{64}{77}K^2\right]\alpha_2 L^2$$

$$+\left[\frac{192}{7}+\frac{256}{77}K+\frac{192}{143}K^2\right]\alpha_3 a^2+\left[\frac{192}{77}+\frac{192}{1001}K^2\right]\alpha_4 a^2L^2$$

$$=-\frac{9.7.5.5}{128L^9a^7}\int_0^L\int_0^a\left[\frac{\partial^2\phi_0}{\partial x^2}\cdot\frac{\partial^2\phi_3}{\partial x^2}+\frac{\partial^2\phi_0}{\partial y^2}\cdot\frac{\partial^2\phi_3}{y^2}\right.$$

$$\left.+2.\frac{\partial^2\phi_0}{\partial x\partial y}\cdot\frac{\partial^2\phi_3}{\partial x\partial y}\right]dx\,dy \qquad [15]$$

$$\left[\frac{64}{11}+\frac{64}{11}K^2\right]\alpha_1+\left[\frac{192}{143}+\frac{192}{11}K^2\right]\alpha_2 L^2$$

$$+\left[\frac{192}{11}+\frac{192}{143}K^2\right]\alpha_3 a^2+\left[\frac{576}{143}+\frac{256}{121}K+\frac{576}{143}K^2\right]\alpha_4 a^2L^2$$

$$=-\frac{9.7.7.5.5}{128L^{11}a^7}\int_0^L\int_0^a\left[\frac{\partial^2\phi_0}{\partial x^2}\cdot\frac{\partial^2\phi_4}{\partial x^2}+\frac{\partial^2\phi_0}{\partial y^2}\cdot\frac{\partial^2\phi_4}{\partial y^2}\right.$$

$$\left.+2.\frac{\partial^2\phi_0}{\partial x\partial y}\cdot\frac{\partial^2\phi_4}{\partial x\partial y}\right]dx\,dy \qquad [16]$$

For various symmetrical distribution of stress over the ends $x = \pm L$ it is only necessary to change the form of the function ϕ_0 in Eqn [12]. This change effects only the right hand side of Eqns [13] [14] [15] and [16] The left hand side of the equations remains as stated for all conditions of symmetrical loading to which the ϕ function of Eqn [12] is applicable.

The remaining problem for any given loading condition is to determine the function ϕ_0 that will satisfy the boundary conditions.

If the ends of the beam are loaded at $x = \pm L$ by a stress given by $f(y)$, ϕ_o has to be determined such that:-

$$\frac{\partial^2 \phi_0}{\partial y^2} = \sigma_x = f(y) \quad \text{at } x = \pm L$$

$$\frac{\partial^2 \phi_0}{\partial x^2} = \sigma_y = 0 \quad \text{at } y = \pm a$$

$$-\frac{\partial^2 \phi_0}{\partial x \partial y} = \tau_{xy} = 0 \quad \text{at } y = \pm a \text{ and } x = \pm L$$

These conditions can be achieved simply by taking

$$\phi_0 = \iint f(y)\, dy\, dy \qquad [17]$$

For a distribution of end stresses at $x = \pm L$ that is symmetrical about the y axis but anti-symmetrical about the x axis, the stress system will be odd with respect to (x) and even with respect to (y). These conditions will be satisfied by taking the stress function:-

$$\phi = \phi_0 + (x^2 - L^2)^2 (y^2 - a^2)^2 \left[\alpha_1 y + \alpha_2 y x^2 + \alpha_3 y^3 + \alpha_4 x^2 y^3 \ldots \right] \quad [18]$$

ϕ_0 as before, being such as to satisfy the prescribed boundary conditions of the problem and determined from Eqn [17] .

A typical loading condition for which this would be a suitable stress function is shown in Fig. 10.2.2.

Again, if only four parameters ($\alpha_1, \alpha_2, \alpha_3$ and α_4) are used in Eqn [18] for the solution of a given problem then the four equations for the solution of the unknown (α) parameter are:-

Writing $\frac{a^2}{L^2} = K$

$$\left[\frac{64}{7} + \frac{256K}{105} + \frac{64}{55} K^2 \right] \alpha_1 a + \left[\frac{64}{77} + \frac{64}{385} K^2 \right] \alpha_2 L^2 a$$

$$+ \left[\frac{64}{21} + \frac{512}{1155} K + \frac{192}{715} K^2 \right] \alpha_3 a^3 + \left[\frac{64}{231} + \frac{192}{5005} K^2 \right] \alpha_4 L^2 a^3$$

$$= - \frac{9.7.5}{128 L^9 a^6} \int_0^L \int_0^a \left[\frac{\partial^2 \phi_0}{\partial x^2} \cdot \frac{\partial^2 \phi_1}{\partial x^2} + \frac{\partial^2 \phi_0}{\partial y^2} \cdot \frac{\partial^2 \phi_1}{\partial y^2} \right.$$

$$\left. + 2 \frac{\partial^2 \phi_0}{\partial x \partial y} \cdot \frac{\partial^2 \phi_1}{\partial x \partial y} \right] dx.dy \quad [19]$$

$$\left[\frac{64}{7}+\frac{64}{35}K^2\right]\alpha_1 a + \left[\frac{192}{91}+\frac{256}{105}K+\frac{192}{35}K^2\right]\alpha_2 L^2 a$$

$$+\left[\frac{64}{21}+\frac{192}{455}K^2\right]\alpha_3 a^3 + \left[\frac{192}{273}+\frac{512}{1155}K+\frac{576}{455}K^2\right]\alpha_4 L^2 a^3$$

$$= -\frac{11.9.7.5}{128 L^{11} a^6}\int_0^L\int_0^a\left[\frac{\partial^2\phi_0}{\partial x^2}\cdot\frac{\partial^2\phi_2}{\partial x^2}+\frac{\partial^2\phi_0}{\partial y^2}\cdot\frac{\partial^2\phi_2}{\partial y^2}\right.$$

$$\left.+2\frac{\partial^2\phi_0}{\partial x\,\partial y}\cdot\frac{\partial^2\phi_2}{\partial x\partial y}\right]dx\,dy \qquad [20]$$

$$\left[\frac{64}{21}+\frac{512}{1155}K+\frac{192}{715}K^2\right]\alpha_1 a + \left[\frac{64}{231}+\frac{192}{5005}K^2\right]\alpha_2 L^2 a$$

$$+\left[\frac{832}{231}+\frac{4352}{15015}K+\frac{64}{715}K^2\right]\alpha_3 a^3 + \left[\frac{832}{2541}+\frac{192}{15015}K^2\right]\alpha_4 L^2 a^3$$

$$= -\frac{9.7.5}{128 L^9 a^8}\int_0^L\int_0^a\left[\frac{\partial^2\phi_0}{\partial x^2}\cdot\frac{\partial^2\phi_3}{\partial x^2}+\frac{\partial^2\phi_0}{\partial y^2}\cdot\frac{\partial^2\phi_3}{\partial y^2}\right.$$

$$\left.+2\frac{\partial^2\phi_0}{\partial x\partial y}\cdot\frac{\partial^2\phi_3}{\partial x\,\partial y}\right]dx\,dy \qquad [21]$$

$$\left[\frac{64}{21}+\frac{192}{455}K^2\right]\alpha_1 a + \left[\frac{192}{273}+\frac{512}{1155}K+\frac{576}{455}K^2\right]\alpha_2 L^2 a$$

$$+\left[\frac{832}{231}+\frac{192}{1365}K^2\right]\alpha_3 a^3 + \left[\frac{64}{77}+\frac{4352}{15015}K+\frac{576}{1365}K^2\right]\alpha_4 L^2 a^3$$

$$= -\frac{11.9.7.5}{128 L^{11} a^8}\int_0^L\int_0^a\left[\frac{\partial^2\phi_0}{\partial x^2}\cdot\frac{\partial^2\phi_4}{\partial x^2}+\frac{\partial^2\phi_0}{\partial y^2}\cdot\frac{\partial^2\phi_4}{\partial y^2}\right.$$

$$\left.+2\frac{\partial^2\phi_0}{\partial x\partial y}\cdot\frac{\partial^2\phi_4}{\partial x\,\partial y}\right]dx\,dy \qquad [22]$$

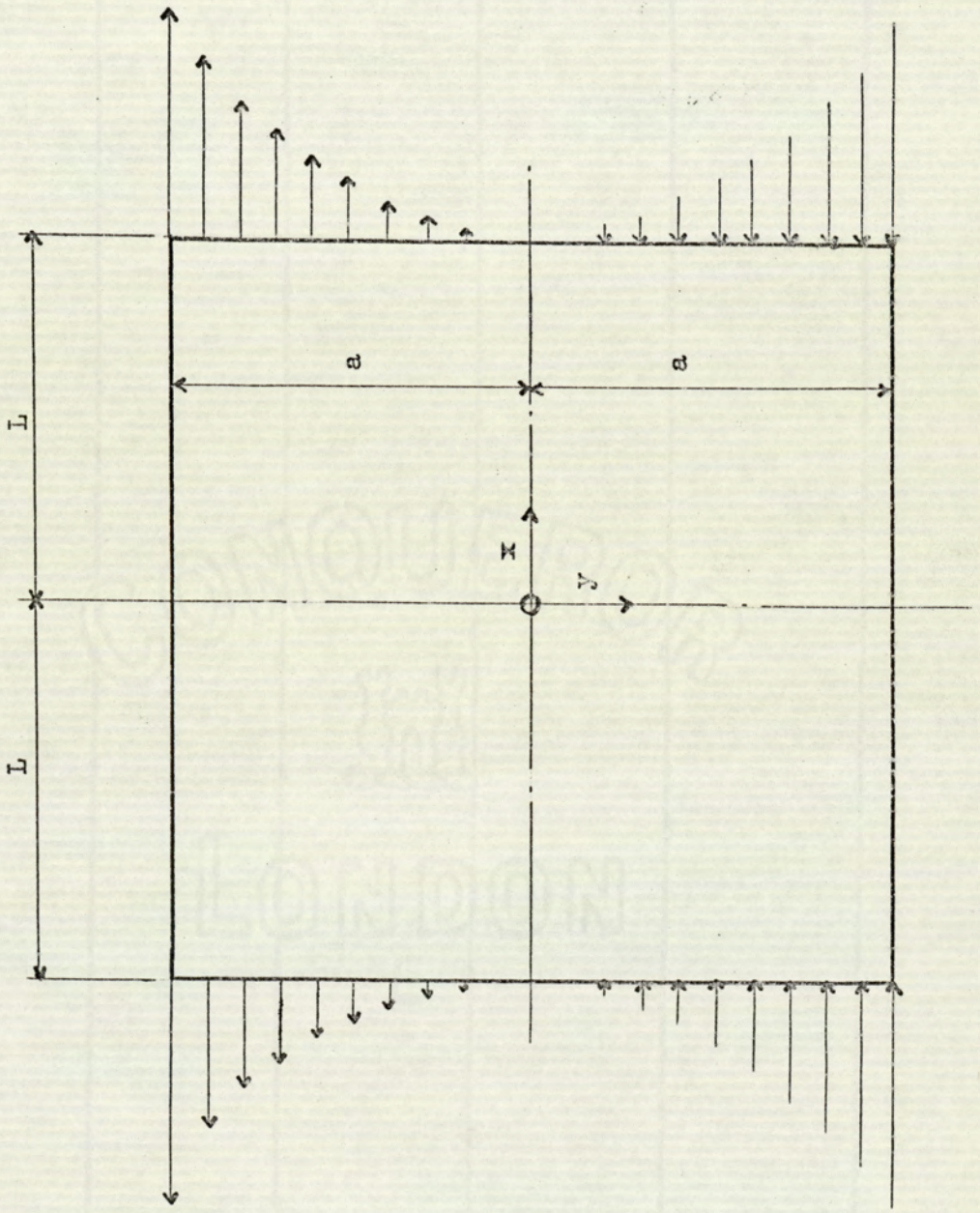

Fig.10.2.2

10.3 The determination of the Stress Equations for the elimination of end stresses

10.3.1 Consider the rectangular deep beam of unit thickness bounded by $x = \pm L$ and $y = \pm a$ subject to its self weight (unit density = D) and an imposed load on the top edge of 160 A a^3 per unit area.

This beam was considered in Chapter 9 where it was shown that the resultant end stresses from the Theory of Elasticity are:-

1) Due to the self weight of the beam

$$\sigma x = \frac{D}{80a^2}\left(80\,y^3 - 48\,a^2 y\right) \qquad [23]$$

2) Due to the imposed load

$$\sigma x = A\left(80\,y^3 - 48\,a^2 y\right) \qquad [24]$$

To eliminate these end stresses it will be necessary to apply to the vertical ends of the beam stresses equal in magnitude and opposite in sign to the stresses given by Eqns [23] and [24] .

Clearly, Eqns [23] and [24] give similar curves for the distribution of stress $(80\,y^3 - 48\,a^2 y)$ the variation being in the constants $\frac{D}{80a^2}$ and A.

These distributions of stress are shown in Fig. 10.3.1.

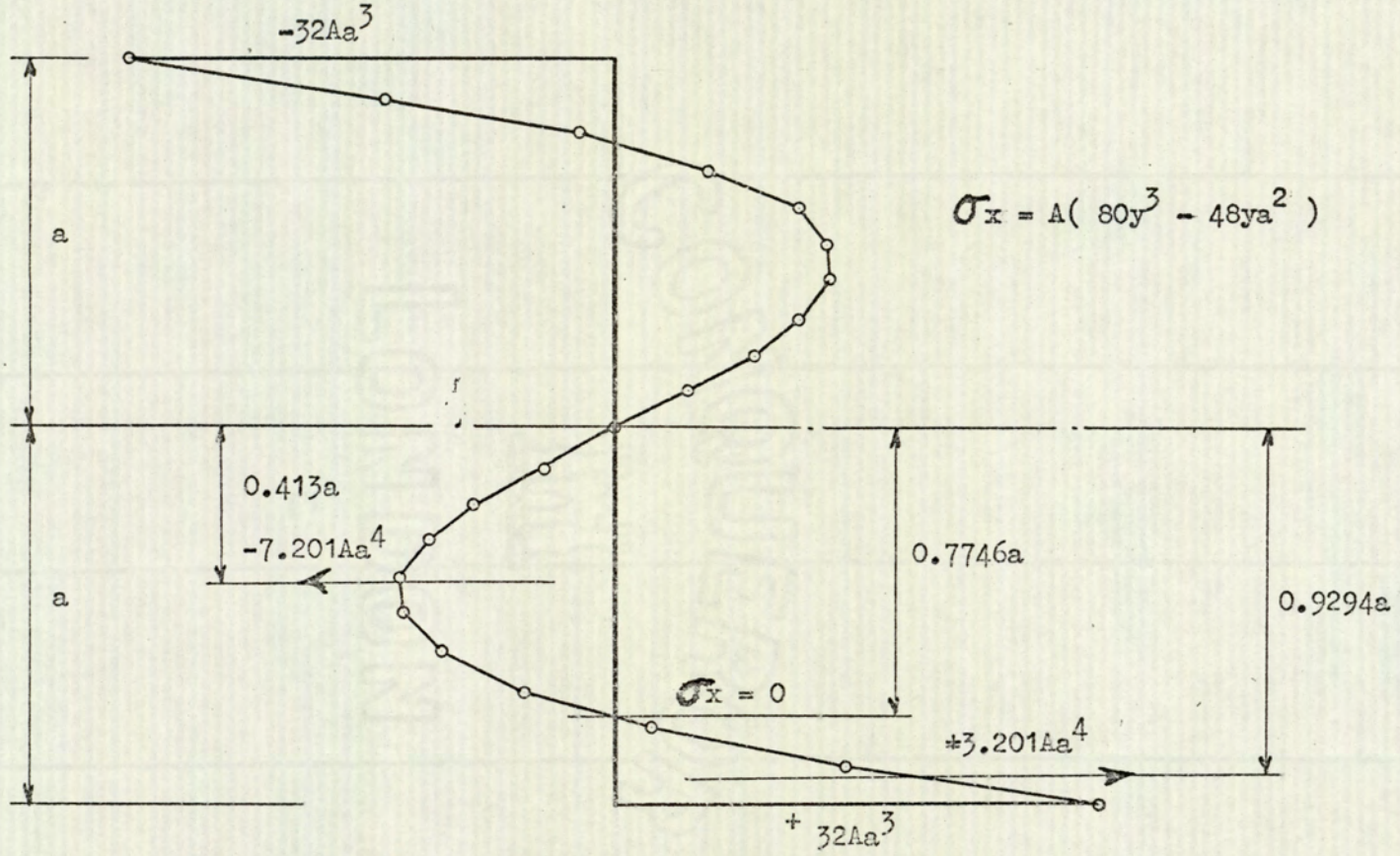

DISTRIBUTION OF END STRESSES DUE TO AN IMPOSED LOAD OF $w = 160Aa^3$

RESULTANT END STRESSES FROM CHAPTER 9 STRESS FUNCTION.

Fig 10. 3. 1

Stress equations will therefore be determined to eliminate the end stresses due to the imposed load, these equations will then be modified to give stress equations that will eliminate the end stresses due to the self weight of the beam.

10.3.2.

Fig. 10.3.1. shows that the stress distribution is symmetrical about the y axis and anti-symmetrical about the x axis. The stress function will therefore be of the form of Eqn [18] .

To satisfy the prescribed boundary conditions

$$\sigma_x = -A(80\,y^3 - 48\,a^2y) \quad \text{at } x = \pm L$$
$$\sigma_y = 0 \quad \text{at } y = \pm a$$
$$\tau_{xy} = 0 \quad \text{at } y = \pm a \text{ and } x = \pm L$$

ϕ_0 can be determined from Eqn [17]

$$\phi_0 = \iint -A(80y^3 - 48\,a^2y)\,dy\,dy$$

$$\therefore \phi_0 = -A(4y^5 - 8\,a^2y^3) \qquad [25]$$

The stress function can now be written

$$\phi = -A(4y^5 - 8a^2y^3) + (x^2 - L^2)^2\,(y^2 - a^2)^2\left[\alpha_{1y} + \alpha_{2yx}{}^2 + \alpha_3 y^3 + \alpha_4 x^2 y^3\right] \qquad [26]$$

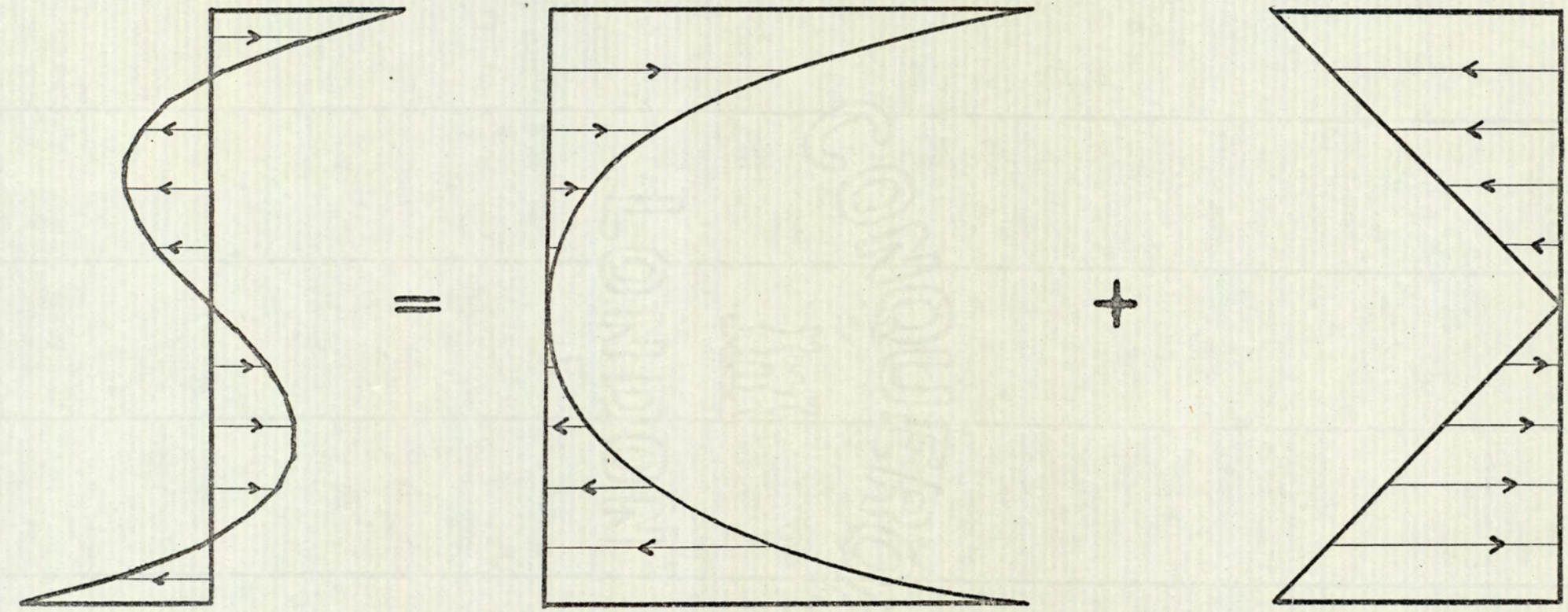

APPLIED STRESS DISTRIBUTION TO ELIMINATE RESULTANT END STRESSES

Fig 10. 3. 2.

Fig. 10.3.2. shows the distribution of stress that will be applied to the ends of the beam at $x = \pm L$ to eliminate the end stresses that result from the stress function obtained in Chapter 9.

The total stress distribution can be broken down into two simpler distributions:

a) $-80 A y^3$

b) $+48 A a^2 y$

Both of these distributions are symmetrical about the y axis and anti-symmetrical about the x axis. The stress function for each case will therefore be of the form of Eqn [18] .

Clearly, $40 A a^2 y$ is a linear distribution of stress

The stress function that will suit this distribution is

$$\phi = 8 A a^2 y^3 + (x^2 - L^2)^2 (y^2 - a^2)^2 \left[\alpha_{1y} + \alpha_{2yx^2} + \alpha_{3y^3} + \alpha_{4x^2y^3}\right] \quad [27]$$

Using Eqns [19] [20] [21] and [22] to determine the unknown (α) parameters results in the right hand side of all equations equal to zero.

Since ϕ_0 is independant of x, $\frac{\partial_2 \phi_0}{\partial x^2} = 0$ and $\frac{\partial_2 \phi_0}{\partial x \, \partial y} = 0$

the right hand side of Eqns [19] [20] [21] and [22] will all contain the term

$$\int_0^L \int_0^a \left[\frac{\partial_2 \phi_0}{\partial y^2} \cdot \frac{\partial_2 \phi_n}{\partial y^2}\right] dx \, dy \quad [28]$$

Then for example solving this term for Eqn [19]

$$\phi_0 = 8 A a^2 y^3$$

$$\therefore \frac{\partial_2 \phi_0}{\partial y^2} = 48 A a^2 y$$

$$\phi_1 = (x^2 - L^2)^2 (y^2 - a^2)^2 y$$

After the expansion of ϕ_1

$$\frac{\partial_2 \phi_0}{\partial y^2} \cdot \frac{\partial_2 \phi_1}{\partial y^2} = 48 A \left[-12x^4y^2a^4 + 24x^2y^2L^2a^4 - 12y^2L^4a^4 + 20x^4y^4a^2 - 40x^2y^4L^2a^2 + 20y^4L^4a^2 \right]$$

$$\int_0^L dx = 48A \left[-\frac{12}{5} y^2 L^5 a^4 + \frac{24}{3} y^2 L^5 a^4 - 12y^2 L^5 a^4 + \frac{20}{5} y^4 L^5 a^2 - \frac{40}{3} y^4 L^5 a^2 + 20 y^4 L^5 a^2 \right]$$

$$\int_0^a dy = 48AL^5a^7 \left[-\frac{12}{15} + \frac{24}{9} - \frac{12}{3} + \frac{20}{5} - \frac{40}{15} + \frac{20}{5} \right]$$

$$= 0$$

This shows that a linear distribution of stress applied to the end of the beam is transmitted without change throughout the length of the beam.

The mathematical solution for the complete problem where $\phi_0 = -A(4y^5 - 8a^2y^3)$ can therefore be simplified by considering only the term $-4Ay^5$ when using Eqns [19] [20] [21] and [22] for the determination of the unknown (α)parameters.

Therefore, using Eqns [19] [20] [21] and [22] to determine the values of $\alpha_1, \alpha_2, \alpha_3$ and α_4 the right hand sides of these equations become:-

Eqn [19]

$$-\frac{9.7.5}{128L^9a^6}\int_0^L\int_0^a\left[\frac{\partial_2\phi_0}{\partial y^2}\cdot\frac{\partial_2\phi_1}{\partial y^2}\right]dx.dy \qquad [29]$$

$$\frac{\partial_2\phi_0}{\partial y^2} = -80A\,y^3 \quad (\text{i.e. neglecting the term } 48Aa^2y)$$

$$\phi_1 = (x^2-L^2)^2(y^2-a^2)^2y$$

$$\frac{\partial_2\phi_1}{\partial y^2} = \left[-12\,x^4y\,a^2 + 24\,x^2y\,L^2a^2 - 12yL^4a^2 + 20x^4y^3 - 40x^2y^3L^2 + 20y^3L^4\right]$$

$$\frac{\partial_2\phi_0}{\partial y^2}.\frac{\partial_2\phi_1}{\partial y^2} = -80A\left[-12x^4y^4a^2 + 24x^2y^4L^2a^2 - 12y^4L^4a^2 + 20x^4y^6 - 40x^2y^6L^2 + 20y^6L^4\right]$$

$$\int_0^L dx = -80A\left[-\frac{12}{5}\,y^4L^5a^2 + \frac{24}{3}\,y^4L^5a^2 - 12y^4L^5a^2 + \frac{20}{5}\,L^5y^6 - \frac{40}{3}\,L^5y^6 + 20\,L^5y^6\right]$$

$$\int_0^a dy = -80AL^5a^7\left[-\frac{12}{25} + \frac{24}{15} - \frac{12}{5} + \frac{20}{35} - \frac{40}{21} + \frac{20}{7}\right]$$

$$= -\frac{10240}{525}\,A\,L^5\,a^7$$

Eqn [29] then becomes

$$-\frac{315}{128L^9a^6} \times -\frac{10240}{525}\,A\,L^5\,a^7 = \frac{48\,A\,a}{L^4}$$

Eqn [20]

$$-\frac{11.9.7.5}{128L^{11}a^6}\int_0^L\int_0^a\left[\frac{\partial_2\phi_0}{\partial y^2}\cdot\frac{\partial_2\phi_2}{\partial y^2}\right]dx\,dy \qquad [30]$$

$$\frac{\partial_2\phi_0}{\partial y^2} = -80\,A\,y^3$$

$$\phi_2 = x^2\phi_1$$

$$\frac{\partial_2\phi_0}{\partial y^2}\cdot\frac{\partial_2\phi_2}{\partial y^2} = -80A\left[-12x^6y^4a^2 + 24x^4y^4L^2a^2 - 12x^2y^4L^4a^2 + 20x^6y^6 - 40x^4y^6L^2 + 20x^2y^6L^4\right]$$

$$\int_0^L dx = -80A\left[-\frac{12}{7}y^4L^7a^2 + \frac{24}{5}y^4L^7a^2 - \frac{12}{3}y^4L^7a^2 + \frac{20}{7}y^6L^7 - \frac{40}{5}y^6L^7 + \frac{20}{3}y^6L^7\right]$$

$$\int_0^a dy = -80AL^7a^7\left[-\frac{12}{35} + \frac{24}{25} - \frac{12}{15} + \frac{20}{49} - \frac{40}{35} + \frac{20}{21}\right]$$

$$= -\frac{2048}{735}\,A\,L^7\,a^7$$

Eqn [30] then becomes

$$-\frac{3465}{128L^{11}a^6}\times-\frac{2048}{735}\,A\,L^7\,a^7 = \frac{11088}{147}\,\frac{A\,a}{L^4} = \frac{528}{7}\,\frac{A\,a}{L^4}$$

Eqn [21]

$$-\frac{9.7.5}{128L^9a^8}\int_0^L\int_0^a\left[\frac{\partial^2\phi_0}{\partial y^2}\cdot\frac{\partial^2\phi_3}{\partial y^2}\right]dx\,dy \qquad [31]$$

$$\frac{\partial^2\phi_0}{\partial y^2} = -80\,A\,y^3$$

$$\phi_3 = y^2\phi_1 = \Big[x^4y^3a^4 - 2x^2y^3L^2a^4 + y^3a^4L^4 - 2x^4y^5a^2 + 4x^2y^5a^2L^2 - 2y^5L^4a^2 + x^4y^7 - 2x^2y^7L^2 + y^7L^4\Big]$$

$$\frac{\partial^2\phi_3}{\partial y^2} = \Big[6x^4ya^4 - 12x^2yL^2a^4 + 6ya^4L^4 - 40x^4y^3a^2 + 80x^2y^3a^2L^2 - 40y^3L^4a^2 + 42x^4y^5 - 84x^2y^5L^2 + 42y^5L^4\Big]$$

$$\frac{\partial^2\phi_0}{\partial y^2}\cdot\frac{\partial^2\phi_3}{\partial y^2} = -80A\Big[6x^4y^4a^4 - 12x^2y^4L^2a^4 + 6y^4L^4a^4 - 40x^4y^6a^2 + 80x^2y^6L^2a^2 - 40y^6L^4a^2 + 42x^4y^8 - 84x^2y^8L^2 + 42y^8L^4\Big]$$

$$\int_0^L dx = -80A\Big[\frac{6}{5}y^4L^5a^4 - \frac{12}{3}y^4L^5a^4 + 6y^4L^5a^4 - \frac{40}{5}y^6L^5a^2 + \frac{80}{3}y^6L^5a^2 - 40y^6L^5a^2 + \frac{42}{5}y^8L^5 - \frac{84}{3}y^8L^5 + 42\,y^8L^5\Big]$$

$$\int_0^a dy = -80AL^5a^9\Big[\frac{6}{25} - \frac{12}{15} + \frac{6}{5} - \frac{40}{35} + \frac{80}{21} - \frac{40}{7} + \frac{42}{45} - \frac{84}{27} + \frac{42}{9}\Big]$$

$$= -\frac{6144}{945}\,A\,L^5a^9$$

Eqn [31] then becomes

$$-\frac{315}{128L^9a^8} \cdot -\frac{6144AL^5a^9}{945} = \frac{16\,Aa}{L^4}$$

Eqn [22]

$$-\frac{11.9.7.5}{128L^{11}a^8} \int_0^L \int_0^a \left[\frac{\partial^2\phi_0}{\partial y^2} \cdot \frac{\partial^2\phi_4}{\partial y^2} \right] dx\,dy \qquad [32]$$

$$\frac{\partial^2\phi_0}{\partial y^2} = -80\,A\,y^3$$

$$\phi_4 = x^2\phi_3$$

$$\frac{\partial^2\phi_0}{\partial y^2} \cdot \frac{\partial^2\phi_4}{\partial y^2} = -80A\left[6x^6y^4a^4 - 12x^4y^4L^2a^4 + 6x^2y^4L^4a^4 \right.$$
$$-40x^6y^6a^2 + 80x^4y^6L^2a^2 - 40x^2y^6L^4a^2$$
$$\left. + 42x^6y^8 - 84x^4y^8L^2 + 42x^2y^8L^4 \right]$$

$$\int_0^L dx = -80A\left[\frac{6}{7}y^4L^7a^4 - \frac{12}{5}y^4L^7a^4 + \frac{6}{3}y^4L^7a^4 \right.$$
$$-\frac{40}{7}y^6L^7a^2 + \frac{80}{5}y^6L^7a^2 - \frac{40}{3}y^6L^7a^2$$
$$\left. + \frac{42}{7}y^8L^7 - \frac{84}{5}y^8L^7 + \frac{42}{3}y^8L^7 \right]$$

$$\int_0^a dy = -80\,A\,L^7a^9\left[\frac{6}{35} - \frac{12}{25} + \frac{6}{15} - \frac{40}{49} + \frac{80}{35} - \frac{40}{21} + \frac{42}{63} - \frac{84}{45} + \frac{42}{27} \right]$$

$$= -\frac{2048}{2205}\,A\,L^7a^9$$

Eqn [32] then becomes

$$-\frac{99 \times 35}{128L^{11}a^8} \cdot -\frac{2048}{2205}\,A\,L^7a^9 = \frac{176}{7}\,\frac{Aa}{L^4}$$

For the problem under consideration the α equations can now be written in detail from Eqns [19], [20], [21] and [22]

$$\left[\frac{64}{7} + \frac{256}{105}K + \frac{64}{55}K^2\right]\alpha_1 a + \left[\frac{64}{77} + \frac{64}{385}K^2\right]\alpha_2 L^2 a$$

$$+ \left[\frac{64}{21} + \frac{512}{1155}K + \frac{192}{715}K^2\right]\alpha_3 a^3 + \left[\frac{64}{231} + \frac{192}{5005}K^2\right]\alpha_4 L^2 a^3 = \frac{48Aa}{L^4} \qquad [33]$$

$$\left[\frac{64}{7} + \frac{64}{35}K^2\right]\alpha_1 a + \left[\frac{192}{91} + \frac{256}{105}K + \frac{192}{35}K^2\right]\alpha_2 L^2 a$$

$$+\left[\frac{64}{21} + \frac{192}{455}K^2\right]\alpha_3 a^3 + \left[\frac{192}{273} + \frac{512}{1155}K + \frac{576}{455}K^2\right]\alpha_4 L^2 a^3 = \frac{528}{7}\frac{Aa}{L^4} \qquad [34]$$

$$\left[\frac{64}{21} + \frac{512}{1155}K + \frac{192}{715}K^2\right]\alpha_1 a + \left[\frac{64}{231} + \frac{192}{5005}K^2\right]\alpha_2 L^2 a$$

$$+ \left[\frac{832}{231} + \frac{4352}{15015}K + \frac{64}{715}K^2\right]\alpha_3 a^3 + \left[\frac{832}{2541} + \frac{192}{15015}K^2\right]\alpha_4 L^2 a^3 = \frac{16Aa}{L^4} \qquad [35]$$

$$\left[\frac{64}{21} + \frac{192}{455}K^2\right]\alpha_1 a + \left[\frac{192}{273} + \frac{512}{1155}K + \frac{576}{455}K^2\right]\alpha_2 L^2 a$$

$$+ \left[\frac{832}{231} + \frac{192}{1365}K^2\right]\alpha_3 a^3 + \left[\frac{64}{77} + \frac{4352}{15015}K + \frac{576}{1365}K^2\right]\alpha_4 L^2 a^3 = \frac{176}{7}\frac{Aa}{L^4} \qquad [36]$$

Eqns [33] [34] [35] and [36] can now be used to determine the values of $\alpha_1, \alpha_2, \alpha_3$ and α_4 for various values of K.

These result in Table No. 10.3.1.

For a given beam shape it is now possible to write the final stress function from Eqn [26] using the determined (α) parameters from Table 10.3.1.

SPAN / DEPTH	K	$\alpha_1 \frac{A}{L^4}$	$\alpha_2 \frac{A}{L^6}$	$\alpha_3 \frac{A}{L^4 a^2}$	$\alpha_4 \frac{A}{L^6 a^2}$
2.0	0.25	3.773	12.449	-0.131	3.115
1.8	0.309	3.815	10.906	-0.119	3.444
1.6	0.391	3.837	9.111	-0.087	3.731
1.4	0.510	3.811	7.097	-0.018	3.896
1.2	0.694	3.683	4.959	0.111	3.825
1.0	1.0	3.357	2.920	0.328	3.382
0.8	1.563	2.700	1.280	0.643	2.523
0.6	2.778	1.625	0.291	0.962	1.426
0.4	6.250	0.467	-0.016	0.903	0.453
0.2	25.00	0.015	-0.003	0.197	0.021

(α) PARAMETERS FOR TOP FACE LOADING = $160A\,a^3$ per UNIT AREA

TABLE NO. 10.3.1

10.3.3.

Before proceeding with the equations for stress it is convenient to consider the final stress function ϕ in the form given in Eqn [5] .

$$\phi = \phi_0 + \alpha_1\phi_1 + \alpha_2\phi_2 + \alpha_3\phi_3 + \alpha_4\phi_4 \ldots\ldots$$

$$\phi_0 = -A(4y^5 - 8a^2y^3)$$

$$\alpha_1\phi_1 = \alpha_1 y \left[(x^2 - L^2)^2 (y^2 - a^2)^2\right]$$

$$\alpha_2\phi_2 = \alpha_2 yx^2 \left[(x^2 - L^2)^2 (y^2 - a^2)^2\right]$$

$$\alpha_3\phi_3 = \alpha_3 y^3 \left[(x^2 - L^2)^2 (y^2 - a^2)^2\right]$$

$$\alpha_4\phi_4 = \alpha_4 x^2y^3 \left[(x^2 - L^2)^2 (y^2 - a^2)^2\right]$$

Then, writing the equations for stress in detail

$$\sigma_x = \frac{\partial_2\phi}{\partial y^2}$$

$$\therefore \sigma_x = -A(80y^3 - 48a^2y)$$

$$+\alpha_1(-12x^4ya^2 + 24x^2yL^2a^2 - 12yL^4a^2 + 20x^4y^3 - 40x^2y^3L^2 + 20y^3L^4)$$

$$+\alpha_2(-12x^6ya^2 + 24x^4yL^2a^2 - 12x^2yL^4a^2 + 20x^6y^3 - 40x^4y^3L^2 + 20x^2y^3L^4)$$

$$+\alpha_3(6a^4x^4y - 12x^2yL^2a^4 + 6yL^4a^4 - 40x^4y^3a^2 + 80x^2y^3L^2a^2 - 40y^3L^4a^2 + 42x^4y^5 - 84x^2y^5L^2 + 42y^5L^4)$$

$$+\alpha_4(6a^4x^6y - 12x^4yL^2a^4 + 6x^2yL^4a^4 - 40x^6y^3a^2 + 80x^4y^3L^2a^2 - 40x^2y^3L^4a^2 + 42x^6y^5 - 84x^4y^5L^2 + 42x^2y^5L^4) \quad [37]$$

$$\sigma_y = \frac{\partial_2 \phi}{\partial x^2}$$

$$\therefore \sigma_y = \alpha_1(12a^4x^2y - 4yL^2a^4 - 24x^2y^3a^2 + 8y^3L^2a^2 + 12x^2y^5 - 4y^5L^2)$$
$$+ \alpha_2(30a^4x^4y - 24x^2yL^2a^4 + 2yL^2a^4 - 60x^4y^3a^2 + 48x^2y^3L^2a^2 - 4y^3L^4a^2$$
$$+ 30x^4y^5 - 24x^2y^5L^2 + 2y^5L^4)$$
$$+ \alpha_3(12a^4x^2y^3 - 4y^3L^2a^4 - 24x^2y^5a^2 + 8y^5L^2a^2 + 12x^2y^7 - 4y^7L^2)$$
$$+ \alpha_4(30a^4x^4y^3 - 24x^2y^3L^2a^4 + 2y^3L^4a^4 - 60x^4y^5a^2 + 48x^2y^5L^2a^2$$
$$- 4y^5L^4a^2 + 30x^4y^7 - 24x^2y^7L^2 + 2y^7L^4) \qquad [38]$$

$$\tau_{xy} = -\frac{\partial_2 \phi}{\partial x \partial y}$$

$$\therefore \tau_{xy} = -\alpha_1(4a^4x^3 - 4xL^2a^4 - 24x^3y^2a^2 + 24xy^2L^2a^2 + 20x^3y^4 - 20xy^4L^2)$$
$$-\alpha_2(6a^4x^5 - 8x^3L^2a^4 + 2xL^4a^4 - 36x^5y^2a^2 + 48x^3y^2L^2a^2 - 12xy^2L^4a^2$$
$$+ 30x^5y^4 - 40x^3y^4L^2 + 10xy^4L^4)$$
$$-\alpha_3(12a^4x^3y^2 - 12xy^2L^2a^4 - 40x^3y^4a^2 + 40xy^4L^2a^2 + 28x^3y^6 - 28xy^6L^2)$$
$$-\alpha_4(18a^4x^5y^2 - 24x^3y^2L^2a^4 + 6xy^2L^4a^4 - 60x^5y^4a^2 + 80x^3y^4L^2a^2$$
$$-20xy^4L^4a^2 + 42x^5y^6 - 56x^3y^6L^2 + 14xy^6L^4) \qquad [39]$$

An examination of Eqns [37] [38] and [39] shows that the prescribed boundary conditions are completely satisfied.

10.3.4

The problem here is the determination of the effect of the Theory of Elasticity on the maximum value of the flexural stress in deep beams. The present investigations will therefore be limited to the mid-span section of the beam.

From Eqn [37] for x = 0 th e simplified stress equation for σx can be written

$$\sigma x = -A(80y^3 - 48a^2y) + \alpha_1 yL^4(20y^2 - 12a^2) + \alpha_3 yL^4(6a^4 - 40y^2a^2 + 42y^4) \quad [40]$$

The total σx stress for a rectangular beam of unit thickness subject to a top face loading equal to 160 A a^3 per unit area will be given by the addition of Eqn [40] and the stress at mid-span resulting from Chapter 9 Eqn [23].

$$\sigma x = 120yL^2A + \alpha_1 yL^4(20y^2 - 12a^2) + \alpha_3 yL^4(6a^4 - 40y^2a^2 + 42y^4) \quad [41]$$

The values of α_1 and α_3 being taken from Table 10.3.1.

The maximum value of σx will clearly be at the extreme outer fibres of the beam at $y = \pm a$. Substituting for $y = + a$ in Eqn [41] the maximum value of the flexural stress is given by:-

$$\sigma x = 120aL^2A + 8a^3L^4(\alpha_1 + \alpha_3 a^2) \quad [42]$$

The two elements of this equation are the stress due to simple bending ($120aL^2A$) and the additional stress due to the Theory of Elasticity $\left[8a^3L^4(\alpha_1 + \alpha_3 a^2)\right]$

The following figures 10.3.4. 1 to 10.3.4. 5 show the distribution of σ_x stress at mid-span sections of beams of unit thic kness for various Span/Depth ratios, subject to a load applied to the top face equal to 160 A a^3 per unit area.

These stress distributions are calculated from Eqn. [41]

In each case the σ_x distribution calculated on the basis of the simple theory of bending is shown by a dotted line.

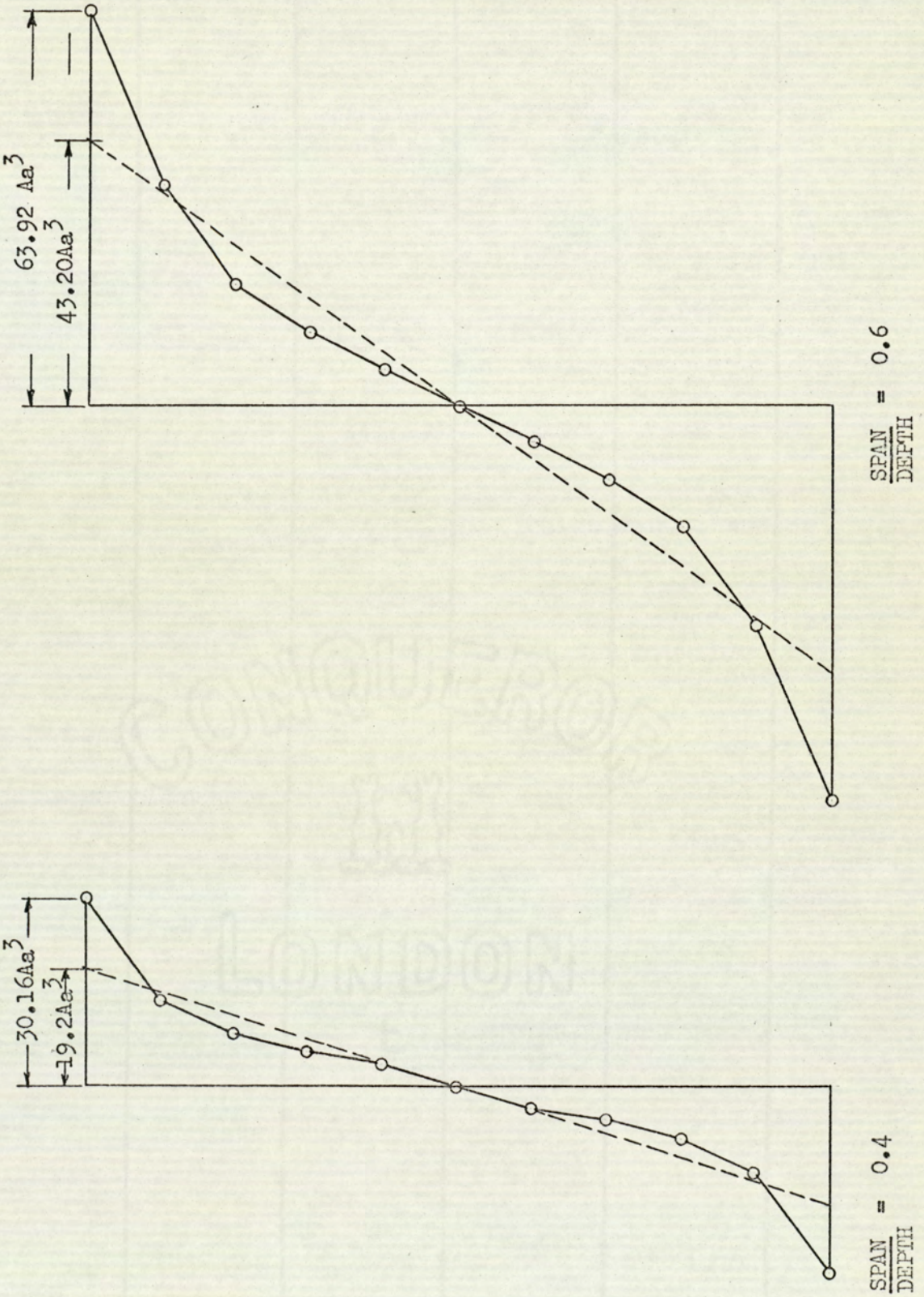

Fig. 10.3.4. 1

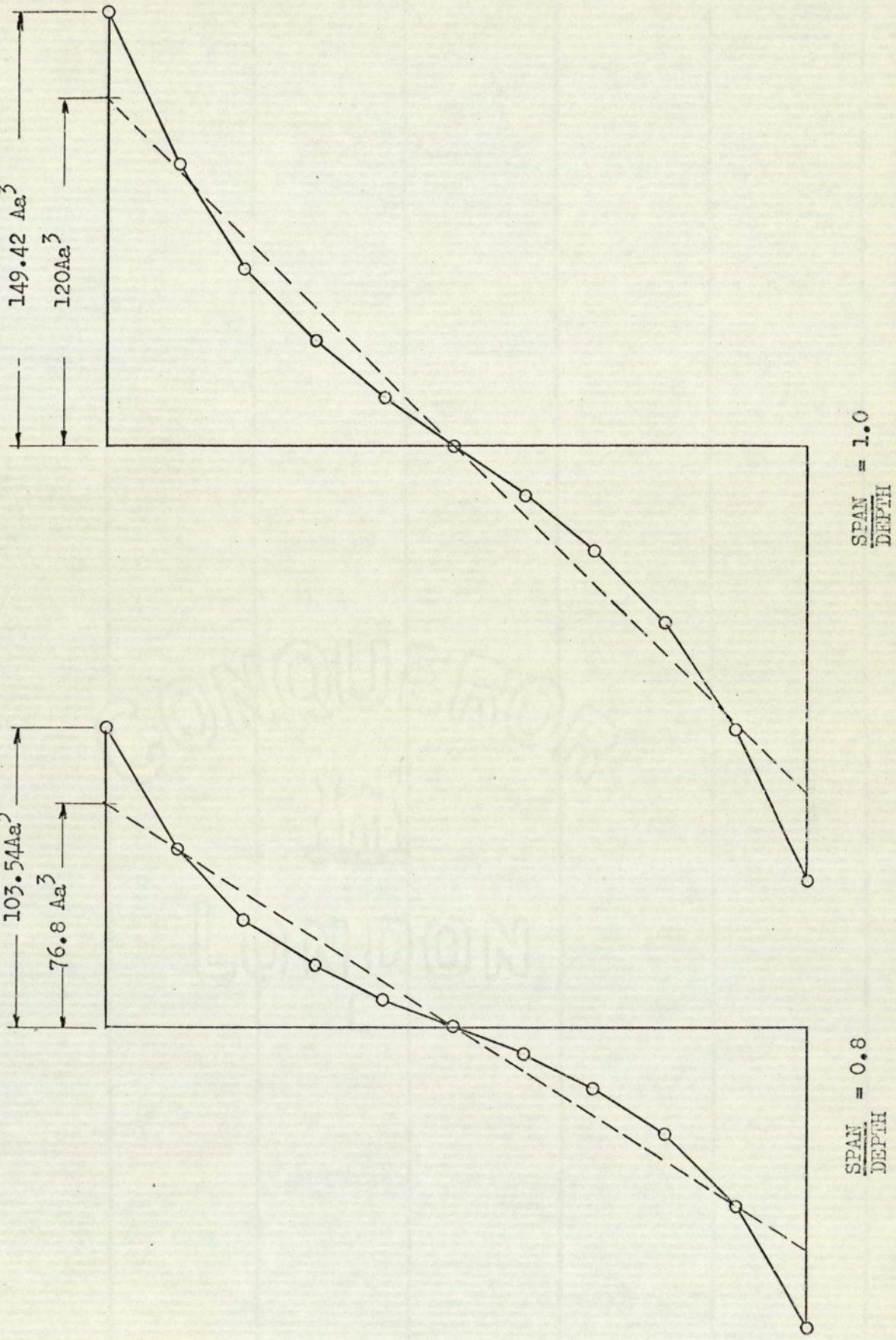
149.42 Aa3
120Aa3
SPAN / DEPTH = 1.0
103.54Aa3
76.8 Aa3
SPAN / DEPTH = 0.8

Fig. 10.3.4. 2

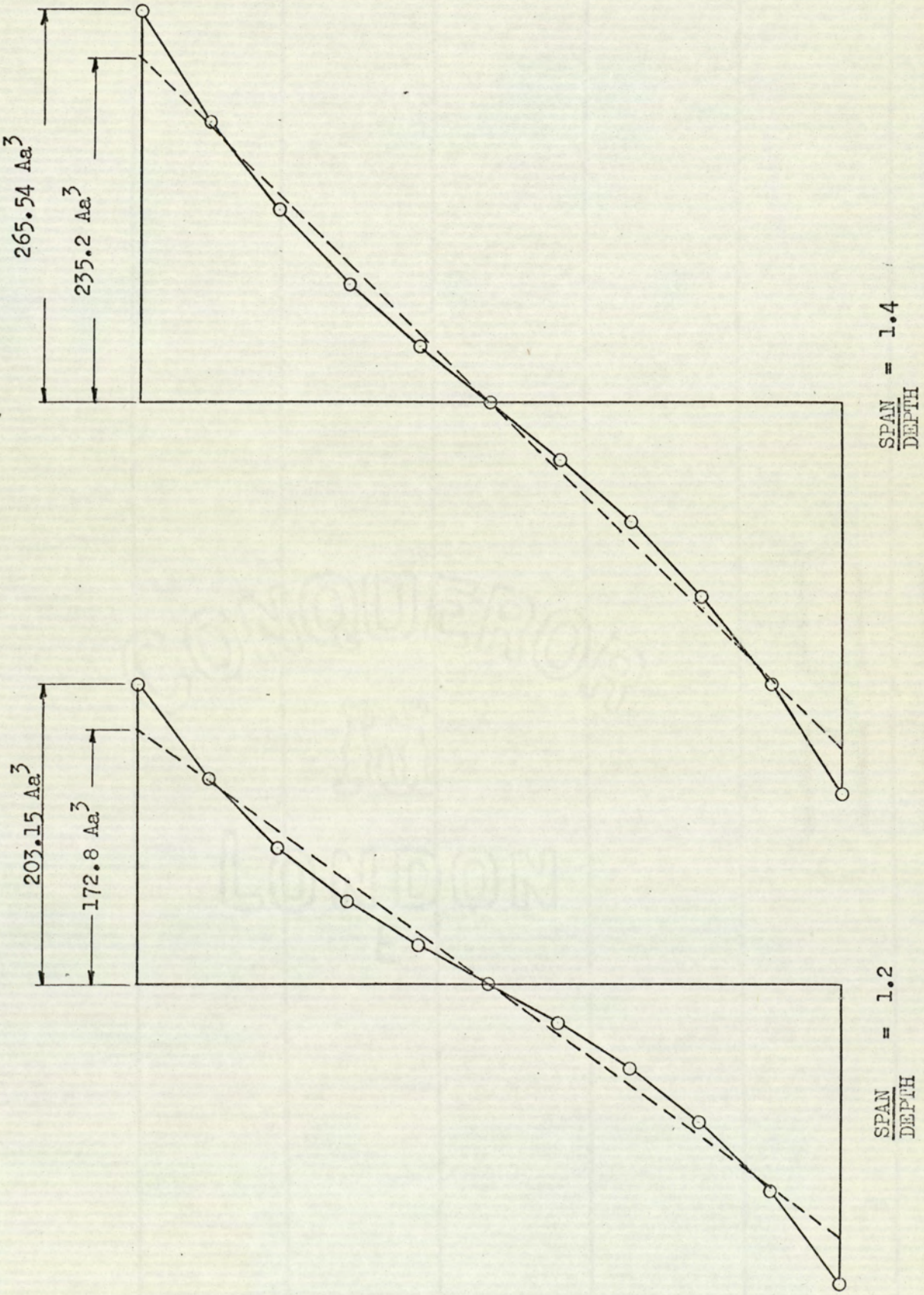
265.54 Aa3
235.2 Aa3
SPAN / DEPTH = 1.4
203.15 Aa3
172.8 Aa3
SPAN / DEPTH = 1.2

Fig. 10.3.4. 3

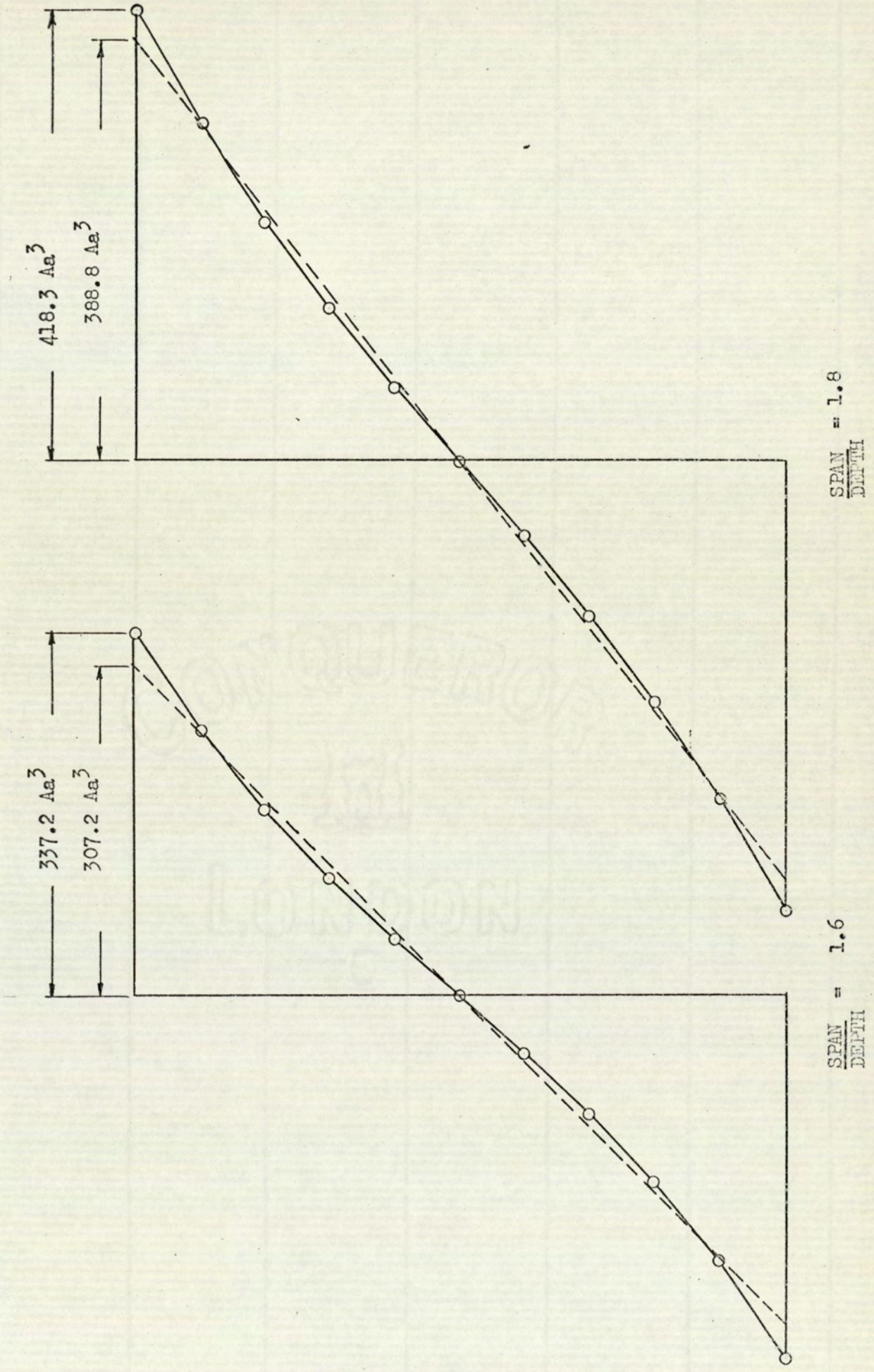
418.3 Aa3
388.8 Aa3
SPAN / DEPTH = 1.8
337.2 Aa3
307.2 Aa3
SPAN / DEPTH = 1.6

Fig.10.3.4. 4

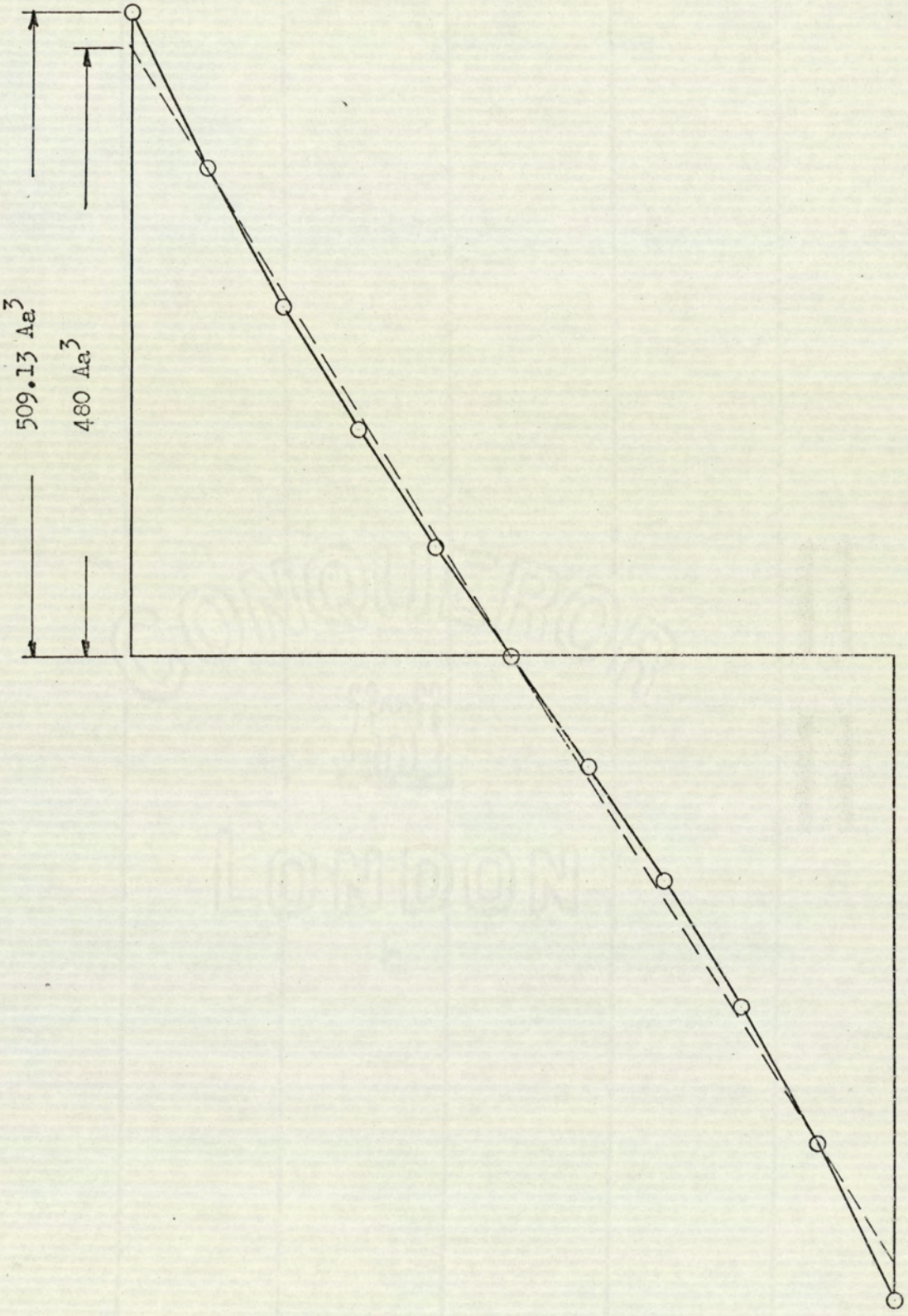

Fig. 10.3.4. 5

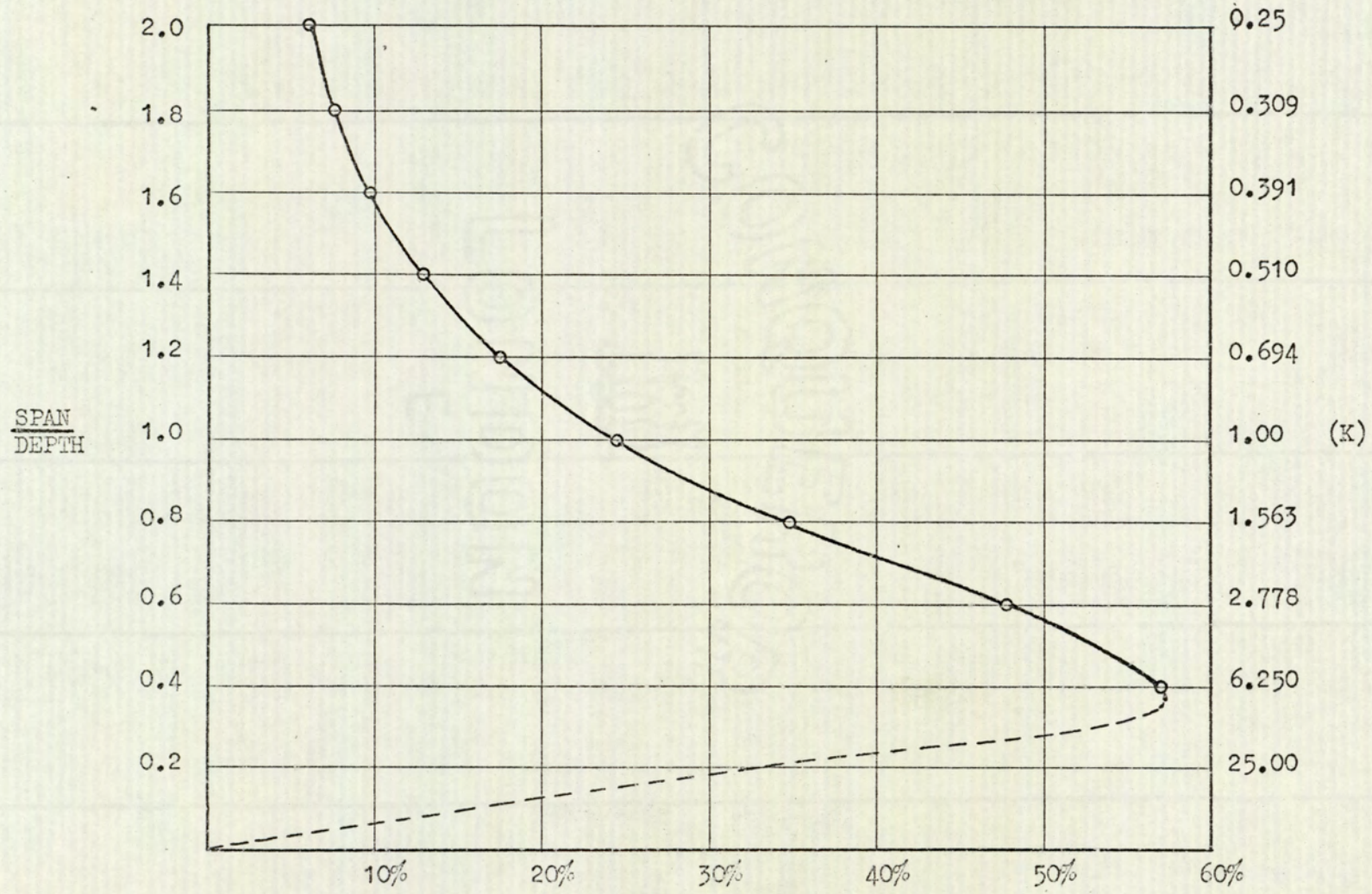

EFFECT OF THE THEORY OF ELASTICITY ON σ_x AS A PERCENTAGE OF σ_x DUE TO SIMPLE BENDING.

Fig 10.3.4. 6

10.3.5

The flexural stress due to the self weight of the beam

In consideration of the stresses due entirely to the self weight of the beam the preceding equations for an applied load of 160 A a^3 can be modified by substituting for $A = \frac{D}{80a^2}$

Table 10.3.5. shows values for the (α) parameters modified from Table 10.3.1. on the basis of this substitution.

Modification of Eqn [40] gives the following simplified stress equation for σx at mid-span of the beam.

$$\sigma x = -\frac{D}{80a^2}(80y^3 - 48a^2y) + \alpha 1 y L^4(20y^2 - 12a^2) + \alpha 3 y L^4(6a^4 - 40y^2a^2 + 42y^4) \qquad [43]$$

The total σx stress for a rectangular beam of unit thickness and density=D subject to the self weight of the beam only will be given by the addition of Eqn [43] and the stress at mid-span resulting from Chapter 9 Eqn [27].

$$\sigma x = \frac{3}{2}\frac{yL^2D}{a^2} + \alpha 1 y L^4(20y^2 - 12a^2) + \alpha 3 y L^4(6a^4 - 40y^2a^2 + 42y^4) \qquad [44]$$

The values of $\alpha 1$ and $\alpha 3$ being taken from Table 10.3.5.

The maximum value of σx will again be at the extreme outer fibres of the beam at $y = \pm a$.

Substituting for $y = +a$ in Eqn [44] the maximum value of the flexural stress is given by:-

$$\sigma x = \frac{3}{2}\frac{L^2D}{a} + 8a^3L^4(\alpha 1 + \alpha 3\, a^2) \qquad [45]$$

The two elements of this equation are the stress due to simple bending $\left(\frac{3}{2} \frac{L^2 D}{a} \right)$ and the additional stress due to the Theory of Elasticity

$$\left[8a^3 L^4 (\alpha_1 + \alpha_3 a^2) \right]$$

SPAN / DEPTH	K	$\alpha_1 \frac{D}{L^4 a^2}$	$\alpha_2 \frac{D}{L^6 a^2}$	$\alpha_3 \frac{D}{L^4 a^4}$	$\alpha_4 \frac{D}{L^6 a^4}$
2.0	0.25	0.047	0.156	-0.0016	0.039
1.8	0.309	0.048	0.137	-0.0015	0.043
1.6	0.391	0.048	0.114	-0.0011	0.047
1.4	0.510	0.048	0.089	-0.0002	0.049
1.2	0.694	0.046	0.062	0.0014	0.048
1.0	1.0	0.042	0.037	0.0041	0.042
0.8	1.563	0.034	0.016	0.0080	0.032
0.6	2.778	0.020	0.0036	0.012	0.018
0.4	6.250	0.006	-0.0002	0.011	0.006
0.2	25.00	0.0002	-0.00004	0.0025	0.00026

(α) PARAMETERS FOR LOADING DUE TO SELF WEIGHT ONLY

MATERIAL UNIT DENSITY = D

TABLE 10.3.5

10.4 Conclusions

The development of the stress function for the elimination of end stresses, which was assumed to be in the form of a series with adjustable parameters and determined by the application of the principle of least work to the strain energy integral, results in a logical solution to the problem of the simply supported single span beam, carrying loads due to the self weight of the beam together with an applied uniformly distributed load.

A combination of the stress functions resulting from Chapter 9 and 10 produce a 'Theory of Elasticity' solution that completely satisfies the prescribed boundary conditions of the problem.

It is of particular interest to examine the effect of the 'Theory of Elasticity' on the longitudinal flexural stress in beams.
The Chapter 9 solution showed that there was an increase in the flexural stress as calculated by the 'simple' theory of $A(80y^3 - 48a^2y)$ for beams of all span/depth ratios and that the value was constant throughout the length of the beam. This clearly was in error, since the solution resulted in stresses at the vertical ends of the beam which does not satisfy the prescribed boundary conditions of the simply supported single span beam.
The Chapter 10 solution which gives the correction to this error, has the effect of eliminating the stresses at the end of the beam and by reason of the diminishing properties of the assumed stress function has a diminishing effect on the stresses due to the 'Theory of Elasticity' as the considered be am sections are moved from the end of the beam towards the centre of the span.
A combination of the two solutions then shows that the 'Theory of Elasticity' has a maximum effect on the longitudinal flexural stress at the mid-span section of the beam and zero effect at the vertical ends of the beam for any given span/depth ratio.

The natural sequence then follows that the effect of the 'Theory of Elasticity' as shown in Fig. 9.2. will be in error for span/depth ratios where the presence of resultant end stresses cannot be ignored.

Fig. 10.3.4. 6 shows the final effect of the combined solution on the maximum value of σx at the mid-span section of the beam for various span/depth ratios.

For span/depth ratios greater than 1.25 this figure indicates no significant difference from Fig.9.2. However below span/depth = 1.25 the curves depart and take up a significantly different shape such that the final solution shows that below span/depth = 0.4 the effect of the 'Theory of Elasticity' rapidly reduces to zero.

This clearly must be the case, the elimination of the end stresses, which are the effect of the 'Theory of E lasticity', do not diminish at the centre of the beam by any appreciable magnitude for beams with a span whic h is small in relation to its depth. Therefore the effect of the 'Theory of Elasticity' becomes insignificant at the extreme low values of span/depth ratio.

Although span/depth ratios below 0.4 can be considered to be below the range of practical use the assumed probable curve is shown by a dotted line in Fig. 10.3.4. 6.

In order that the diminishing effect of the stress function for the elimination of end stresses can be clearly illustrated, Table 10.4.1. has been prepared to show the values of σx at various vertical sections calculated from Eqn. [37] for a beam span/depth ratio = 2.0.

Fig. 10.4.1. graphically illustrates the conditions at these vertical sections and qualifies the effect of St. Venant's principle.

The figure has been simplified to show the separate effect of the two applied stresses, $\sigma x = -80Ay^3$ and $\sigma x = 48a^2y$.

It has been previously shown in para 10.3.2. that the linear distribution of stress $\sigma x = 48a^2y$ is transmitted without change throughout the length of the beam, this is shown in the figure by a dotted line.
The initial parabolic distribution $\sigma x = -80Ay^3$ however behaves very differently. The figure shows that as vertical sections move away from the point of application of the load then the initial parabolic curve gradually changes to a linear distribution. At the point where $\sigma x = -80Ay^3$ becomes a linear distribution equal to $\sigma x = 48a^2y$ then the stress at any point in the section is zero. i.e. the average value of the self equilibrating system of stresses that was applied to the end of the beam. For span/depth ratio = 2.0 this situation is virtually achieved at x = 0.25 L, in consideration of the maximum value of the flexural stress at mid-span the effect of end stresses could be ignored and the stresses could be confidently calculated from the stress equations of Chapter 9. Fig. 10.4.1. shows that at x = 0 there is some deviation from the almost linear distribution at x = 0.25 L. This should not be the case, since at x = 0 the curve should be even more linear than at x = 0.25 L.
The apparent error in the use of only 4 (α) parameters in what is strictly an infinite series. The next term in the series would have been $\alpha_5 \phi_5$ where $\phi_5 = \phi_1 y^4$. This would produce an additional term in y at x = 0 resulting in a more linear distribution.

Figs. 10.3.4. 1 to 10.3.4. 5 show the distribution of σx stress at mid-span of beams of unit thickness for various span/depth ratios subject to a load applied to the top face of the beam equal to $160\ Aa^3$ per unit area.

These figures can readily be converted to the state of stress due to the self weight of the beam by substituting for $A = \frac{D}{80a^2}$.

Again, the figures graphically show the effect of the 'Theory of Elasticity' on σ_x at mid-span.
As the span/depth ratio increases the total σ_x stress tends to become more linear, the important conclusion here however is that within the span/depth range considered there is no case where a reversal of stress is shown (as in Fig. 9.5) above or below the neutral axis where the stress could be expected to be either entirely tensile or entirely compressive. This,is the result of the true effect of the 'Theory of Elasticity' on beams with span/depth ratio less than 1.0 being significantly less than the effect predicted by the Chapter 9 solution.

The final stress Equations [42] and [45] for the maximum value of σ_x due to an applied uniformly distributed load and the self weight of the beam are in a simple form that can readily be used for practical design purposes.

A by-product of this solution is that the determination of the Chapter 10 stress function makes a solution readily available for the analysis of the stress distribution in members subject to non-uniform tension or compression.

With particular reference to brickwork beams, consider a square beam simply supported and subject only to its own weight. The density of the material (D) = 0.073 lb/in^3 (125 lb/ft^3)

Using Fig. 10.3.4. 2 and substituting $A = \frac{0.073}{80a^2}$

the maximum value of σ_x will be $149.42 \times \frac{0.073}{80}\ a$

$\therefore \quad \sigma_x\ (max) = 0.136\ a$

Although CP.111 states that in general no reliance should be placed upon the tensile strength of brickwork, it does state that at the discretion of the designer a tensile stress of 20 lb/in^2 can be used when the direction of tensile stress is at right angles to the perpend joints.

On this basis,

$$\sigma x = 0.136\ a = 20\ \text{lb/in}^2 \qquad \therefore\ a = \frac{20}{0.136} = 147\ \text{inches}$$

This indicates that a square brick beam would require to be of dimensions greater than 24' x 24' (in elevation) before an extraneous support would be required.

The uncertain factor in the tensile strength of brickwork is singularly the s trength of adhesion between brick and mortar. If this adhesive (bond) strength alone could be relied upon even at the very low permissable value of 20 lb/in^2 the necessity for the provision of permanent lintol beams would become obsolete in the majority of practical construction examples.

Fig. 10.4.2 shows the value of σx at the centre of the beam compared to τxy at the end of the beam for various Span/Depth ratios, indicating that for values of Span/Depth less than 0.7 the diagonal tensile stress will be greater than the mid-span flexural stress.

For beams in this range it would be necessary to determine the ultimate values of diagonal tensile strength and flexural tensile strength of the brickwork in order that the criterion value could be used for design purposes.

$\frac{x}{L}$ \ $\frac{y}{a}$	VALUES OF σ_x (Aa^3)					
	0	0.2	0.4	0.6	0.8	1.0
1.0	0	+8.96	+14.08	+11.52	-2.56	-32
0.75	0	+4.34	+6.90	+5.03	-1.82	-13
0.50	0	+0.63	+0.56	-0.26	-0.78	+1.9
0.25	0	+0.05	+0.05	-0.021	-0.11	+0.442
0	0	+0.39	+0.77	+0.89	+0.10	-2.86

BEAM SPAN/DEPTH = 2.0

σ_x DISTRIBUTION CALCULATED FROM EQN. [37]

TABLE 10. 4. 1.

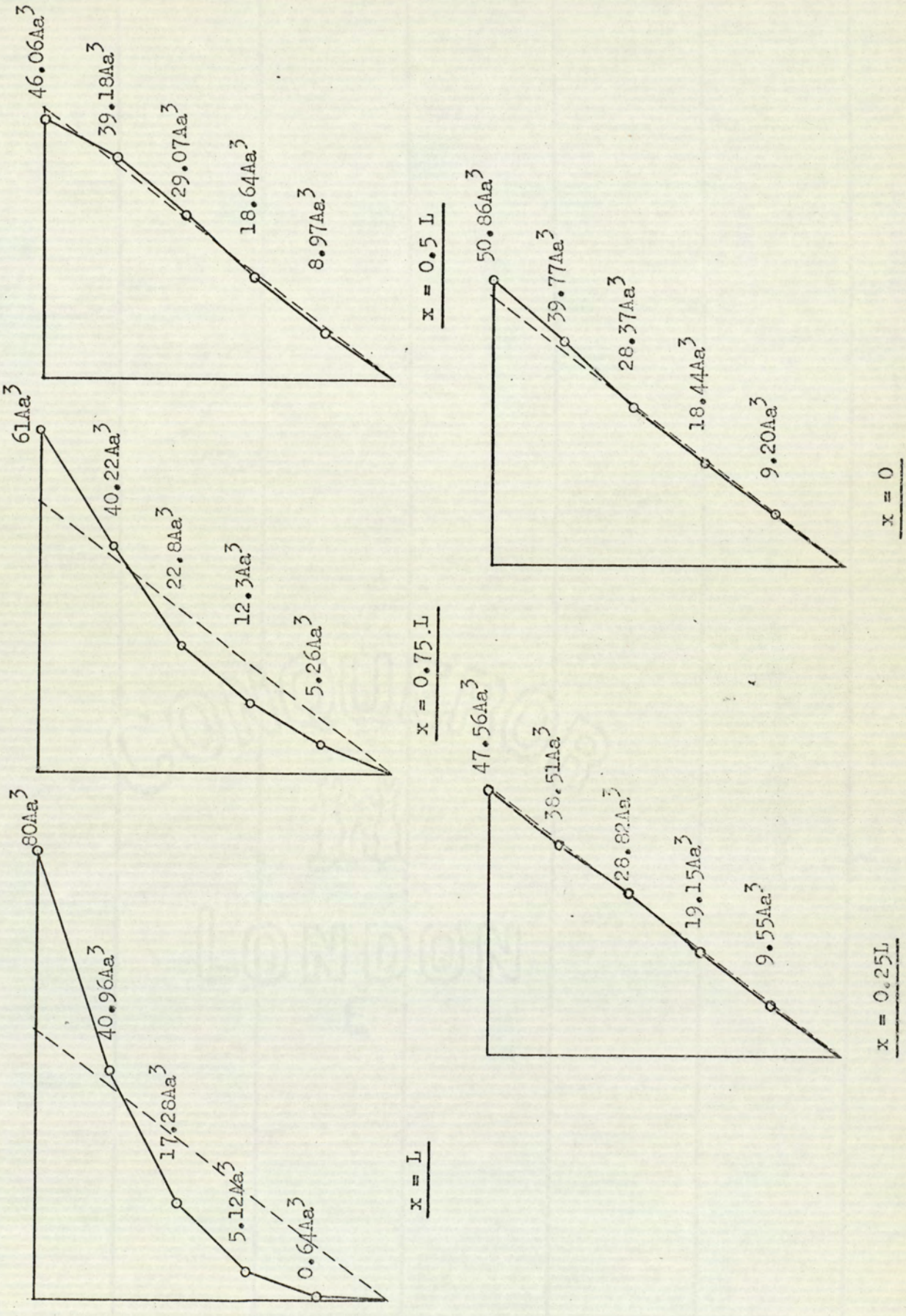

DISTRIBUTION THROUGH BEAM OF APPLIED $\sigma_{x = 1} = 80Ay^3$ AT x = L

$\frac{\text{SPAN}}{\text{DEPTH}} = 2.00$

FIG.10.4.1

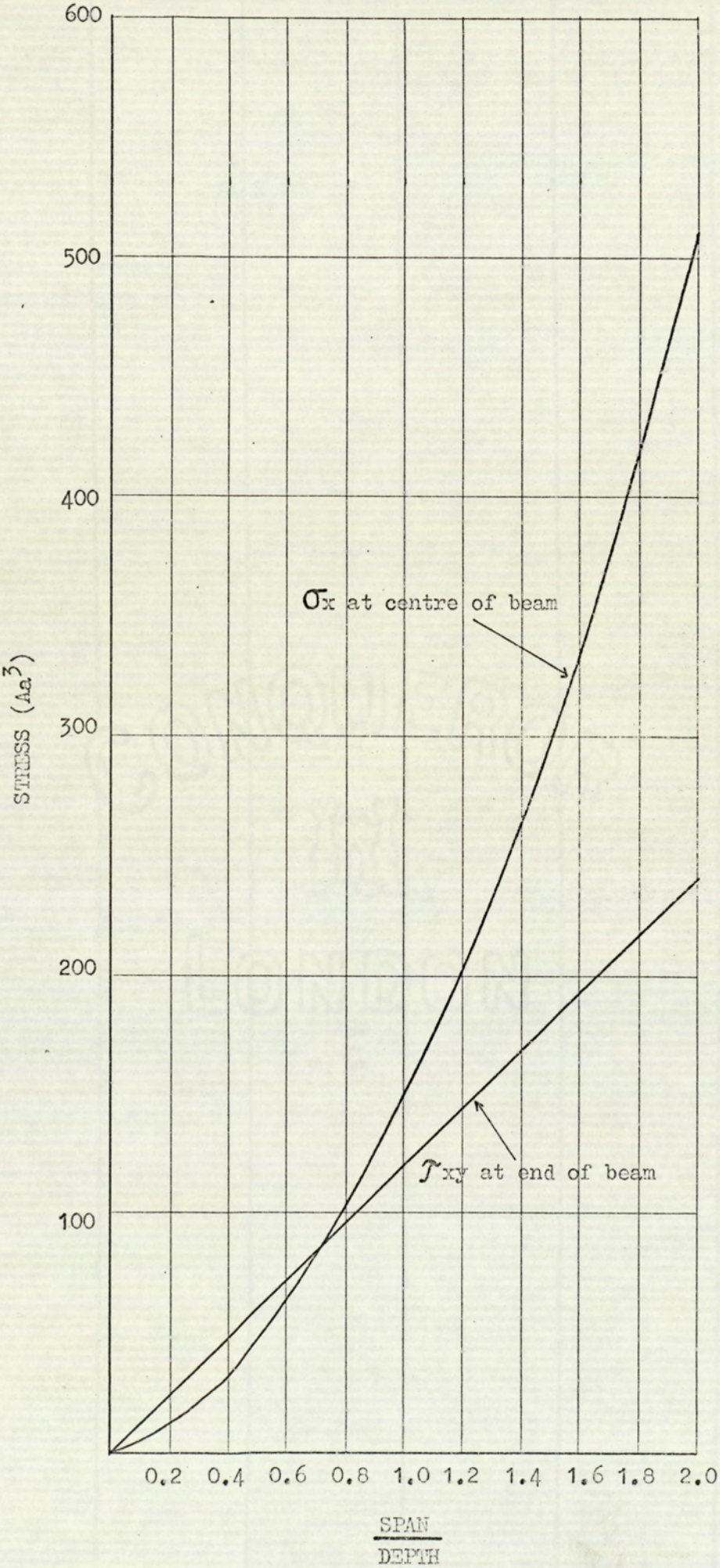

RELATIONSHIP BETWEEN THE MAXIMUM VALUES OF σ_x and τ_{xy} FOR BEAMS OF VARIOUS SPAN/DEPTH RATIOS

Fig 10. 4. 2.

10.5 Commentary on the work of some previous authors

For the specific problem of a beam simply supported by a shear force at each vertical end face, the solution of which has been developed in this chapter, the author is unable to locate any published work that gives the solution for the stress distribution in a beam that satisfies the prescribed boundary conditions for stress free vertical ends.

COULL (12) presents a method of stress analysis of the two-dimensional plane stress problem by expressing the stresses in the form of a FOURIER series in one direction, the coefficients of the series being functions of the other co-ordinate only. After satisfying the equilibrium and boundary conditions, the coefficients are determined by the minimisation of the strain energy , by the calculus of variations. Coull then uses the method of analysis to investigate the problem of a deep cantilever beam subjected to a uniformly distributed load applied to the top edge of the beam. The effect of gravitational forces is neglected.
The solution offered is complex and mathematically laborious resulting in equations that could not be readily used for practical design consideration.

UHLMANN (13) investigates the problem of a deep beam supported by vertical forces at the bottom edge of each end of the beam. Although the paper does not give the mathematical solution to the problem it is stated that the principles of finite difference are used and that Richardson's method of successive approximation was adopted.

The mathematical derivation of these stress functions is not given by these authors but it is stated that the Rayleigh-Ritz method was employed.

A computer analysis was carried out for beams of various span/depth ratios subject to a varying loading condition for beam supported along the bottom edge for a length of 0.1 Span from each end and the results are tabulated.

For a beam of span/depth ratio = 1.0 subject to a uniformly distributed load along the top edge the resulting distribution of σ_x at mid-span of the beam is similar to that obtained by Uhlmann although the numerical values of stress cannot easily be compared.

CONWAY, CHOW and MORGAN (15) offer a method of analysing the stress distribution in deep beams of finite length again by superimposing two stress functions.

The first stress function is chosen in the form of a trigonometric series which satisfies all but one of the boundary conditions, that of zero normal stress on the vertical ends of the beam.

The second stress function is then determined in a similar method to that adopted in this thesis (by the principles of least work) to obtain the distribution of normal stress at the beam ends that is left by the first stress function.

The Fourier series chosen for the first stress function results in equations for stress that are lengthy and difficult to handle, the distribution of normal stress at the ends of the beam is given in the form of an infinite trigonometric series for which the authors give an approximate polynomial.

This solution is then used to investigate a deep beam which is a square plate loaded and supported such that it has a loaded span and clear distance between the supports equal to one half of the plate length. The resulting distributions of σ_x at mid-span and τ_{xy} at the ends of the beam are however symmetrical diagrams and contrary to the results of other authors investigating beams with similar support conditions. This gives further support to the conclusion that the distribution of shearing stress at the end of the beam is dependant upon the method of beam support and that this in turn has a direct influence on the distribution of bending stress at mid-span for beams that have a depth comparable to their span.

Conway, Chow and Morgan mention that data obtained from photoelastic tests confirm, in a general manner, the results given by the mathematical analysis presented in their paper.

It is unfortunate that published work on the analysis of deep beams makes little reference to the effects of body forces due to the self weight of the beam material, when deep beams form part of a building structure whether they are in brickwork or reinforced concrete the self weight of the beam is usually the principle load that the beam has to carry. It is therefore of paramount importance that the self weight stresses are analysed. A mathematical solution has been given in this thesis.

Experimental work has probably been neglected in this field by reasons of the difficulty of reproducing in the laboratory gravitational forces on model structures.

Important experimental work in this field has been carried out by PROF. A. W. HENDRY and SHAWKI SAAD (16) who overcame the difficulty on a laboratory scale by using a large centrifuge in conjunction with the frozen stress method of photo-elasticity.

The equipment used and the general technique were described in a paper (17) read at the 50th Anniversary Conference of the Institution of Structural Engineers.

It is not possible to c ompare the experimental results given in this paper with the theoretical solution offered in this present thesis since, again, the experimental work was limited to beams that were supported for some short distance along their bottom edge rather than by a shear force along the vertical ends of the beam.

However, probably the most interesting point from the work on Hendry and Saad is the conclusion that a beam whose depth is greater than its span acts roughly (as far as self weight is concerned) as a beam of depth equal to span with the top part merely resting on it. The top portion of the beam hardly contributes any resistance to the bending moment due to the self weight of the beam.

It is further confirmed that an analysis of the gravitational stresses in deep beams based upoh the simple straight line theories of bending would be seriously in error.

10.6 An experimental investigation into the strain distribution in some deep beams

Following the conclusion to the theoretical work of this chapter and the commentary on the work of some previous authors it was considered necessary to carry out some experimental work to validate the theory and confirm that the diagram of strain distribution at mid-span varies with the conditions of end support.

For this purpose, 3 beams as shown in Table 10.6.1. were constructed from half scale model bricks using 1:0:3 C/L/S mortar.
For ease of handling, the specimen beams were constructed on a 2" thick reinforced concrete slab base.
The model bricks were 'commons' supplied by the London Brick Company Ltd. and having been stored in the Laboratory for some 12 months were wetted before laying to reduce the suction rate in an attempt to obtain an acceptable degree of adhesion between brick and mortar.

Specimen beams of span depth ratios 2:1 and 0.75 were selected to be representative of the range of deep beams under consideration.

To assimilate the theoretical conditions of end support considered in the theory of this chapter the beams were constructed between piers such that for all practical purposes they can be considered to be supported by a shear force at the vertical end.

The arrangement of the testing apparatus is shown in Plates Nos: 10.6.1., 10.6.2 and 10.6.3. which are photographs of each beam before testing.

To produce a close approximation to a uniformly distributed load a system of rollers and spreader beams was adopted such that a single point load applied by a hand operated hydraulic jack through a calibrated proving ring was distributed throughout the length of the beam.

Initially, a continuous spreader beam was bedded in plaster of paris on the top edge of the beam, as testing commenced it became apparent that the stiffness of the continuous spreader was influencing the bending of the brick beam. The spreader was then cut into short segments such that during the tests it did not influence the deflection of the brick beams.

All strains were measured by the use of 1" long felt backed electrical resistance gauges taken at increments of the proving ring dial gauge. The test results are recorded in Tables 10.6.2., 10.6.3 and 10.6.4. Since it was the intention of this experimental work to investigate the strain diagram patterns, the arithmetic mean of the strains measured throughout the tests were plotted to show the general tendency of strain pattern rather than the strain distribution for specific values of applied load.

The diagrams of mean strain distribution at the mid-span sections of the beams are shown in Figs. 10.6.1., 10.6.2 and 10.6.3.

SPECIMEN TEST BEAMS

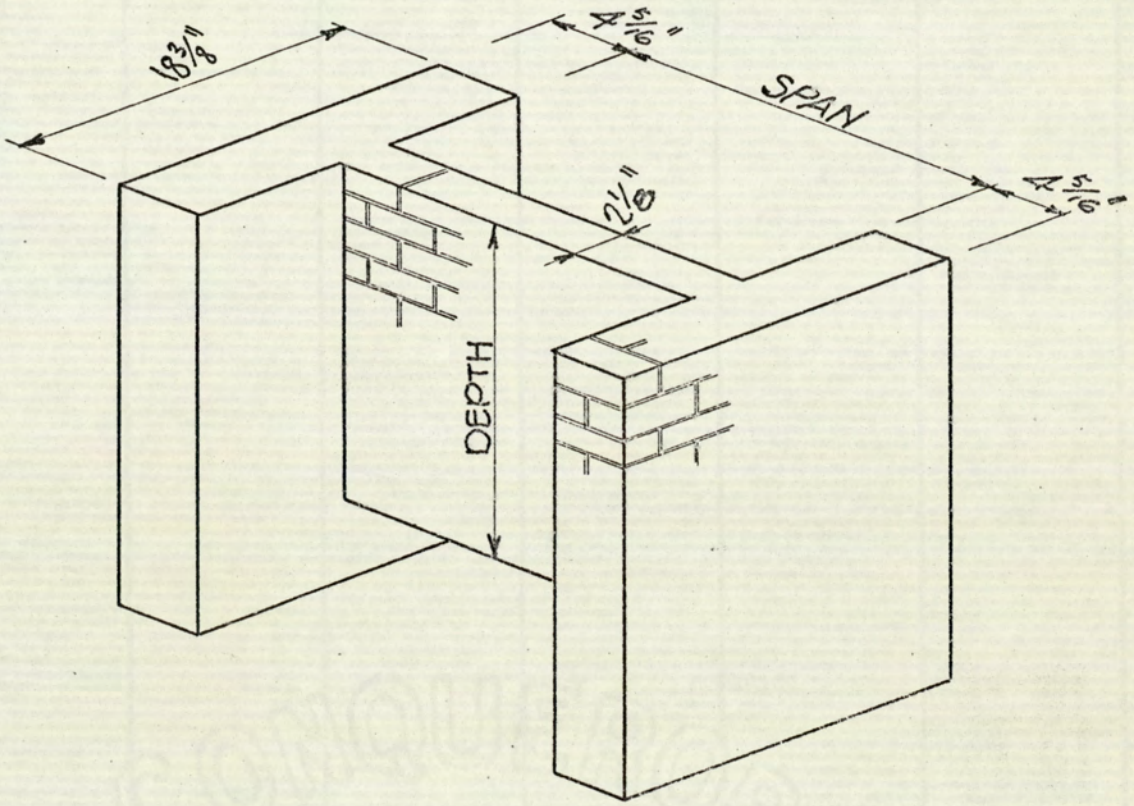

BEAM NO.	SPAN	DEPTH	$\frac{\text{SPAN}}{\text{DEPTH}}$
1	$46\frac{7}{8}$"	$23\frac{3}{16}$"	2.0
2	$24\frac{3}{4}$"	$24\frac{13}{16}$"	1.0
3	$17\frac{3}{4}$"	$23\frac{1}{4}$"	0.75

TABLE 10.6.1

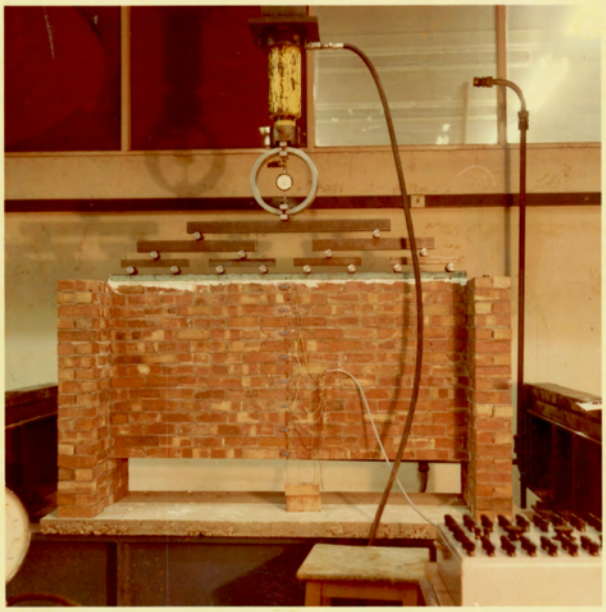

PLATE NO. 10.6.1.

BEAM NO. 1 BEFORE TESTING

BEAM NO.1 S/D = 2

CONSTRUCTED 10.12.71
TESTED 3.1.72

APPLIED LOAD (PROVING RING DIVS)	MICROSTRAINS							
	G1	G2	G3	G4	G5	G6	G7	G8
25	-7	-9	-2	-1	+8	+6	+5	+8
50	-9	-12	-9	-11	+4	+6	+5	+7
75	-14	-23	-13	-13	+9	+7	+18	+14
100	-18	-21	-13	-15	+6	+7	+14	+19
125	-24	-23	-14	-11	+4	+7	+16	+26
150	-36	-25	-16	-14	+8	+4	+18	+27
175	-41	-25	-17	-15	+5	+4	+25	+35
200	-45	-28	-21	-13	+5	+9	+29	+35
225	-46	-31	-20	-11	+2	+17	+33	+45
250	-54	-33	-22	-8	+2	+15	+35	+49
275	-58	-39	-26	-9	+3	+17	+37	+55
300	-66	-39	-28	-10	+1	+23	+44	+61
325	-64	-40	-30	-6	+3	+26	+44	+71
350	-74	-42	-32	-2	+4	+40	+38	+75
375	-76	-41	-32	-2	+4	+41	+42	+83
$\bar{x}$	-42	-28	-19	-9	+5	15	27	+40

TABLE 10.6.2

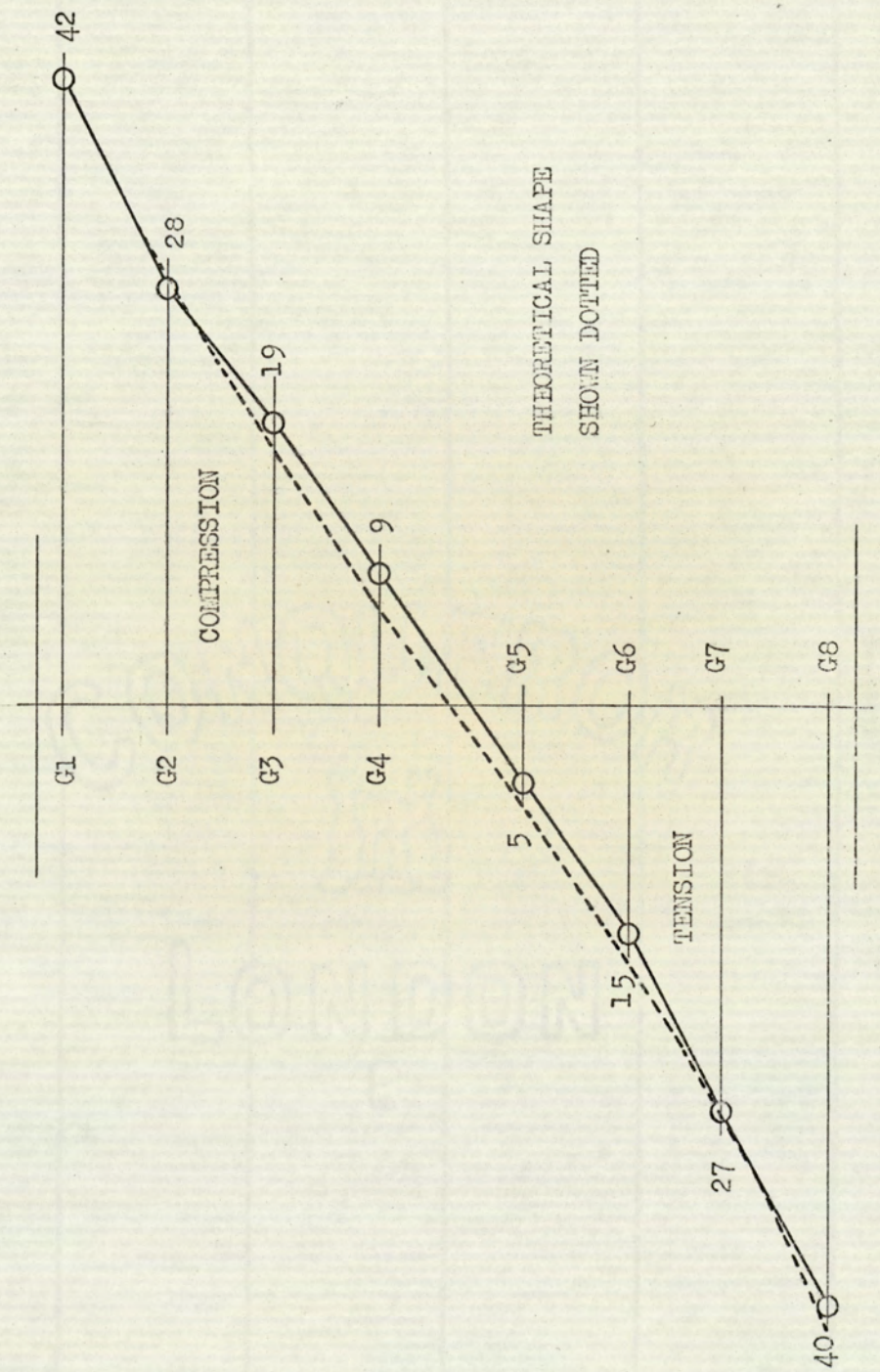

BEAM NO.1

DIAGRAM OF MEAN STRAIN AT MID-SPAN

Fig.10.6.1

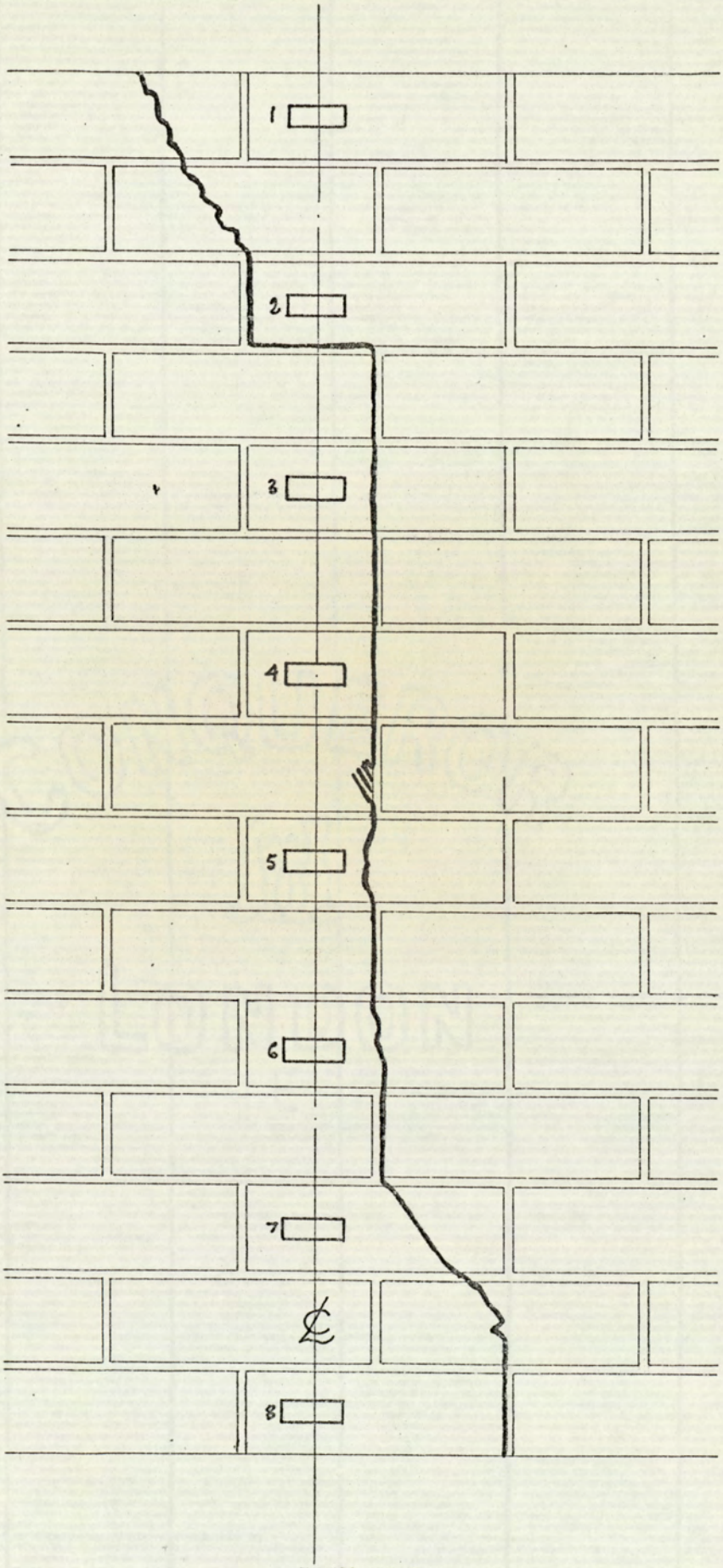

BEAM NO.1

CRACK PATTERN AT FAILURE

Fig.10.6.4

PLATE NO. 10.6.4.

BEAM NO. 1 AFTER FAILURE

PLATE NO. 10.6.5.

BEAM NO.1

CRUSHING ON INSIDE EDGE OF PIER

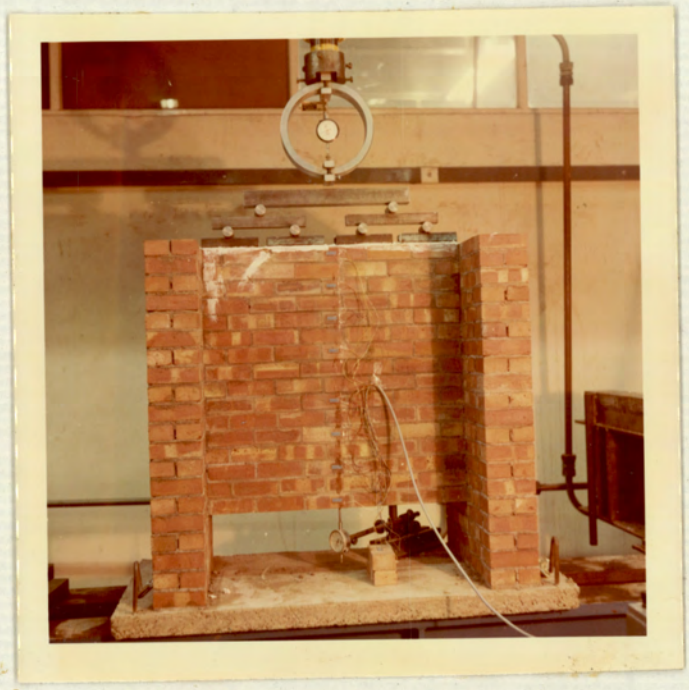

PLATE NO. 10.6.2

BEAM NO. 2 BEFORE TESTING

BEAM NO.2 S/D = 1

CONSTRUCTED 16.12.71

TESTED 4. 1.72

LOAD PROVING RING DIVS	MICROSTRAINS							
	G1	G2	G3	G4	G5	G6	G7	G8
20	-16	0	-12	-14	+10	+9	+17	+5
40	-15	-6	-14	-5	+13	+3	+18	+17
60	-21	-4	-11	-6	+14	+6	+25	+14
80	-34	-8	-8	-8	+20	+17	+28	+14
100	-33	-8	-14	-5	+20	+31	+42	+16
120	-33	-13	-13	-4	+25	+28	+51	+20
140	-45	-20	-11	-3	+28	+38	+52	+21
160	-58	-14	-18	-4	+27	+43	+57	+21
180	-70	-17	-11	-4	+29	+44	+60	+24
200	-81	-19	-13	-4	+30	+48	+63	+24
220	-88	-22	-13	-3	+31	+50	+66	+25
240	-94	-22	-14	-1	+35	+63	+75	+25
260	-97	-24	-14	+1	+39	+64	+84	+25
280	-104	-24	-18	-6	+39	+71	+83	+20
300	-115	-27	-13	-2	+44	+75	+88	+23
320	-129	-25	-17	-1	+46	+82	+84	+22
340	-127	-33	-12	-3	+48	+90	+90	+23
360	-139	-36	-15	0	+48	+91	+93	+23
$\bar{x}$	-72	-18	-14	-4	30	47	59	20

Table 10.6.3

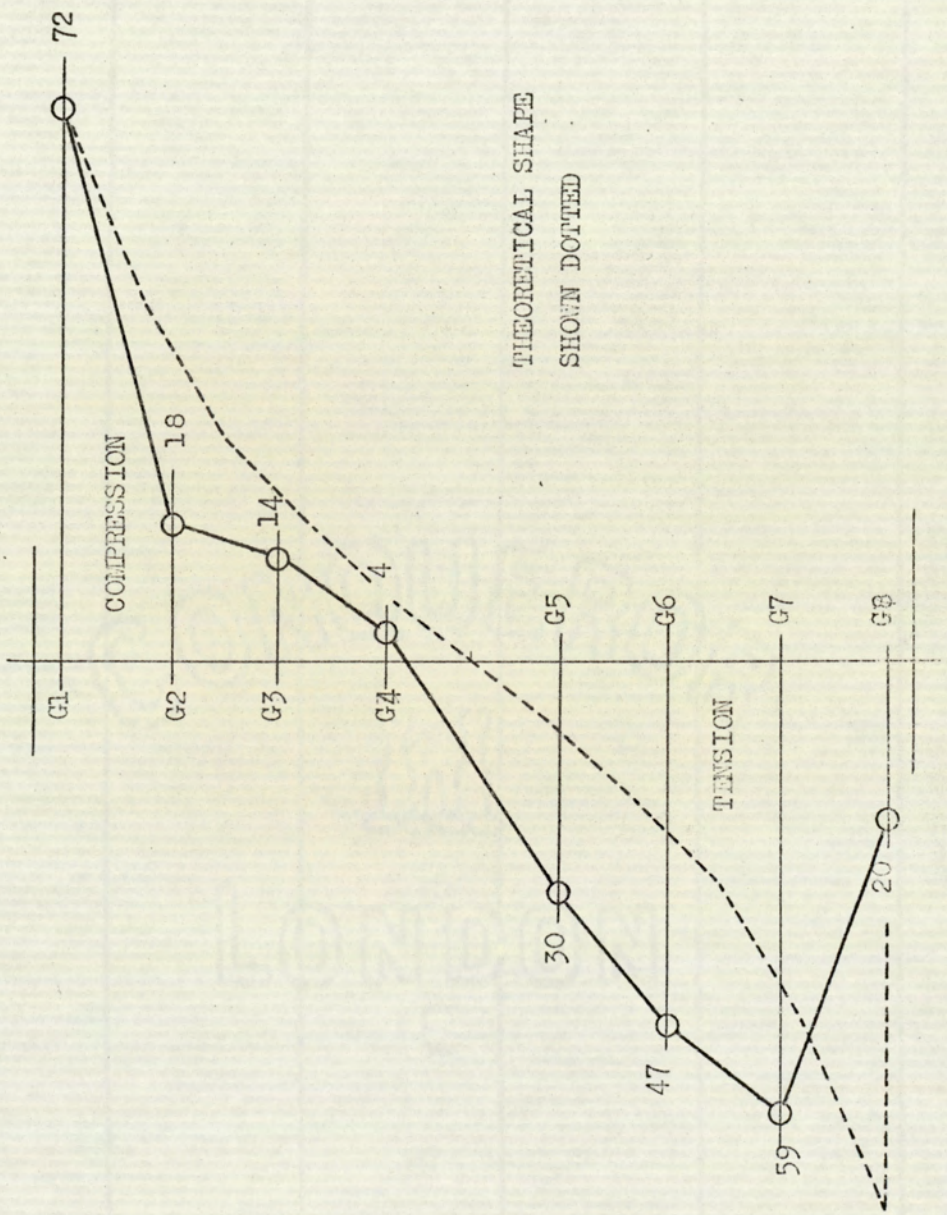

BEAM NO.2

DIAGRAM OF MEAN STRAIN AT MID-SPAN

Fig. 10.6.2

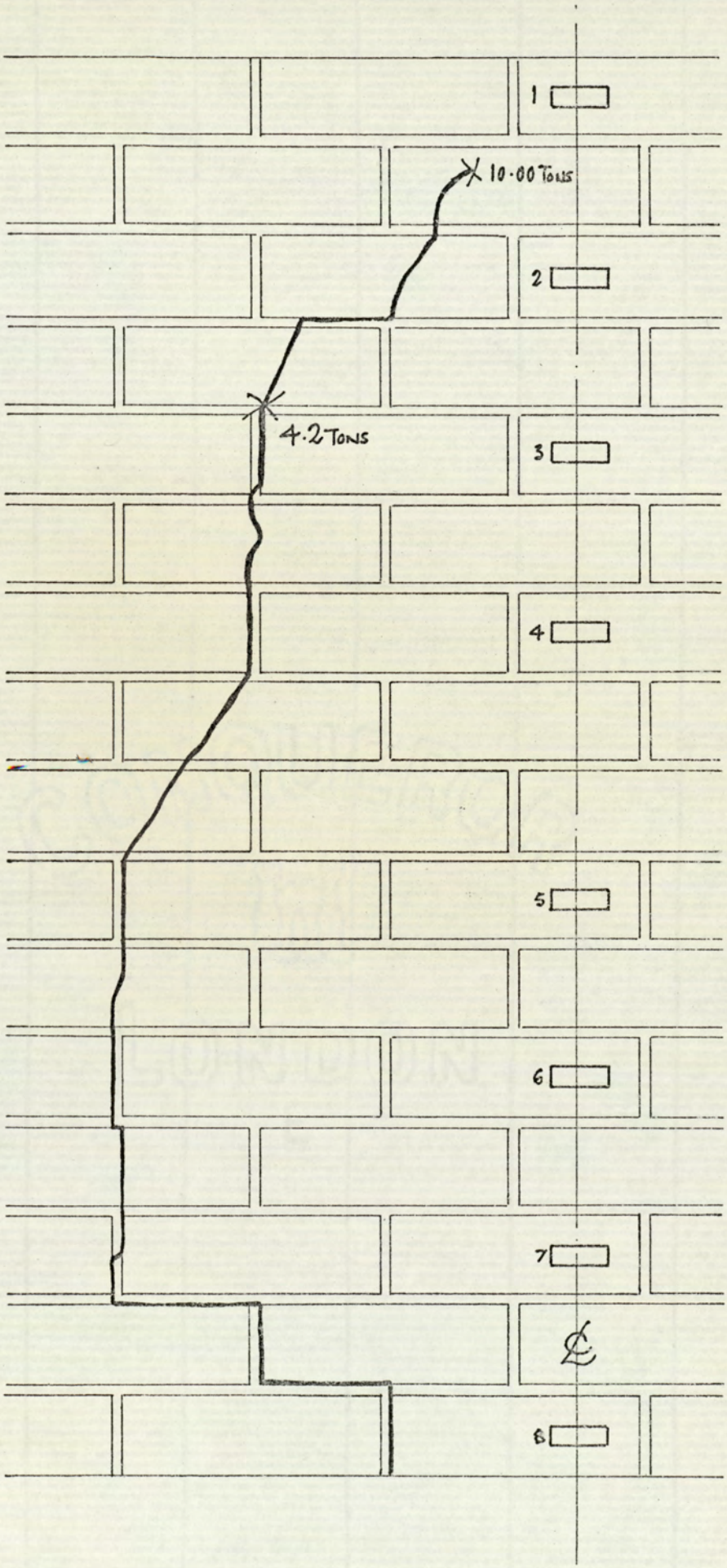

BEAM NO.2

CRACK PATTERN AT FAILURE

Fig.10.6.5

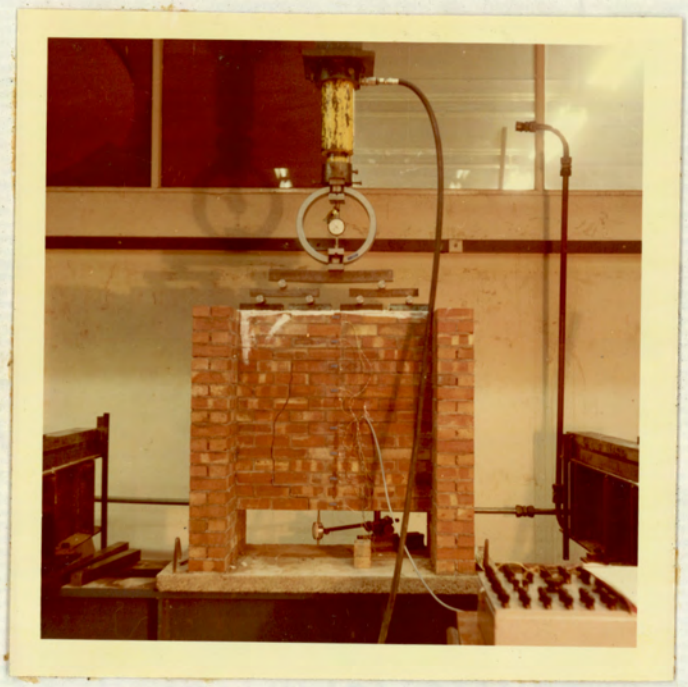

PLATE NO. 10.6.6

BEAM NO.2 SUSTAINING A LOAD OF 10.00 TONS

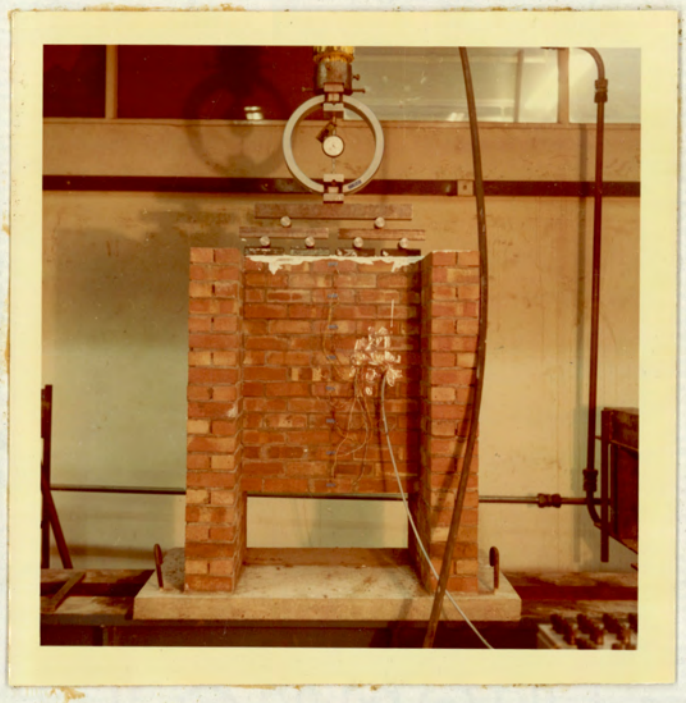

PLATE NO. 10.6.3

BEAM NO. 3 BEFORE TESTING

BEAM NO.3 S/D = 0.75

CONSTRUCTED 17.12.71

TESTED 4. 1.72

LOAD PROVING RING DIVS	MICROSTRAINS							
	G1	G2	G3	G4	G5	G6	G7	G8
100	-16	-2	+4	+12	+8	+2	+8	+3
200	-31	-2	+4	+17	+11	+2	+8	+13
300	-52	-3	+5	+13	+11	+5	+8	+13
400	-68	-2	+13	+24	+15	+7	+12	+22
500	-83	-4	+9	+23	+23	+9	+15	+22
600	-103	-6	+13	+26	+30	+12	+18	+25
700	-120	-9	+17	+37	+35	+16	+23	+31
800	-134	-13	+20	+40	+43	+19	+29	+35
900	-154	-12	+24	+46	+44	+17	+34	+38
1000	-172	-15	+27	+54	+53	+18	+38	+41
1100	-182	-18	+33	+51	+61	+18	+43	+46
1200	-213	-23	+33	+61	+67	+20	+50	+49
$\ddot{\bar{x}}$	-111	-9	+17	+34	+33	+12	+24	+28

TABLE 10.6.4

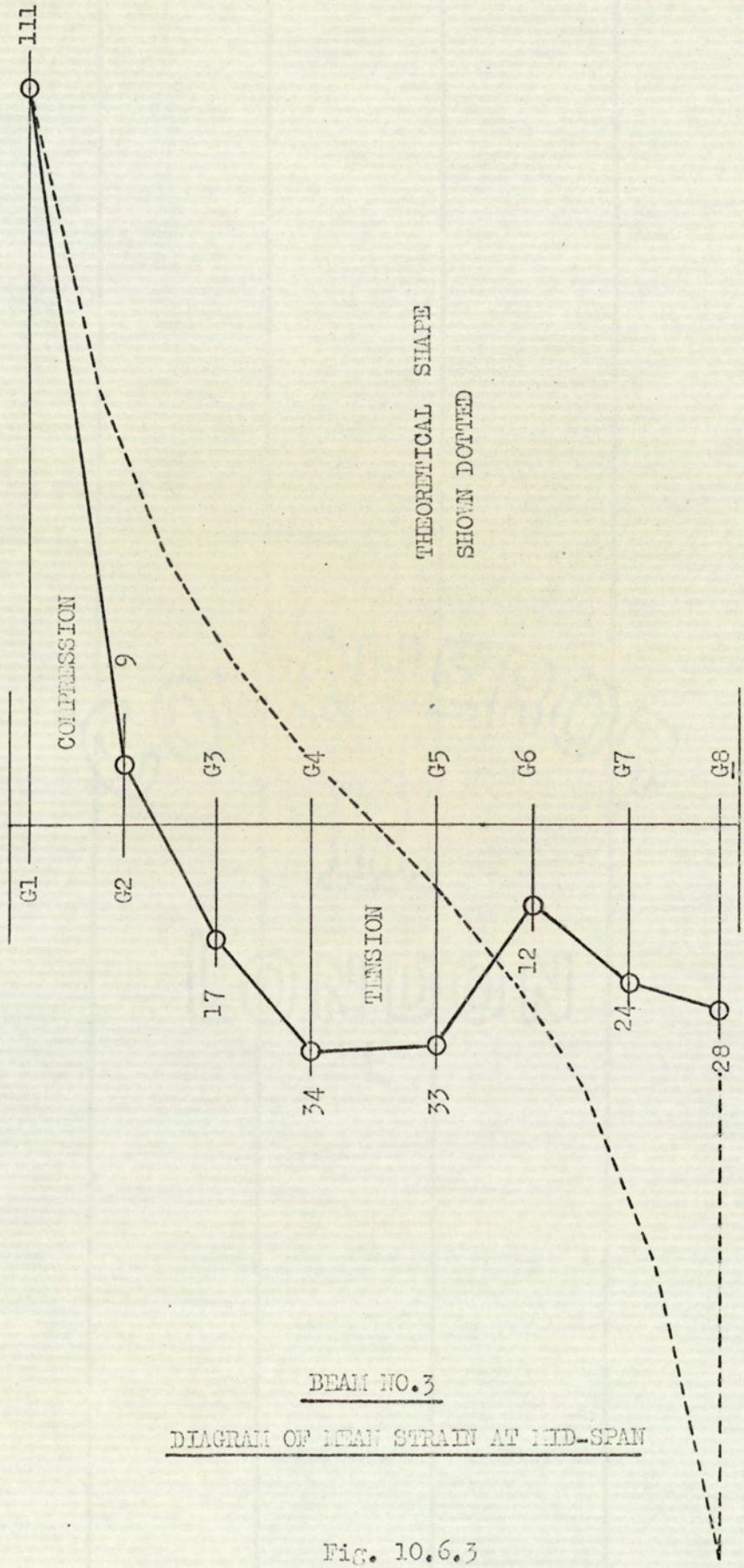

BEAM NO.3

DIAGRAM OF MEAN STRAIN AT MID-SPAN

Fig. 10.6.3

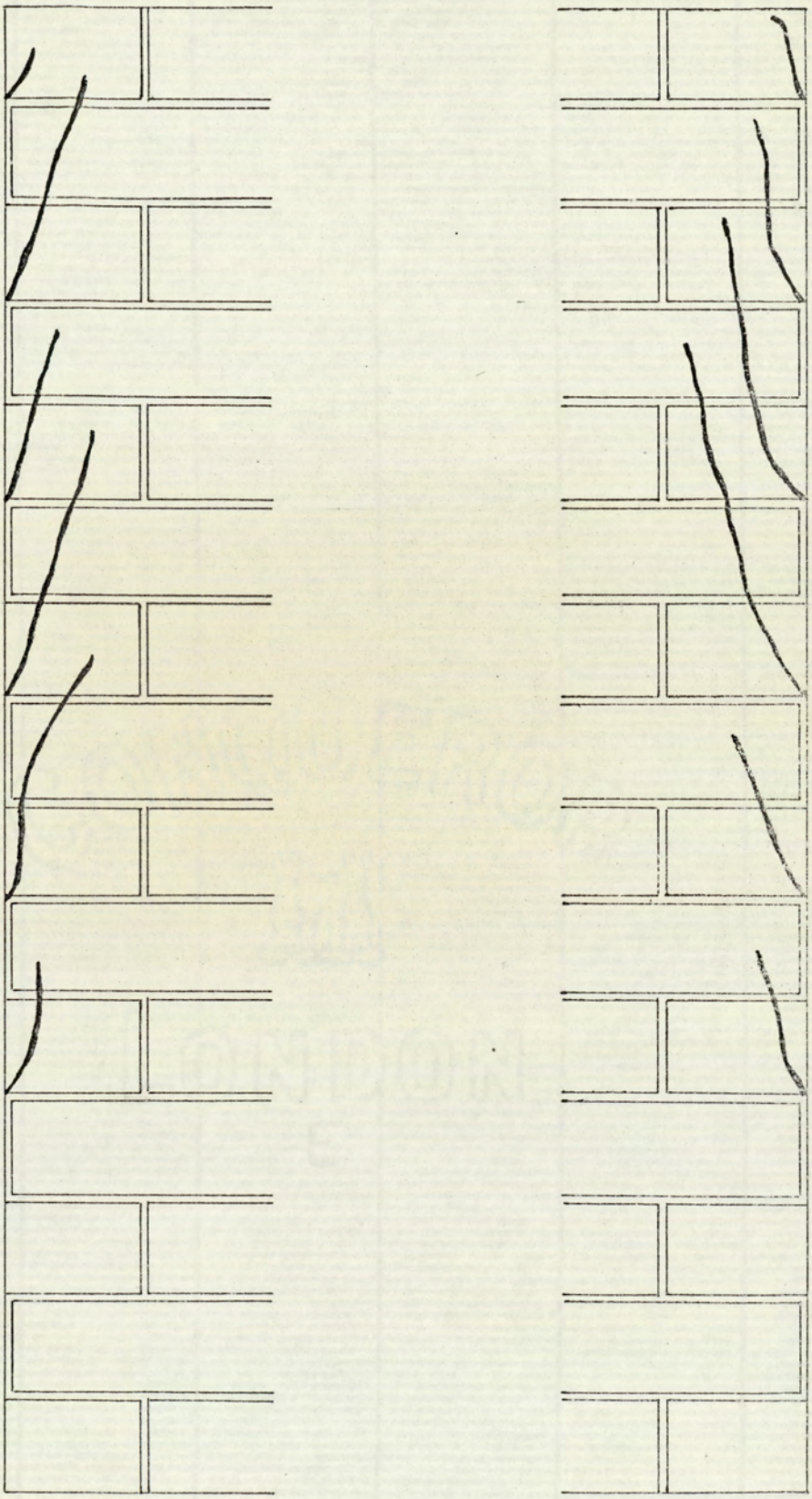

BEAM NO.3

SHEAR CRACK PATTERN AT FAILURE

Fig.10.6.6

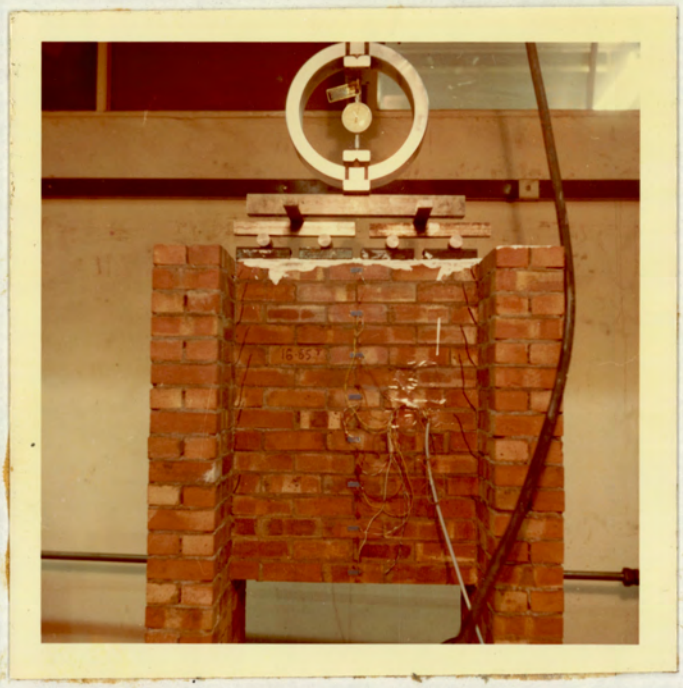

PLATE NO. 10.6.7

BEAM NO. 3 AT SHEAR FAILURE

Commentrary on Test Results

BEAM NO.1

The diagram of mean strain shown in Fig. 10.6.1 can be favourably compared to the theoretical diagram shown in Fig. 10.3.4. 5 (p.221) indicating that this beam behaved almost exactly as the theory would predict.

Ultimate failure of the beam occurred at an applied load of 5600 lb.

From Fig. 10.3.4. 5 the theoretical failure stress is given by:-

$$\sigma_x = 509.13\ Aa^3$$

$$\text{Top face loading} = 160\ Aa^3 = \frac{5600}{2.125 \times 46.875} \quad \text{lb/in}^2$$

$$\therefore \text{ Modulus of Rupture} = \frac{5600 \times 509.13}{2.125 \times 46.875 \times 160} = 178.9 \text{ lb/in}^2$$

The crack pattern at failure shown in Fig. 10.6.4. can be said to be the typical tension mode of failure for a brickwork beam.

Failure occurred at the extreme outer tension fibres in a perpend joint by a breakdown in the adhesion between brick and mortar. After this initial failure the tension crack rapidly moved towards the perpend joint adjacent to the point of maximum bending moment, then continuing to rise through the depth of the beam along the weakest line always between brick and mortar; until at a point near the top of the beam a weak bed joint is found which naturally produces a change in the direction of the developing crack.

Plate No. 10.6.4. shows the beam after failure.

During the period of the development of the tension failure crack a secondary failure occurred in the right hand supporting brick pier. Rotation of the pier during the beam deflection set up a high intensity of vertical stress at the base of pier giving rise to crushing of the bottom course of bric kwork on the inside face of the pier.
This is shown in Plate No. 10.6.5.

BEAM NO.2

The diagram of mean strain shown in Fig.10.6.2. does not give a favourable comparison with the theoretical diagram shown in Fig.10.3.4.2 (page 218)

The experimental results do however indicate that the beam behaved along the general lines that could be expected for a symmetrical section subject to bending.
A neutral axis exists near to the centre of the section with zones of tension and compression increasing in numerical value towards the extreme outer fibres of the section.
The decrease in tensile strain between gauges No. 7 and 8 suggest that there was some additional factor influencing the flexural behaviour of the beam.

As a first thought, it may be suggested that this factor could well be the stiffness of the supporting piers, thei r reluctance to rotate and the inability of the horizontal distance between the piers to freely increase as the applied load to the beam is increased.

By a simple mathematical solution, the effects of this factor can be shown.

Consider the specimen to be of the nominal dimensions shown on Fig.10.6.7 the thickness of the beam being $2\frac{1}{8}$"

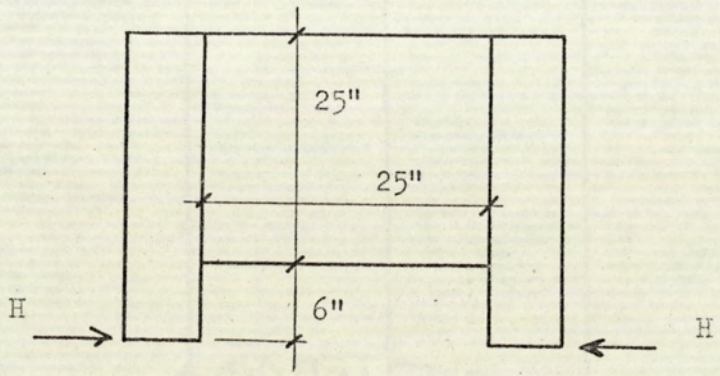

Fig.10.6.7

When the specimen acts as a "structure" a horizontal force H is set up at the supports, this reaction being generated principally by the friction between the supporting piers and the concrete base slab.

At the mid-span section of the beam the stress diagram due to simple bending from the applied load will be of the form:-

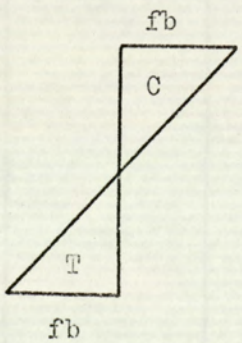

The section modulus of the beam is $\frac{2.125 \times 25^2}{6} = 221.35 \text{ in}^3$

The area of the beam section = $25 \times 2.125 = 53.125 \text{ in}^2$

The effect of the horizontal force (H) on the mid-span section of the beam will therefore be:-

a) A direct compressive stress = $\frac{H}{53.125}$

b) A bending stress = $\pm \frac{18.5\ H}{221.35}$

The combined effect of (a) and (b) will be:-

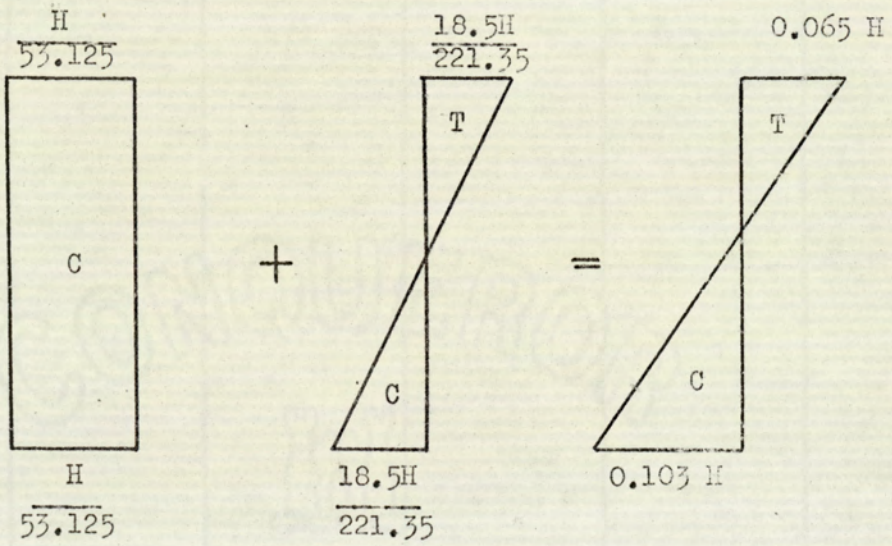

Adding the effect of H to the stress due to simple bending from the applied load results in a diagram of stress distribution at mid-span:-

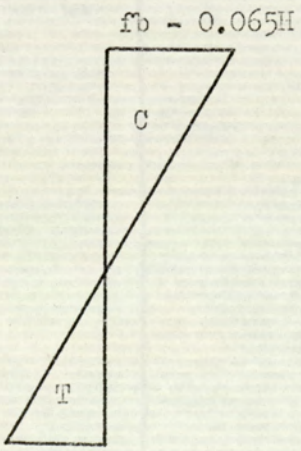

fb - 0.103H

Indicating a move of the neutral axis position from the centre towards the bottom face of the beam.

The experimental work clearly shows that the neutral axis position moves towards the TOP face of the beam.

For a simply supported beam of span = L carrying a uniformly distributed load (W) the angular rotation can be shown to be:

$$\theta = \frac{WL^2}{24EI} \quad \text{radians}$$

For the beam being considered here

$$\theta = \frac{W \times 25^2}{24 \times 1.77 \times 10^6 \times \frac{2.125 \times 25^3}{12}} = 0.0053 \times 10^{-6} \, W \text{ radians}$$

This value is extremely small and the effect of any outside influence restricting this rotation can be neglected when considering the strain distribution at mid-span.

It is therefore suggested that the influence of the piers can be neglected and that the disturbance to the theoretically predicted strain diagram must be due to some factor other than the presence of the supporting piers.

Referring again to the diagram of mean strain (Fig.10.6.2) it can be justly concluded that the beam is acting ina manner that would be predicted by the theory if a depth of beam between gauges No. 1 and No.7 is considered.

Fig.10.6.8 has been prepared neglecting that part of the beam below gauge No.7. The theoretical shape drawn for comparison is based on a strain value at the extreme outer fibres of $\frac{59 + 72}{2} = 65.5$ which is the average of the maximum experimental values for the extreme outer fibres strains.

The experimental mean position of the neutral axis is shown to be in a position in close approximation to the centre of the beam, the distribution of tensile and compressive strain give some evidence to support the conclusion that the element is principally acting as a beam could generally be expected to behave. At the same time, there must exist again some external factor that is giving rise to the deviation of the mean strain diagram from the symmetrical diagram predicted by the theory.

From the results of the test carried out on Beam No. 1 it was calculated that the Modulus of rupture was 179 lb/in^2.

For a beam of span/depth ratio = 1.0, Fig.10.3.4. 2 shows that the maximum stress at the extreme outer fibres is 149.42 Aa^3.

On this basis, using the Modulus of rupture value obtained for Beam No.1 the theory could predict:-

$$\sigma_x = 149.42\ Aa^3 = 179\ lb/in^2$$

$\therefore$ Top face loading per unit area = $160\ Aa^3$

$= 191.67\ lb/in^2$

$\therefore$ The total applied load at predicted failure = W

$$W = 25 \times \frac{2.125}{2240} \times 191.67 = 4.55 \text{ tons}$$

Beam No. 2 actually failed at W = 4.2 tons

This further indicates that the beam which had a span/depth ratio equal 1.00 behaved within an acceptable limit as the theory would predict.

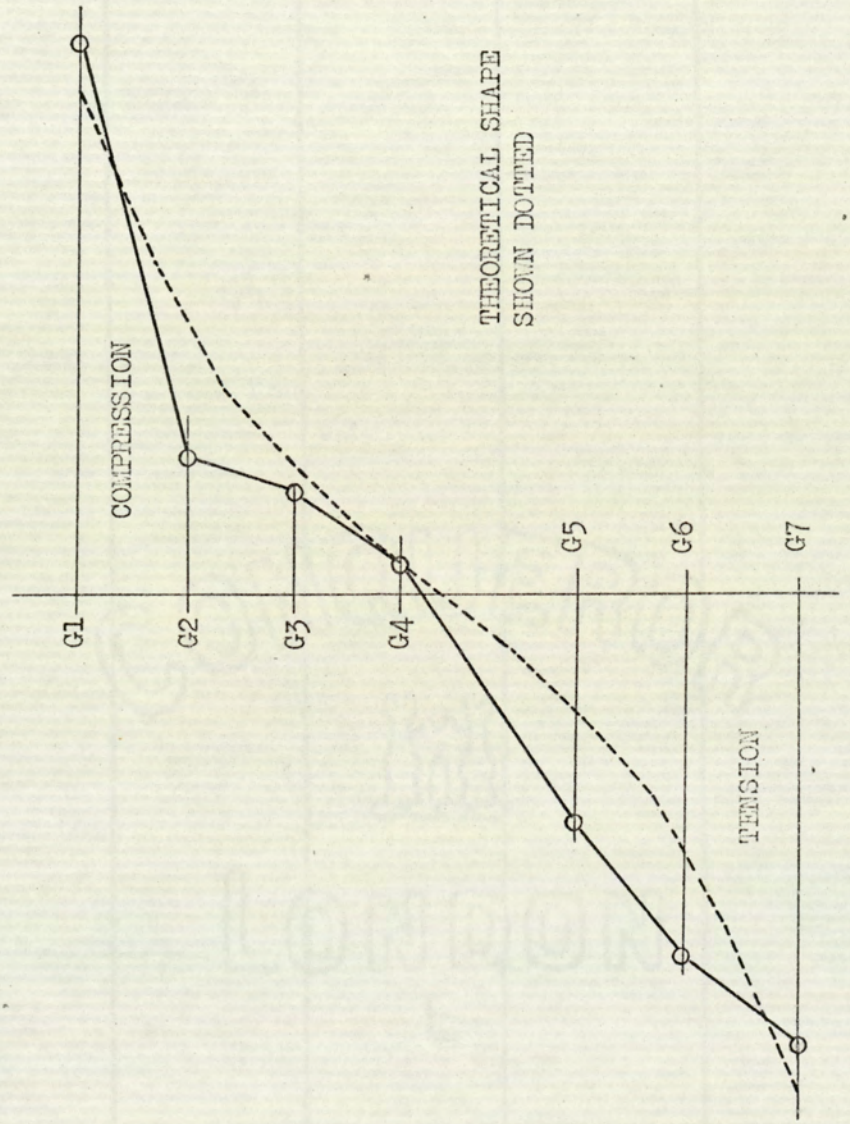

BEAM NO.2

STRAIN DISTRIBUTION FOR MODIFIED DEPTH

Fig.10.6.2

It is apparent from the mean strain diagram that the bottom 2 courses of brickwork in the beam are for some reason ineffective in the resistance to the applied bending moment. Probably, there was a failure in the perpend joint that was undetected during the test. If the bottom two courses are neglected the beam still had a span/depth ratio of 1.13 resulting in a calculated modulus of rupture value that would be very little less than that for a beam with span/depth = 1.0.
The mode of failure of brickwork beams will be discussed in the conclusion to this chapter.

Undetected perpend cracks on the extreme tension face may well be a contributory factor to the interference with the theoretical mean strain diagram. Bricks and mortar on this face which have been in a state of tensile stress before perpend cracking are relieved of some stress when the crack takes place; due to the elastic properties of the material a relief of stress sets up a desire for the extended material to contract and since the next bed joint is still intact a compression will be set up in the next course of bric kwork. This would have an effect on the distribution of stresses in the beam and would consequently modify the distribution of strain across a given section.

The crack pattern of Fig.10.6.5. again shows the typical flexural failure for brickwork beams. The first fracture is a breakdown in the adhesion between brick and mortar in a perpend joint, the crack progresses along a weak bed joint and then rises through the next perpend joint, again a weak bed joint is found and then the crack rises through the beam moving towards the plane of maximum bending moment.

At an applied load of 4.2 tons the fracture travelled from the bottom tension face of the beam to the bed joint of the fourth course from the top face of the beam. This was considered to be the failure load of the beam but was indeed not the collapse load.
The applied load was then increased to 10.00 tons which was the maximum allowable load of the proving ring in use, at this load the structure still remained intact although the tension crack had now extended into the next 3 courses of the beam. Plate No. 10.6.6 shows the specimen sustaining an applied load of 10.00 tons.

Obviously, full arching action was now taking place, the specimen was behaving as a deep arch with the resistance to horizontal thrust being provided by the friction between the brickwork piers and the reinforced concrete base slab. This evidence provides some solution to the problem of interference with the mid-span strain distribution at lower values of applied load, clearly if a beam of this span/depth is capable of full arching action at high values of applied load then it will exhibit characteristics of partial arching action for lower values of load thus having some effect on theoretically predicted strain distribution based upon an assumption that the beam is in a state of simple bending.

BEAM NO.3

Again, the diagram of mean strain shown in Fig.10.6.3. is not representative of the theoretical strain distribution.

Based upon the theory of this chapter and using a modulus of rupture of 179 lb/in^2 as determined for Beam No.1, it would be predicted that a tension failure in the beam would occur at an applied load of 4.60 tons.

At this load the specimen showed no sign of distress whatsoever, the applied load was increased to 16.85 tons when failure of the structure occurred by diagonal tension cracks due to shear at the supporting face between beam and piers.

This further emphasises the fact that deep beams are capable of exhibiting arching action. In this case the beam had a span/depth ratio of 0.75, the test results indicate that the beam element did not at any stage behave as a simple beam and that full arching action took place from the very commencement of loading. The dimensions of the specimen can be likened to a very deep arch where the horizontal thrust which would be of a comparatively low value could easily be taken up by shear in the brickwork piers and by friction between the piers and the concrete base slab.

The experiment however further illustrates the high ultimate strength that a brickwork structure of this shape possesses. The mode of failure is particularly interesting since this was the only instance in the whole of t his work that a shear failure was achieved.

The crack pattern at failure is reproduced in Fig.10.6.6. showing diagonal tension fractures on the face of the beam element at each end where the beam is built into the supporting piers.
The cracks generate from alternate course lines where the brick is bonded into the pier and rise upwards at an approximate angle of 20^{o} to the vertical.

In order that the test specimen could be preserved the applied load was removed at 16.85 tons before complete collapse had occurred.

At this failure load of 16.85 tons a mathematical investigation of the shear failure can be given assuming that the "arch" was such that the vertical shear was carried uniformly down a vertical line of the beam of a length equal to that which became cracked under the loading conditions. It can further be assumed that only the alternate bricks that were bonded into the pier were effective in resisting this shear such that the shear carried by each brick was $\frac{16.85}{2 \times 6}$ = 1.404 tons.

The "vertical" shear stress in each brick was therefore:-

$$fs = \frac{1.404}{2.125} \times \frac{2240}{1.3125} = 1127.6 \text{ lb/in}^2$$

The stress system on an element of brick at the support can then be represented by:-

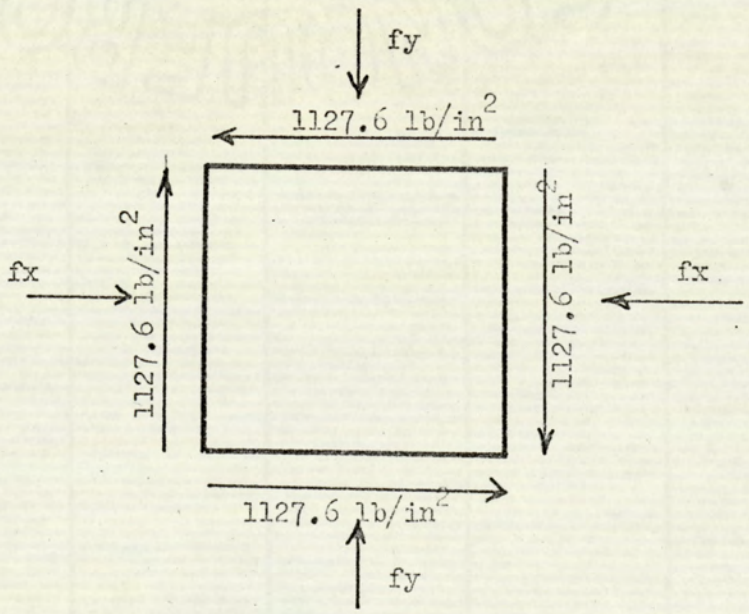

then considering the principal plane at 20° to the vertical the principal tensile stress (ft) which will be the tensile stress in the brick at failure will be taken as 344 lb/in^2, the arithmetic mean of ultimate tensile strength of similar bricks obtained by previous experiment.

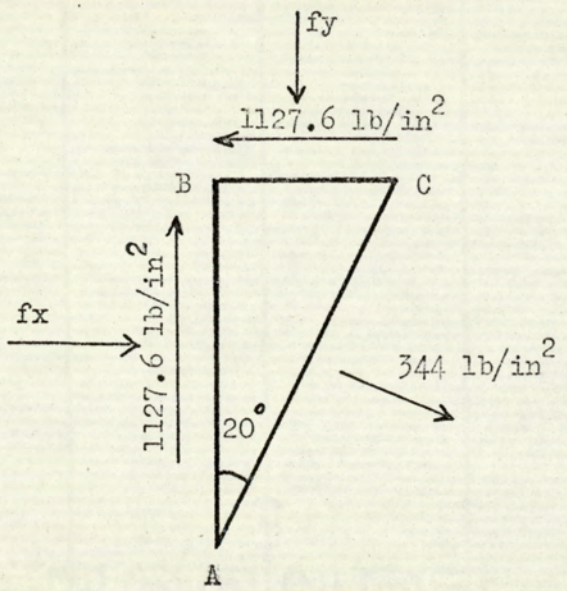

Considering the equilibrium of the wedge ABC

$$344\ AC \sin 20^\circ = 1127.6\ AB - fy\ BC$$

$$344 \sin 20^\circ = 1127.6 \cos 20^\circ - fy \sin 20^\circ$$

$$117.655 = 1059.59 - 0.34202\ fy$$

$$\therefore\ fy = 2754\ lb/in^2$$

$$344\ AC \cos 20^\circ = 1127.6\ BC - fx\ AB$$

$$344 \cos 20^\circ = 1127.6 \sin 20^\circ - fx \cos 20^\circ$$

$$323.25 = 385.66 - 0.93969\ fx$$

$$\therefore\ fx = 66.42\ lb/in^2$$

The resulting stresses acting on the wedge are:-

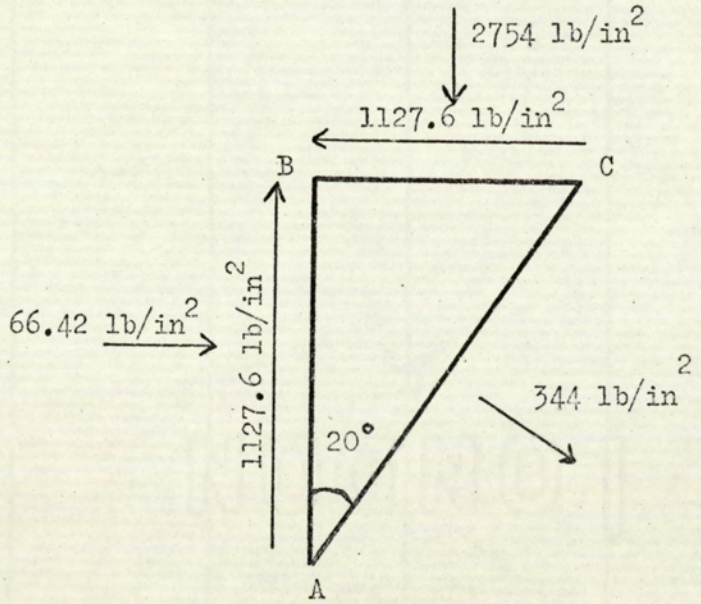

Confirming that the horizontal stress, being the reaction due to the arch thrust, is small compared to the vertical compressive stress. i.e. as would be expected for a deep arch.

Conclusions:

The results of the test on Beam No. 1 can be taken as conclusive evidence that the theory correctly predicts the behaviour of a beam with a span/depth ratio equal to 2.00.
The theory based upon a beam composed of a homogenerus material can be successfully applied to a brickwork beam which can be described as a 'plate' where the individual size of the elements i.e. brick and mortar is small compared to the overall size of the plate.

The calculated Modulus of Rupture value is of the same order as that obtained for shallow beams and again indicates that a load factor of 8 or 9 can be readily achieved if design stresses are employed based upon the value of 20 lb/in^2 allowed by CP.111 when the direction of principal bending stress is at right angles to the perpend joints.

A particular factor meriting further investigation is the discrepancy between Modulus of Rupture values for brickwork beams and the bond strength or values of ultimate stress for the adhesion of brick to mortar as determined by the experimental work of Chapter 4.
The bond strength as determined by a direct tensile test gives results that are only one third of the beam modulus of rupture values.

As a first thought, it may well be anticipated that the breakdown in adhesion between brick and mortar in a perpend joint at the extreme outer tension fibre would result immediately in the beam failure.
From the experimental results, this obviously cannot be true, it is suggested by the author that two principal factors account for the discrepancies. Firstly, the flexural bond strength has a greater value

than the direct tensile bond strength this is shown in the flexural strength test of small scale assemblies in Chapter 7. Secondly, after the first failure in the outer perpend joint (the failure would only show as a hair line crack and would be difficult to observe) the tensile strength of the brick would then become predominant. The typical tension failure crack progresses vertically through the beam and by reason of the general staggered arrangements of perpend joints on any vertical line the fracture must progress alternately through a joint and then through a brick which must be the cause of considerable re-distribution of stress throughout the non-homogenerus material of the brickwork.

For practical design purposes it would be more sensible to employ a simple tensile strength test for the brickwork proposed and then to apply a specified load factor to determine the allowable flexural tension design stress.

The all embracing figure of 20 lb/in^2 allowed by CP.111 is not dependent on the types of brick and mortar and may well be either dangerous or very conservative.

From the discussion on the results of the test on Beam No.2 it can be said that the theory successfully predicts the behaviour and ultimate load carrying capacity for a beam of span/depth ratio = 1.0 that is supported by the theoretical end conditions of a shear force at the vertical end of the beam. Evidence is given that this span/depth ratio is the probable limit to which the theory should be applied since at these beam proportions the ability for arching action to take place is beginning to have some effect on the theoretical predictions. However, for design purposes within the elastic range of the brickwork materials these arching effects could be ignored and the beam may for all practical

purposes be assumed to be in a state of simple bending.

The results of the test on Beam No.3 give the conclusion that a beam of span/depth ratio equal to 0.75 will not act in a state of simple bending and that it is more likely that full arching action takes place from the commencement of loading. In practice, beams of such proportions should be analysed by one of the 'arching theories'.

From these experiments it has been shown that brickwork structures of the type tested possess a high ultimate strength in the lower span/depth ratios, this factor would be worthy of further mathematical and experimental investigation.

In many instances of present day design cross walls are supported on what must be superfluous lintolbeams designed to carry the full weight of the wall when in actual fact the wall itself is probably capable of carrying a load many times its own weight without the necessity for the provision of extraneous support.

Similarly, walls supported on strip foundations are assumed to impose a uniformly distributed load over the length of the foundation. If the wall is deep in relation to its span the results of this programme of work indicate that arching action will take place, friction between the wall and its foundation will be more than sufficient to accommodate the thrusts set up by the arch. The result of this behaviour would be high concentration of stress in the foundations at each end of the wall whilst atthe centre, a non-reinforced foundation would be ineffective.

Finally, it can be concluded from the work of this chapter and from the work of previous authors who considered deep beams supported along a short distance of the bottom face, that the distribution of strain at the mid-span section will be dependant upon the beam support conditions.

CHAPTER 11

THE ARCHING ACTION OF BRICK BEAMS RESTRAINED IN THE LONGITUDINAL DIRECTION

11.1 Introduction

It is well known that in certain cases restrained bric kwork in a state of flexure has been able to sustain much greater loads than could be predicted by an analysis based upon the simple theories of bending using a defined value for the ultimate tensile strength of the brickwork.

A practical example of this condition is the case of brickwork panel walls that are subjected to horizontal wind loads, the walls being built between rigid piers, reinforced concrete columns or beams such that for practical purposes there can be no horizontal movement, similar conditions could be applied to the internal spans of continuous beams subject to loads in either the vertical or horizontal direction.

The additional load that such beams are able to sustain can be attributed to the behaviour of the internal stresses in the plane of the beam after the initial tension cracks have developed and crushing taken place in the remaining compression areas at the beam centre and supports.
This process will be referred to as the 'arching action' of the brick beam.

In this Chapter it is proposed to develop a mathematical investigation into the 'arching action' from the stage of a fully cracked tension zone to the elastic failure of the beam, which is considered to be the point at which first crushing of the brickwork takes place.

For this purpose it will therefore be assumed that the brickwork is incapable of developing a resistance to tensile forces and that upon the immediate application of the load a tensile crack will occur at the centre of the beam and at its points of support. The crack extending initially from the extreme outer fibre to the neutral axis.

At this point in the loading cycle the beam begins to function as an arch, further increases in load will give a rotation of the beam thus increasing the length of the tension cracks and decreasing the compression area at the cracked sections.

11.2 The Loading Cycle

STAGE 1

Immediately upon the application of an applied load, at the points of maximum tensile stress cracks will be produced from the extreme outer fibres to the neutral axis of the beam (Fig. 11.1)

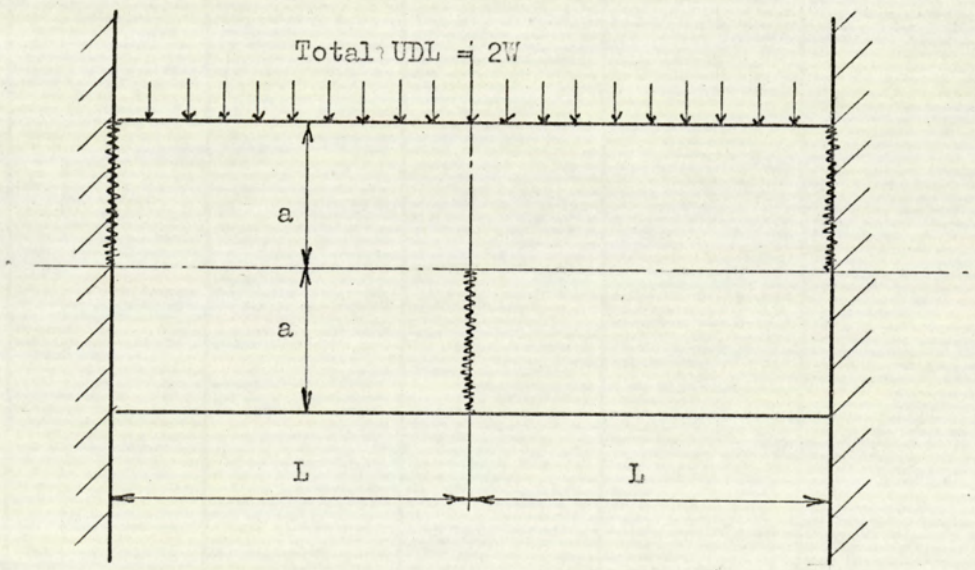

Fig. 11.1

The beam now begins to function as an arch.

STAGE 2

A further increase in the applied load will result in a deflection of the beam (Fig. 11.2).

For a brickwork beam it will be assumed that each half of the beam remains in a straight line rectangular shape and that it rotates as a rigid body.

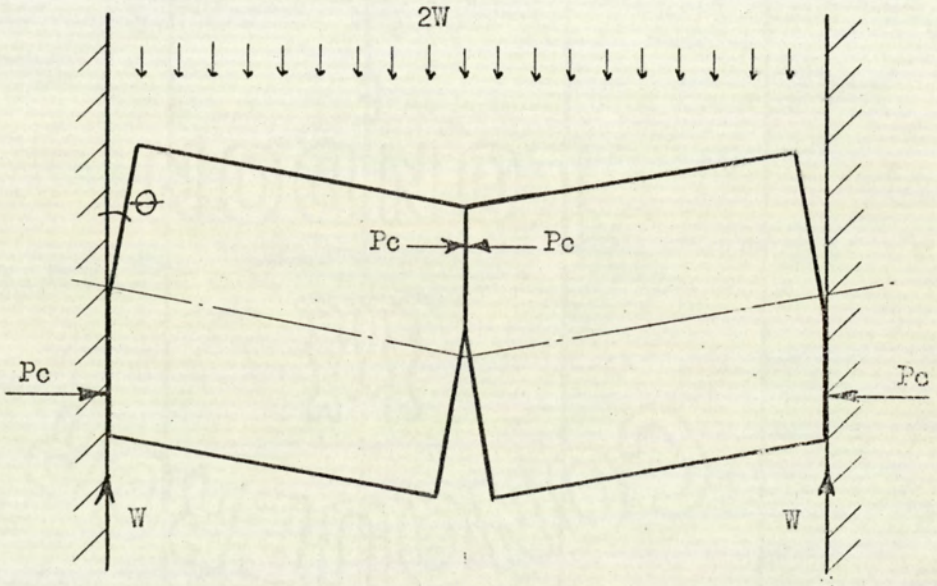

Fig. 11.2

Equilibrium of the beam 'arch' is maintained by the shear force between the compression interfaces and the couple produced by the compressive forces PC.

For the conditions of equilibrium the compression contact areas at the ends of the beam and at the centre must be equal.

The result of this deflection will be an increase in the original crack depth and a consequent decrease in the compression contact area.

A rotation of the beam can only occur by reason of a strain in the compression fibres of the material, clearly, the angle of rotation for any specific value of W will be entirely dependant upon the stress/strain relationship of the brickwork material.

STAGE 3

The beam 'arch' will be capable of sustaining further increases in the applied load until either the couple of the internal forces (PC) disappears or until a physical crushing of the beam material permits a mechanical failure.

11.3 The Increase in Crack Depth

Consider the geometry of the deflected half beam shown in Fig. 11.3.

θ = angle of rotation in degrees

$\frac{\beta a}{\cos\theta}$ = compression contact length

$a(1-\beta)$ = increase in crack depth

αL = shortening of the extreme outer fibres

In terms of the beam length, depth and angle of rotation the deflected beam position is given by:-

$$\beta = \frac{\alpha L}{a \tan\theta} \qquad [1]$$

$$\alpha L = \tfrac{1}{2}\left[L\left(1 - \frac{1}{\cos\theta}\right) + 2\, a \tan\theta \right] \qquad [2]$$

$$\text{Compression contact length} = \frac{\beta a}{\cos\theta} = \frac{\alpha L}{\tan\theta \cos\theta} = \frac{\alpha L}{\sin\theta}$$

$$\frac{\beta a}{\cos\theta} = \frac{1}{2 \sin\theta}\left[L\left(1 - \frac{1}{\cos\theta}\right) + 2\, a \tan\theta \right] \qquad [3]$$

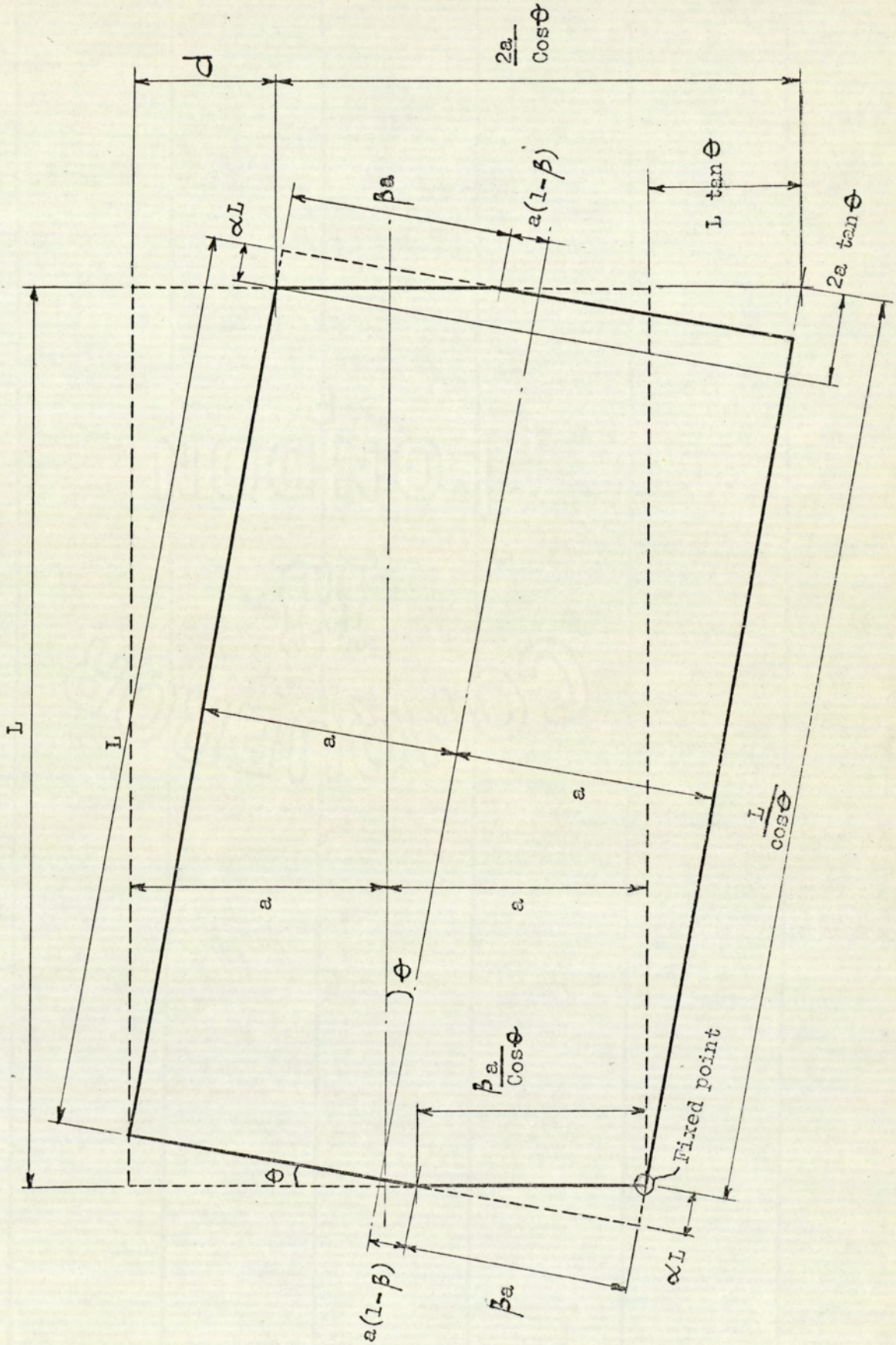

THE DEFLECTED HALF BEAM

Fig. 11.3

Crack Extension $= a(1 - \beta)$

$$= a\left(1 - \frac{\alpha L}{a \tan\theta}\right)$$

$$= a\left\{1 - \frac{1}{2a \tan\theta}\left[L\left(1 - \frac{1}{\cos\theta}\right) + 2a \tan\theta\right]\right\}$$

$$= a\left[1 - \frac{L}{2a \tan\theta}\left(1 - \frac{1}{\cos\theta}\right) - 1\right]$$

$$= -\frac{L}{2 \tan\theta}\left(1 - \frac{1}{\cos\theta}\right)$$

$$= -\frac{L}{2}\left(\frac{1}{\tan\theta} - \frac{1}{\tan\theta \cos\theta}\right)$$

$$= \frac{L}{2 \sin\theta} - \frac{L}{2 \tan\theta}$$

$$= \frac{L}{2 \sin\theta}\left(1 - \frac{\sin\theta}{\tan\theta}\right)$$

$$\therefore \quad a(1 - \beta) = \frac{L}{2}\,\frac{(1 - \cos\theta)}{\sin\theta} \qquad [4]$$

This equation for $a(1 - \beta)$ therefore shows a linear relationship between the crack extension and $L\theta$.

In approximate terms

$$\text{Crack extension} = 0.0044 \quad L\theta \qquad [5]$$

The solution of the problem now clearly becomes dependant upon the determination of αL which is in itself the total shortening of the extreme outer fibre and is directly dependant upon the stress/strain characteristics of the beam material.

Reference to Fig. 11.3. shows that the outer fibres of each half of the beam are stressed at one end of the fibre only, the end of the fibre at the developing crack must therefore be in a state of zero longitudinal stress. The resulting distribution of stress and consequential distribution of strain along a longitudinal fibre in the conditions of this problem cannot be readily assessed. The mathematical solution to this problem would be complex in the extreme since to obtain a solution for the distribution of stress in an outer fibre would necessitate a mathematical solution for the complete half beam. Such a solution is outside the scope of this programme of work.

For the purposes of the mathematical solution being considered here, the total shortening of the extreme outer fibres (αL) is given by Eqn.[2] in terms of the angle of rotation (θ). The numerical value of the outer fibre strain is unknown since the effective length of the fibre that is strained is unknown. It is therefore not possible to calculate αL for a given load and the known elastic constants of the beam material.
It is proposed here to determine by experiment the load/deflection relationship for beams of various span depth ratios. From this relationship the angular rotation can be calculated in terms of the applied load and hence αL can be determined.

11.4 The Compression Zone and Lever Arm

Fig. 11.3 shows a sudden change in the end face from that part of the face in compression contact with support to that part of the face forming the developing tension crack.
In practice, the condition could only be approached if the beam were made of a very brittle material. An elastic material would of course exhibit a gradual transition from contact face to crack face.
For the purpose of this investigation it will be assumed that the elasticity of brickwork is such that the properties of the beam material

will permit conditions approaching a sudden transition to take place.

Again, considering the geometry of Fig. 11.3. the conditions over the Compression Zone that will be considered are:-

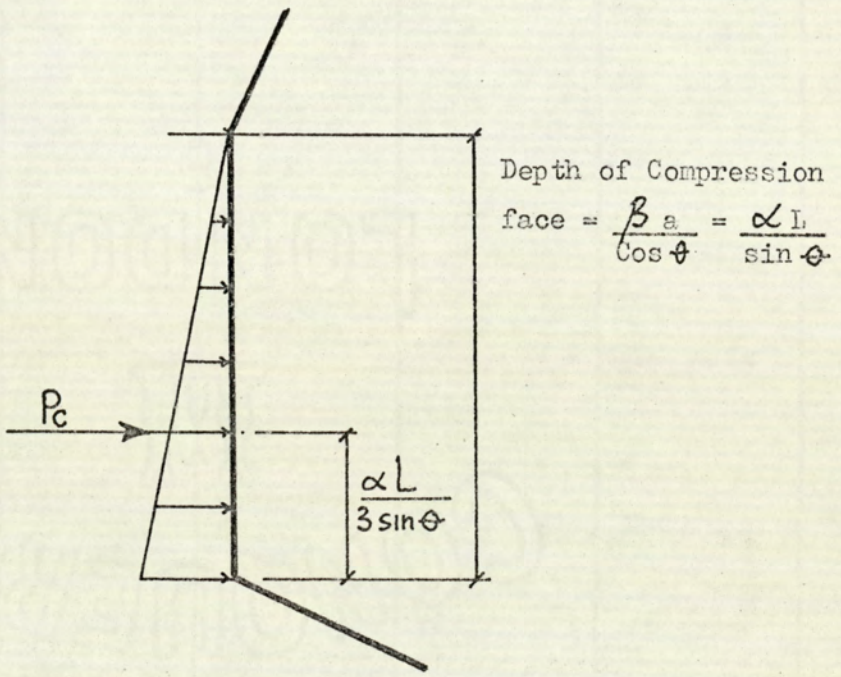

Considering the beam to be of unit thickness

Pc = the total compressive force

The average compressive stress over the compression contact area will be $\frac{Pc \sin\theta}{\alpha L}$ resulting in a maximum compressive stress at the extreme outer fibres of $2 \frac{Pc \sin\theta}{\alpha L}$ this of course is the horizontal component of the maximum stress in the beam.

From Fig 11.3. the lever arm (l_a) of the compressive faces (Pc) will be:-

$$l_a = \frac{2a}{\cos\theta} - L \tan\theta - \frac{2}{3} \frac{\alpha L}{\sin\theta} \qquad [6]$$

The conditions of moment equilibrium for the loading condition being cons idered demands that

$$\frac{WL}{2} = Pc \cdot l_a \qquad [7]$$

$$\therefore \quad Pc = \frac{WL}{2\left(\frac{2a}{\cos\theta} - L\tan\theta - \frac{2}{3}\frac{\alpha L}{\sin\theta}\right)} \qquad [8]$$

Therefore since 2 Pc $\frac{\sin\theta}{\alpha L}$ is the horizontal component of the maximum stress in the beam, the maximum stress (fc) at the extreme outer fibres can be calculated from

$$2\,Pc\,\frac{\sin\theta}{\alpha L} = fc\,.\cos\theta$$

$$fc = \frac{\tan\theta}{\alpha L}\left[\frac{WL}{\left(\frac{2a}{\cos\theta} - L\tan\theta - \frac{2}{3}\frac{\alpha L}{\sin\theta}\right)}\right] \qquad [9]$$

If the angle of rotation is small and measured in radians, then

$$\cos\theta = 1$$

$$\sin\theta = \tan\theta = \theta$$

Eqn [2] can then be simplified

$$\alpha L = a\theta \qquad [10]$$

substitution into Eqn [10] then results

$$fc = \frac{WL}{a\left(\frac{4a}{3} - L\theta\right)} \qquad [11]$$

in a more convenient form where $\frac{L}{a} = R$

this equation can be written:

$$fc = \frac{W}{\frac{L}{R}\left(\frac{4}{3R} - \theta\right)} \qquad [12]$$

where

W = the applied load

θ = the angular rotation caused by the applied load

2L = the span of the beam

R = the span/depth ratio

If the beam material were such that it could accept the resulting deformations without crushing of the material taking place then a mechanical collapse would occur when $\ell a = 0$

$\therefore$ From Eqn [7]

$$\ell a = \frac{2a}{\cos\theta} - L\tan\theta - \frac{2}{3\cos\theta}\left[a - \frac{L}{2}\left(\frac{1-\cos\theta}{\sin\theta}\right)\right] = 0 \qquad [13]$$

Again substituting for $a = \frac{L}{R}$

$$\frac{2L}{R\cos\theta} - L\tan\theta - \frac{2}{3\cos\theta}\left[\frac{L}{R} - \frac{L}{2}\left(\frac{1-\cos\theta}{\sin\theta}\right)\right] = 0 \qquad [14]$$

Within the limits of application of the 'small angle' Eqn [14] reduces to

$$\frac{2L}{R} - L\theta - \frac{2L}{3R} = 0$$

$$\therefore \theta = \frac{4}{3R} \text{ radians} \qquad [15]$$

in the specific case of brickwork beams Eqn. [15] could be used with sufficient accuracy for beams with a span depth ratio greater than 7.50 this being the limit at which the author suggests that results using the small angle theory would be acceptable.

11.5 The Distribution of Strain along a fibre due to the application of a point load

Although it was stated in 11.3 that a mathematical solution to the problem of the distribution of strain along a fibre due to the application of a distributed end load is not available, an approximate analogy can be obtained by an application of the equations developed by FROCHT [18] for the stresses due to the application of a point load to the apex of an infinite wedge (Fig. 11.5.1)

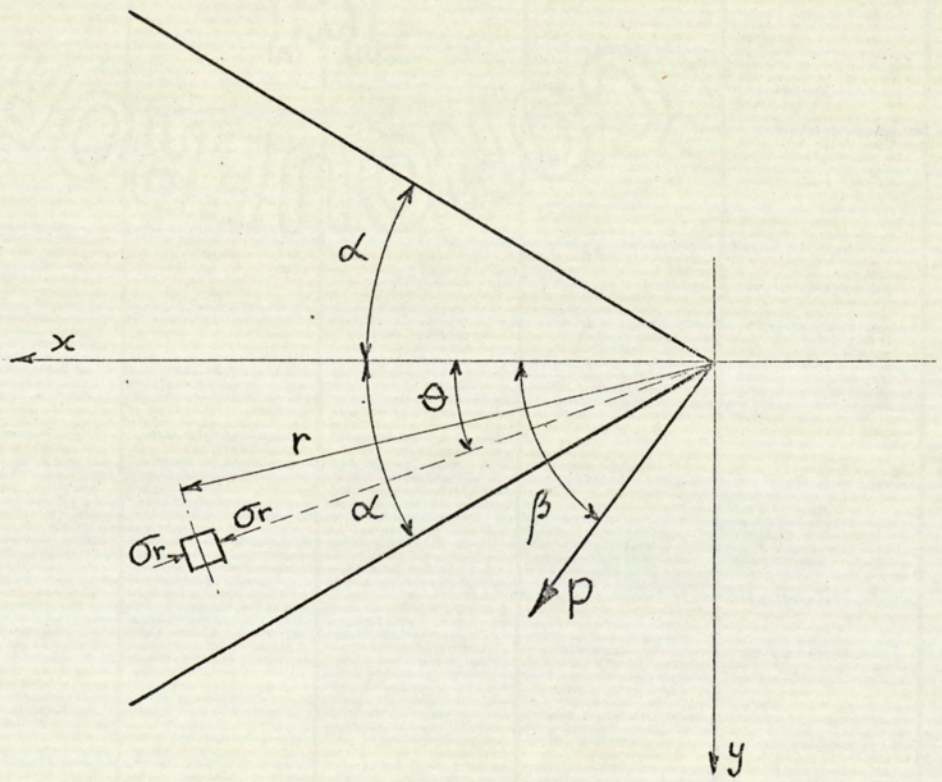

Fig. 11.5.1

The solution to this problem is given as:-

$$\sigma_r = \frac{2P}{rt}\left[\frac{\cos\beta\cos\theta}{2\alpha + \sin 2\alpha} + \frac{\sin\beta\sin\theta}{2\alpha - \sin 2\alpha}\right] \qquad [16]$$

where t = the thickness of the material at right angles to the plane of the diagram.

Considering the special case of a right angled corner of an infinite plate subjected to a point load (P) applied at the corner and in line with one edge (Fig. 11.5.2)

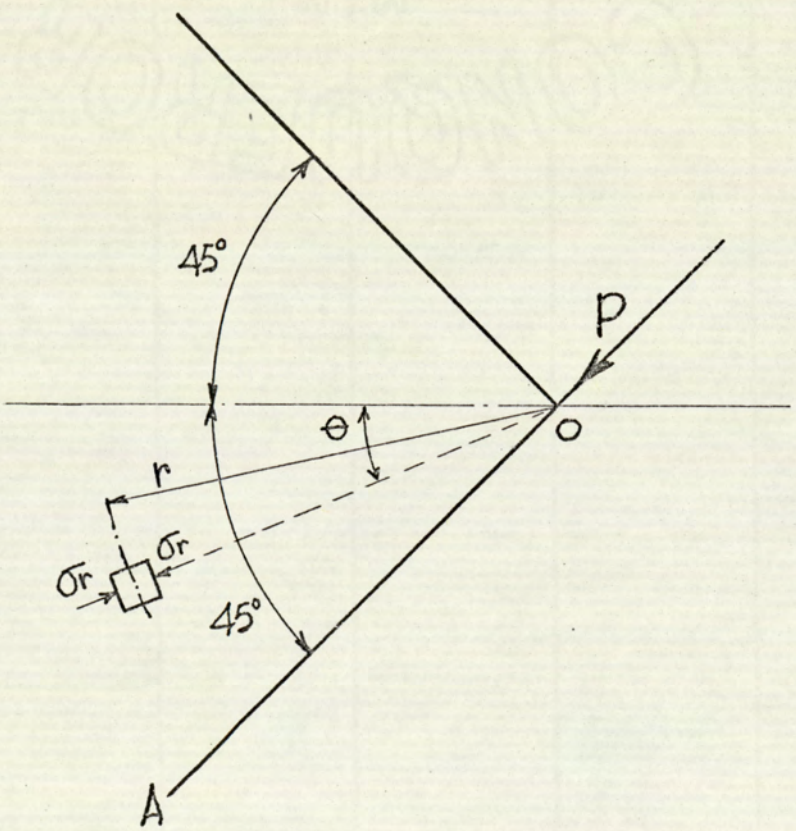

Fig. 11.5.2

In this special case, $\alpha = \beta = 45^\circ$

Eqn [16] then becomes

$$\sigma_r = \frac{2P}{rt}\left[\frac{\cos 45.\ \cos\theta}{\frac{\pi}{2} + \sin 90} + \frac{\sin 45.\ \sin\theta}{\frac{\pi}{2} - \sin 90}\right] \qquad [17]$$

giving

$$\sigma_r = \frac{2P}{rt}\left[\frac{\frac{1}{\sqrt{2}}\cos\theta}{\frac{\pi}{2} + 1} + \frac{\frac{1}{\sqrt{2}}\sin\theta}{\frac{\pi}{2} - 1}\right]$$

$$\therefore \sigma_r = \frac{\sqrt{2}\,P}{rt}\left[0.389\cos\theta + 1.75\sin\theta\right] \qquad [18]$$

Thus, when considering the fibre (OA) along which the load (P) is acting, $\theta = 45^\circ$.

Eqn [18] then gives

$$\sigma_r = \frac{2.139\,P}{rt} \qquad [19]$$

Showing that at the point of application of the load (i.e. r = 0) then $\sigma_r = \infty$.

At an infinite distance along the fibre from the point of application of the load (i.e. $r = \infty$) then $\sigma_r = 0$.

This is mathematically correct since a point load must by definition be applied over an infinitely small area, thereby producing an infinitely large stress.

The problem here is the determination of the strain along the fibre OA.

The total dis placement of O along the line OA is given by:-

$$D = \int_0^{\infty} \frac{2.139\ P}{Ert}\ dr$$

$$= \frac{2.139\ P}{Et} \left[\log_e r \right]_0^{\infty} = \infty$$

The distribution of strain along OA can now be readily plotted by considering the fibre to be split up into small elements of length.

From Eqn [19]

The average strain in an element is given by

$$\mathcal{C} = \frac{2.139\ P}{r.t.E} \qquad [20]$$

where

E = the value of Young's Modulus for the plate material

r = the distance along OA to the centre of the element

Then, tabulation of Eqn [20] gives:-

r x t	Strain $\frac{P}{E}$
0	∞
1	2.139
2	1.069
3	0.713
4	0.535
5	0.428
6	0.357
7	0.306
8	0.267
9	0.238
10	0.214
15	0.143
20	0.107
25	0.086
30	0.071
∞	0

These values are plotted in Fig. 11.5.3 and show clearly that the variation of strain along the fibre OA is non-linear.

Although the strain must have some value throughout the length of the fibre it can be said that for practical considerations the value of strain in elements beyond rt = 20 are of such a small magnitude that they could be neglected.

Fig.11.5.3 of course represents the truly theoretical case of a point load applied over an infinitely small area; again, in practice this would not be achieved.

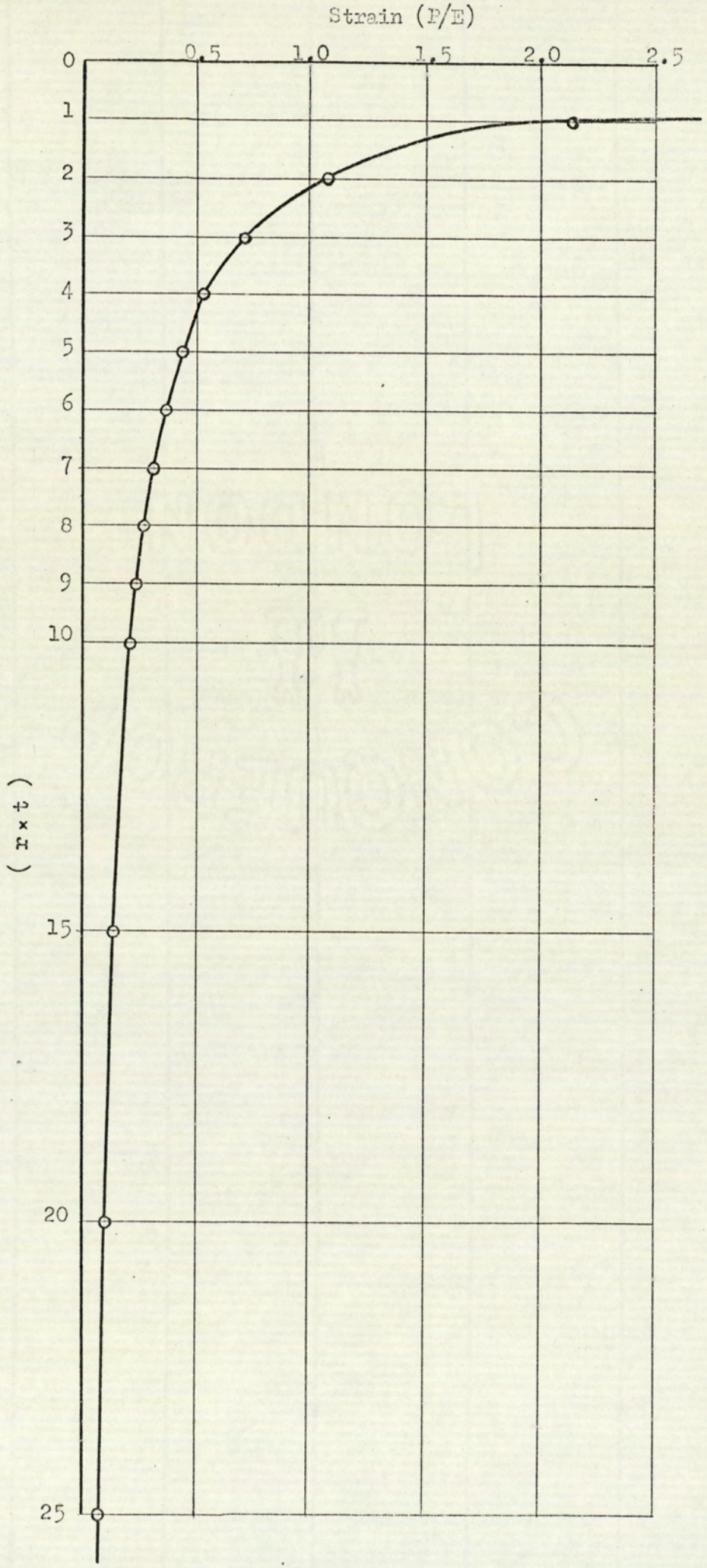

DISTRIBUTION OF STRAIN ALONG FIBRE OA

Fig. 11.5.3

11.6 An experimental determination of the load/deflection relationship

The theoretical work of this chapter gives an explanation of the arching action of brick beams that are restrained from movement in the longitudinal direction. The theory is based upon the beam being constituted from a homogenerus material, it was therefore necessary to investigate specimens of such a material in order that the resulting strain constants may be substituted into the theoretical equations.

For this purpose, 9 cement/lime/sand mortar beams were constructed as shown in Table No. 11.6.1 and tested to obtain their relevant load/deflection characteristics and mode of failure.

The modes of failure are compared to the theoretical predictions and from the experimental results the apparent crushing stress at failure is calculated.

Several attempts were made to cast a beam 2" deep using 1.1.5 C/L/S; in each case during the curing period the specimen suffered severe shrinkage cracking, it was finally decided to abandon a specimen of this thickness and mix from the testing programme.

All beams were made from locally obtained building sand with ordinary Portland cement and were cast using a water cement ratio of 0.86 by volume in 'Formica' lined timber moulds.
After casting the specimens were cured under a damp hessian covering in the laboratory.

To obtain the elastic properties of each mortar mix 3 No. 4" cubes were cast at the same time as the beam and were tested on the same day as the beam tests.

Tests to obtain the value of Young's Modulus and crushing strength were carried out as previously described in this thesis and resulted in the following:

1. 0. 3 Mortar

Average value of Young's Modulus (E) = 1.43×10^6 lb/in^2

Crushing strength

Arithmetic mean	($\bar{x}$)	2319 lb/in^2
Standard deviation	(S)	178.37 lb/in^2
Coefficient of Variation	(V)	7.69%

1. 1. 5 Mortar

Average value of Young's Modulus (E) = 0.82×10^6 lb/in^2

Crushing strength

Arithmetic mean	($\bar{x}$)	835.8 lb/in^2
Standard deviation	(S)	97.37 lb/in^2
Coefficient of variation	(V)	11.65%

TEST BEAM SPECIMENS

BEAM NO.	MIX C/L/S	LENGTH	WIDTH	DEPTH	SPAN/DEPTH (R)	CAST	TESTED
1	1.0.3	30"	8"	6"	5	22.11.71	21.12.71
2	1.0.3	30"	8"	5"	6	22.11.71	21.12.71
3	1.0.3	30"	8"	4"	7.5	22.11.71	21.12.71
4	1.0.3	30"	8"	3"	10	22.11.71	21.12.71
5	1.0.3	30"	8"	2"	15	22.11.71	21.12.71
6	1.1.5	30"	8"	6"	5	26.11.71	22.12.71
7	1.1.5	30"	8"	5"	6	26.11.71	22.12.71
8	1.1.5	30"	8"	4"	7.5	26.11.71	22.12.71
9	1.1.5	30"	8"	3"	10	26.11.71	22.12.71

TABLE NO. 11.6.1

Method of Test

The general arrangement of the testing apparatus is shown in Plate No. 11.6.1.

A steel rig was manufactured of welded c onstruction from 17" x 4" R.S. Channels, $\frac{3}{8}$" gussets plates and 3" x 3" x $\frac{3}{8}$" bracing angles. To accommodate possible veriations in the specimen dimensions a $\frac{3}{4}$" M.S. bearing plate was provided at each end such that it could be adjusted in horizontal location and vertical alignment by the use of 12 No. $\frac{3}{4}$" dia. B.S.W set screws. (Plate No. 11.6.2.)

The specimen to be tested was placed in the rig and supported vertically at each end by a 1" wide x $\frac{3}{4}$" thick rubber strip upon which was placed a 1" wide x $\frac{1}{8}$" thick M.S. plate.
The end bearing plates were then adjusted by means of the set screws such that the plates provided a firm and even fit to the vertical end surface of the mortar beam. Care was taken to ensure that the plates were only sufficiently adjusted to the beam length and verticality of the ends and that no measurable pre-compression was applied to the longitudinal axis of the beam.

A further 1" wide x $\frac{3}{4}$" thick rubber strip was placed at the mid-span point on the top face of the beam through which the load was applied by means of a hand operated hydraulic jack through a proving ring.
A $1\frac{1}{2}$" square x 9" long steel spreader separated the proving ring from the rubber strip.

For the purpose of measuring vertical deflections, dial gauges were positioned on each side of the central loading strip and at each end on

the plates between the beam and the rubber strip providing the vertical support.

It should be noted that the vertical supports were provided simply to locate the beam during setting up of the experiment. The vertical reaction to the applied load is provided by friction between the vertical end of the beam and the end bearing plates. Dial gauges were provided in this position to indicate any vertical slip that had taken place.

For convenience the load was applied in increments of the proving ring dial gauge, the load/deflection curves are plotted on this basis. Calibration of the proving ring dial gauge is given in Table No. 11.6.2 showing the applied load in pounds and tons equivalent to divisions of the dial gauge.

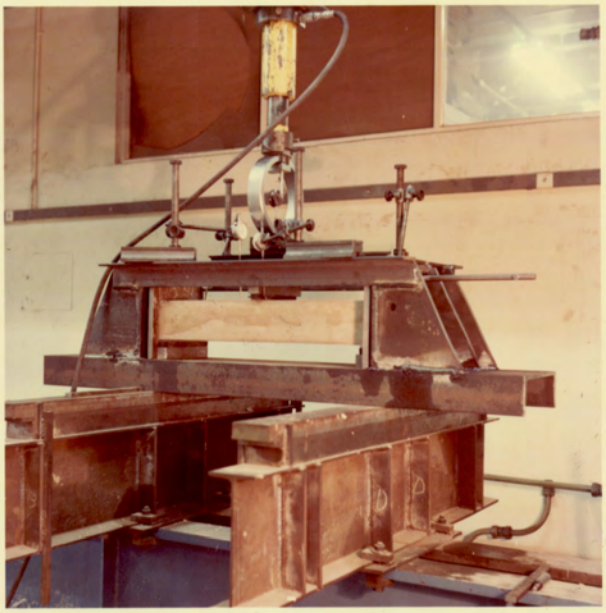

PLATE NO. 11.6.1

ARRANGEMENT OF TESTING APPARATUS

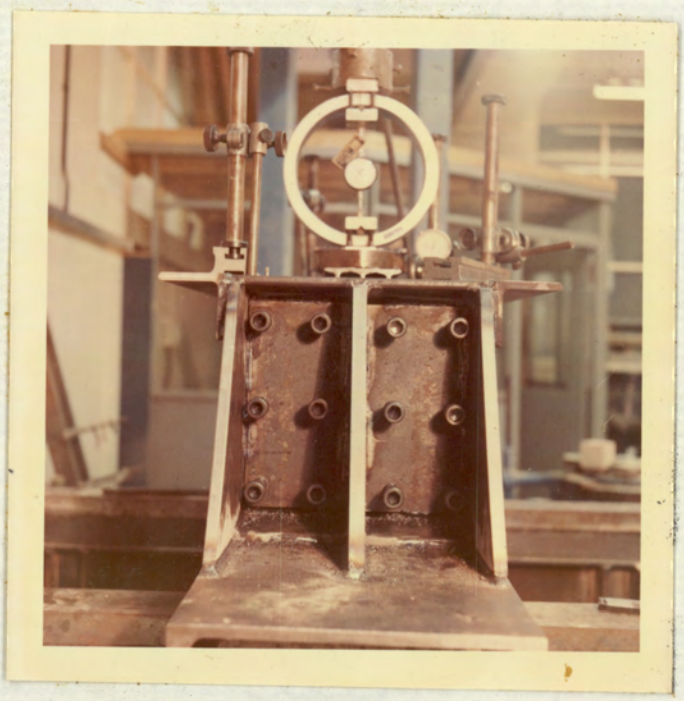

PLATE NO. 11.6.2

ADJUSTING SCREWS FOR END BEARING PLATE

CALIBRATION OF PROVING RING NO.914

DIAL GAUGE DIVISIONS	TONS	lb
10	0.0843	188.87
20	0.1686	377.74
30	0.2529	566.61
40	0.3373	755.48
50	0.4216	944.35
60	0.5059	1133.22
70	0.5902	1322.09
80	0.6745	1510.96
90	0.7589	1699.83
100	0.8432	1888.7
125	1.0540	2360.87
150	1.2637	2830.66
175	1.4743	3302.44
200	1.6849	3774.22
225	1.8955	4245.99
250	2.106	4717.78
275	2.308	5170.68
300	2.578	5640.74
325	2.728	6110.89
350	2.938	6580.86
375	3.145	7044.03
400	3.354	7513.63
450	3.774	8452.83
500	4.193	9392.03
550	4.602	10307.90
600	5.02	11244.98
650	5.432	12167.13
700	5.850	13103.06
750	6.253	14006.67
800	6.670	14940.45
850	7.086	15871.63
900	7.502	16805.25

TABLE NO. 11.6.2

TEST RESULTS

BEAM NO.1

APPLIED LOAD (PROVING RING DIVS)	DEFLECTION (0.001")	
	L.H.GAUGE	R.H.GAUGE
10	0.5	0.5
20	1	1.5
30	2	2
40	2.5	3
50	3	3.5
60	4.5	4.5
70	6	6
80	7.5	9.5
90	16	24.5
100	21.5	31
150	33	37
175	38	41.5
200	44	50
225	49	59
250	54	71
275	57	81
300	58	92
325	61	110
500	90	139.5
550	98	149
600	106	156.5
650	116	166.5
700	125	180
750	130	196

TABLE NO. 11.6.3

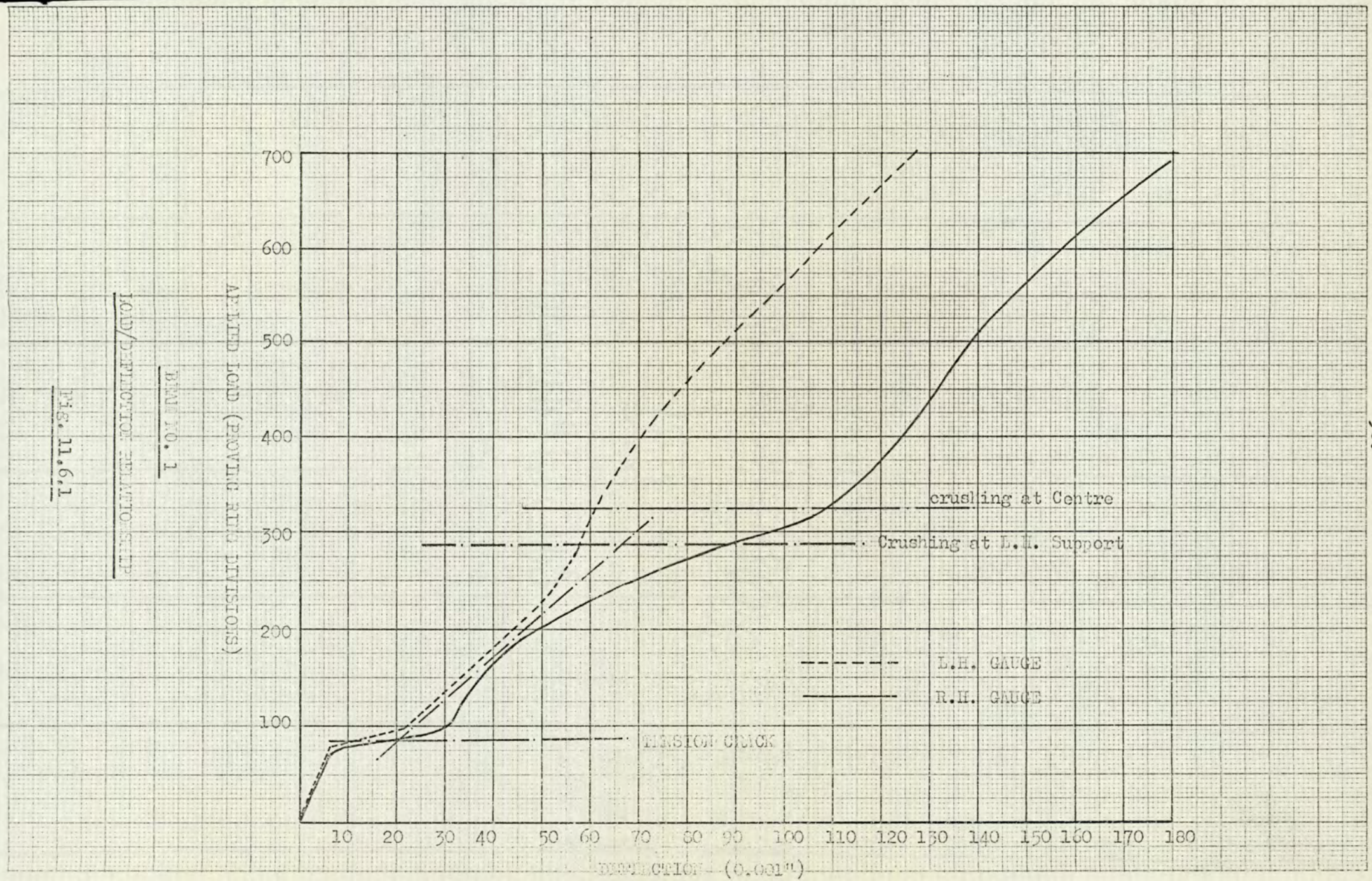

BEAM NO. 1

LOAD/DEFLECTION RELATIONSHIP

Fig. 11.6.1

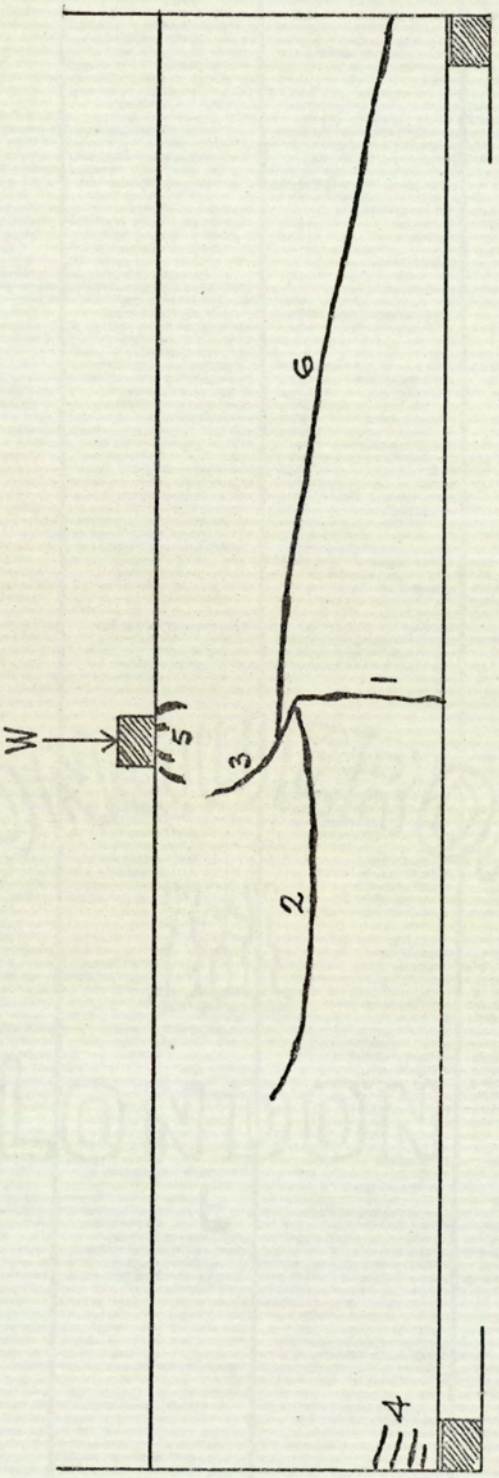

BEAM NO.1

FAILURE PATTERN

Fig. 11.6.2

BEAM NO.2

APPLIED LOAD (PROVING RING DIVS)	DEFLECTION (0.001")	
	L.H.GAUGE	R.H.GAUGE
10	2.25	0.5
20	2.75	1
30	3.25	2
40	5	2
50	5.5	3
60	5.75	3
70	6.25	4
80	20.5	20
90	23.25	23
100	25.5	26
125	32.25	33
150	39	40
175	45	46.5
200	70	54
225	75.5	60
250	81.5	66
275	87.5	72
300	94	78
350	106	91
400	120	105
450	132.5	117
500	100.5	135
550	173	164

TABLE NO. 11.6.4

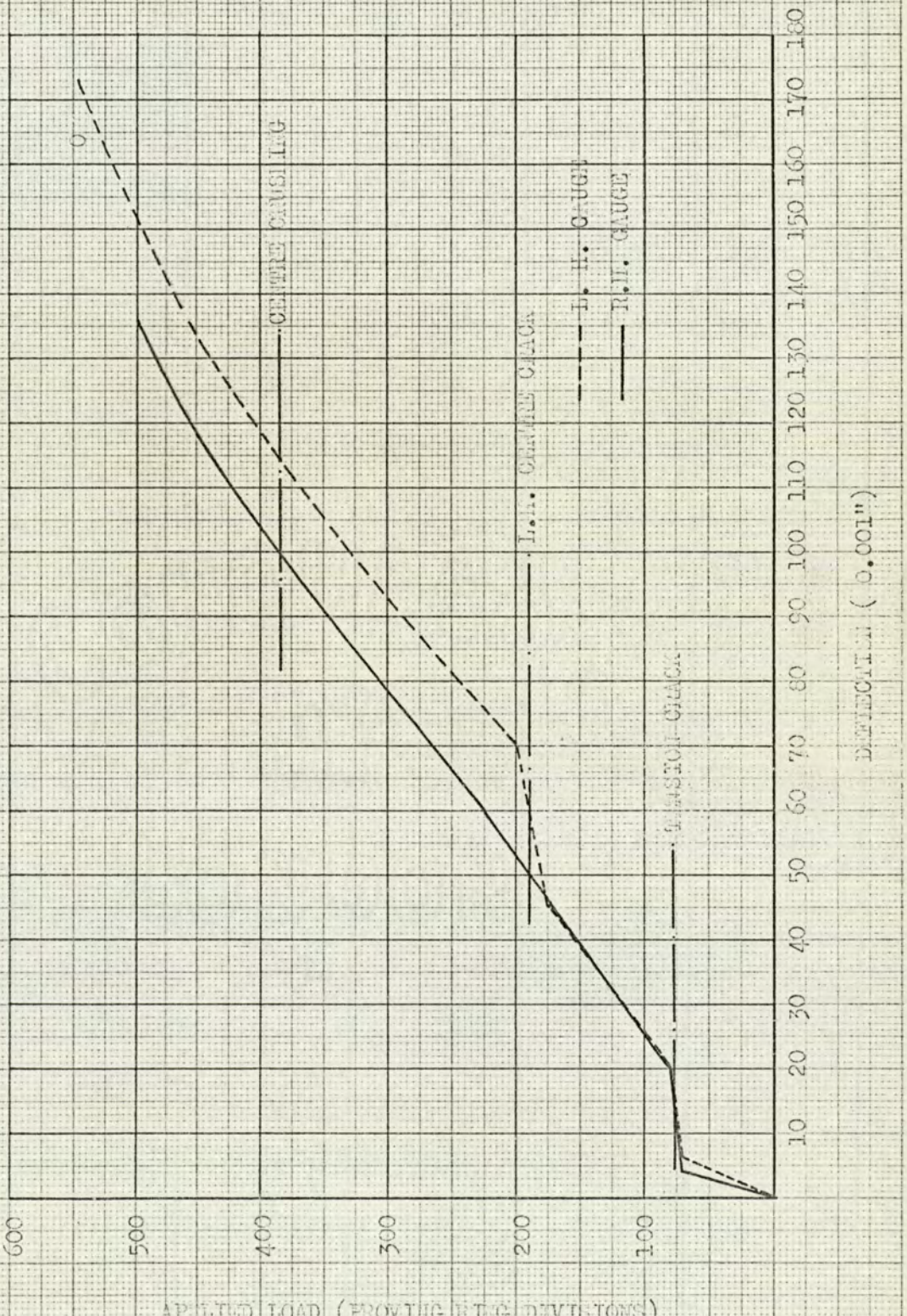

BEAM NO. 2

LOAD/DEFLECTION RELATIONSHIP

Fig. 11.6.3

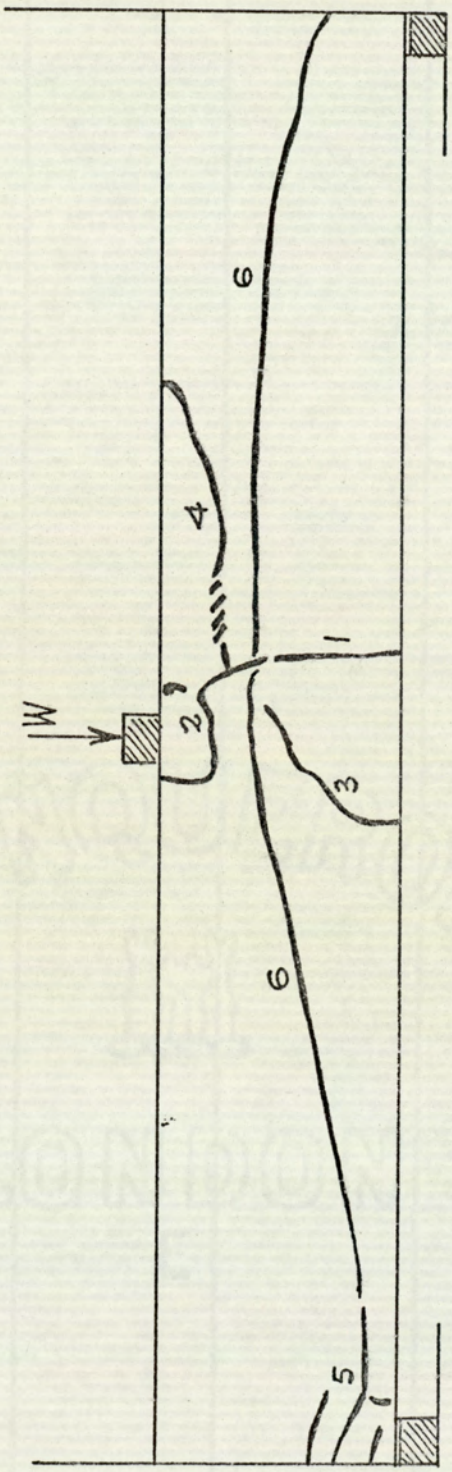

Beam No 2

FAILURE PATTERN

Fig 11. 6. 4.

BEAM NO.3

APPLIED LOAD (PROVING RING DIVS)	DEFLECTION (0.001")	
	L.H.GAUGE	R.H.GAUGE
10	4	4
20	5.5	6
30	6.5	7
40	7.5	8
50	23.5	29
60	34	40.5
70	38.5	45
80	42.5	49.5
90	47.5	54.5
100	52.5	59
125	62.5	69
150	72.5	80
175	82.5	91
200	93.5	102.5
225	104	114
250	113.5	123
275	125.5	137
300	138.5	151
325	151.5	163
350	167.5	179
375	188.5	200
400	237.5	242

TABLE NO. 11.6.5

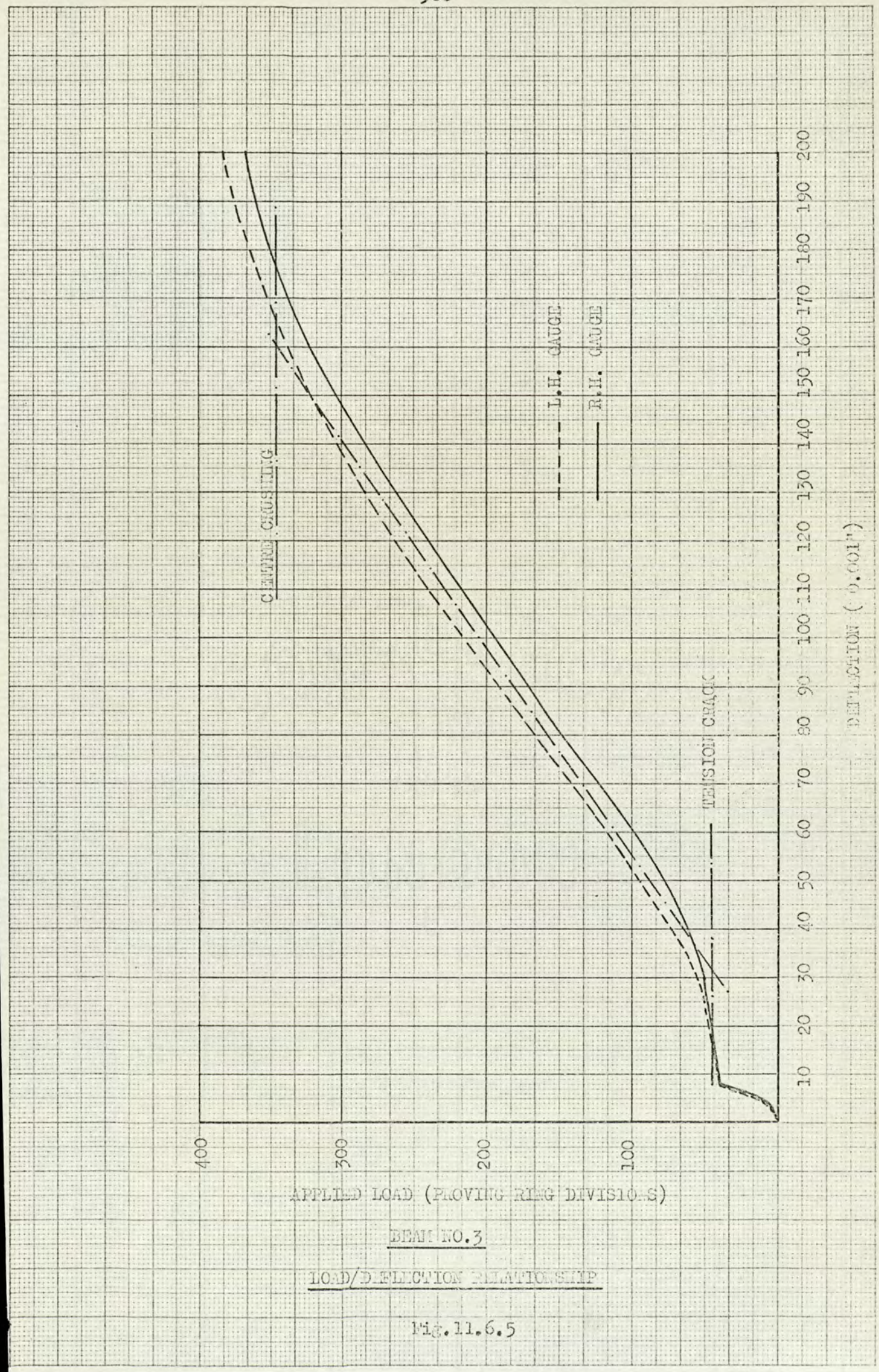

BEAM NO.3

LOAD/DEFLECTION RELATIONSHIP

Fig.11.6.5

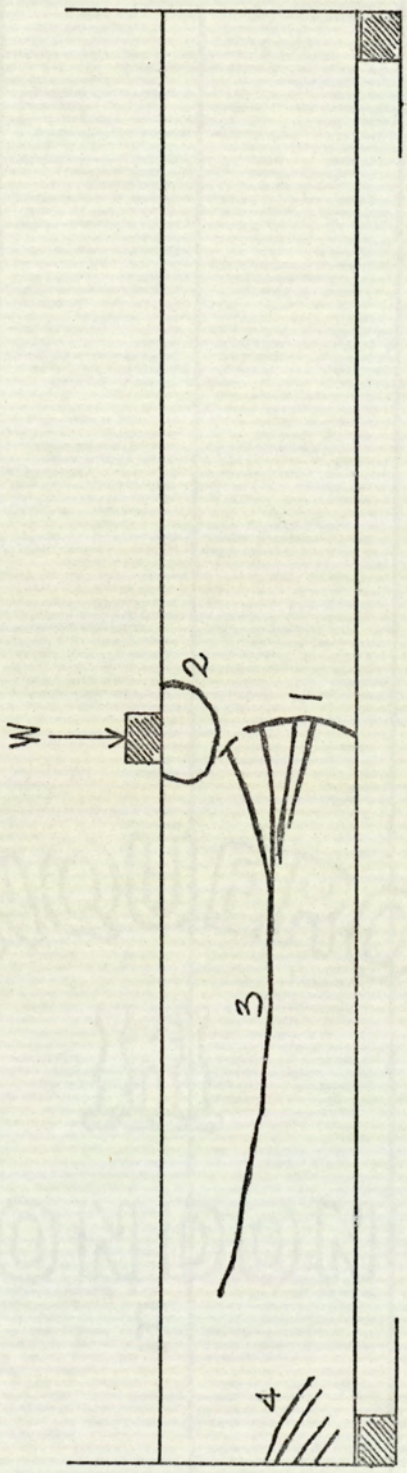

BEAM NO.3

FAILURE PATTERN

Fig.11.6.6

BEAM NO.4

APPLIED LOAD (PROVING RING DIVS)	DEFLECTION (0.001")	
	L.H.GAUGE	R.H.GAUGE
10	6	6
20	16	17
30	23	21
40	32	30
50	40	40
60	47	48
70	55	56
80	68	68
90	78	79
100	82	81
110	95	98
120	106	125
130	118	142
140	136	159
150	146	187
160	161	205
170	174	223
180	191	238

TABLE NO. 11.6.6

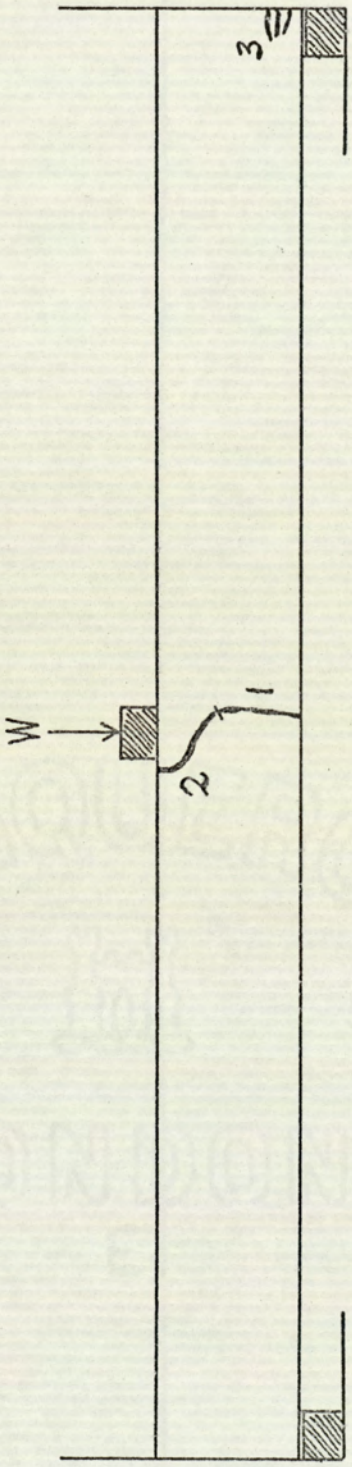

BEAM No.4

FAILURE PATTERN

Fig. 11.6.8

BEAM NO.5

APPLIED LOAD (PROVING RING DIVS)	DEFLECTION (0.001")	
	L.H.GAUGE	R.H.GAUGE
5	92	97
10	122	117
15	144	152
20	185	176
25	218	212
30	248	232
35	274	268
40	298	305
45	338	334

TABLE NO. 11.6.7

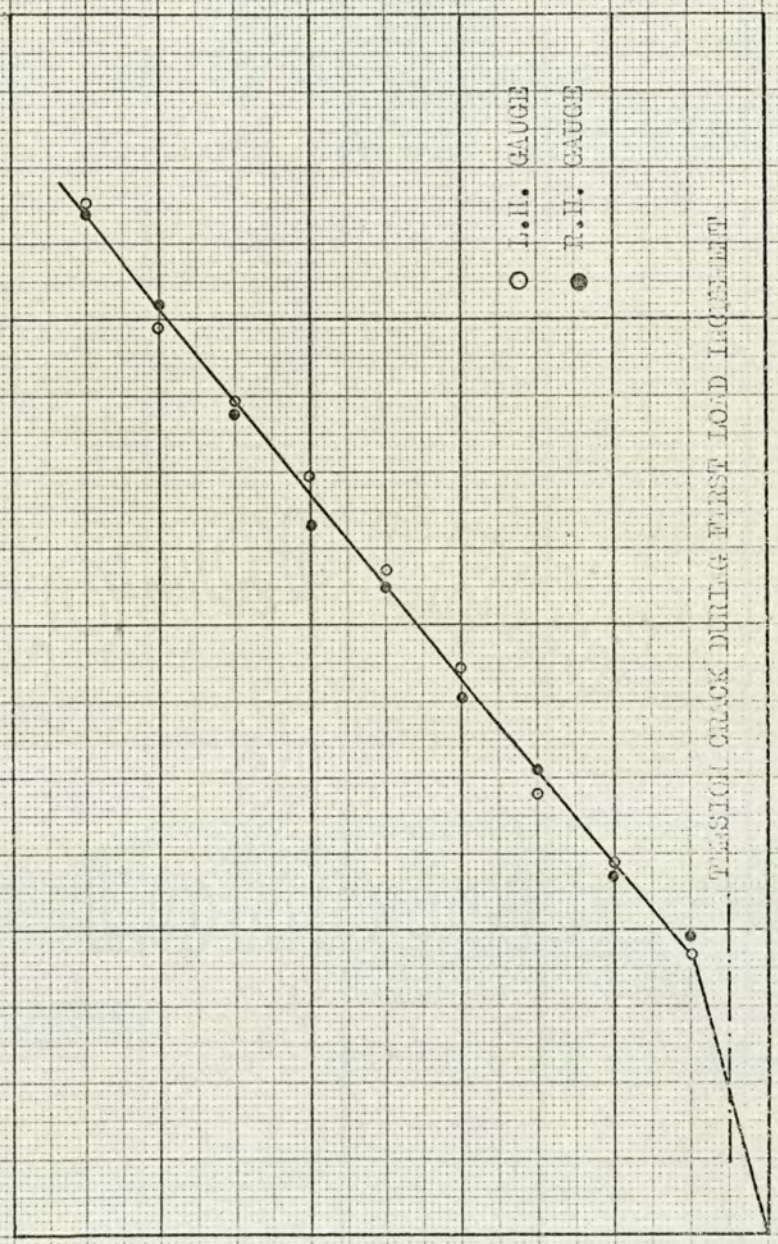

BEAM NO.5

LOAD/DEFLECTION RELATIONSHIP

Fig.11.6.9

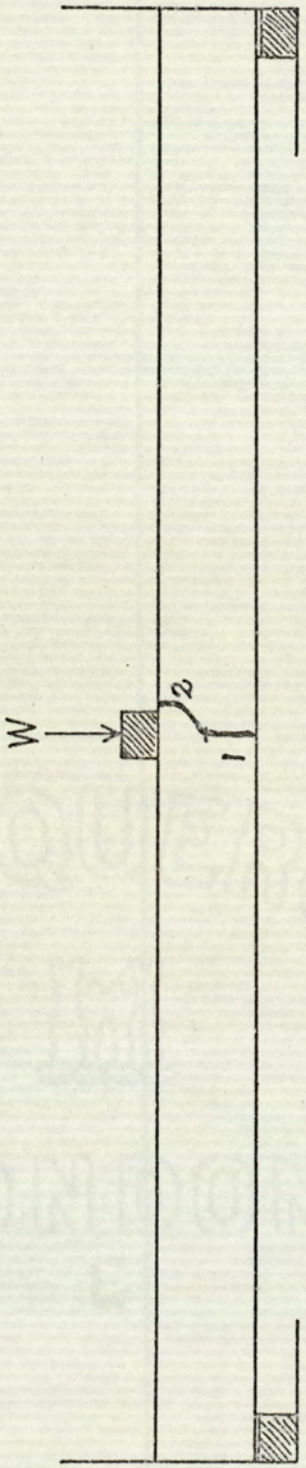

BEAM NO.5

FAILURE PATTERN

Fig.11.6.10

BEAM NO.6

APPLIED LOAD (PROVING RING DIVS)	DEFLECTION (0.001")	
	L.H.GAUGE	R.H.GAUGE
10	1	1
20	2	1.5
30	2.5	2.5
40	3	3
50	4	4
60	6	7
70	10	10
80	15	14
90	19	18
100	25	25
125	34	34
150	43	42
175	56	66
200	63	73
225	72	83
250	82	93
275	94	104
300	110	119
350	137	148
400	186	254

TABLE NO. 11.6.8

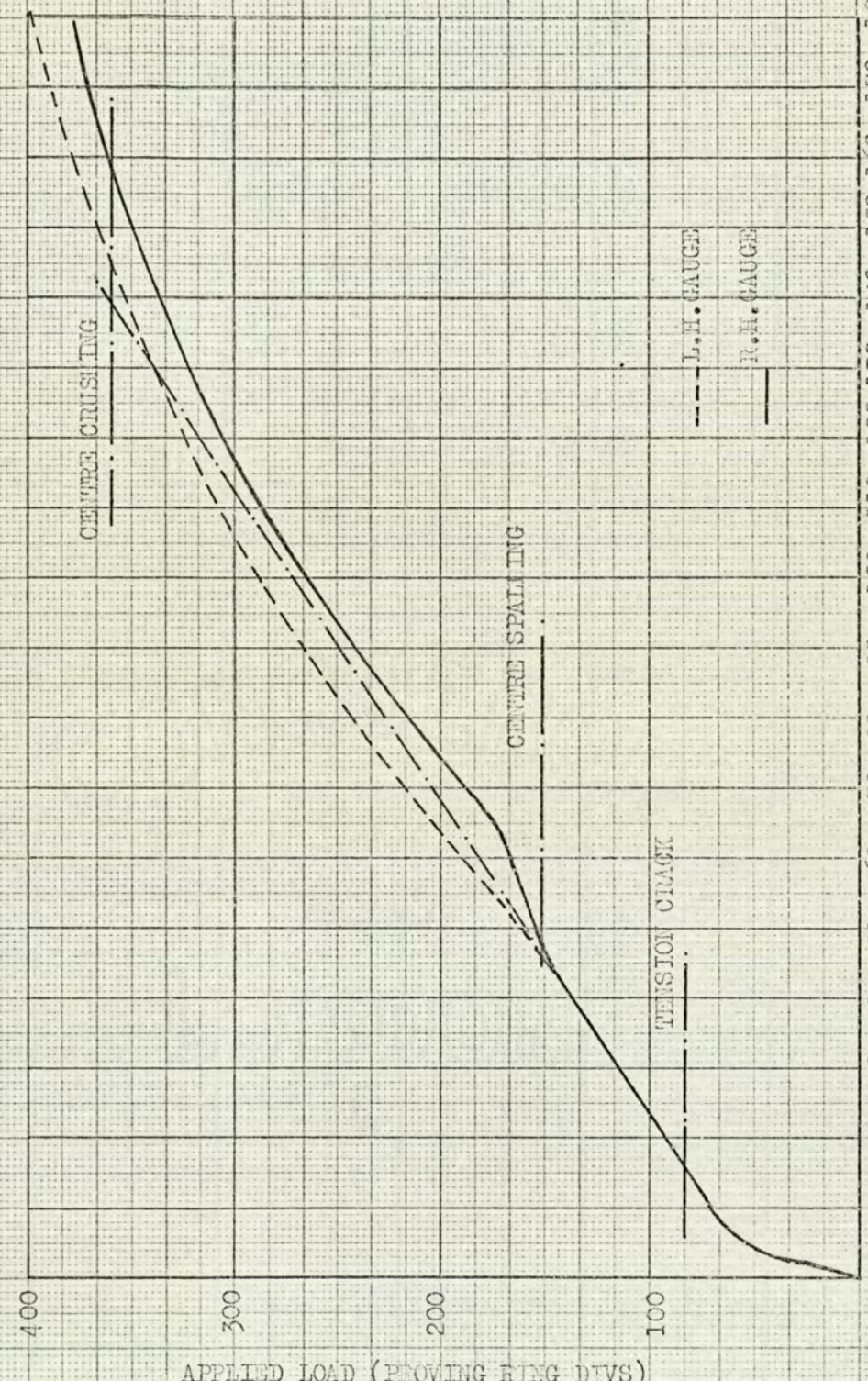

BEAM NO.6

LOAD/DEFLECTION RELATIONSHIP

Fig. 11.6.11

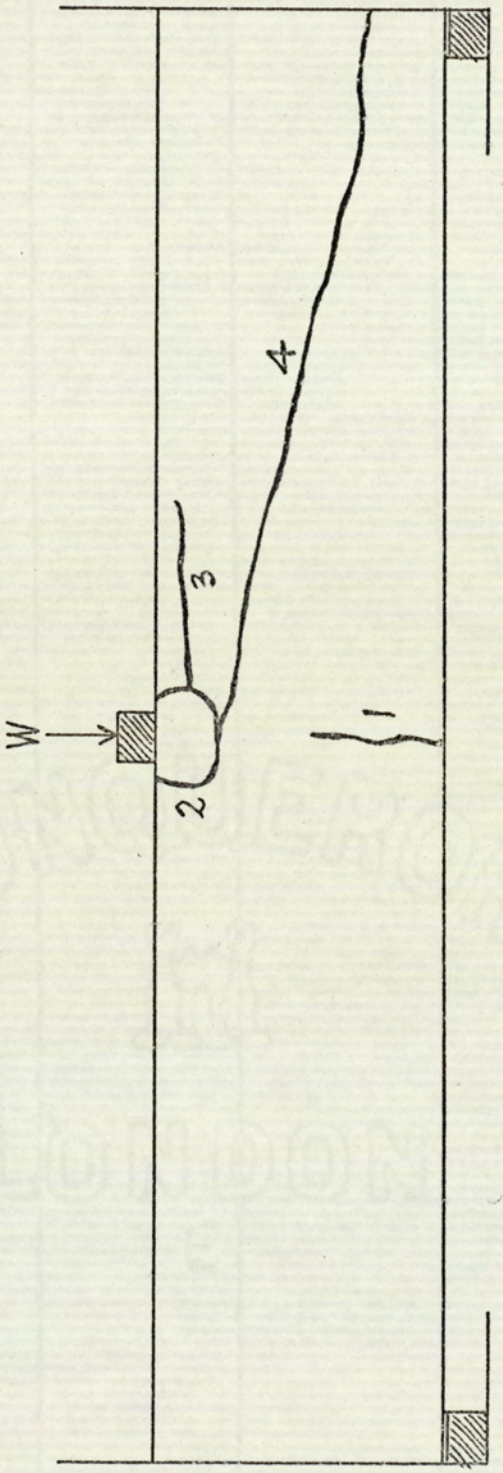

BEAM NO.6

FAILURE PATTERN

Fig.11.6.12

BEAM NO.7

APPLIED LOAD (PROVING RING DIVS)	DEFLECTION (0.001")	
	L.H.GAUGE	R.H.GAUGE
10	2	2
20	3	3
30	4	4
40	6	5
50	14	14
60	20	20
70	27	27
80	35	34
90	41	41
100	48	47
125	60	60
150	70	73
175	73	88
200	84	105
225	95	120
250	110	139
275	140	175

TABLE NO. 11.6.9

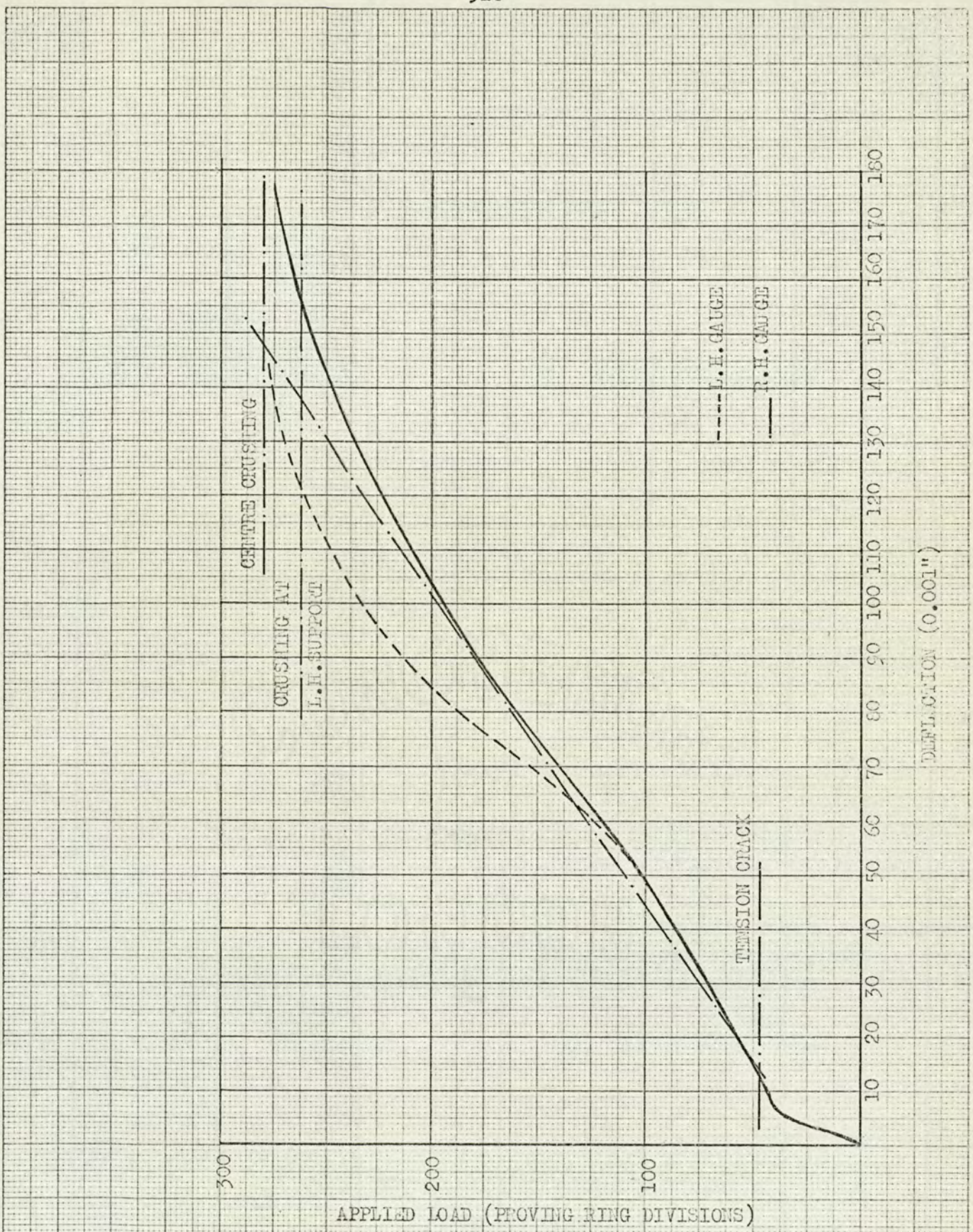

BEAM NO.7

LOAD/DEFLECTION RELATIONSHIP

Fig.11.6.13

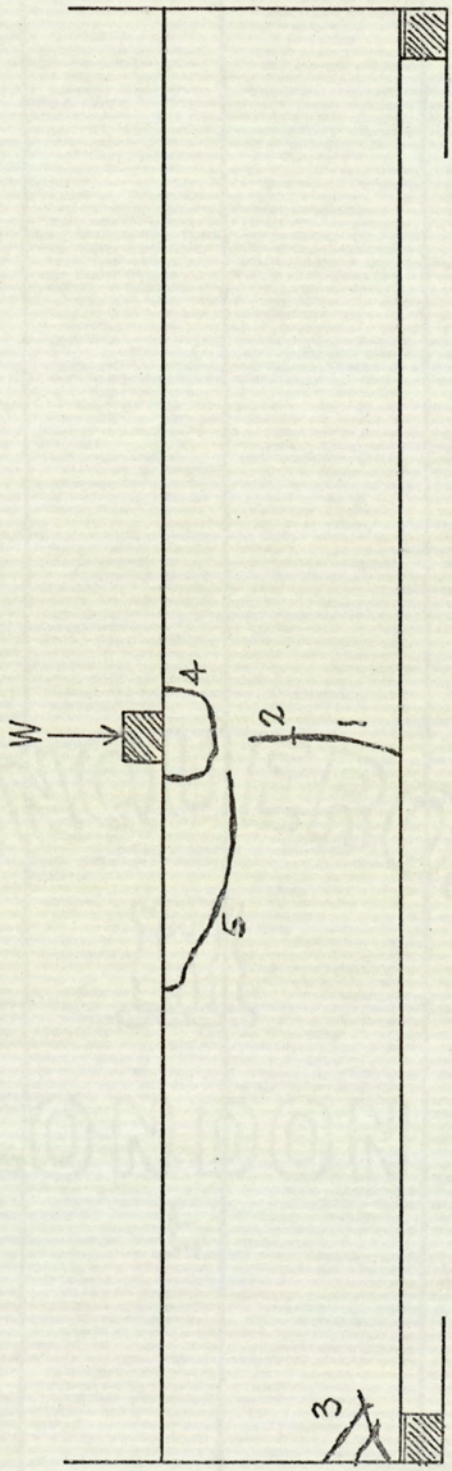

BEAM NO.7

FAILURE PATTERN

Fig.11.6.14

BEAM NO.8

APPLIED LOAD (PROVING RING DIVS)	DEFLECTION (0.001")	
	L.H.GAUGE	R.H.GAUGE
10	5	5
20	7	7
30	9	9
40	11	11
50	20	21
60	30	31
70	39	40
80	50	52
90	63	63
100	75	76
110	88	88
120	101	101
130	115	115
140	134	133
150	156	157
160	185	184
170	204	201

TABLE NO. 11.6.10

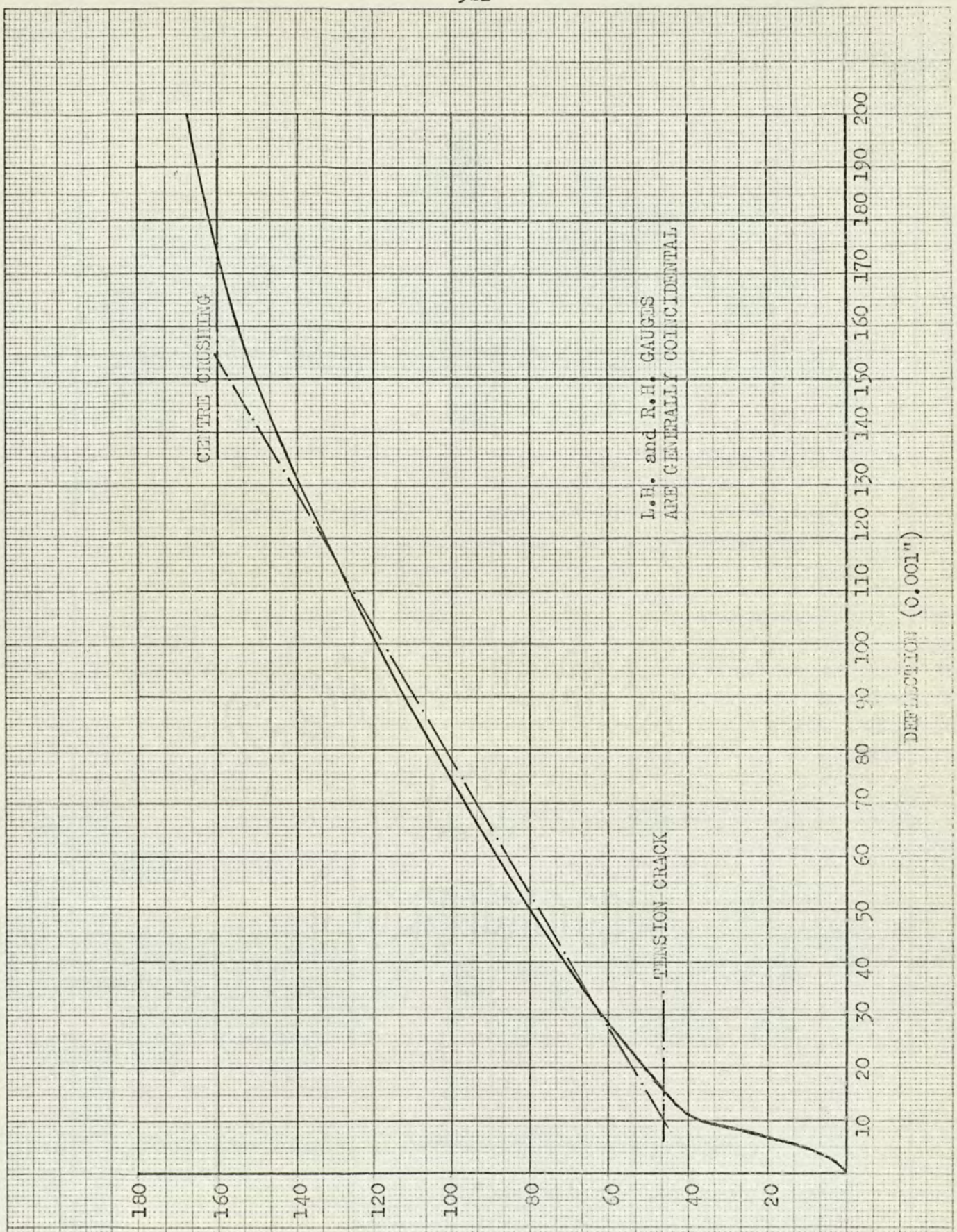

BEAM NO.8

LOAD/DEFLECTION RELATIONSHIP

Fig.11.6.15

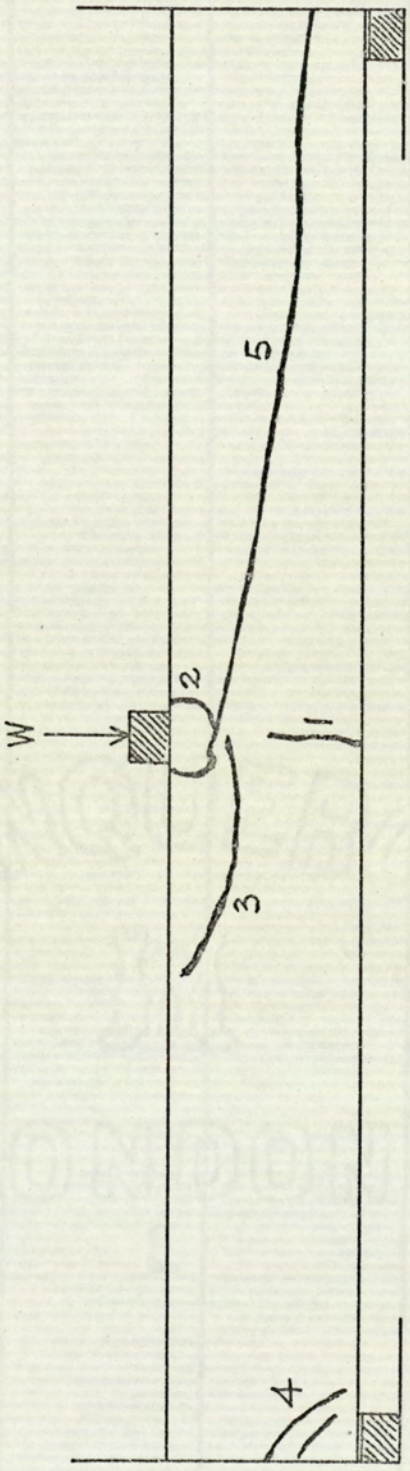

BEAM NO.8

FAILURE PATTERN

Fig. 11.6.16

BEAM NO.9

APPLIED LOAD (PROVING RING DIVS)	DEFLECTION (0.001")	
	L.H.GAUGE	R.H.GAUGE
10	19	19
20	54	56
30	78	83
40	104	108
50	138	141
60	174	178
70	287	221

TABLE NO.11.6.11

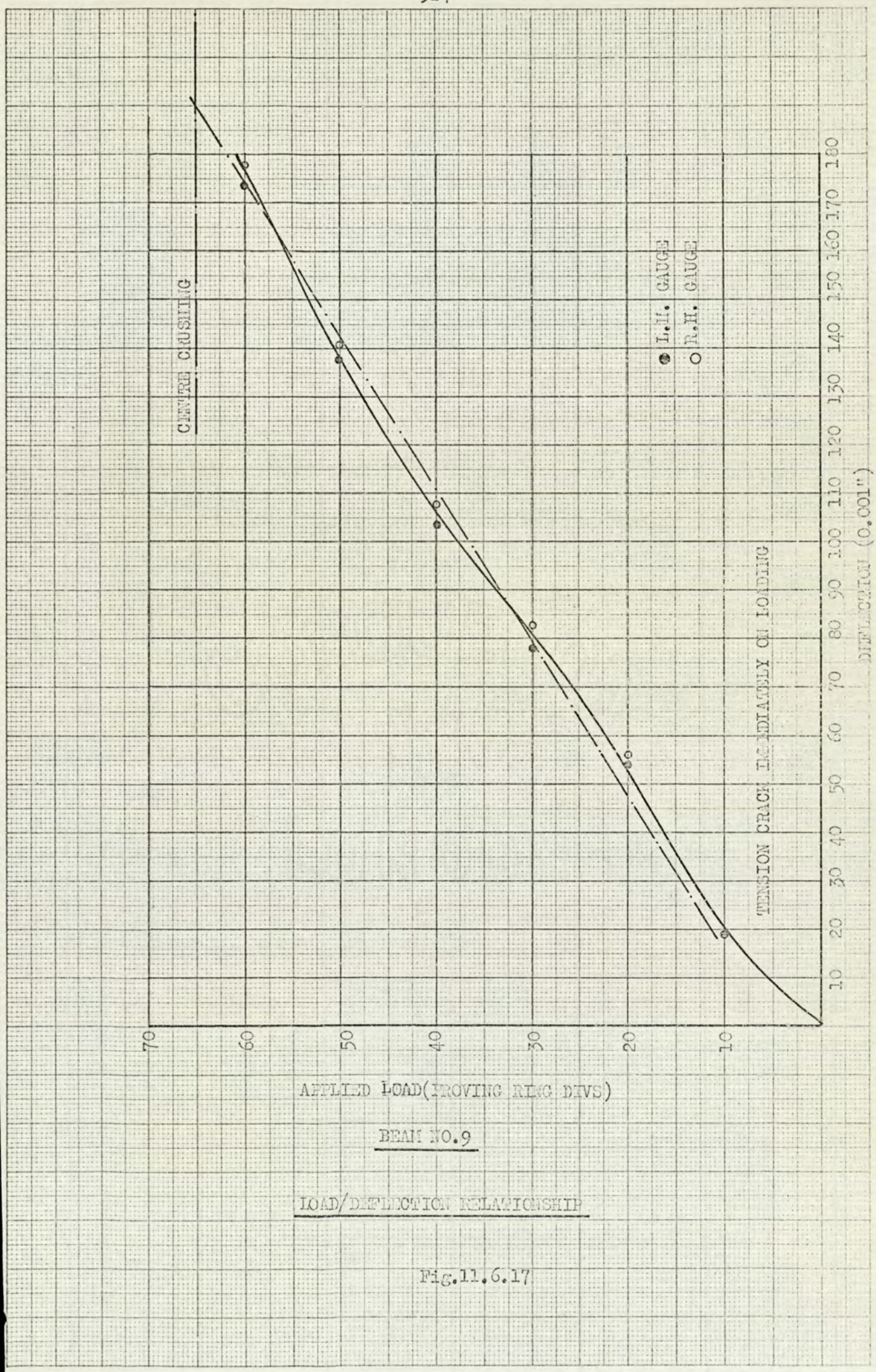

BEAM NO.9

LOAD/DEFLECTION RELATIONSHIP

Fig.11.6.17

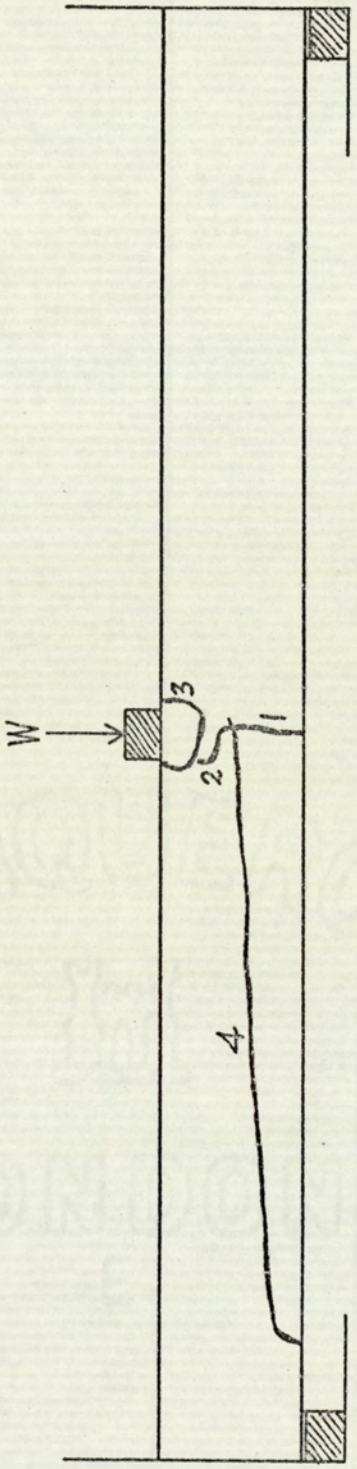

BEAM NO.9

FAILURE PATTERN

Fig.11.6.18

11.7 Interpretation of Test Results

1) UP TO FIRST TENSION CRACK

The conditions of loading and support are considered to be approximate to those of a fixed end beam supporting a point load (W lb) at mid span. On thi s basis the bending moment at mid-span for a beam 30" long is given by:-

$$M = \frac{15\,W}{4} \quad \text{lb ins} \qquad [21]$$

For a beam 8" wide and depth (D) the section modulus is:-

$$Z = \frac{4\,D^2}{3} \quad \text{in}^3 \qquad [22]$$

From an observation of the applied load (W) causing the first tension crack the apparent stress at first cracking is calculated from:-

$$f_{bt} = \frac{45}{16} \cdot \frac{W}{D^2} \quad \text{lb/in}^2 \qquad [23]$$

2) POST TENSION CRACK CONDITION

Considering a point load of W per unit thickness applied at the centre of the beam

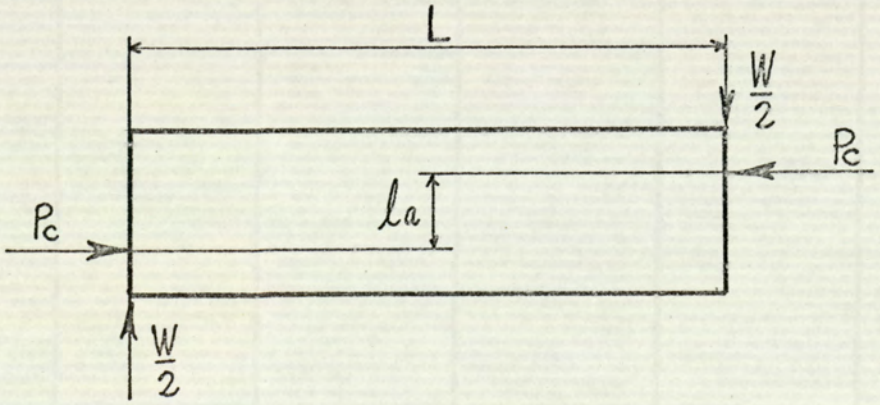

By simple moments, $\frac{WL}{2} = Pc.\,la$

Eqns [9] and [10] will therefore remain valid for this experimental loading condition.

From Fig. 11.3 the vertical deflection at the top of the beam at mid-span is given by:-

$$d = 2a\left(1 - \frac{1}{\cos\theta}\right) + L\tan\theta \qquad [24]$$

For small angles when θ is measured in radians and L = 15", Eqn [24] can be written:-

$$d = 15\theta \qquad [25]$$

On the load deflection curve for each beam, a mean straight line is drawn to give the linear relationship of deflection to applied load for the stage between the development of the initial tension crack and the first crus hing of the beam.

From this straight line and substituting for $d = 15\theta$ from Eqn [25], θ is calculated in terms of W and hence $\propto$L is determined in terms of W.

The applied loads producing the first tension crack, first signs of crushing and final collapse are given in Table No. 11.6.12.

For each specimen beam the load to cause first crushing and the angular rotation related to this load is used by substitution in Eqn [12] to calculate the apparent crushing stress at failure.

The results of these calculations are shown in Table No. 11.6.13.

	APPLIED LOAD (W lb)		
BEAM NO.	TENSION CRACK	CRUSHING	COLLAPSE
1	1590	5360	16152
2	1416	7214	12354
3	944	6581	7894
4	661	2455	3774
5	-	887	HINGE
6	1590	6766	9392
7	906	5171	HINGE
8	944	3019	HINGE
9	-	1228	HINGE

TABLE NO. 11.6.12

BEAM NO. 1

FROM EQN [23]

$$f_{bt} = \frac{45}{16} \times \frac{1590}{36} = 124.22 \text{ lb/in}^2$$

FROM Fig.11.6.1

$$\frac{W}{d} = \frac{3660}{0.047 \times 8} = 9734 \text{ per UNIT THICKNESS}$$

FROM EQN [25] $d = 15\theta$

$$\therefore \theta = \frac{W}{15 \times 9734} = \frac{W}{146010} \quad \text{(W per UNIT BEAM THICKNESS)}$$

FROM EQN [10]

$$\alpha L = 3\theta = 20.55 \times 10^{-6} W \quad \text{(W per UNIT THICKNESS)}$$

FROM EQN [12]

$$f_c = \frac{5360}{8 \times 3(0.27 - \frac{5360}{8 \times 146010})} = 843 \text{ lb/in}^2$$

The calculation presented here for Beam No. 1 gives the method of calculation used for an analysis of the test results.
Calculations for Beams No. 2 - 9. inclusive were carried out by the same method, the results of these calculations although not presented in detail are tabulated in Table No. 11.6.13.

				W lb per unit thickness			
BEAM NO.	R	a(ins)	W/d (per unit thickness)	Θ(rads)	$\propto$ L	fbt(lb/in^2)	fc(lb/in^2)
1	5	3	9734	$\frac{W}{146010}$	$20.55 \times 10^{-6}W$	124.22	843
2	6	2½	8320	$\frac{W}{124800}$	$20.03 \times 10^{-6}W$	159.30	1693
3	7.5	2	5453	$\frac{W}{81795}$	$24.45 \times 10^{-6}W$	165.94	2419
4	10	1½	2951	$\frac{W}{44265}$	$33.89 \times 10^{-6}W$	206.56	1663
5	15	1	394	$\frac{W}{5910}$	$169.2 \times 10^{-6}W$	-	1562
6	5	3	5268	$\frac{W}{79020}$	$37.97 \times 10^{-6}W$	124.22	1088
7	6	2½	4063	$\frac{W}{60945}$	$41.02 \times 10^{-6}W$	101.93	1237
8	7.5	2	1895	$\frac{W}{28425}$	$70.36 \times 10^{-6}W$	165.94	1130
9	10	1½	743	$\frac{W}{11145}$	$134.59 \times 10^{-6}W$	-	882

TABLE NO. 11.6.13

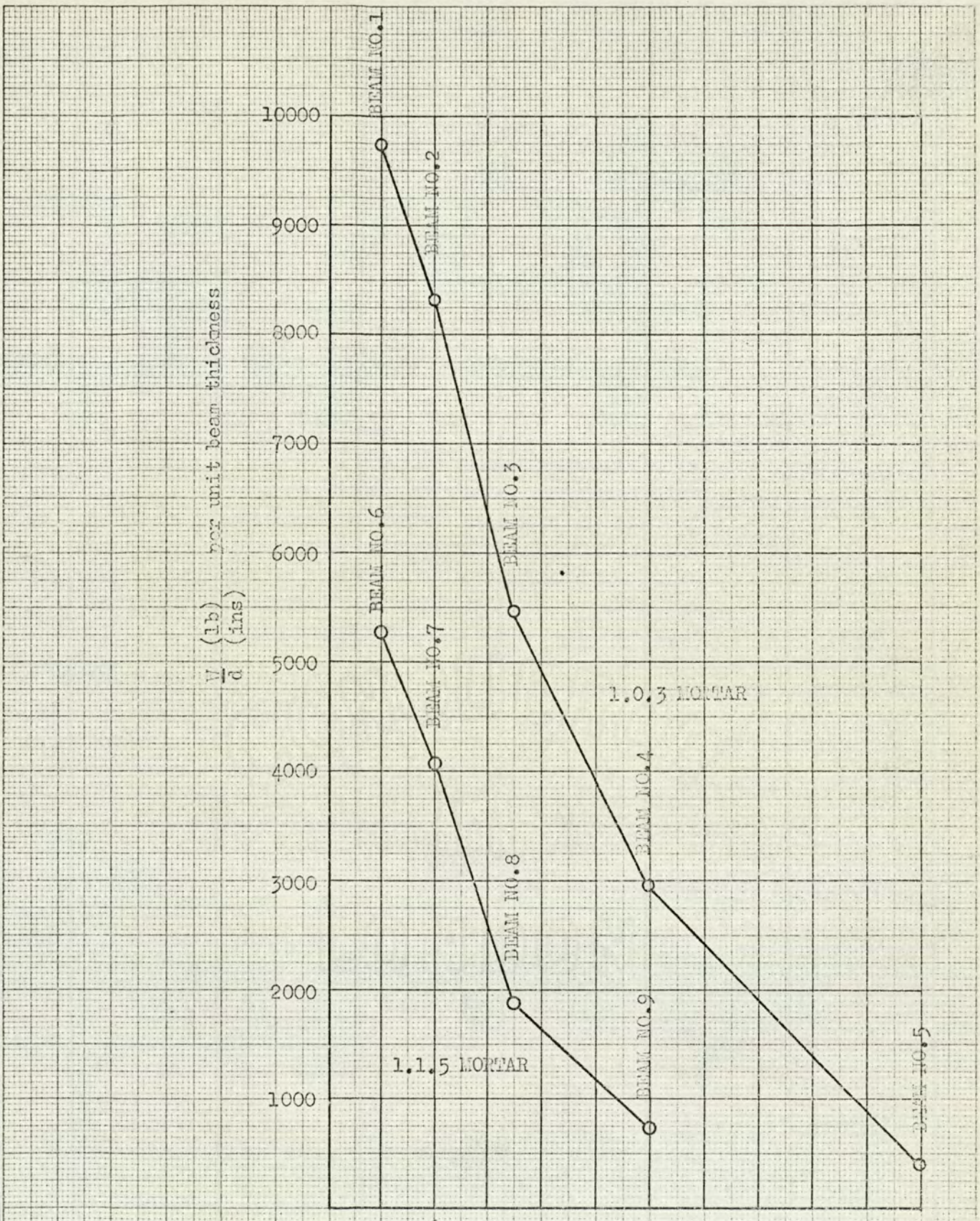

EXPERIMENTAL RELATIONSHIP

LOAD / DEFLECTION TO SPAN / DEPTH

Fig.11.6.19

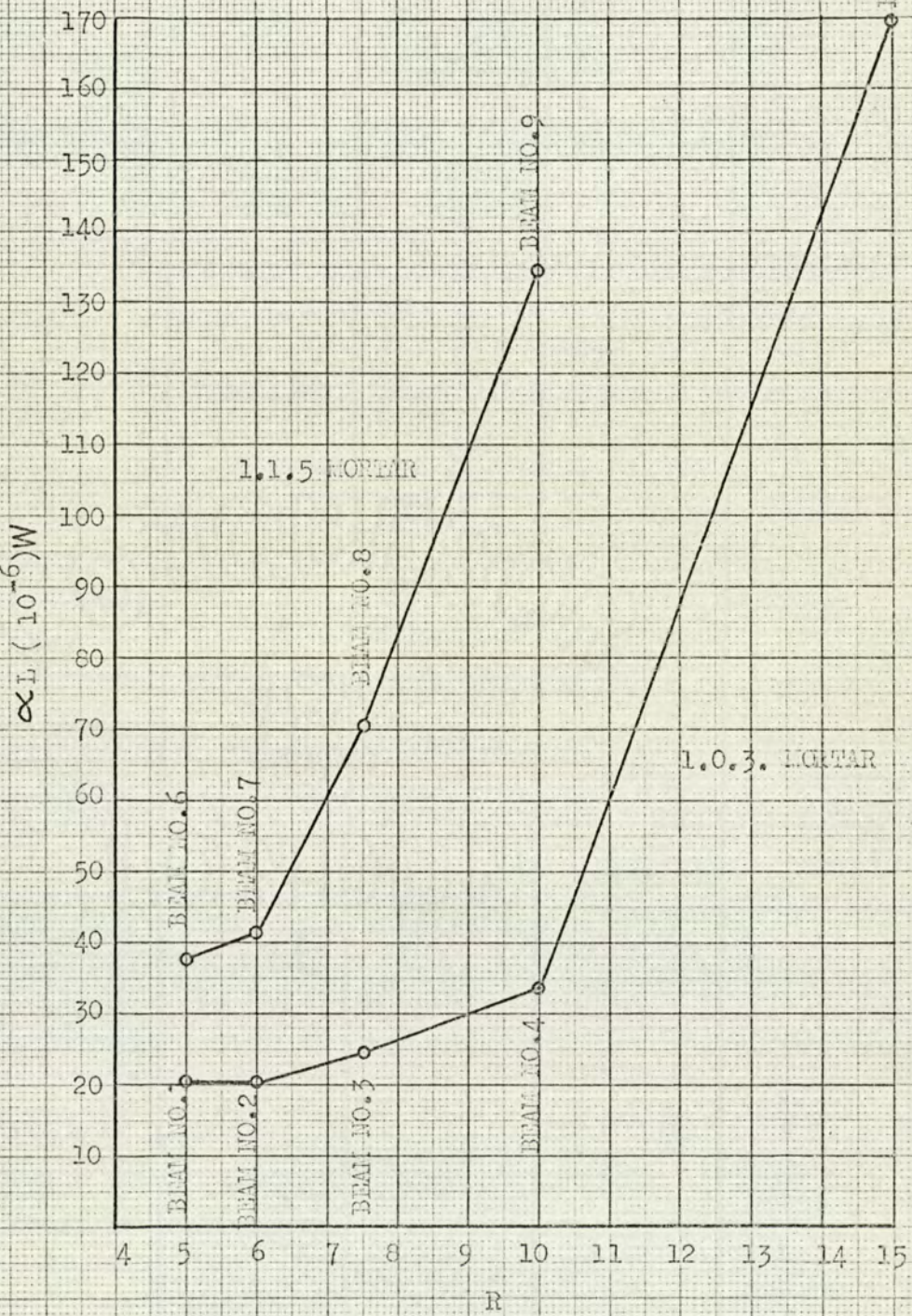

EXPERIMENTAL RELATIONSHIP OF α_L TO R

Fig.11.6.20

BEAM NO.1 (6" Deep: 1.0.3. Mix)

The first cycle loading produced the initial tension crack (Plate No. 11.6.3.) which travelled from the bottom face of the beam vertically to a point almost exactly on the centre line of the beam at the mid-span position.

Fig.11.6.1. showing the load/deflection relationship indicates a linear behaviour up to the first tension crack. Subsequent applied loads produced a widely differing deflection characteristic on either side of the loading point, although in general terms the LH gauge indicated a linear load/deflection relationship between first tension crack and first crushing. During this stage of loading there was no visual damage at the loading point. It must therefore be assumed that some internal weakness existed.

Fig.11.6.2. diagramatically shows the crack failure pattern, cracks are numbered in the order in which they developed.

For this beam, a video tape recording was made during the loading cycles, it is therefore possible to follow the development of the failure cracks very precisely.

Crack No. 2 develops fairly quickly and then remains stationary, Crack No. 3 which is the developing tension crack does not rise vertically but travels around the zone of high compression from the

applied point load. This is followed by crushing at the LH support and then by crushing at the centre of the beam, this is considered to be the elastic failure of the beam and at this stage the applied load was 5360 lb.

The beam did not however collapse at this load and in fact went on to support a load of 16152 lb which is some three times the load to cause crushing before the beam finally collapsed. The beam in the collapsed condition is shown in Plate No.11.6.4. Collapse was sudden and produced an interesting mode of failure.

Crushing of the beam material was not sufficient to allow a hinge to develop at the centre of the beam before a longitudinal tension failure (Crack No.6) occurred, generating from the RH support and progressing towards the centre of the beam. Ultimate failure of the specimen was therefore the result of a longitudinal tension fracture clearly brought about by what must have been the very high magnitude of the arch thrust forces.

BEAM NO.2 (5" Deep: 1.0.3. Mix)

The load/deflection curve for the RH gauge plotted in Fig.11.6.3. shows what may be considered to be the classical behaviour for the tests of this programme. Initial loading produces a linear relationship up to the first tension crack which results in a sudden deflection, from the tension crack to centre crushing again a linear relationship is indicated and then on a non-linear curve to failure.

The effect of the left hand centre crack is shown in the plot for the LH gauge, a sudden deflection takes place and is followed again by a linear relationship up to the stage of crushing which occurred at an applied load of 7214 lb.

The crack failure pattern and sequence, Fig.11.6.4. shows that the initial tension crack did not occur in the centre of the beam as would normally be predicted; this crack (2) progressed fairly rapidly through the depth of the beam and travelled round the zone of high compression to the top face. Crack No. (3) developed from the bottom face of the beam and as such must have been a secondary tension crack. The local tension crack (4) was followed by crushing at the LH support (5).

The condition of the beam at this point is shown in Plate No. 11.6.5.

The load was then increased to 12354 lb at which point failure occurred in the same mode as Beam No. 1. The longitudinal tension cracks (6) occurred simultaneously and finally the specimen collapsed as shown in Plate No. 11.6.6.

BEAM NO. 3 (4" Deep: 1.0.3.Mix)

Fig.11.6.5. further illustrates what can now be predicted to be the typical load/deflection curve.

The sequence of cracking and failure pattern reproduced in Fig.11.6.6. is interesting since this beam had a mode of failure different to that of Beam No. 1 and 2. The initial tension crack (1) again progressed through the depth of the beam avoiding the high compression zone (2). At an applied load of 6581 lb, at which centre crushing took place

only cracks No. 1 and 2 existed, from this load to the collapse load of 7894 lb the longitudinal cracks (3) and end crushing (4) occurred (see Plate No. 11.6.7).

Without the application of a further increase in load the hydraulic jack was extended to impose a further deflection on the beam, this resulted in a complete crushing of the fan shaped longitudinal fractures (3) thus permitting a central hinge to develop with the consequent collapse of the beam.

BEAM NO.4 (3" deep: 1.0.3. Mix)

The initial tension crack occurred immediately on loading, thereafter the load/deflection relationship remained linear up to a point just before centre crushing took place at an applied load of 2455 lb. At this stage, the tension crack had again progressed through the beam avoiding the zone of a high compression beneath the point load. The load was then increased to 3774 lb when complete crushing at the centre of the beam allowed a hinge to form and the specimen to collapse.

BEAM NO.5 (2" Deep: 1.0.3. Mix)

This beam behaved almost exactly in the manner of Beam No.4 up to centre crushing at an appli ed load of 887 lb, however the beam was incapable of resisting a further increase in applied load and a hinge mechanism of failure immediately occurred.

BEAM NO.6 (6" Deep: 1.1.5 Mix)

The load/deflection relationship shown in Fig.11.6.11. differs from that for Beam No. 1 which was of the same span/depth ratio in that the pre-tension crack part of the curve exhibits a non-linear

relationship and that there was no sudden increase in deflection when the tension crack occurred. This suggests that the crack must have developed slowly and probably commenced at a comparatively low value of applied load. Thereafter, the load/deflection relationship is of a linear form with interuptions after centre spalling had been observed.

The failure pattern (Fig.11.6.12) should be particularly noted for in this instance the tension crack (1) did not progress into the line of crushing failure (2) as had been observed in previous tests.

Centre crushing was observed at an appliedload of 6766 lb.

After a further increase in load the longitudinal fracture line (3) immediately preceded the collapse failure line (4) at an applied load of 9392 lb.

This mode of failure is similar to Beams Nos. 1 and 2 and again is the result of the large thrust forces set up by the arching action.

BEAM NO.7 (5" Deep: 1.1.5. Mix)

Fig.11.6.13 shows that in a similar manner to Beam No.6 the pre-tension crack behaviour is non-linear and there was no sudden increase in deflection at cracking. The non-linear characteristics of the load/deflection curve between cracking and observed crushing suggest that the first crushing of the material was not observed during the experiment and that a major crushing failure was observed and recorded.

The failure pattern of Fig.11.6.14 shows that again the tension crack did not progress through the beam, the first crushing observed was at the LH support (3) at an applied load of 5171 lb. This was followed by centre crushing and the progression of the longitudinal crack (5).

In this instance the longitudinal crack did not reach some position and remain stationary as had previously been experienced, but it progressed through to the top face of the beam thereby permitting a hinge failure to take place.

BEAM NO.8 (4" Deep: 1.1.5. Mix)

Fig.11.6.15 again shows that for this mortar mix the initial tension crack must progress from the commencement of loading and is probably at first a hair line crack that is difficult to detect during experime nt. The beam exhibits an approximate linear load/deflection relationship for the loading cycle between tension crack and crushing.

The failure sequence and pattern of Fig.11.6.16 indicates once more that the tension crack (1) did not progress very far beyond the centre of the beam, the longitudinal crack (3) terminated before reaching the top face of the beam and elastic failure occurred at an applied load of 3019 lb when crushing occurred at the centre of the beam. Final collapse immediately followed during the next increment of applied load when a longitudinal fracture resulted from the arch thrust forces.

BEAM NO.9 (3" Deep: 1.1.5. Mix)

Fig.11.6.17 suggests that a tension crack occurred immediately upon the application of the load and that the load/deflection relationship was within acceptable limits linear up to the stage of centre crushing at an applied load of 1228 lb.

The tension crack had in this instance progressed during the test into the compression zone at the point of the applied load.

Whilst maintaining the load at the crushing value the specimen crept to failure by a hinge mechanism after the longitudinal crack (4) had reached the bottom face of the beam.

BEAM NO. 1

INITIAL TENSION CRACK

PLATE NO. 11.6.3

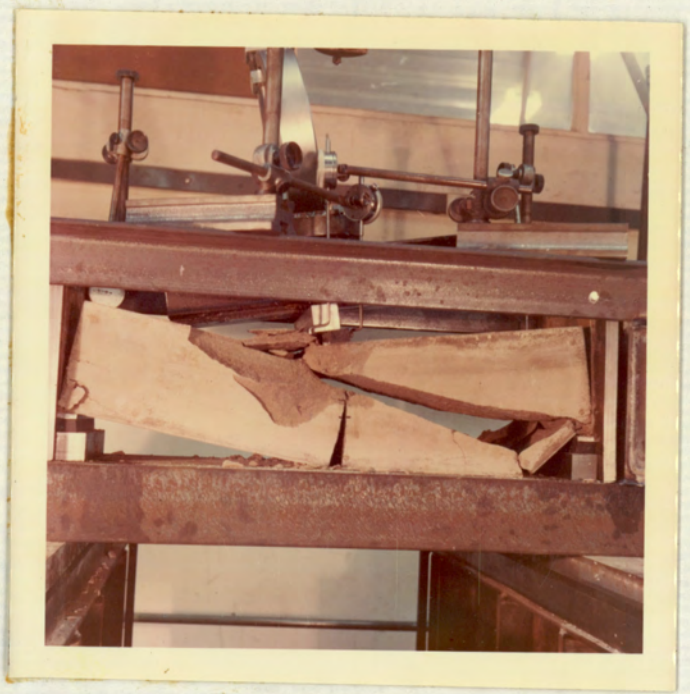

BEAM NO. 1

BEAM AFTER COLLAPSE

PLATE NO. 11.6.4

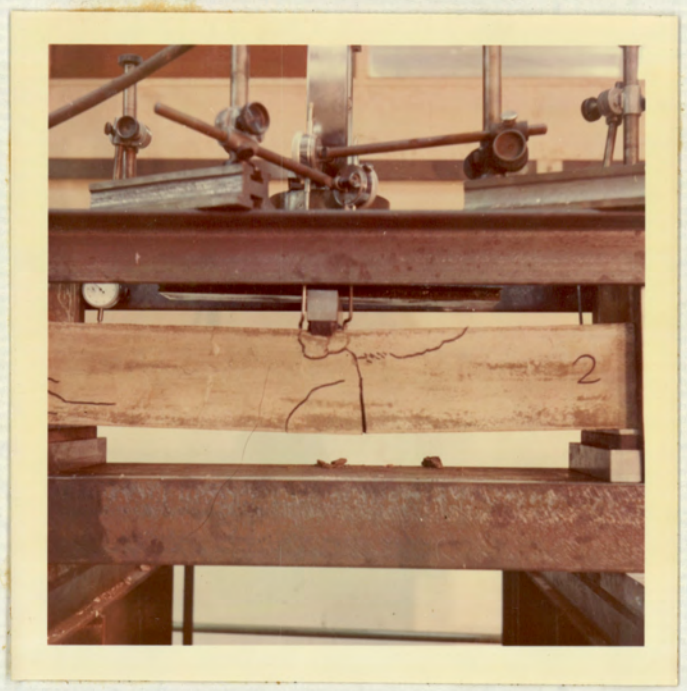

BEAM NO. 2

BEAM AT ELASTIC FAILURE

PLATE NO. 11.6.5

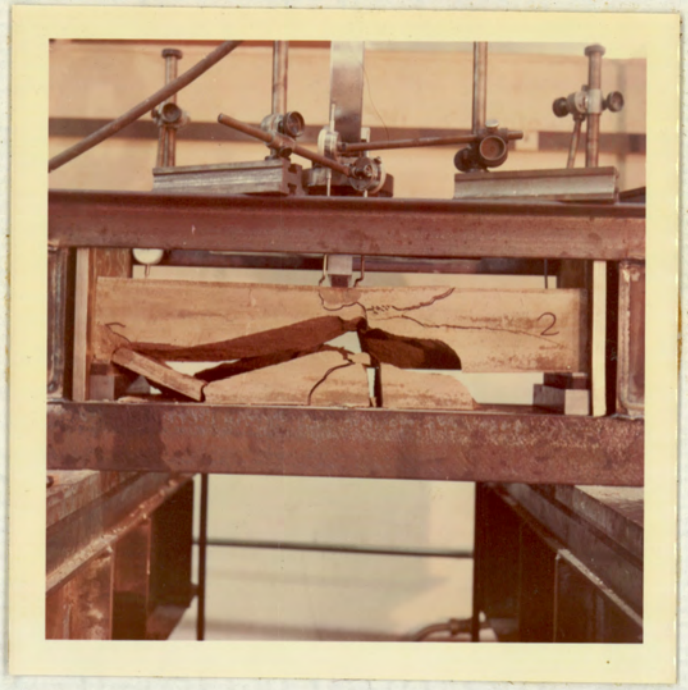

BEAM NO. 2

BEAM AFTER COLLAPSE

PLATE NO. 11.6.6

BEAM NO. 3

BEAM AT ELASTIC FAILURE

PLATE NO.11.6.7

11.8 Conclusions

The experimental work clearly confirms the validity of the theoretical assumed loading cycle.

In the initial stages of loading the specimen behaves in the manner of a fixed end beam for the consideration of stress distribution at the mid-span section, the moment of resistance to the applied bending moment is provided by tensile and c ompressive forces across the section. The calculated values of ultimate flexural tensile strength result in an arithmetic mean of 164 lb/in^2 for 1.0.3. mortar and 130 lb/in^2 for 1.1.5. mortar indicating that for certain span/depth ratios the beams exhibited a fair degree of strength before the initial tension crack occurred.

For the sp ecimens R = 15 (1.0.3. mortar) and R = 10 (1.1.5. mortar) the initial tension crack occurred immediately upon loading, it can therefore be said that these specimens exhibited no tensile strength whatsoever, if the theory presented here was applied to shallow beams perhaps for example in the case of panel walls subject to lateral loads then it would be reasonable to assume that the beam possesses no appreciable tensile strength and that arching action would be operative from the very commencement of loading.

It has been shown in the previous chapter that deep beams subject to vertical loads would, in most practical instances, be capable of providing sufficient tensile strength for the theories of elastic bending to be applicable, however, when the initial tension crack has taken place in a beam that is restrained in the longitudinal direction the work of this chapter suggests that the brickwork beam w ould have such strength as an arch that the value of applied load at ultimate collapse would be more likely to be dependant upon the ability of the supports to provide the lateral restraint than on the physical properties of the brickwork that constitute the beam.

For the range of beams considered here, Eqn [8]could be used to determine the value of the longitudinal restraint force that must be provided by the supports for any given value of applied load. It must be noted that if the theory is used in this way then some modification to the equations would be necessary to include for the deflection characteristics of the support when subject to the horizontal forces imposed by the brickwork arch.
Examples of this application would provide scope for further interesting research, e.g. The specific case of an isolated brick panel built between columns of reinforced concrete, steel or brickwork as part of a framed building, where due to the thrust forces from the arching panel the deflection in the column would vary throughout the length of the Column.

The load/deflection curve for each beam can be idealised to predict a linear relationship from first loading to the initial tension crack at which point there is a magnified deflection as the crack opens, the specimen ceases to act as a beam and then takes on the characteristics of an arch. This is then followed by a linear load/deflection relationship until crushing occurs either at the centre or supports, the relationship then becoming non-linear as progressive crushing through the depth of the compression zone takes place.

Although elastic failure of the beams may be considered to be the point at which first crushing takes place, ultimate collapse was in a number of specimens well in excess of the load at the first observed signs of crushing.

In all cases the initial tension crack extended only to an approximate position at the mid-span depth point of the section, any extension of this crack due to further applied load showed that the fracture line did not travel vertically through the beam but was deflected to take up a course avoiding the zone of high compression beneath the point of application of the applied load. Obviously, at this point there exists a state of complex stress distribution, the distribution of direct vertical stress beneath the loaded area is analogous to the 'bulb of pressure' beneath a foundation, the theory of which is well known. It would not therefore be acceptable to apply the theoretical equations to the ultimate load conditions of the beams without some reservations, since the constituent materials of brickwork possess very definite non-linear stress/strain characteristics.

However, for comparison, the ultimate crushing stress values given in Table No. 11.6.12. have been calculated from Eqn [12] which is of course based upon an elastic analysis. These values can be concluded to give the theoretical value of longitudinal stress due to the thrust forces, if the value of the maximum principal stress at a point beneath the applied load is required then account must be taken of the variation in direct vertical stress due to the loading condition.

The calculated values of compressive stress (fc) at failure given in Table 11.6.13. are based upon the values of applied load at the first observed signs of material crushing. By reason of the arrangement of the test apparatus it was only possible to visually inspect the outside faces of the beam under test, it is therefore suggested by the author that no real conclusive evidence can be drawn from this part of the work.

From crushing tests carried out on 4" mortar cubes it would have been expected that the stresses at beam crushing would have been in the region of 2300 lb/in^2 for 1.0.3. mix and 830 lb/in^2 for 1.1.5. mix. The low value obtained for B eam No. 1 (1.0.3.) at 843 lb/in^2 gives further support to the conclusions obtained from the load/deflection curve that there was some internal deficiency in the material of this beam.

A further investigation of the load/deflection curves for Beams Nos. 6 - 8 suggests that crushing took place at some time before it was observed during the test, in these cases the curve becomes non-linear at applied loads well below that of the value given for visual crushing. This factor in itself would account for the high values of (fc) for the mortar mix 1.1.5. C/L/S.

The load/deflection curves for Beams Nos. 3 and 9 can be seen to remain linear from the states of tension crack to first crushing, the calculated value of (fc) for these beams is 2419 lb/in^2 and 882 lb/in^2 respectively which are both in the region that could be reasonably expected based upon the crushing strength values given by the cube tests. The variation between calculated crushing stress and mortar cube strength suggests that at the level of stress observed for first crushing the assumed diagram of linear stress distribution over the compression contact area was no longer entirely a valid assumption. Test results for the 1.0.3. mix show a tendancy for the calculated stress based upon a triangular distribution to be less than the experimental cube strength of the material. Fig.11.8.1. shows a diagram of stress distribution that would satisfy these conditions. The areas of the two diagrams would be equal giving the total thrust force of Pc in each case.

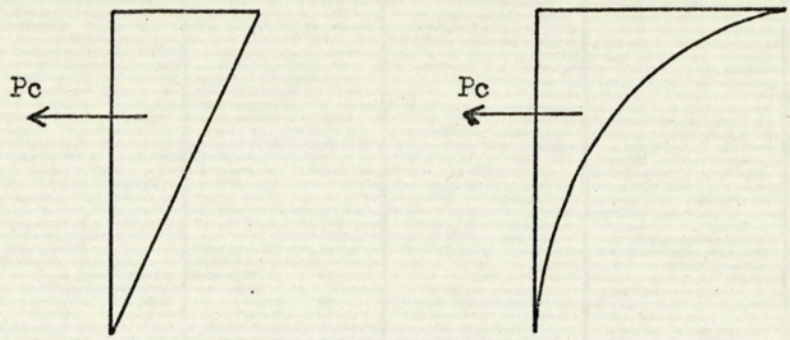

Fig.11.8.1.

Test results for the 1.1.5. mortar mix show a tendancy for the calculated stress based upon a triangular distribution to be greater than the experimental cube strength of the material. Fig.11.8.2. shows a diagram of stress distribution that would satisfy these conditions. Again, the areas of the two diagrams would be equal giving the total thrust force of Pc in each case.

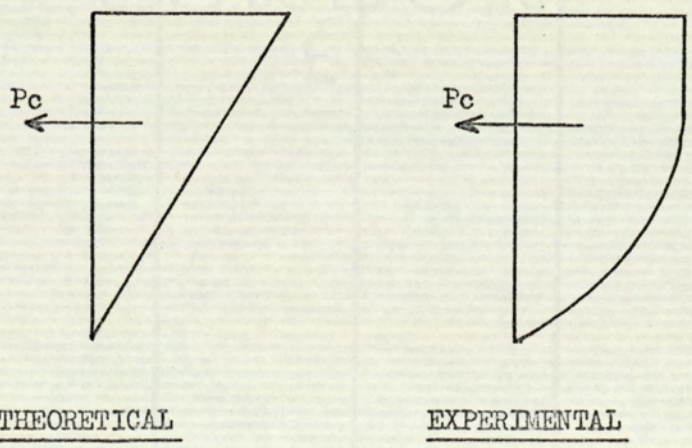

Fig. 11.8.2.

It is known that the strain at crushing for concrete specimens varies from approximately 0.005 for weak concrete to 0.002 for strong concrete, indicating that the higher strength concretes tend to be more brittle and that the lower strength concretes tending to be more ductile would more readily re distribute stresses beyond the elastic limit and exhibit properties of plasticity.

It is not unreasonable therefore to assume that mortars of varying strengths would have relative behaviour similar to those of concrete specimens.

It is therefore concluded that if a greater number of beams were tested and the crushing stage more accurately defined then Eqn [12] would predict a crushing stress more closely related to the experimentally obtained crushing strength of the material.

Ultimate collapse of the test beam specimens occurred by one of two modes, either a longitudinal tension failure or a hinge mechanism permitted by progressive crushing over the compression zone at the centre of the beam.

The longitudinal fracture occurred along the line of maximum thrust from the compression zone at the centre of the beam to the compression zone at the support. The magnitude of the compressive forces would be such that in the beam a high intensity of compressive stress would be set up. It is concluded that the longitudinal fracture exhibited in some beams was a tension failure due to the compressive forces, the result being very similar to the conditions obtained by the well known 'Brazilian Test' for obtaining the tensile strength of a material by the application of a compressive force over a small area of the specimen.

The hinge type of failure was brought about by reason of the ability of the beam to allow a progression of the crushed area of the compression zone to progress in advance of the effects of the thrust forces along the compression axis, thereby allowing sufficient beam deflection to give a resulting negative lever arm of the compressive forces.

From the limited number of tests carried out there is insufficient evidence to enable a failure pattern to be predicted, however it could be expected with some certainty that shallow beams with a high value of span/depth ratio, as would be the case for infill panels walls would have an ultimate mode of failure of the hinge mechanism type.

The conditions of vertical support are assumed in the theoretical consideration to be developed entirely by friction between the vertical end face of the beam and the face of the supporting member. In the experimental condition, this was the face of the adjustable end bearing plate. During each test, checks were made with respect to the deflection of the vertical end supports that were used to locate the specimen in the test rig, it was found without exception that from the first increment of applied load the horizontal expansion of the specimen was sufficient to generate the necessary frictional support to provide the

vertical reaction to the applied load. There was no measurable slip between the beam end support, even at the highest values of applied load there was no indication of vertical compression in the rubber blocks at each end of the beam.

Fig. 11.6.19. shows the experimental relationship of load/deflection to span/depth, the experimentally obtained values for each beam are plotted according to mortar mix and result in an acceptable diagram of non-linear relationship for each material. From the experimental values of the load/deflection relationship values of ($\propto$L) are calculated for each beam. Fig. 11.6.20. has been plotted to show the resulting relationship of ($\propto$L) to R for each mortar mix. With the limited amount of information by reason of the fact that only one beam of each span/depth ratio per mix was tested, the inter-relationship between ($\propto$L) for beams of equal span/depth ratios but of different mortar mixes must at present remain to some degree inexplicable.
The value of ($\propto$L) which is the total shortening of an extreme outer fibre at the centre of the beam and at the supports, is dependant upon the stress/strain characteristics of the beam material. As such it could reasonably be expected that the value of ($\propto$L) for similar beams of different material would be in proportion to the value of Young's Modulus for the respective materials. The results of the tests carried out in this programme do not confirm the validity of this assumption.
For the production of accurate design data it would therefore be necessary for this programme of work to be extended to include probably at least six beams of the same span/depth ratio for each mortar mix in order that the specific relationship between different materials may be determined.

The basic assumption of the theory of arching action presented here is that after the initial tension crack has taken place each half of the beam then deflects as a rigid body, the effects of local deflection due to a uniformly distributed load are neglected. On this basis, since the beam deflection is related to the value of αL, which is in turn the resultant of the arch compressive forces, the diagram of load/deflection due to a point load (W) applied at the centre of the beam will be identical to a diagram of load deflection due to a total uniformly distributed load on the beam of (2W). Both loading conditions will produce the same value of horizontal compressive force (Pc) at the centre of the beam and at the supports, thereby resulting in equal deflections at mid-span.

Table 11.6.14. shows a comparison between the value of the applied load (W) for the theoretically predicted elastic failure and actual collapse. The theoretical load is based upon the cube strength of the respective materials and with the exception of Beam No. 5 results in a predicted crushing failure that is below the value of the applied load at collapse.

BEAM NO.	APPLIED LOAD (Wlb)		W (COLLAPSE) / W (CRUSHING)
	AT THEORETICAL CRUSHING	AT EXPERIMENTAL COLLAPSE	
1	14059	16152	1.15
2	9774	12354	1.26
3	6197	7894	1.27
4	3414	3774	1.11
5	1175	887	-
6	5147	9392	1.82
7	3567	5171	1.44
8	2231	3019	1.35
9	1194	1228	1.02

TABLE NO. 11.6.14

CHAPTER 12

FINAL CONCLUSIONS AND SUGGESTIONS FOR FURTHER RESEARCH

12.1 Introduction

Throughout this thesis it has been shown that brickwork possesses a potential tensile strength of sufficient magnitude that would produce further economies if the tensile properties were included in the design of loadbearing brickwork structures.

It is unfortunate that during the last three or four decades the art and craft of the bricklayer has been allowed to degenerate into a state of poor workmanship that is readily accepted by those who are responsible for present day constructions. Surprisingly, the decrease in standards has been accompanied by a corresponding decrease in productivity.

If the full potential strength of brickwork is to be exploited then for reasons of reliability the labour must be educated to produce work of a satisfactory standard. There is no reason at all why the standard of site supervision for brickwork could not be equal to that at present achieved for reinforced concrete.

Modern methods of brick production and mortar mixing are such that the designer can place complete reliability on the physical properties of the constituent materials, if the same reliability could be accepted for the simple art of bringing together the bricks and mortar to form a composite material then further advances could be made in the adventurous use of brickwork.

Probably the most important single factor influencing the production of brickwork with a fair degree of reliable tensile strength is the moisture content of the bricks at the time of laying. It has been known for many centuries that dry bricks result in poor brickwork, nevertheless it is a rare sight indeed in the present day to see bricks that have been satisfactorily wetted before use.

If the only possible way to reduce the initial suction rate of a brick is by soaking in water, then the time required for soaking must be specified by the brick manufacturer and not left to the site labour to arbitrarily decide.

The use of a mortar additive may well provide a solution to the suction rate problem, for these answers we must look to those expert in the chemistry of the hydration process.

It may well be that a suitable alternative to the age old use of sand/cement mortars will be found, there have been many advances in the field of construction adhesives, after all, the mortar is really only required as a medium for bedding the bricks and bonding them together.

The theoretical and experimental work of this thesis provides the designer with a better understanding of the behaviour of brickwork in flexure and will enable a more scientific approach to be made in the specific field of the analysis of stresses in unreinforced brickwork beams.

12.2 The Physical properties of brickwork

There exists a wealth of knowledge with respect to those physical properties of brickwork concerned with the compressive strength of the material. Limits on allowable design stresses are given in CP.111 and the designer is specifically advised by this Code of Practice that no reliance should be placed on the tensile strength of brickwork in calculations, it is further stated that it should be assumed that part of the section will be inactive and the remainder will carry compressive stress only.

Regardless of the results of this thesis, there exists many practical examples of brickwork exhibiting a great deal of tensile strength. It must be concluded that in this respect CP.111 is very conservative and that the provision of such limitations on brickwork in tension prevent the designer from taking full advantage of the material.

It is suggested by the author that the Code of Practice should be amended to permit reliance to be placed on tensile strength where it can be shown to reliably exist. It would be sensible to specify a suitable load factor to the values of ultimate strength obtained by experiment for the particular brick and mortar being used.

The tests for diagonal tensile strength described in Chapter 6 give a reliable assessment for the flexural shear strength of the material, to obtain the tensile strength of a particular brickwork sample a similar test could be carried out by orientating the axis of the applied load to suit the direction in which it is required to obtain the tensile strength.

To determine the tensile strength parallel to the bed joint of brickwork constructed with L.B.C. 'commons' using 1.0.3 and 1.1.5 cement/lime/sand mortars the author has carried out 'splitting' tests on 18" square panels of brickwork. The mode of failure is shown in Plate No. 12.2.1. On the basis of calculation that $ft = \frac{2P}{\pi.D.t}$ the test results give arithmetic means of tensile strength of 138 lb/in^2 for 1.0.3. mortar and 119 lb/in^2 for 1.1.5. mortar. These values are below those obtained for flexural strength tests and by the use of a suitable load factor would satisfactorilly give values of allowable tensile strength that could be permitted for practical design purposes.

The numerical value of the load factor could only be determined after a more extensive series of tests using various bricks and mortar mixes. This could well form a part of some future research programme.

12.3 Shallow brickwork beams

The theory developed here for shallow brickwork beams based upon the analogy of a laminated section could readily be applied to a beam manufactured from any number of different materials bonded together to form a composite section.

With particular reference to brickwork beams there remains the question at which stage can the beam be considered to be a plate of homogeneous material and therefore up to what limits must the various properties of brick and mortar be considered.

In Chapter 8 it was shown that for the purposes of deflection calculations the beam would be considered to be homogeneous but for the purposes of a stress analysis the non-homogeneous properties must be considered

since the shift in the position of the neutral axis at various cross-sections will influence the calculated value of the flexural stresses. Calculations show that for beams greater than 5 courses deep the effect of the change in neutral axis position is negligable.

Further investigation could be carried out to determine the relationship between tension strengths obtained from a splitting test on sample panels to the ultimate flexural strength of shallow beams constructed from various bricks and mortar mixes.

If it is required to determine the true distribution of stress in the elements of a shallow brickwork beam then it is essential to use a theory that takes into account the various physical properties of the bricks and mortar. For practical design purposes based upon a limiting value of flexural stress it is suggested that beams greater than 5 courses deep could be analysed without significant error on the basis of a homogeneous section assuming the application of the simple theories of bending.

12.4 The application of the theory of elasticity to the solution of stresses in beams

This work is of significant importance since a polynomial solution is achieved for the ideal condition of stress free ends for a beam supported by a shear force at each end and subject to a uniformly distributed load applied to the top face. Although the theory has been developed for the application to brickwork beams the parameters are such that the theoretical solution could be applied to beams manufactured from any homogeneous material. The work could be suitably extended to reinforced concrete deep beams.

The expansion of a doubly infinite power series to obtain the stress function places the search for the stress function on a logical basis. Wit hout further mathematical research the method can be immediately employed to determine suitable stress functions for deep cantilever beams as may be the case in retaining walls, shear wall constructions or gravity dams.

Applied loads of varying intensity can be readily solved; quite simply for a linear variation and without very much complexity for non-linear variations. The complexity of course being dependant upon the applied load intensity equation.

This method for the determination of a stress function has so far not been investigated for discontinuous loads such as a system of point loads.

The polynomial solution to problems in elasticity usually results in the most convenient stress equations, it would therefore be worth while for further research in this field to determine a method by which the expansion of a power series could be adapted to produce stress equations for discontinuous loading systems.

In modern multi-storey brickwork structures the case often arises where walls acting as beams supporting floor loads also act to provide the reaction against horizontally imposed wind forces. The theoretical sol utions given in this thesis make it possible for such loading cases to be analysed simply by the superposition of one loading system upon another, similarly it could be extended to beams subject to compression in the longitudinal axis.

12.5 Deep Brickwork beams

The evidence obtained from the tests carried out in this programme to validate the proposed theory clearly shows that for beams with a span/depth ratio less than 1.0 there is a considerable difference between elastic failure and complete collapse.

The effect of arching action is responsible for the magnitude of the ultimate strength, no special effort was made to provide a reaction to the horizontal thrust forces resulting from the arching action, the reactions resulted entirely from the construction of the test specimens.

It follows therefore that there is considerable scope for further research into the arching of deep beams and into the ultimate strenght of complete brickwork structures, the behaviour of piers supporting flexural members would be of particular interest.

A simple tie, which could be in the form of steel reinforcement in a bottom course bed joint would have a significant influence on the ultimate load carrying capacity of a deep brickwork beam. It would not be necessary for an analysis to be made on the theory of a reinforced beam since simple arching action would be more likely to be the mode of behaviour.

The work undertaken in this programme has been restricted to solid brickwork, it is often the case in practical construction that external walls are not only of cavity construction but each leaf of the wall is of a different material eg. External leaf in facing bricks with an internal leaf in lightweight blocks.

Each leaf of the wall would of course be capable of acting as a deep beam, they are however connected by some form of ties across the cavity and there must be an interaction between the beams of disimilar materials.
The composite behaviour in flexure requires a complete investigation.

There are numerous examples of panel wall construction that would merit further research, particular reference could be made to the possible variation in restraint conditions.

The experimental behaviour of the deep beams recorded in Chapter 10 suggests that the theory of arching action given here would not be applicable to deep beams with a span/depth ratio equal to or less than 0.75 since the beam tested did not produce a flexural tension crack which is a basic assumption of the theory.
There are at present published theories relating to the arching action of brickwork supported on steel and reinforced concrete beams, there is a further necessity for a theoretical solution to be given for the arching action in deep beams that are supported by a vertical shear force at each end.

PLATE No 12. 2. 1.

TENSION SPLITTING TEST ON 18" SQUARE SAMPLE PANELS.

REFERENCES

1. PLUMMER, H. C.

'Brick and Tile Engineering'
(Structural Clay Products Institute, Washington D.C.)
pp. 33, 61 and 153.

2. ALBRECHT, W. and SCHNEIDER, H.

'The Influence of the Suction Capacity of Hollow Blocks on the Loadbearing Capacity of Masonry'
Ziegelindustrie 16, (24) 906,1963;
17, (1), 3, (2), 31: 1964

3. Draft British Standard Code of Practice for Structural Recommendations for Walls Constructed of Brickwork, Blockwork or Masonry.
BSI Ref BLCP/29. Jan 1970.
(Revision of CP111: 1964 'Structural Recommendations for Loadbearing Walls')

4. PLOWMAN, J. M.

'The Modulus of Elasticity of Brickwork'
Proceedings of the British Ceramic Society
Loadbearing Brickwork No. 4 July 1965

5. STAFFORD-SMITH, B. and CARTER, C.

'A Hypothesis for the Shear Failure of Brickwork'
University of Southampton.

6. HENDRY, Prof A. W.

'Wind Load Analysis of Multi-Storey Brickwork Structures'
B. D. A. Research Note
Vol, 1 No. 3, Jan. 1971

7. STAFFORD-SMITH, B., CARTER, C. and CHOUDHURY, J. R.

'The Diagonal Tensile Strength of Brickwork'
The Structural Engineer, Vol. 48 No. 6 June 1970

8. Structural Clay Products Research Foundation
Small Scale Specimen Testing
Progress Report No. 1.
Geneva, Illinois. 1964.

9. 'History of Strength of Material'
Timoshenko S. P.
McGraw-Hill Book Company, Inc.

10. TIMOSHENKO, S. P. and GOODIER, J.N.
'Theory of Elasticity' Third Edition
McGraw-Hill Book Company

11. GOODIER, J. N.
'Compression of Rectangular Blocks and the Bending of Beams by Non-Linear Distribution of Bending Forces'
The American Society of Mechanical Engineers
APM - 54 - 17

12. COULL, A.
'Stress Analysis of Deep Beams and Walls'
The Engineer - Feb.1966

13. UHLMANN, H. L. B.
'The Theory of Girders Walls with Special Reference to Reinforced Conc rete Design'
The Structural Engineer. August 1952

14. ARCHER , F. E. and KITCHEN, E.M.
'Stress Distributions in Deep Beams'
Civil Engineering and Public Works Review
Vol. 55. No. 643. Feb 1960

15. CONWAY, H. D., CHOW, L. and MORGAN, G.W.
'Analysis of Deep Beams'
The American Society of Mechanical Engineers
Annual Meeting 1950

16. HENDRY, Prof. A. W. and SHAWKI SAAD
'Gravitational Stresses in Deep Beams'
The Structural Engineer June 1961

17. HENDRY, A.W. and SAAD, S.
'The Determination of Gravitational Stresses by Photo-Elasticity'
Proceedings of the Fiftieth Anniversary Conference of the
Institution of Structural Engineers
October 1958.

18. FROCHT, M. M.
Photoelasticity Vol. II
Chapman and Hall Ltd.